

# **Historical Growth Rates and Changing Climatic Sensitivity of Boreal Conifers**

**Thomas Michael Melvin**

**PhD Thesis**

Climatic Research Unit  
School of Environmental Sciences  
University of East Anglia

**May 2004**

© This copy of the thesis has been supplied on condition that anyone who consults it is understood to recognise that its copyright rests with the author and that no quotation from this thesis, nor any information derived therefrom, may be published without the author's prior permission

## ***Abstract***

This thesis is concerned with the expression of relatively long-timescale growth forcing in tree-ring chronologies. The operation of different standardisation techniques, used in dendroclimatology to remove internal, non-climate related growth trends in measured series of ring-widths, is explored with an emphasis on the efficiency of the Regional Curve Standardisation (RCS) technique. The approach adopted here makes extensive use of concepts taken from tree-growth models and is based on the assumption that common external growth forcing operates through its influence on photosynthesis. A definition, of the growth rate of trees in terms of the carbon production by unit foliage, is the rationale that underlies this work and leads to the use of a multiplicative model for processing individual tree and chronology indices. The presence of a “common signal” in series of tree measures can lead to the distortion of the shape of detrending curves and a problem with bias in chronologies. Problems of the RCS technique are identified which are associated with tree age and diameter-related bias, arising from the use of ring-width to establish tree growth rates, regardless of tree diameter. These problems are manifest as “end effects” in chronology development and are most significant in the most recent century. Alternative, significant modifications of the RCS approach are proposed: the Multiple RCS (MRCS) and the Size-Adjusted RCS (SARCS) methods which greatly mitigate these problems. These are made possible by the introduction of two new concepts in dendroclimatology: the “best fit means” method and the use of “signal-free measures”. The concept of the mechanical strength of trees is used to simulate tree growth from series of ring-width measures and a “process based standardisation” (PBS) model is developed. The PBS model is tested and shown to be a feasible alternative to existing standardisation techniques.

## ***Acknowledgements***

I wish to thank the following people:

Keith Briffa my supervisor for his help and support throughout this project.

Tim Osborn and Phil Jones for helpful advice and also for reading and commenting on this manuscript.

Ed Cook for helpful comments and discussion.

Those Finnish and Swedish colleagues in the Advance 10K project for providing the raw tree ring measures used in this project.

Matti Eronen, Jouku Meriläinen, Mauri Timonen, Pentti Zetterberg and Marcus Lindholm for developing the long sub-fossil Finnish-Lapland chronology which was vital to this project and again Mauri Timonen for his assistance in arranging permissions and sites in Finland for the fieldwork of this project.

Håken Grudd, Wibjörn Karlén, and Thomas Bartholin for developing the Tornetrask chronology.

Annikki Mäkelä for developing the series of process-based tree growth models upon which the PBS model is based.

Ben Smith and Andrew Friend for providing the source code for the GUESS and HYBRID tree-growth models.

This project was funded by NERC, Ref GT04/1999/TS/0063

Last, but not least, I would like to thank June, my wife, for encouragement and support over the years and also help with the fieldwork.

## **List of Contents**

Abstract.....	i
Acknowledgements .....	ii
List of Contents .....	iii
Glossary .....	vii
List of Figures and Tables .....	ix
<b>Chapter 1. Introduction .....</b>	<b>1</b>
1.1. Climate Change .....	1
1.2. Tree Growth and Climate .....	1
1.3. Long-timescale Variance in Tree Ring Chronologies .....	3
1.4. The Growth Rate of Trees .....	4
1.5. This Thesis.....	5
1.6. Structure of this Thesis .....	6
<b>Chapter 2. Background .....</b>	<b>8</b>
2.1. Tree Structure .....	8
2.2. Tree Rings.....	9
2.3. Time Series .....	10
2.4. Dendroclimatology .....	11
2.5. Standardisation .....	12
2.5.1. Introduction .....	12
2.5.2. Curve-fitting Standardisation Methods .....	13
2.5.3. Estimating the age-related growth curve .....	15
2.5.4. Hughschoff Method of Standardisation .....	16
2.5.5. Long-timescale Variance using Curve-fitting Methods.....	18
2.5.6. Regional Curve based Standardisation Method.....	19
2.5.7. RCS Method .....	20
2.5.8. RCS Method Restrictions .....	21
2.6. Summary.....	22
<b>Chapter 3. Chronologies and Meteorological Data .....</b>	<b>23</b>
3.1. Introduction .....	23
3.2. Choosing Sites, Data and Samples .....	23
3.2.1. Site Selection.....	23
3.2.2. Data and Sample Selection .....	25
3.3. Source and Processing of Data .....	26
3.3.1. Meteorological Data .....	26
3.3.2. Sub-Fossil Chronologies .....	27
3.3.3. Tree Core Sampling.....	27
3.3.4. Tree Core Data Processing .....	29
3.3.5. End-Aligned Chronologies .....	30
3.3.6. Randomly Generated Trees .....	31
3.4. Data Comparisons and Relationships .....	32
3.4.1. Meteorological Data Comparisons .....	32
3.4.2. Meteorological Data Correlations .....	35
3.4.3. Tree ring data - Statistics .....	36
3.4.4. Tree-ring data - Correlations .....	40
3.5. Summary.....	41
<b>Chapter 4. Tree Growth.....</b>	<b>42</b>
4.1. Growth Rate and Amount of Growth .....	42
4.1.1. Introduction .....	42

4.1.2.	Climate controls photosynthesis.....	43
4.1.3.	Expected Growth Rate is proportional to Foliage Mass.....	44
4.1.4.	Foliage mass increases while trees get bigger.....	45
4.1.5.	Variation in Growth Rates.....	46
4.1.6.	Tree Measures Demonstrate Variation in Growth Rates.....	48
4.1.7.	Predicting Ring Width Decay.....	50
4.1.8.	Discussion.....	52
4.2.	Mathematical Chronology Model.....	53
4.2.1.	Introduction.....	53
4.2.2.	Creating Chronology Indices.....	53
4.2.3.	Signal-free Measures.....	54
4.2.4.	Resetting Means or Rescaling.....	55
4.2.5.	Resetting the Slope.....	55
4.2.6.	Summary.....	57
4.3.	Best Fit Means (BFM).....	57
4.3.1.	Introduction.....	57
4.3.2.	Trend in Mean.....	58
4.3.3.	Overlapping Trees.....	58
4.3.4.	Best Fit Examples.....	59
4.3.5.	Best Fit Means Procedure.....	61
4.3.6.	Evaluation – Best Fit Means.....	63
4.3.7.	Discussion.....	69
4.4.	Trend distortion.....	70
4.4.1.	Introduction.....	70
4.4.2.	Demonstration of the Problem.....	71
4.4.3.	Trend distortion.....	73
4.4.4.	Why and When a Problem.....	74
4.4.5.	Simulated Trees with Known Signals.....	76
4.4.6.	Avoidance of Trend distortion.....	79
4.4.7.	Discussion.....	82
4.5.	Conclusions.....	83
<b>Chapter 5. RCS Method – Problems and Improvements.....</b>		<b>84</b>
5.1.	Introduction.....	84
5.2.	Variation of Mean Growth Rate.....	85
5.3.	RCS Indices are Larger and Slope.....	86
5.4.	Modern sample bias.....	89
5.4.1.	Introduction.....	89
5.4.2.	Random variations in growth rates.....	90
5.4.3.	Modern chronologies.....	91
5.4.4.	Incomplete Samples.....	94
5.4.5.	Real and Apparent Problems.....	96
5.4.6.	Discussion.....	98
5.5.	The Slope of the RCS Curve.....	99
5.5.1.	Introduction.....	99
5.5.2.	Low-frequency limits of RCS Curves.....	99
5.5.3.	Randomly Generated Chronologies.....	103
5.5.4.	Problems with the Slopes.....	104
5.5.5.	Slope Removal and Trend-free Chronologies.....	105
5.5.6.	Rotation of Chronologies.....	107
5.5.7.	Chronology Slope Correction.....	110
5.5.8.	Expected Growth and Common Forcing.....	113
5.6.	Smoothing the RCS Curve.....	117
5.7.	Multiple RCS Curve Method (MRCS).....	118
5.7.1.	Introduction.....	118
5.7.2.	MRCS Method.....	120
5.7.3.	MRCS Method - Examples.....	122
5.8.	Size adjusted RCS Method (SARCS).....	126

5.8.1.	Introduction .....	126
5.8.2.	SARCS Method .....	128
5.9.	Conclusions .....	132
<b>Chapter 6.</b>	<b>RCS, MRCS and SARCS Comparisons .....</b>	<b>135</b>
6.1.	Introduction .....	135
6.2.	Comparison of RCS, MRCS and SARCS Methods .....	135
6.2.1.	Expected growth curves and tree indices.....	135
6.2.2.	Means of tree indices by ring age.....	138
6.2.3.	Random Chronologies.....	140
6.2.4.	Chronology comparisons.....	140
6.2.5.	Artificial step increase or decrease.....	144
6.2.6.	Growth rate, Age and Size.....	146
6.3.	Errors and Uncertainty.....	148
6.3.1.	Introduction .....	148
6.3.2.	Bootstrapped Confidence Limits .....	149
6.3.3.	Overlapping by BFM as a source of Error.....	155
6.3.4.	Overlapping Errors for Sample Chronologies .....	159
6.3.5.	SARCS Method used on Modern chronologies.....	164
6.4.	Tree Growth and Temperature .....	165
6.4.1.	Correlations .....	165
6.4.2.	Regressions.....	167
6.4.3.	Low and High pass Filtered Comparisons.....	173
6.5.	Conclusions .....	175
<b>Chapter 7.</b>	<b>Process Based Standardisation (PBS).....</b>	<b>178</b>
7.1.	Introduction .....	178
7.2.	PBS Model Overview .....	180
7.3.	PBS Model - General Properties .....	183
7.3.1.	State Variables.....	183
7.3.2.	Parameters .....	185
7.3.3.	Conservation of Mass.....	186
7.3.4.	Some Assumptions .....	186
7.3.5.	Mathematical Procedures .....	187
7.4.	Growth Processes .....	187
7.4.1.	Photosynthesis .....	187
7.4.2.	Allocation .....	189
7.4.3.	Respiration .....	189
7.4.4.	Senescence .....	190
7.4.5.	Reproduction .....	194
7.4.6.	Mortality.....	194
7.4.7.	Mechanical Strength.....	195
7.4.8.	Stem Diameter and Compartment Lengths.....	197
7.5.	PBS Model Calculations.....	198
7.5.1.	Overview .....	198
7.5.2.	Foliage and Fine Root Mass .....	199
7.5.3.	Sapwood Volume and Mass .....	200
7.5.4.	Wood Profile from Mechanical Strength.....	202
7.5.5.	Branch Wood.....	203
7.5.6.	Trunk Root Wood.....	204
7.5.7.	Par1 - Increases as Trees Grow .....	204
7.5.8.	Par1 - Open Grown > Closed Canopy .....	207
7.5.9.	Height Growth Strategy.....	208
7.5.10.	Estimating Initial Height .....	211
7.6.	Evaluating the PBS Model .....	212
7.6.1.	Testing Methods.....	212
7.6.2.	The PBS Program.....	213
7.6.3.	Parameter Values.....	214

7.6.4.	Trees and the PBS Model.....	215
7.6.5.	Measured v Calculated Sapwood Areas .....	220
7.6.6.	PBS Indices by Year, Ring Age and Diameter.....	222
7.6.7.	Growth Efficiency of the PBS Model.....	227
7.6.8.	Comparisons of the PBS model and other methods .....	229
7.7.	Conclusions and Further Development .....	234
<b>Chapter 8.</b>	<b>Conclusions.....</b>	<b>241</b>
8.1.	Project description and methods.....	241
8.2.	Summary of major findings.....	241
8.3.	Project's strengths and weaknesses .....	243
<b>Reference List.....</b>		<b>248</b>

## **Glossary**

For the convenience of the reader, a number of terms with specific meaning in this thesis are described briefly.

### **Age-related Growth Curve**

The medium-frequency change of the size of ring-width measurements over the life of a tree is described as the age-related growth trend.

### **Curve-fitting**

Methods of generating *expected growth curves* by fitting values to the series of measures of an individual tree, which includes fitting by eye, least squares methods, and deterministic methods are called curve-fitting methods.

### **End-aligned chronology**

A end-aligned chronology created by setting the final ring of each tree to the same calendar date and earlier rings to the corresponding, sequentially ordered, earlier dates.

### **Expected growth curve**

The expected growth curve is the value of growth, for each ring age, expected in an average growth year i.e. a year in which the common forcing on tree growth will produce the average amount of growth.

### **High-frequency**

Variance at periods of about a decade and less is referred to as high-frequency variance.

### **Life-span trend**

A series of indices have a life-span trend if the mean values of first half of the series differs from the mean values of the second half of the series i.e the series have an overall slope.

### **Low-frequency**

Variance at periods over a century and beyond the lifespan of a tree is referred to as *low-frequency* variance.

### **Mäkelä model**

A series of carbon balance tree-growth models developed for *Pinus sylvestris* with the investigation of height growth strategies amongst the objectives are referred to as the Mäkelä model ( Mäkelä & Hari 1986; Mäkelä 1986; Mäkelä & Sievanen 1992; Mäkelä 1997).

### **Medium-frequency**

Variance at periods from decades to half the lifespan of a tree is referred to as *medium-frequency* variance

### **Modern chronology**

A chronology or group of trees sampled from predominantly living trees and with samples taken at roughly the same time (year or decade), usually in the recent period are referred to as a modern chronology.



**Modern sample bias**

Modern sample bias is an age related growth rate bias which can distort modern chronologies developed from mean tree growth rates over time.

**Multiple RCS method (MRCS)**

MRCS is a method of standardisation using a family of RCS curves for varying growth rates (Section 5.7).

**Process Based Standardisation (PBS) model**

The PBS is a computer model of tree growth designed to standardise series of ring measurements.

**PBS Indices**

Series of tree indices generated by the PBS model and based on the rate of carbon production by unit foliage.

**Size Adjusted RCS method (SARCS)**

SARCS is a method of standardisation based on the RCS method but using ring-age and diameter to select expected growth curves from the RCS curve (Section 5.8).

**Signal-free**

A series of measurements, or an RCS curve generated from measurements, which have been divided by chronology indices in order to remove the effects of common forcing are referred to as signal-free.

**Trend distortion**

This is the distortion of *expected growth curves* created by using series of measures which contain the effects of the common forcing signal as compared to the use of series of *signal-free* measures.

## **List of Figures and Tables**

<b>Figure 2.5.1</b> Sample trees from Luosto, Finland showing ring width and <i>expected growth curves</i> generated using (a) Hegershoff curve, (b) modified negative exponential curve, (c) negatively sloping straight line, and (d) and a horizontal line.	17
<b>Figure 3.2.1</b> Location map showing meteorological stations (white), sub-fossil tree regions (green), and “modern” tree regions (red).	24
<b>Table 3.3.1</b> Meteorological data, site names and calendar ranges.	26
<b>Table 3.3.2</b> Site names, sample references, brief description, elevation, and grid refs for the modern-tree samples used in this study.	28
<b>Figure 3.4.1</b> Means of mean monthly temperatures for Sodankyla, Bødö and Tornedalen for (a) Summer (June, July and August), (b) Winter (December, January and February), (c) Annual mean (all months), and (d) normalised summer temperatures.	33
<b>Table 3.4.1</b> Mean monthly temperature, within site correlations.	34
<b>Table 3.4.2</b> Correlations of mean monthly temperature between meteorological stations, over their common period (indicated) for each pair. (All correlations significant at the 99.9% level)	35
<b>Table 3.4.3</b> Summary statistics for the seven chronologies of this study: Tree counts, mean age, mean radius, and mean ring width (means with standard deviations).	36
<b>Figure 3.4.2</b> Mean ring widths, standard deviations (plotted from zero), and tree counts by calendar year (shaded area). (a) Tornetrask AD (smoothed), (b) Finnish-Lapland AD (smoothed), (c) Tornetrask End Align, (d) Finnish-Lapland End Align.	37
<b>Figure 3.4.3</b> Mean ring widths, standard deviations (plotted from zero), and tree counts by calendar year (shaded area) for (a) Luosto, Finland, (b) Rutajarvi, Finland, and (c) Helldalisen, Norway.	38
<b>Figure 3.4.4</b> Means of current tree radius, current ring age, and final tree age for rings and trees contributing to each calendar year at (a) Luosto, Finland and (b) Helldalisen, Norway.	39
<b>Table 3.4.4</b> Mean between tree and mean tree to chronology correlations, with standard deviations, for each region, based on high-pass filtered series of tree indices.	40
<b>Table 3.4.5</b> Region to region correlations between each region, based on high-pass filtered chronologies.	41
<b>Figure 4.1.1</b> (a) Tornetrask AD mean ring-width of the fastest, slowest and all trees by ring age. (b) Tornetrask AD ring-width of the fastest and slowest trees by calendar year with tree counts. (c) and (d) as (a) and (b) but for the Finnish-Lapland AD trees.	49

<b>Figure 4.3.1</b> (a) Two generated series of tree indices, (b) Chronologies from these by arithmetic mean and by BFM method, and (c) Chronologies from series of tree indices with a mean of 1.0 by arithmetic mean and by BFM method.	60
<b>Table 4.3.1</b> Simultaneous equations relating the mean values of tree indices.	62
<b>Figure 4.3.2</b> (a) and (c) Chronologies created using arithmetic and BFM methods. (b) and (d) The mean values of series of tree indices created using the RCS and BFM methods, both sorted on the RCS method mean.	64
<b>Figure 4.3.3</b> Comparison of chronologies made using indices created by the RCS method, (a) and (c) chronologies by arithmetic means and (b) and (d) chronologies created by BFM method. Fastest and slowest trees based on time to reach 10cm radius.	66
<b>Figure 4.3.4</b> Chronologies made from indices created by the RCS method and averaged using BFM method. Series of differing maximum lengths sub-divided to obtain each chronology. Slopes set to zero and means to 1.0 for period 600 to 1600.	68
<b>Figure 4.3.5</b> Comparison of mean-tree chronologies by RCS and BFM methods. All indices of each tree replaced by the series mean.	69
<b>Figure 4.4.1</b> Hegershoff standardisation of chronologies created using the Luosto and Helldalisen trees. Ring-width values from 1920 onward adjusted by factors of 1.3, 1.0, 0.7 and 0.4.	72
<b>Figure 4.4.2</b> Illustration of trend distortion using alternative expected growth curves on a randomly generated tree with a two-decade long growth increase.	74
<b>Figure 4.4.3</b> Randomly-generated chronologies with a variety of common signals, standardised using the Hegershoff method, and used to demonstrate the effects of trend distortion.	78
<b>Figure 4.4.4</b> Demonstration of the effects of removing the common forcing signal from raw measures. Measures (a), signal-free chronologies (b), and rotated (over period to 1900) chronologies (c).	81
<b>Figure 5.3.1</b> Mean ring width (a and c) and mean tree indices (b and d) using the RCS method at the Tornetrask AD (a and b) and Finnish-Lapland (c and d) sites plotted by ring age separately for the fastest and slowest growing thirds of trees.	87
<b>Figure 5.4.1</b> Plots of the mean ring width of rings aged between 40 – 60 year from trees of final diameter between 12 and 14 cm. Ring counts and mean ring width of all trees from the Tornetrask and Finnish-Lapland end aligned chronologies.	91
<b>Table 5.4.1</b> Site statistics, all radii and ages include pith estimates and standard deviations are shown in brackets.	92
<b>Figure 5.4.2</b> Scatter plots of final radius against final age and growth rate (mean during first 100 years) against final tree age for trees from Luosto and Helldalisen.	93

**Figure 5.4.3** Simulated modern chronologies from sub-fossil chronologies at 200-year intervals. Demonstrating that chronologies developed from modern samples have a more positive slope than chronologies built from overlapping trees.

95

**Figure 5.4.4** Plots of mean ring-width and mean indices showing the differences between the youngest and oldest trees in a modern sample. Trees from Luosto and Helldalisen sites were combined and plots were smoothed with a 20 year spline.

97

**Figure 5.5.1** Demonstration of the incorporation of the mean slope of series into the RCS curve and the removal of this slope from resultant tree indices.

100

**Figure 5.5.2** Sensitivity of the RCS and BFM methods to the slope of the RCS curve, (a) RCS curves, (b) RCS created chronologies, and (c) BFM created chronologies.

102

**Figure 5.5.3** RCS curves for (a) random no signal, step up and step down chronologies and (b and c) RCS curves for all, fastest and slowest growing trees from the Tornetrask (b) and Finnish-Lapland (c) end aligned chronologies.

106

**Figure 5.5.4** Comparison of chronologies created with RCS, “best fit means RCS”, and “trend-free best fit means” RCS methods using the (a) random no signal, (b) random step up, and (c) random step down chronologies.

109

**Figure 5.5.5** “Trend-free”, “means-equal”, and “trend corrected” chronologies for (a) random step up, (b) random step down, (c) Tornetrask AD, and (d) Finnish-Lapland AD chronologies.

112

**Figure 5.5.6** Plots showing the 1<sup>st</sup>, 3<sup>rd</sup>, and 6<sup>th</sup> stages of the iterative removal of a “common signal” from the random step up trees. (a) RCS curves, (b) means of signal-free tree indices, and (c) the resulting chronologies.

116

**Figure 5.6.1** Smoothing RCS curves using an age-related smoothing spline.

118

**Figure 5.7.1** Multiple RCS curves for the Tornetrask AD site, (a) first iteration RCS curves, (b) final signal-free curves and age-dependent spline smoothed curves.

123

**Figure 5.7.2** Multiple RCS curves for the Finnish-Lapland AD site, (a) first iteration RCS curves, (b) final signal-free curves and age-dependent spline smoothed curves.

124

**Figure 5.7.3** RCS and MRCS curves for the Tornetrask and Finnish-Lapland sites.

125

**Figure 5.8.1** Comparison of mean indices by ring age of the fastest and slowest growing trees at the Finnish-Lapland AD site using the SARCS method with (a) one RCS curve, (b) two RCS curves, and (c) three RCS curves.

130

**Figure 5.8.2** Comparison of mean indices by ring age of the smallest and largest trees at the Finnish-Lapland site using the SARCS method with (a) one RCS curve, (b) two RCS curves, and (c) three RCS curves.

131

**Figure 5.8.3** Overlap of trees from the Finnish-Lapland site in the AD 530 to 550 period.

132

<b>Figure 6.2.1</b> Sample series of measurements and expected growth curves using the RCS, MRCS, and SARCS methods for fast (a) and (b), medium (c), and slow (d) growing trees from the Tornetrask AD site.	136
<b>Figure 6.2.2</b> Sample series of measurements and tree indices created using the RCS, MRCS, and SARCS methods for fast (a) and (b), medium (c), and slow (d) growing trees from the Tornetrask site.	137
<b>Figure 6.2.3</b> Comparison of the mean indices by ring age of the fastest and slowest growing trees at the Finnish-Lapland site using the RCS (a), MRCS (b), and SARCS (c) methods.	139
<b>Figure 6.2.4</b> Chronologies from the RCS, MRCS and SARCS methods using the random no signal (a), random step up (b), and random step down (c) trees.	141
<b>Figure 6.2.5</b> Chronologies created with the RCS, MRCS and SARCS methods using the Tornetrask AD (a) and Finnish-Lapland AD (b) sites.	142
<b>Figure 6.2.6</b> Test of the RCS (a), MRCS (b), and SARCS (c & d) methods ability to retain an artificial step increase or step decrease in the middle of a chronology using trees are from the Finnish-Lapland AD site.	143
<b>Figure 6.2.7</b> Test of the RCS (a), MRCS (b), and SARCS (c) methods ability to retain an artificial step increase or step decrease at the end of a chronology using trees from the Finnish-Lapland AD site.	145
<b>Figure 6.2.8</b> Tree indices created by (a) RCS and (b) MRCS methods. Mean values of tree indices by year, for the 50% slowest, fastest, youngest, oldest, smallest and largest trees from the Tornetrask AD site.	146
<b>Figure 6.2.9</b> Tree indices created by (a) Hegershoff and (b) SARCS methods. Mean values of tree indices by year, for the 50% slowest, fastest, youngest, oldest, smallest and largest trees from Luosto, Finland.	148
<b>Figure 6.3.1</b> Chronology indices and 95% confidence error using (a and c) RCS and (b and d) MRCS methods on trees from (a and b) Tornetrask AD and (c and d) Finnish-Lapland AD.	150
<b>Figure 6.3.2</b> Bootstrapped 95% confidence error bars of chronologies created from low-pass filtered (50-year spline) series of tree indices derived from (a and c) RCS and (b and d) MRCS methods using trees from (a and b) Tornetrask AD and (c and d) Finnish-Lapland AD.	151
<b>Figure 6.3.3</b> Bootstrapped 95% confidence errors plotted from zero for 100-year Spline, RCS, MRCS and SARCS chronologies using trees from (a) Tornetrask AD and (b) Finnish-Lapland AD.	153
<b>Figure 6.3.4</b> Bootstrapped error bars from Tornetrask trees derived using the MRCS method showing a sequence of sorting and scaling processes.	154

<b>Figure 6.3.5</b> Tree counts by year for a hypothetical chronology with a gap and three sample series with least squares fitted lines, offset for clarity (counts and trees from Tornetrask).	155
<b>Table 6.3.1</b> Means and standard deviations of the absolute error (chronology index – tree index) for Tornetrask AD and Finnish-Lapland AD chronologies developed using various standardisation method and various filtering techniques.	157
<b>Figure 6.3.6</b> Progressively reduced overlap at 750 AD using all Tornetrask AD trees with a ring between 500 and 1000 AD, showing strength of overlap, tree counts and chronology indices (red).	160
<b>Figure 6.3.7</b> Standard deviation of chronology section means derived from 100 samples and plotted by overlapping ring count and square root of tree count.	161
<b>Figure 6.3.8</b> Chronologies of SARCS derived indices, series sub-divided to reduce mean length and averaged using BFM, with each chronology slope set to zero and mean to 1.0 for period 600 to 1600 AD. Chronologies (a) and (c) and counts of overlapping rings (b) and (c).	163
<b>Figure 6.3.9</b> Comparison of modern chronologies, with adjusted slopes and means, created with the SARCS and RCS methods using trees from (a) Luosto, (b) Helldalisen, (c) Tornetrask, and (d) Finnish-Lapland.	164
<b>Table 6.4.1</b> Cross-correlation table of Bödö mean monthly temperatures (previous May to current September) against chronologies using various (specified) standardisation methods and sites.	166
<b>Table 6.4.2</b> Cross-correlation table of Tornedalen mean monthly temperatures (previous May to current September) against chronologies using various (specified) standardisation methods and sites.	167
<b>Table 6.4.3</b> Variance explained by the regression model (1) using Tornetrask chronologies against the Bödö temperature data for full period, first half of period, and second half of period.	168
<b>Table 6.4.4</b> Variance explained by the regression model (1) using Finnish-Lapland chronologies against the Bödö temperature data for full period, first half of period, and second half of period.	168
<b>Table 6.4.5</b> Variance explained by the regression model (1) using Helldalisen chronologies against the Bödö temperature data for full period, first half of period, and second half of period.	169
<b>Table 6.4.6</b> Variance explained by the regression model (1) using Luosto chronologies against the Tornedalen temperature data for full period, first half of period, and second half of period.	169

<b>Table 6.4.7</b> Variance explained by regression models for the Tornetrask and Finnish-Lapland sites using RCS chronologies.	169
<b>Figure 6.4.1</b> Measured and estimated mean July temperature showing two standard error limits, from RCS generated chronologies for (a) Tornetrask AD regressed against Bödö and (b) Finnish-Lapland AD regressed against Tornedalen.	170
<b>Figure 6.4.2</b> Various mean July temperature reconstructions based on chronologies created by different standardisation techniques: RCS, Hugershoff, MRCS and SARCS methods from regression against current and previous years growth indices for (a) Tornetrask AD and (d) Helldalisen to Bödö and (b) Finnish-Lapland AD and (c) Luosto to Tornedalen.	172
<b>Table 6.4.8</b> Correlations of chronologies created using various (specified) standardisation methods and mean July temperature series which have been filtered using high-pass and band-pass filters.	173
<b>Figure 6.4.3</b> Tornedalen mean July temperatures and Finnish-Lapland RCS chronology filtered as (a) high-pass 180-year, (b) band-pass 10 to 180 year, and (c) high-pass 10-year series.	174
<b>Figure 7.1.1</b> Schematic diagram of PBS model chronology processing showing inputs (green), processes (yellow), processes (white) and outputs (red).	181
<b>Table 7.3.1</b> State variables used in the PBS model	183
<b>Figure 7.3.1</b> (a) schematic diagram of a tree, (b) schematic diagram of a stem cross section, and (c) stem vertical cross-section.	184
<b>Table 7.3.2</b> Parameters used in the PBS model	185
<b>Table 7.6.1</b> Parameter values selected for the Luosto, Helldalisen, and Rutajarvi sites.	214
<b>Figure 7.6.1</b> Growth, carbon per unit foliage, by calendar year (with standard deviation), ring age, and diameter for (a) Luosto and (b) Rutajarvi. Scales for calendar year add 1550 (a) and 1700 (b), ring age units of years, and diameter units of mm.	216
<b>Figure 7.6.2</b> Ring-width, stem area, sapwood area and tree height over the life of each tree for sample trees from Luosto. (1.0 on the vertical scale represents the magnitude and units shown separately for each variable.)	218
<b>Figure 7.6.3</b> Sample trees showing ring-width and tree indices over the life of the trees.	219
<b>Figure 7.6.4</b> Comparison of tree indices for sample trees from Luosto created using the SARCS, PBS and Hugershoff methods of standardisation.	220
<b>Figure 7.6.5</b> Comparison of measured sapwood area and calculated sapwood area sorted on ascending final tree diameter for (a) Luosto, (b) Helldalisen, and (c) Rutajarvi.	221

<b>Figure 7.6.6</b> Mean PBS Indices (carbon per unit foliage) for Luosto and Helldalisen (a) by calendar year, (b) signal-free by ring age, and (c) signal-free by diameter.	223
<b>Figure 7.6.7</b> Mean PBS Indices for the Luosto site by calendar year showing (a) slowest and fastest growing trees, (b) youngest and oldest trees, and (c) smallest and largest trees.	226
<b>Figure 7.6.8</b> Mean PBS Indices for the Luosto site by ring age showing (a) slowest and fastest growing trees, (b) youngest and oldest trees, and (c) smallest and largest trees.	227
<b>Figure 7.6.9</b> Fraction values and standard deviations plotted by (a) ring age and (b) calendar year with calculated upper and lower efficiency limits.	228
<b>Figure 7.6.10</b> PBS model and SARCS method chronologies from (a) Luosto and (b) Helldalisen and PBS model chronologies and July temperatures (c) Helldalisen and Bödö, and (d) Luosto and Tornedalen.	230
<b>Figure 7.6.11</b> Chronology indices and their 95% confidence error limits, after smoothing tree indices with a 20-year spline, for (a) Luosto using SARCS method, (b) Luosto using PBS model, (c) Helldalisen using SARCS method, and (d) Helldalisen using PBS model.	231
<b>Figure 7.6.12</b> Comparison of SARCS and PBS chronologies after smoothing with a 20-year spline, for (a) Luosto, Finland and (b) Helldalisen, Norway.	232
<b>Table 7.6.2</b> Statistics comparing tree and chronology indices created using the SARCS and PBS methods and the Luosto and Helldalisen trees.	233
<b>Table 7.6.3</b> Correlations between SARCS and PBS chronologies from Luosto and Helldalisen (Filters using spline with 50% cut-off at 10-years).	233



## **Chapter 1. Introduction**

### **1.1. Climate Change**

The climate system and the biosphere are related by many factors, operating at multiple time scales, and form a complex, dynamic system (Dickinson et al. 1996). The carbon cycle is an important component of both climate and biosphere systems (Schimel et al. 1995). The carbon dioxide content of the atmosphere modifies the absorption of outgoing terrestrial long-wave radiation by the atmosphere, which leads to changes in air temperature. Air temperature controls the exchange of carbon with the oceans, the absorption of carbon by land based vegetation, and the release of carbon from soils. The concentration of carbon dioxide in the atmosphere also has some control on the growth of vegetation (Beerling & Woodward 1996). Anthropogenic effects over recent centuries, related to the release of fossil carbon to the atmosphere and changes in land use, have direct effects on both the biosphere and climate. Natural and/or anthropogenically induced climate changes have the potential to disrupt human society. The need to assess the risk and take action to reduce this risk is the driving force behind a large body of research (Houghton et al. 1990; Houghton 2001). Scientists are developing and refining climate and earth system models to assess and predict the effects of climate change on human society in the 21<sup>st</sup> century. The existence of both positive and negative feedbacks within the climate / earth system leads to quasi-stable states at various time scales. There are lags in the system and it is likely that a truly stable state is never achieved and that continuous change is normal. Ice ages come and go over hundreds of millennia, El-Nino events occur every few years, and the weather can change in days. Knowledge of the role that the biosphere plays in moderating the carbon content of the atmosphere is critical to predictions of climate change (Woodward 1987). Knowledge of past climate is required in order to assess the range of natural variability of the climate system and to evaluate the role of anthropogenically induced changes over recent centuries. Instrumental and historical records of past climate are usually only available for the most recent century, and the inference of meaningful long-term climatic information requires the rigorous interpretation of proxy data (Bradley & Jones 1992; Bradley et al. 2003).

### **1.2. Tree Growth and Climate**

Large proportions of both the carbon exchange between atmosphere and biosphere, and the carbon storage in plants and soil are controlled by the growth of trees. Trees, as living

organisms, are sophisticated entities with the ability, at cell level, to sense their immediate environment and to adjust their growth in response to changes in this environment. Foresters have developed yield tables from the statistics of tree growth measures which can be used to predict tree growth at a site (Hamilton & Christie 1971). Foresters and ecologists have studied the detailed processes involved in tree growth and have also developed sophisticated tree-growth models which can predict the growth of trees and forests (Bonan et al. 1992) in specified environmental conditions (measured or predicted). Tree-growth models are not limited to the prediction of the growth of individual trees in a given climate but, by modelling germination, inter-species competition, and mortality, can develop statistical descriptions of the evolution and changing distribution of forest communities over time (Foley et al. 1998). Wherever tree growth is limited by a climatic variable there is a possibility that tree growth measures can be used to reconstruct some information about past environmental conditions. Pollen, leaves, and tree stems are preserved in the environment by various naturally occurring processes. Inferences can be made about the range of past climate using knowledge of the empirically derived climate tolerance of plant species, stratigraphic and isotopic dating methods, and study of the spatial distribution of sub-fossil remains (Prentice & Webb 1998).

Dendrochronology has developed techniques to date exactly the growth years of some tree stems. Dendroclimatology has developed empirical methods that enable measures taken from exactly-dated wood samples, obtained from living and sub-fossil tree stems, to be used as proxies for various climatic variables. The relationships between tree growth measures and climate variability are used to reconstruct past values of climate variables and these reconstructions are used in the assessment of climate change. The ability to reconstruct past climate using tree growth is based on the assumption of “uniformitarianism”. Specifically this states that the relationship between tree growth and climate forcing has remained unchanged over recent millennia (Briffa et al. 1992a). The dendroclimatic study of the relationship between tree growth measures and climate is mainly empirical; a statistical relationship is sought between instrumental measures of climate variables and measures representing tree growth over a common period and this relationship is used to estimate the values of climatic variables in periods prior to the establishment of climate measurements. Dendroclimatologists use empirical techniques to retrodict the past values of climatic variables from tree growth measures (Fritts 1976c;

Briffa 1995), whilst foresters use process based models to predict tree growth using the values of climatic variables (Botkin et al. 1972).

### **1.3. Long-timescale Variance in Tree Ring Chronologies**

This project is concerned with the identification and interpretation of relatively long-timescale, i.e. multi centennial, climate change as inferred from the annual growth measures of trees. This project arose from the recent emphasis in dendroclimatic research on the reconstruction of long-timescale variability from various tree measures. A large effort is being expended to develop long chronologies of tree growth measures, existing methods of chronology production are being pushed to their limits, and new chronology processing / construction techniques have been introduced in order to establish the long-timescale variance of climatic variables from tree growth measures. Dendroclimatic methods seek to isolate specific climatic information from series of tree growth measures e.g. temperature values from ring width measures in the boreal forest. There are many biological and environmental factors which can exert control over observed tree growth and these produce variance in tree growth measures (noise) which must be removed in order to isolate the variance created by changes in the factor of interest (the climatic signal). Generally only two types of noise, classified by their frequency, are removed from series of measurements. High-frequency noise is removed by averaging the signals from many trees within the process of chronology production. Low-frequency noise, seen as the age-related reduction of ring-width increments in trees, is estimated and removed from each tree explicitly. The term standardisation is used to describe the dendroclimatic methods used to both remove the noise from series of measures and to generate a chronology representing the common variance of tree growth on as long timescales as possible.

The dendroclimatic methods used to isolate the signal of interest from the low-frequency noise impose limits on the timescale at which the variance of interest can be isolated (Briffa et al. 1995). Traditional curve-fitting standardisation methods limit the preservation of long-timescale variance to that of the age of trees (Cook et al. 1995). A recently introduced approach, using the Regional Curve Standardisation (RCS) method (Briffa et al. 1992a), has the ability to preserve longer-timescale variance in the signal of interest from multiple series of tree measures, but the method has specific limitations, most notably by the requirement for large numbers of sub-fossil trees and in the need for

careful sample selection. The problem of isolating long-timescale variance from tree growth measures is one of standardisation and this thesis concentrates on the area of standardisation that estimates and removes the low-frequency noise (age related reduction of ring-width) from series of growth measures.

The need to examine process-based tree-growth models arose as a result of recent findings about apparent changes in the rates of tree growth and in the climate sensitivity of that tree growth across the northern boreal forest (Briffa et al. 1998b). Averaged over large geographic areas, the maximum density and ring width of trees, specially selected because their annual growth is limited primarily by summer warmth, showed a close correlation with summer temperature but the relationship between decadal mean growth and temperature was seen to break down in recent decades. The existence of an unexplained change in the sensitivity of tree growth to climate casts doubt on the assumptions of uniformitarianism, limits confidence in climate reconstructions, and impacts on the investigation of climate change (Briffa et al. 1998b). The ideal of “unambiguously” isolating the long-timescale variance in tree growth is dependent on explaining this “change in sensitivity” issue. The decision was made to explore whether or not the apparent change in sensitivity of tree growth to climatic forcing could be explained by known tree growth processes.

#### **1.4. *The Growth Rate of Trees***

There are a number of measures that can be used to describe the “growth rate” of trees. In dendroclimatology the growth rate of a tree is often considered in terms of the size of ring width measures. In the boreal forest, tree rings are larger for years with warmer summers than for years with colder summers and this empirical relationship between tree growth rates and temperature enables the retrodiction of past summer temperatures. In tree-growth models the growth rate of a tree is considered in terms of the mass of new material added to a tree each year. In the boreal forest, in warmer summers, foliage produces more growth material than in years with colder summers. Newly generated growth material is added to the tree stem leading to climate-related variation in ring-width. In this study the assumption is made that the control of climate on tree growth is on the production rate of foliage and that the relationship between ring-width and climatic forcing is thus indirect. This assumption places some restrictions on the mathematical procedures that can be used to isolate the long-timescale variance found in tree growth

measures. This assumption, of climate control of foliage production rates, leads to a dependency of the age-related reduction in ring-width on the effects of the climatic forcing on tree growth; i.e. the age-related decline of tree growth is modified by the climate controlled-supply of growth material.

### **1.5. This Thesis**

Investigating the “apparent change in sensitivity”, initially an important aspect of this thesis, became a secondary issue because it was found that the magnitude of the effect of the modification of the age-related decline of tree growth by climatic forcing is sufficient to cast doubt on the conclusions concerning a change of sensitivity. This thesis, therefore, concentrates on elucidating and removing the problems within standardisation methods and leaves the establishment (and investigation) of the apparent change in sensitivity of tree growth to climatic forcing to a future study.

The aim of this project is to explore the implications of the use of specific chronology production techniques for the expression of dendroclimatic reconstructions of climate variability at medium and long timescales. This encompasses a study of different methodologies for establishing the growth rates of trees in the Fennoscandian boreal forest. Methods of standardisation will be re-examined, problems identified, and possible improvements developed. In addressing this task a combination of empirical and process-model based approaches will be explored. The intention is to exploit the body of knowledge, relating climate to tree growth, incorporated within existing tree-growth models in order to improve existing dendroclimatic methods. Standardisation methods have been extensively studied in the past and in order to add value to those studies, the alternative definition of tree growth, (i.e. the rate of production of growth material) was adopted in this study. This thesis will concentrate on the aspects of standardisation that relate to the removal of the age-related growth trend in the development of chronologies representing tree growth. Existing standardisation methods will be examined but the objective of isolating long-timescale variance dictates a concentration of effort on resolving problems with the RCS standardisation method. The methods used in process-based tree-growth models lead to the possibility of a novel, process-based standardisation method which will be explored. It is necessary to demonstrate that the sought-after climate signal is contained within the chronologies developed here, and this is achieved using standard, simple calibration / correlation methods.

## 1.6. Structure of this Thesis

Chapter 2 provides background, introduces concepts, defines terms, and describes some relevant aspects of the existing status of dendroclimatic work. The structure of trees and tree rings is discussed along with some mathematical background (Sections 2.1-2.3). Dendroclimatic methods are considered within this study largely as a collection of “black box” procedures. The dendroclimatic procedures that are used in their “unopened” or unmodified state are described briefly, whereas the procedures that are adjusted or replaced as part of this work, such as some standardisation methods, are described in far greater detail (Sections 2.4 - 2.10). The latter part of this Chapter consists of a selected review of the history and current status of methods designed to isolate long-timescale climatic variance from tree measures.

Chapter 3 introduces and describes the data sets used to test and verify the procedures defined and used later. A full description of the collection and measurement of tree cores sampled specifically for this study is provided (Section 3.1). The sources, processing, and characteristics of the temperature measurements that are used in this project are described (Section 3.2). The testing of new standardisation methods and comparison with existing standardisation methods requires the use of chronologies of ring-width measures containing sub-fossil trees. The Tornetrask (Grudd et al. 2002) and Finnish-Lapland (Eronen et al. 2002) tree-ring data bases are the principal data sets used here for this purpose. Background information about these is provided (Section 3.3). Series of simulated tree measures are developed and known signals are superimposed on the ring-width measures of these simulated trees in order to illustrate or evaluate the performance of standardisation methods. These methods of chronology generation and the characteristics of these simulated chronologies are described (Section 3.4).

Chapter 4 starts with a description of the concepts of *growth rates*, *foliage mass* and *expected growth*. (Italicized terms are defined in the relevant sections.) The concept of evaluating expected growth in terms of foliage mass is introduced, its use is justified, and its relationship to existing standardisation methods is explored (Section 4.1). A model formulating the rules, used later to manipulate tree measures, tree indices, and chronology indices, is described. The concept of *fractional deviation* needed to remove a signal from a series of measures and the method of *chronology rotation* are described and defined (Section 4.2). A procedure called *best fit means*, which allows the retention of long-

timescale variance in the absence of known growth rates, is described and some of the characteristics of this procedure are demonstrated (Section 4.3). The problem caused by having long-timescale climate-related variance in ring-width measures when using curve-fitting detrending methods is described and methods of removing this statistical *common signal* from tree measures is explored (Section 4.4).

Chapter 5 is concerned with a re-evaluation of the “Regional Curve Standardisation” (RCS) method of chronology construction. Problems are identified, and adjustments devised to overcome these problems. The implicit use of mean growth rates inherent in the RCS method (Section 5.2) and the potential for bias in resulting indices is demonstrated (Section 5.3). The problem in of using samples from living trees to represent the growth rates of trees over extended periods, described as *modern sample bias*, is introduced and described (Section 5.4). Some problems with the slope of the RCS curve are demonstrated and techniques required to overcome these problems are presented. The frequency characteristics and some aspects of the retention of long-timescale variance by RCS type methods are discussed and explored (Sections 5.5). The new ideas and techniques are used to develop two new refinements of the RCS method: *Multiple Regional Curve Standardisation* (MRCS) method (Section 5.7) and the *Size Adjusted Regional Curve Standardisation* (SARCS) method (Section 5.8).

In Chapter 6, the MRCS, SARCS and RCS methods are compared and discussed with particular attention paid to the “robustness” of generated chronologies. A comparison of the variance in chronologies with the variance in measured temperature data, including simple reconstructions of past summer temperatures, are presented using both the old and new standardisation methods.

Chapter 7 is concerned with the development of a *Process-Based Standardisation* model (PBS). A model is developed using methods extracted from tree-growth models and a full description is given. The chronologies output by this model are compared to chronologies developed earlier and compared to series of temperature measures.

Chapter 8 consists of a summary of the findings of this thesis, a discussion of further developments and final conclusions

## **Chapter 2. Background**

It is necessary to provide some background and introduction to a number of terms that will be encountered in this study. The selection of topics discussed here are of specific relevance to the work undertaken.

### **2.1. Tree Structure**

Trees are complicated and this initial description is simplified to encompass the minimum concept of Structure, Function and Development over Time to a level suitable for this study. A more detailed description of tree structure and functioning can be found in Chapter 7. The structural scheme described here is loosely based on that set out by Mäkelä (Mäkelä & Hari 1986; Mäkelä 1997) which relates to *Pinus sylvestris* but will apply to most conifers. A tree is considered to consist of compartments of fine roots, trunk roots, stem, branches, bark, foliage and reproductive organs. The foliage and fine roots are active organs which extract material from the external environment. The stem, branches and trunk roots give the tree shape, and form a structural support mechanism for the active organs. The outer parts of this support structure are made of living cells (sapwood) which provide the tree with a storage and internal transport mechanism, while the inner part of this structure consists of enclosed dead cells (heartwood). The stem, branches and trunk roots are covered by a protective layer of bark. The crown is that part of the tree containing branches and foliage, below which there is a bare stem connected to the root system. The canopy is a continuous system of branches and foliage created where trees grow in close proximity.

The cambium is a thin layer of cells situated behind the bark and the cambium forms a sheath surrounding the tree. Growth takes place at the cambium, with inner growth providing new sapwood for the stem, branches and trunk roots, and outer growth providing bark, foliage, fine roots and reproductive organs. Trunk roots provide structural support, anchoring the tree securely to the ground and forming a support and distribution mechanism which allows fine roots to access various sections of the soil. Trunk roots develop over the life of the tree but also adapt over multi-annual periods to the ongoing support and nutrient requirements of the tree by the growth of new trunk roots and the loss of any existing trunk roots which are not required. The stem of the tree provides structural support for branches. Stem growth takes place at the cambium layer over the life of a tree and growth is limited, with the exception of daily hydration cycles and



physical damage repair, to increase in height and increase in radial diameter. The branches provide a support and distribution mechanism to allow foliage to access light. Branches develop over the life of the tree from active nodes in the stem. Branches will be lost when no longer needed to support foliage (Mäkelä 1997). Foliage consists of individual leaves containing stomata which control the absorption of carbon from the atmosphere (via photosynthesis). Foliage is distributed to intercept light (photosynthetically active light or PAR). In conifers, leaves (needles) may be active from one to a few years (Nikinmaa 1990) after which they are lost by a process called senescence. Fine roots absorb water and nutrients from the soil and in *Pinus sylvestris* can be grown, used, and senesced over monthly to annual time scales (Mäkelä & Vanninen 2000). Fine roots can adapt to changing soil conditions at sub-annual timescales. The fine roots of many tree species will not operate below the water table and a high water table can produce considerable restrictions in tree growth (Nicoll & Ray 1996) and may lead to tree mortality. Bark is grown as a layer of protection around the cambium and has a life span of years to decades. Bark is lost from the outside and requires continuous growth to cover a steadily increasing surface area. In the event of damage to an area of cambium, growth proceeds from the adjacent healthy cambium and both bark and sapwood will grow over and around the area of damage.

## **2.2. Tree Rings**

The science of dendrochronology stems from the existence of radial tree rings and the ability to use tree rings to date the wood in tree stems exactly. The growth of the woody parts of a tree (stem, branches and trunk roots) takes place at the cambium by adding layers of cells to the sapwood surface. Many species of trees have periods of growth and dormancy and this cyclic activity can produce distinct layers of two types of cells. In conifers, layers of relatively large, thin-walled cells (earlywood) are laid down early in the growing season and layers of cells which are narrower and have thicker walls (latewood) are laid down later in the growing season, prior to the dormancy period (Schweingruber 1996a). The anatomical and colour contrast between these layers can be seen in a stem cross section as a series of concentric tree rings. In areas that experience strong and regular contrasts in seasonal climate, rings are formed annually (Fritts 1976b). The radial width of the rings seen in a cross section can vary. Comparison of series of rings from different trees at a site often shows some measure of consistency in relative growth levels in some calendar years; wider rings in high growth years and narrower

rings in poor growth years. The pattern formed over time by the different relative sizes of ring width in each year, particularly in trees from the same site, can be matched from tree to tree. The visual matching of tree rings along with some statistical analysis allow dendrochronologists to eliminate any dating errors and produce series of ring-width measures which are exactly dated relative to each other. In the presence of a link to a calendar date, the “crossdating” of ring width measures enables the calendar date of each growth ring to be determined (Stokes & Smiley 1968). The consistent variation of ring width common to particular calendar years suggests the existence of one or more underlying growth forcing mechanisms exerting a variable influence from year to year. A series of values representing the magnitude of this net common forcing of tree growth over time is described as a chronology. The ability to crossdate living tree ring records and those from sub-fossil material, in some situations spanning many millennia, demonstrates the continued existence of such common forcing over long periods.

### **2.3. Time Series**

Some specialised statistical terms are commonly used when describing the processing of tree measures and these need to be introduced. The terms *mean*, *variance*, *standard deviation*, *normalisation* and *correlation* all have standard, mathematically-defined meanings (Mendenhall et al. 1990). A dated sequence of ring measurements forms a time series with a value for each calendar year. A chronology is a single time series of indices produced by combining the data from many trees. The variance of a series of measurements is a measure of the dispersion or variation from the arithmetic mean of the series. The variance can be considered at different frequencies. **In this study, variance at periods over a century and beyond the lifespan of a tree is referred to as low-frequency, variance from decades to half the lifespan of a tree is referred to as medium-frequency, and variance at periods of about a decade or less is referred to as high-frequency.** Inter-annual variance is the year-to-year change of value.

Trend is the average rate of change in the mean values of the series over some specified period. If the mean value of the first half of a series differs markedly from the mean value of the second half of the series, the series will exhibit a trend referred to as a *life-span* trend in this text. In processing time series, it is often convenient to describe the underlying trend, to explicitly define the variance, and to remove the variance of a specified frequency range. The removal of variance in a specified frequency range is

called filtering, and methods of filtering involving subtraction or division are used in dendroclimatology. A simple method of smoothing is the running mean, where each value is replaced by the local mean value, resulting in a series with gradually changing values and the removal of high-frequency variance, a process described as a "low-pass filtering". The subtraction of (or division by) low-pass filtered values from the original values removes the low-frequency variance leaving the high-frequency variance, a process described as a "high-pass filtering".

Many series of measurements are represented as absolute units, such as mms for ring widths, kilograms per cubic metre for wood density, and degrees Celsius for temperature. However it can often be convenient to convert a series of measurements into a series of dimensionless indices, simply a relative value for each year, which can be manipulated for comparison purposes. A series of indices with a roughly normal distribution can be *normalised*, or scaled so that the series have zero mean and unit standard deviation.

#### **2.4. Dendroclimatology**

The study of the annual growth of trees and the subsequent assembly of long, continuous chronologies for use in dating wood is called dendrochronology. The study of the relationships between the annual growth of trees and climate is called dendroclimatology which is a specialised area of study within the science of dendrochronology (Fritts 1976c). Dendroclimatology is an empirical science based on observed relationships. The fact that series of ring widths may, in certain situations, be dated accurately has led to the development of dendrochronology, through the establishment of sets of common procedures and methods. These enable the use of tree growth to study various aspects of the past. Dendrochronologists have developed techniques for sample selection, preparation, measurement, crossdating, and the development of chronologies of different growth indices. Dendrochronologists have developed chronologies of tree growth measurements from living and sub-fossil trees in many areas of the world and for extended periods in the Holocene to date events such as archaeological habitation, forest fires, earthquakes, volcanic eruptions and floods (Schweingruber 1988; Swetnam et al. 1999). Worldwide organisations have been established to enable cooperation among scientists and to promote the development of dendrochronology. The work of these organisations has led to the establishment of standards for data storage, the development of training courses, and the running of regular international conferences. Widely used

computer programs for data manipulation, bibliographies, and large databases of tree growth measures have been made freely available from dedicated internet sites (Grissinomayer & Fritts 1997). Dendroclimatologists use a subset of dendrochronological techniques and have developed methods of sampling, standardisation, and other data analysis specifically to study past climate. A detailed description of the dendroclimatic methods for sampling trees and measuring wood are given in (Fritts 1976a), (Cook & Kairiukstis 1990) and (Schweingruber 1996b).

## **2.5. Standardisation**

### **2.5.1. Introduction**

Standardisation is the name given to the process by which series of ring measurements are converted into a series of chronology indices which represent the magnitude of the annually-varying “common” forcing on tree growth (Cook et al. 1990). Standardisation is a large subject area and it is necessary to limit the scope of the description given here. The focus of this project is on long-timescale variability: the effects on its expression in ring-width chronologies and the extent to which it reliably represents the influence of changing temperatures in northern Fennoscandia. Two types of standardisation methods are distinguished here by whether they can or cannot represent variance at timescales beyond the length of individual tree-ring records to which they are applied. Those that cannot are generally based on “curve-fitting” techniques. The variance represented by curves fitted through the measurement series from individual trees is removed. Those methods that can represent variance at timescales beyond that of the length of individual trees in a chronology can be referred to as “Regional Curve Standardisation” methods because a regional growth curve is used on all trees. Fitting a horizontal line, the mean of a series of measurements, can preserve variance to the length of the series and is a special case of curve-fitting while fitting the same horizontal line to all series, which can preserve variance beyond the lengths of individual series, is a special case of the RCS method. The Ageband Decomposition (Briffa et al. 2001) method is a special case of the RCS method in which tree measures are averaged by ring age class and division is used to create series of indices for each ring age class instead of for each individual tree.

The “traditional” standardisation methods are based on “curve-fitting” and a general description of these methods is presented to introduce the concepts behind standardisation. In this study, specific differences between the various “curve-fitting”

options are not considered important and only a representative description of estimating age-related growth curves is included. Here the Hugeshoff method (Warren 1980) is selected as a general example of these curve-fitting methods and its implementation is described in detail. The long timescale variance limitations of curve-fitting methods are discussed in the specific context of how these problems are addressed in this study. The RCS method (Briffa et al. 1992a) was re-introduced in order to extend the timescales at which low-frequency variance can be identified and this method is described in detail. The ideas behind the use of regional growth curves, the commonly used implementation, and some associated problems are described. There is no generally accepted “theoretical” limit to the isolation of long timescale variance when using the RCS method (Cook et al. 1995) so discussion of the low-frequency characteristics of the RCS method is left to Chapter 5 where specific implementations of the method are considered in detail.

### 2.5.2. Curve-fitting Standardisation Methods

Series of ring-width measurements can be considered as an aggregation of several signals and the process of standardisation is one of disaggregation (Cook et al. 1990). Unwanted signals are considered as noise which must be removed by standardisation in order to isolate the common signal that is required. This noise is usually separated into high-frequency noise and low-frequency noise simply because each can be removed by separate processes. Medium-frequency noise, such as generated by competition between trees over periods of decades, is not separately removed. High-frequency noise common to a proportion of trees, such as generated by insect attacks, is not separately removed. Both these effects can be mitigated in the averaging process by increasing sample depth / sizes. In this thesis the “noise” generated by the year-to-year persistence in tree growth rates (autocorrelation) and the specific methods developed to remove this noise (Cook 1985) are ignored.

Events such as lightning strikes, insect attacks, and local competition cause variations in the ring-width of individual trees in specific years. These variations are not common to all trees, are not wanted by dendroclimatologists, and are considered high-frequency noise. High-frequency noise in series of tree indices is minimised in the chronology by averaging all the tree index values for each calendar year. Early workers "*identified long-term growth trends in measured ring-width data that could confidently be attributed solely to tree aging*" (Cook et al. 1990, p104). In trees with radial growth this trend over

the life of a tree is seen in most trees, irrespective of the period in which the tree grew. In open canopy conifers, if high-frequency variations are ignored, then a series of ring width measurements usually starts with small values which increase to a peak in the first few years (usually less than a decade as in Figure 5.6.1), after which there is a steady decay in ring-width as the tree ages. The change of size of ring-width over the life of a tree is described as the age-related growth trend and because it is not common to calendar years this “signal” is not wanted and is considered as low-frequency noise.

The common forcing signal (along with random noise) appears to be superimposed on the generally larger-magnitude, age-related growth trend of each tree (Briffa et al. 1996). The variance in the tree measures due to the common forcing is generally proportional to the local mean of the measured ring-width series (Cook et al. 1990) which is consistent with the presumption that the common forcing for each year has a similar “fractional deviation” effect on each tree. Treating the common forcing as a fractional deviation has the effect of adjusting each series of tree indices for the differential growth rates of trees (Cook et al. 1990). The value of a tree index (ignoring high-frequency noise) is a fractional deviation and the value of the age-related growth trend for a specific year is a prediction of the amount of growth that would have occurred if the common forcing was constant (at the average rate) over the life of the tree. The age-related growth curve is often referred to as the “expected growth curve” because this is the value of growth, for each ring age, expected in an average growth year and is also (by definition) the value of growth that will produce a tree index value of 1.0. The age-related growth trend forms an estimate of the local mean of a measured ring-width series and a series of tree indices which are fractional deviations can be produced by dividing the measured ring-width values by the estimated expected growth values. The division of measured values by the expected growth curve, results in series of tree indices which are stationary, i.e. relative tree-ring indices with a mean of 1.0 and a relatively constant variance (Cook 1985) and are in a suitable state to be averaged to form a series of chronology indices. A bias problem can occur with the division process if expected growth values approach zero (Cook & Peters 1997) and care is needed.

Curve-fitting standardisation methods thus comprise a sequence of steps:

1. Estimate the age-related growth curve for each tree.

2. Remove the age-related growth curve values from the measures, so creating tree indices.
3. Adjust the series of tree indices for the differential growth rates of trees by resetting means and variances.
4. Average tree indices for each year to minimise *high-frequency* noise and create chronology indices.

Steps 2 and 3 can be achieved (with varying degrees of success) in one process by dividing measured values by expected growth values (Cook et al. 1990). Step 4 is straight-forward, leaving step 1 to be explained further.

### 2.5.3. Estimating the age-related growth curve

The process of estimating and removing the age-related growth curve from a tree is often called detrending. (The standardisation of a chronology involves detrending each series of measures.) There is no generally accepted method of defining the shape of the age-related growth trend, observed in radial ring width measurements, which has led to the pragmatic approach of fitting linear or simple curvilinear functions to each series of measures to represent estimates of the age-related growth trend (Briffa et al. 1996). Early workers fitted a smooth curve by eye to a graphical plot of tree measures (Douglass 1914). Measures were divided by the values of the fitted curve to create series of tree indices and the tree indices were averaged by calendar year to create chronology indices. These procedures were subsequently implemented on computers using mathematical functions to describe expected growth curves whose variance was removed from measurement series automatically by software that operated without any degree of subjectivity. Deterministic methods fit linear or curvilinear mathematical functions to each series of tree measures using least squares methods. The term “curve-fitting” is used here as a general description of methods of generating expected growth curves by fitting values to the series of measures of an individual tree; and this includes fitting by eye, least squares methods, and deterministic methods.

The traditional curve-fitting by eye can be used in conjunction with, or sometimes is replaced by, a hierarchical sequence of mathematical functions such as in program INDEXA (Fritts et al. 1969) where different functions are tried until a “fitting” curve is found. Stochastic or data-adaptive methods of curve-fitting use low-pass digital filtering (Briffa 1984) or cubic smoothing splines (Cook & Peters 1981) to estimate the age-

related growth curve for each tree. The choice of which method of detrending to use for a chronology is based on the known characteristics of the method, the low-frequency characteristics of the signal being sought, and previous experience with the tree species and locations concerned. The choice of curve used for each individual tree is based on how well the selected method or hierarchy of alternatives fits that specific tree.

#### 2.5.4. Hugershoff Method of Standardisation

A description of a typical curve-fitting method of standardisation is included here for illustration purposes. The Hugershoff curve standardisation method (Warren 1980) is selected because it has been used for widespread temperature reconstruction (Briffa et al. 2002) of ring-width chronologies and is used later in this study (Section 4.4). The implementation methods described were originally encapsulated in the INDEXA (Fritts et al. 1969) program and implementation of the Hugershoff method was subsequently incorporated into the widely used ARSTND (Cook 1985) program. In this implementation, indices are produced by the division of measured values by values derived from the fitted curves and the arithmetic means of tree indices for each year are used as chronology indices. For each series of measurements, this method generates an expected growth curve chosen after successive attempts to fit one of a number of curves from a hierarchy of *a priori* defined mathematical models of radial growth using the method of least squares. The hierarchy of mathematical models used in this study is shown below in the sequence used, where function  $G(t)$  is the expected growth curve value over time,  $T$  is time, and  $A$ ,  $B$  and  $C$  are positive constants.

$$G(t) = A * T^B * EXP(- C * T) \quad (\text{HUG})$$

$$G(t) = A + B * EXP(- C * T) \quad (\text{EXP})$$

$$G(t) = A + (-B) * T \quad (\text{LINE})$$

$$G(t) = A \quad (\text{MEAN})$$

HUG fits the generalised exponential or "Hugershoff" function (Warren 1980). EXP fits a modified negative exponential curve (Fritts et al. 1969). LINE fits a negatively sloping linear trend line. MEAN fits a horizontal line through the mean. Ring widths in the early years (first decade) of some trees often start small, rise to a peak, and then decline. The Hugershoff curve may be able to follow this growth pattern (Figure 2.5.1a). Series of ring width measures from open-grown conifers tend to decay over time leading to the use of a negative exponential curve to model this decay (Figure 2.5.1b). Ring width values do not decay to zero but tend to a small roughly constant value which is modelled by adding a



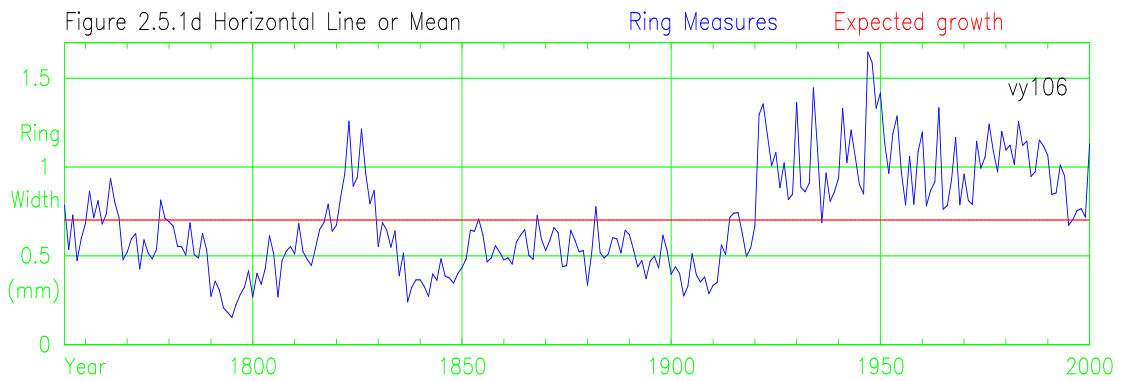
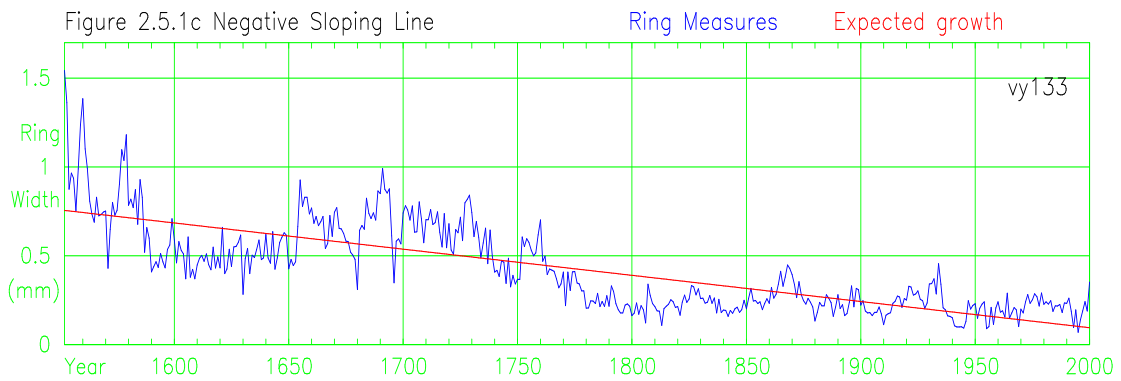
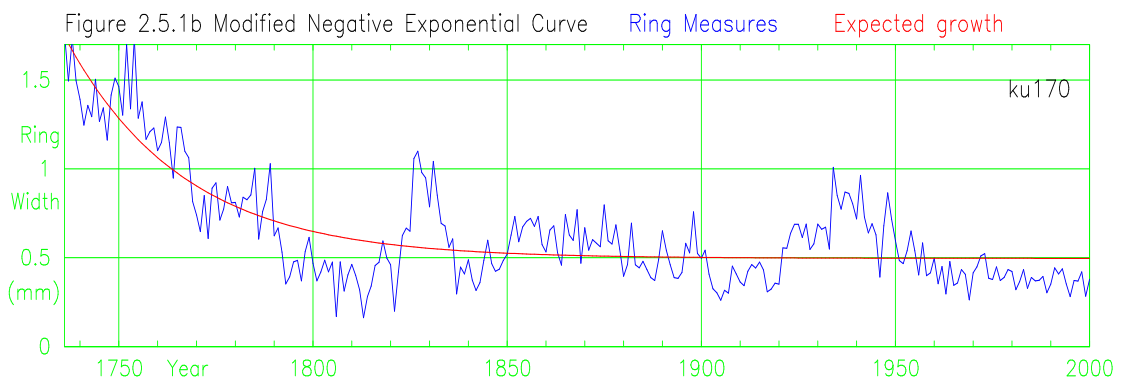
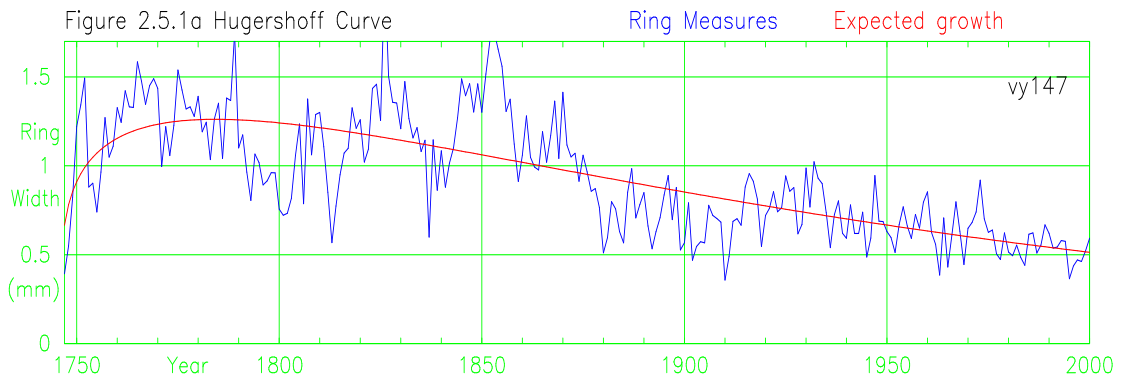


Figure 2.5.1 Sample trees from Luosto, Finland showing ring width and expected growth curves generated using (a) Hugerhoff curve, (b) Modified Negative Exponential Curve, (c) Negative Sloping Line, and (d) Horizontal Line

constant to the negative exponential curve (Fritts et al. 1969). Some series of ring measures, especially from trees growing in closed canopies and trees sampled before they reach old age, do not always show a decay in ring width and series of ring-width measures do not follow decaying curves (Hugershoff or negative exponential) and are modelled using a straight lines. The a priori assumption is often made that expected ring widths will not increase steadily as a tree approaches old age and thus the slope of the fitted line is constrained to be negative (LINE) (Fig 2.5.1c). If the best fit straight line has a positive slope then this is replaced by a horizontal line (MEAN) (Figure 2.5.1d). All values of expected growth must be positive because tree growth is positive and any generated expected growth curve which goes negative will be rejected. Where values of the expected growth curve approach zero then the division method used to create indices can produce excessively large values (Cook & Peters 1997), and in this case the fitted curve is usually rejected. The decision of acceptance or rejection of the fitted expected growth curve is subjective, is made by examining graphical plots of ring measures and expected values, and can lead to the rejection of some trees from the chronology.

#### 2.5.5. Long-timescale Variance using Curve-fitting Methods

A problem arises because the mean value of each series of indices must be approximately 1.0 when produced using curve-fitting detrending methods (Cook et al. 1990). Trees that spent their life in periods favourable to growth will have the same “mean value of indices” as trees that grew in a periods unfavourable to growth. If series of tree indices are averaged to form a long chronology there will be no way to distinguish past periods of good and bad climatic conditions at timescales beyond the life span of individual trees (Cook et al. 1995), a part of the problem described as the “segment length curse”.

Another problem further reduces the long timescale variance limit obtained by curve-fitting methods. This is that series of tree indices will not have a significant overall trend even within their life span (Cook et al. 1995). If a sloping straight line, fitted by the least squares method, is used to detrend a series of tree measures, the indices created by division will have no slope. Other curve-fitting standardisation methods may leave a small slope, but the mean value of the first half of the index series will be approximately equal to the mean value of the second half of the index series, indicating no possibility of any significant overall slope. It should be noted that a horizontal straight line, the mean of a series of measures, is not “fitted” to the slope and this standardisation curve may leave

an overall trend. The practical long timescale limit in the retention of variance by these least squares fitting methods must be the length of a tree or less (Cook et al. 1995).

Mixing different age (length) trees can reduce the retention of low-frequency variance even further. A 400-year long series of tree-indices may contain a 100-year period with the mean value of tree indices above/below 1.0 and with the tree indices having some slope over this sub-period. If this 100-year period of indices is averaged with indices from a 100-year long tree (with zero slope and mean of 1.0) then the magnitude of the mean series (relative to the mean of 1.0) and the slope will both be reduced by half over this sub-period. The retention of low-frequency variance in a chronology is thus limited by the lengths of the shortest trees (Cook & Peters 1981). For long chronologies, created by overlapping sub-fossil trees using curve-fitting methods, the amount of low-frequency variance will vary with the mean age of trees at each point in time. The amount of low-frequency variance can be controlled using data adaptive curve-fitting methods such as smoothing splines (Cook & Peters 1981) but these methods limit the maximum period of low-frequency throughout. The limits in the resolution of long-timescale variance when using curve-fitting standardisation methods are a serious problem in the retrodiction of climatic variables. To reduce this problem some chronologies have been built using only the oldest trees available (LaMarche 1974b; Stahle et al. 1988). For this study the low-frequency problems are simplified to considering the mean value of series of tree indices, the slope of series of tree indices, and methods of diminishing the “dilution” effect on long-timescale variance of averaging together trees of varying age.

#### 2.5.6. Regional Curve based Standardisation Method

Trees are expected to grow faster in periods when the common forcing signal is favourable to tree growth than in periods when the common forcing signal is unfavourable to tree growth. A comparison of measured tree growth rates during the two periods would enable the relative magnitude of the common forcing signal to be estimated. Curve-fitting methods remove the slope from each series of measures because the slope of the expected growth curve is the same as the slope of the series of measures (Cook et al. 1995). In order to preserve an overall trend (life-span trend) in a series of tree indices, the slope of the expected growth curve must be estimated independently of the series of measures.

One proposal to solve these problems was to use a curve of the mean growth by ring age to remove "the mean change in ring width associated with biological factors related to increasing age" (Mitchell 1967). Use of the curve of mean growth by ring age to provide expected growth curves for all trees (Becker 1989) was reintroduced to dendroclimatology under the name Regional Curve Standardisation (RCS) (Briffa et al. 1992a) and the term RCS curve is used to describe the curve of expected mean growth by ring age. The value of the expected growth curve is set by the average value, for all trees from a site or region, of ring width for a specific ring age. The magnitudes of tree indices (created by division) are thus set relative to the "average" magnitude for rings of that ring age. Series of tree indices can have an overall trend, the means of series of tree indices can vary, and the resulting chronology, created as the arithmetic mean of tree indices, can have long timescale variance at periods up to the length of the chronology or beyond (Cook et al. 1995). There is a cost to this dramatic potential improvement in the isolation of long timescale variance, but before exploring this further, a description of the method is first provided.

#### 2.5.7. RCS Method

The difference between the RCS method and curve-fitting methods lies in the way the age-related growth curves are generated. The RCS approach to chronology construction for a site consists of a sequence: creating an RCS curve; detrending individual trees with this curve (creating series of tree indices by division); and averaging the tree indices to produce a chronology (Briffa et al. 1992a; Esper et al. 2002; Cook et al. 2002). Where estimates of the number of missing years to the centre of the tree (pith) are available these are used to establish ring age and in the absence of estimates the first ring of each tree is assumed to have a ring age of one (Briffa et al. 1992a; Esper et al. 2003). Ring widths are aligned by ring age (years from pith) and the arithmetic means of ring width for each ring age are calculated. The curve created from the mean of ring width for each ring age is smoothed using a suitable mathematical smoothing function (Briffa et al. 1996) to create smoothly varying RCS curve values for each ring age. Each ring measure is divided by the RCS curve value for the appropriate ring age to create a tree index value. The chronology indices are created as the arithmetic mean of tree indices for each calendar year.

### 2.5.8. RCS Method Restrictions

This method retains low-frequency variance which is **unrelated** to the common forcing signal being sought, as pointed out by Fritts (1976a, p280) "*However, all individuals of a species rarely attain optimum growth at the same age, and individual trees differ in their growth rates because of differences in soil factors, competition, microclimate and other factors governing the productivity of a site.*". The solution to the problem of non-climate related variation in the overall growth rates of trees when using **curve-fitting** methods of standardisation is to reset the means of series of tree indices to similar values or to rescale, as described by Briffa et al. (1996) "*Besides removing the age trend, the rescaling is generally justified on the grounds that it allows data from trees with different overall growth rates (assumed to be the result of intra-site-related differences) to be averaged without biasing the chronology.*" This rescaling is not available when using the RCS method and the problem of bias caused by differences in the overall growth rates of trees within the same region remains. The effects of this problem are reduced by having greater replication (Briffa et al. 1992a) and the resulting greater uncertainty is considered an acceptable cost (Briffa et al. 1996) for the gain in preservation of low-frequency variance.

The variation in tree growth rates that is not common to all trees increases the number of samples required to estimate the mean value function accurately (Briffa et al. 1996). When using curve-fitting methods, the tree index (fractional deviation) is a measure of the effect of common forcing on that tree. In the RCS method, the tree index is a measure of the fractional deviation of the growth of that tree from the average rate of growth of all trees for that ring age. In the RCS method, the mean and variance of each series of tree indices will be greater for fast growing trees (above average ring sizes) than for slow growing trees and as a consequence fast growing trees will make a larger contribution to the chronology than slow growing trees. Methods are available to "correct" this problem, such as by creating indices as differences and resetting means and variances (Cook 1990).

Another problem is that medium-frequency variance of the common forcing signal could distort the shape of the RCS curve (Briffa et al. 1992a; Briffa et al. 1996). The solution to this problem is to have large numbers of sub-fossil trees from a variety of time periods to "dilute" the effects of contemporaneous common forcing on the RCS curve, especially with respect to the modern era where tree growth may be systematically rising in

response to climate change (Briffa et al. 2002). This requirement restricts the use of the RCS method when using ring-width measures to a handful of sites. Exceptions to this restriction have been made when using maximum latewood density (Briffa et al. 1998a) or using ring-width in conjunction with an RCS type of method called Ageband Decomposition (Briffa et al. 2001). Another problem is that the exact ring age of many wood samples may not be known and this could introduce error into the RCS method (Briffa et al. 1992a; Esper et al. 2003). The magnitude of this effect does not appear to be large and the recommended solution is to use the wood samples themselves to estimate the numbers of missing rings between the first ring and the pith.

## **2.6. Summary**

This section has given a brief introduction to dendroclimatology and standardisation. The problem area, of estimating and removing the medium-frequency age-related growth trend, has been discussed in some detail. There is no consensus among dendroclimatologists as to a definitively best method of processing tree measures in order to express the low-frequency variance found in tree growth. A number of different methods and derivatives / options have been tested and tried, and RCS-based methods have the potential to succeed but suffer from a number of problems. It is from this background that the thesis proceeds and attempts to resolve some of the problems. The starting position is to assemble some sets of well replicated ring-width measures with which to test and demonstrate these problems. The next stage is to use knowledge gained from tree-growth models to examine dendroclimatic methods from an alternative viewpoint and use the findings to direct this research to problem areas.

## **Chapter 3. Chronologies and Meteorological Data**

### **3.1. Introduction**

Data collection is a compromise between ideal requirements, the availability of existing data, and the practical ability to collect and measure new data. Data collection generally takes place near the start of a project and must allow for the possibility that project objectives may evolve. The initial objectives of this thesis included a detailed examination of the apparent change in sensitivity of tree-growth to climate (Briffa et al. 1998a), an investigation of the ability of standardisation methods to express multi-centennial variance in tree growth measures, and an investigation of tree-growth models. The study area was limited to the Fennoscandian boreal forest. Long sub-fossil chronologies of tree-ring data from the Advance 10K project (Briffa & Matthews 2002) were available for multi-century investigations. In order to examine the character of recent temperature change in the longer-term context, data are required that includes tree measures representing the most recent decades. Some measures, not normally available in dendroclimatic samples, are required for validating tree-growth model assumptions. Both of these requirements led to the need to obtain new sets of tree measurements. The availability of meteorological data dictated the choice of sampling sites. The collection of tree growth data requires the establishment of a sampling strategy and subsequent collection and measurement of samples (Schweingruber et al. 1990). For planning purposes, the sequence followed was to decide which data were required, where these data should be taken from, how the data would be collected, and finally what processing of raw data would be required. A number of additional measures were taken that might have been needed but were not subsequently used. These are mentioned below because this data may be of value to others.

### **3.2. Choosing Sites, Data and Samples**

#### **3.2.1. Site Selection**

The study area is constrained to the Fennoscandian boreal forest and the location map, Figure 3.2.1, shows the relative positions of the meteorological sites and tree core sampling regions. The two northern Fennoscandian sub-fossil chronologies from the Advance 10K project; Tornetrask (Grudd et al. 2002) and Finnish-Lapland (Eronen et al. 2002) were selected. The selection of a suitable species was influenced by availability, distribution and, most importantly, the species of the Tornetrask and Finnish-Lapland

chronologies. *Pinus sylvestris* was the chosen species. Climate data are measured regularly in the region and recent data are available for many areas of northern Europe. A decision was made to select regions for tree sampling where long series of daily meteorological observations were available, to allow the investigation of variation in the start of the growing season and its length in relation to tree growth. A precursor project to this thesis produced a chronology of samples from Helldalisen, west Norway which is

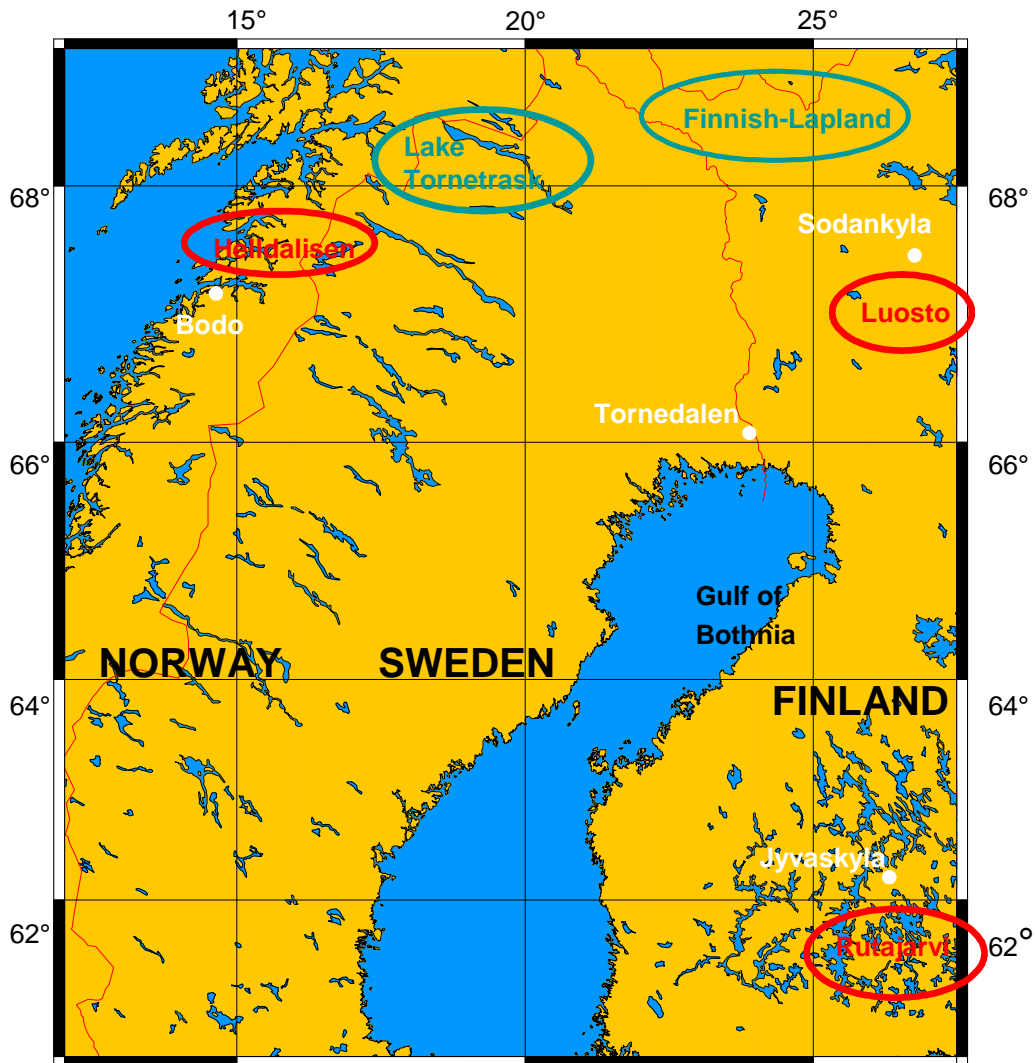


Figure 3.2.1 Location map showing meteorological stations (white), sub-fossil tree regions (green), and “modern” tree regions (red).

close to Böö, a meteorological site with a long record of measurements. The tree cores from the Helldalisen region were chosen as suitable for use in this study. The observation of a north/south variation in the sensitivity of tree growth to climatic forcing (Briffa et al. 1998b) led to a requirement for samples from both northern and southern regions to



enable analysis of the differences. Sodankyla in north Finland and Jyväskylä in south Finland were the selected meteorological stations from which long series of daily meteorological data were available. Luosto in north Finland and Rutajarvi in south Finland were selected as suitable sampling regions close to the locations of the Sodankyla and Jyväskylä meteorological stations.

### 3.2.2. Data and Sample Selection

Meteorological data consist of a series of instrumental measurements taken at regular intervals from a number of measuring devices installed at a site for that specific purpose. Temperature has been shown to constrain tree growth in the Fennoscandian boreal forest (Briffa et al. 1990; Lindholm & Eronen 2000) and mean monthly temperature data were selected for use within this project.

The observation that young trees appear to be growing faster (Briffa & Osborn 1999) than older ones leads to the need to be able to create separate chronologies from trees of different ages or size classes for the same region. Sufficient sampling of different age classes enables the comparison of results by tree age or size. Local site conditions, such as aspect and slope, can create common variance in tree growth which may not represent the wider region. To reduce the effects of local site variation, regions of a few tens of kilometres in diameter were selected, and samples were taken from a number of sites within these regions. To develop chronologies of trees from several sites representing a wider region, at least 30 trees (Schweingruber et al. 1990) are considered suitable. To develop and compare three such chronologies (e.g. young, medium, and old tree chronologies) from a region leads to the need for samples from 90 trees in each region. The practicalities of extraction and measurement limited the number of such additional regions that could be sampled within this thesis to two.

The strongest relationship between tree growth and temperature is seen in open grown, temperature-stressed trees from the tree line (Pilcher 1990). The tree line is a small proportion of the boreal forest and “typical” samples are from closed canopy trees away from the tree line. When using closed canopy trees for the reconstruction of past climate, it is normal to select dominant and co-dominant trees to reduce the effects of competition (Pilcher 1990). In naturally grown, uneven-aged stands, dominance is not achieved until trees are quite large. The requirement to screen out tree age requires the use of naturally

grown, uneven-age stands. The ninety samples from each area need to contain sufficient trees to develop separate “dominant” chronologies if necessary.

The improvement of management practices is the main factor responsible for “*an increase of more than 40% in forest volume growth*” (Mielikainen & Timonen 1996) in southern Finland. A large proportion of tree growth in the boreal forest has been managed over the last century and the decision was made to select samples from locations that showed few signs of recent management in order to avoid the additional effects on tree growth created by management practices. The requirement to consider remote centuries was to be met using sub-fossil chronologies so it was decided to extract all new samples from living trees. Variability in tree radii leads to the recommendation that two cores should be taken from each tree (Pilcher 1990). The need to minimise damage to the trees sampled in this study led to sampling trees of roughly 20cm diameter and above. The planned use of process-based models led to a need to obtain some measurements for validation purposes. The decision was made to estimate tree height and crown height in the year of sampling to allow testing of empirical parameter values in the process based standardisation model (Chapter 7). Distance to nearest neighbour and compass bearing of each tree core were also recorded but were not used in this study.

### 3.3. Source and Processing of Data

#### 3.3.1. Meteorological Data

	Sodankyla	Bödö	Tornedalen
Mean monthly temperature	1908-2000	1868-2000	1816-2002

Table 3.3.1 Meteorological data, site names and calendar ranges.

Instrumental meteorological data are available but there is a need to ensure consistency over the selected temporal and spatial range. Instrumental meteorological data, local to the chosen sampling regions, were obtained from the Finnish and Norwegian Meteorological Services (FMI and DNMI) and extracted from the NORDKLIM data set (Tuomenvirta 2001). The mean monthly temperature data in NORDKLIM had been converted to absolute values by adjustments for changes of equipment, changes of measurement methods, and site location moves over the period of measurement. Missing data entries had been inserted (Tuomenvirta 2001). During the project a long Swedish series of temperature measurements from Tornedalen (Klingbjer & Moberg 2003)

became available. The year 1815 was missing from the Tornedalen data and because of this only data from 1816 and later are utilised. These data from Bödö, Sodankyla and Tornedalen are used in this study without adjustment.

### 3.3.2. Sub-Fossil Chronologies

The isolation of long timescale variance, i.e. longer than the lengths of individual trees, requires long chronologies, necessarily containing sub-fossil trees. In order to test the low-frequency characteristics of the RCS method and some of the “refinements” developed later in this project, data from two sub-fossil chronologies of *Pinus sylvestris*, both from northern Fennoscandia, are used: the Tornetrask chronology (Grudd et al. 2002) from north Sweden and the Finnish-Lapland chronology (Eronen et al. 2002) from Finnish Lapland. The regions from which trees were taken to build these chronologies are shown in Figure 3.2.1. The sub-fossil trees came mainly from small lakes along with some more recent trees surviving as surface wood remnants. Samples from living trees make up the modern portion of both chronologies. Tree and ring age may not be accurate for the sub-fossil chronologies, because estimates of missing wood to the centre of these trees were not used in this study and wood will have been lost from some trees. Data over the last two millennia from these chronologies are used to test the fidelity of standardisation methods in preserving long timescale variance and the two data sets / chronologies are called the Tornetrask AD and Finnish-Lapland AD chronologies. Data from the earlier sections of these chronologies (the BC period), along with more recent data, are used to examine some characteristics of tree growth.

### 3.3.3. Tree Core Sampling

Luosto in north Finland and Rutajarvi were the chosen sampling regions in Finland. Permission to extract cores from trees in public managed forests was obtained from the local Metshallitus offices, which also provided advice and maps showing suitable sampling locations. Locations were examined within 50kms of the meteorological sites (Sodankyla and Jyväskylä) and those selected as sampling sites are briefly described in Table. 3.3.2. Location names, altitudes and grid references were extracted from maps. The Finnish cores were sampled in June 2001. Trees of apparently varying age and social status were selected but generally with diameter greater than 20cm. Two cores were taken from each tree, in directions separated by approximately ninety degrees, in order to eliminate some of the variability found in individual cores (Pilcher 1990). Cores were taken at breast height. Estimates were made of tree height, the height to crown base, and

the distance to nearest neighbour or large stump. The magnetic direction of each sample core taken was measured using a compass. Angles were measured to the nearest 10°, heights to  $\pm 3\text{m}$  and distances to  $\pm 1\text{m}$ . The objective to obtain many samples from open grown trees was not achieved because there were few areas of open grown trees available for sampling. The Norwegian samples from Helldalisen, which contained 50% open grown trees, were extracted from two sites in May 1982, and in June 1998, from mainly living trees. Trees of varying age were selected and two or more cores were extracted from each tree. No measurements of tree dimensions were made at the Norwegian sites.

Site Name (Tree Refs)	Description	Altitude (m)	East	North
<b>Rutajarvi, South Finland</b>				
Rutajarvi RU001 - RU022	Trees on slopes of glacial moraine peninsula in lake, now managed as a nature reserve, closed canopy	125 - 175	26°0'30"	61°55'45"
Ylisjarvi YL023 - YL051	Hill of large rocks, part managed but many large, burnt stumps, uneven aged trees, closed canopy.	120 - 160	25°43'0"	61°56'0"
Rutajarvi RU052 - RU095	Glacial moraine on land, now managed as a nature reserve, closed canopy.	140- 180	26°2'0"	61°55'45"
<b>Luosto, North Finland</b>				
Rahkavaara RA101 - RA105	East facing slope, currently managed forest, closed canopy.	220 - 250	27°8'0"	67°20'0"
Vytamoselka VY106 - VY147	Natural forest, rock strewn ground near swamp, many standing snags and fallen trees, closed canopy.	180 - 200	27°0'0"	67°05'30"
Tutkimusasema TU148 - TU162	Managed forest on flat land, (old peat bog?), currently open canopy.	160 - 180	26°38'0"	67°22'0"
Kuukkeli KU163 - KU190	Natural forest, rock strewn ground near swamp, closed canopy.	180 - 200	27°01'0"	67°05'0"
Luosto LU191 - LU202	Exposed hill made of pile of large rocks, no sign of management, semi-open canopy.	220 - 260	26°59'0"	67°07'0"
<b>Helldalisen, West Norway</b>				
Rorstaddalen RO001 - RO131	North and west facing slopes, glacier smoothed rock, 2 km from open fjord, open canopy.	30 - 150	15°20'	67°36'
Borareloa (river) BO001 - BO134	North facing U shaped glacial valley, strewn with large rocks and glacial till, semi-closed canopy.	120 - 200	15°44'	67°37'

Table 3.3.2 Site names, sample references, brief description, elevation, and grid refs for the modern-tree samples used in this study.

The Luosto, Helldalisen and Rutajarvi regions are considered representative of northern, maritime and southern boreal Fennoscandian sites. The initial intention was to select naturally grown trees from unmanaged forest but it was found that all the sites in south Finland, half of the sites in north Finland, and the Borareloa site in west Norway showed some signs of management. The trees from Norway were growing in more open-canopy

forest whilst the Finnish trees were growing in closed-canopy forest. The Norwegian trees were near their altitudinal tree line on north facing slopes at these sites. The Finnish trees were not close to their northern or altitudinal tree lines.

#### 3.3.4. Tree Core Data Processing

Earlywood and latewood grow during different parts of the year and lead to the potential for more detailed exploration of the relationship with climate (Kalela-Brundin 1999). The decision was made to measure earlywood and latewood separately thus leaving open the option to use these measures separately or to use total ring-width alone. This thesis only uses radial ring-width measures. All cores were glued to wooden supports, sanded, and measurements of earlywood and latewood widths were recorded in microns with an estimated accuracy of  $\pm 3$  microns. The earlywood and latewood measurements were summed to produce ring-width measurements.

Crossdating was achieved using both visual comparison of cores and correlation statistics obtained from program COFECHA (Holmes 1986). First, the measured ring-widths of all cores for each tree were crossdated against each other and second, all trees within each region were crossdated against each other. Sections of cores for which crossdating was uncertain were removed from the chronologies: generally these were where growth was slow and there were coincident missing rings in both cores. For trees with a missing ring on one core and a ring on the other core the missing (zero measure) ring was inserted. Missing rings (zero measure) were inserted for trees that were found to have a missing ring on both cores in situations where the missing ring could be inserted with confidence. Details of these crossdating activities were recorded. Series of ring-width measurements representing each tree were created as the arithmetic mean of the series from each core of that tree. Due to low replication of trees, some of the earliest segments of the oldest trees were removed leaving the Luosto and Helldalisen site chronologies both commencing at 1550 and the Rutajarvi site commencing at 1700. With no need to use the earliest data of the “modern” chronologies, this action reduces the problems of increased variance and decreased signal to noise ratio which are dependent on reduced sample depth (Briffa & Jones 1990). Crossdating was subsequently confirmed by correlation of the site chronologies with the Tornetrask (Grudd et al. 2000) chronology.

Estimates of the radial “pith offset” at coring height and estimates of the number of rings this pith offset represents (Braker 1981) are needed for developing RCS curves and by the PBS model. Radial pith offsets were estimated for each core using series of concentric rings, and the time this pith offset represents in years was estimated from the first few rings of each core. The results from each core were averaged (where necessary) to produce estimated values for each tree. Estimates of sapwood area in the sampling year are needed to test the PBS model. These were obtained for each tree by counting the number of sapwood rings beneath the bark on each core, averaging for each tree, and finally calculating sapwood area from estimated pith offsets and ring-widths using the presumption of radial growth.

### 3.3.5. End-Aligned Chronologies

To demonstrate that the RCS method finds a signal in the absence of a common signal, series of tree measurements are developed into “end aligned” chronologies and these are used to simulate chronologies of trees that are sampled in the same year and that have no common variance. RCS theory makes an implicit assumption that there is no common variance in chronologies when calendar years are mixed up, i.e. re-aligning series of measures by ring age should remove the signal common to calendar years. Tree age (age of the last ring in each tree) appears to be random with respect to both ring age and calendar years and the alignment of trees by “final ring” will remove the signal common to ring age (i.e. that which comprises the RCS curve) and the signal common to calendar years (i.e. climate forcing). Individual trees may contain medium-frequency forcing and decay due to increasing age but, providing these signals are not common, the resulting chronology will not contain significant levels of medium-frequency variance.

Chronologies created from trees that are aligned by final ring are referred to here as “End-Aligned Chronologies”. To ensure a wide spread of calendar dates, chronologies that contain large numbers of sub-fossil trees are used. Trees that grew in the modern period may have a common signal due to “anthropogenic effects” so trees were selected which had ceased growing prior to 1720. Two chronologies of sub-fossil trees with growth spread over more than 50 centuries were used for this study. Trees which grew over a 7000-year period before 1720 were selected and two end aligned chronologies were created using 720 trees from the Tornetrask chronology (Grudd et al. 2002) and 1003 trees from the Finnish-Lapland chronology (Eronen et al. 2002). It is possible to

conjecture that a “mortality based” aging curve may exist but this is not apparent in these chronologies.

The two sets of trees, which grew between 5000 BC and AD 1720, were formed into chronologies by setting the last ring of each tree to the calendar year 2000 and allocating sequentially earlier dates to the preceding rings. These chronologies “resemble” chronologies made up of trees extracted from naturally grown uneven aged forests in the year 2001, but from sites without any temporal common forcing signal. Plots of tree counts, mean ring width, and the standard deviation of ring width are shown for the final 400 years for the Tornetrask End Align chronology (Figure 3.4.2c) and the Finnish-Lapland End Align chronology (Figure 3.4.2d). The mean ring-width curves are reasonably smooth over three centuries because of the large sample sizes and the cancellation, as random noise with respect to calendar year, of the common forcing variance of individual trees. Both mean ring width curves are roughly horizontal in the first three centuries when the decay of ring width of existing trees is offset by the addition of larger rings of younger trees. Both mean ring width curves decay in the last century because there are fewer young trees being added.

### 3.3.6. Randomly Generated Trees

Some testing of standardisation methods is best performed with chronologies that have known low-frequency common signals. Series of tree measures have unknown common signals and series of “randomly generated” tree measures are used to simulate chronologies with known low-frequency characteristics in Sections 4.4.5 and 5.5.3. The methods used to develop chronologies of random trees are outlined here. The assumption that low-frequency chronology signals can be added to series of tree measures by multiplication (Section 4.2.2) is used to develop series of simulated tree measures that contain known low-frequency trends. The *Pinus sylvestris* trees sampled for this study had the property that the oldest trees tend to have slower growth rates than the youngest trees, measured by the time taken to reach 10cm diameter (Table 5.4.1). Tree age is the age of the last ring when the tree was sampled. This consistent growth rate attribute (Enquist et al. 2000) is included in random trees by allocating the youngest trees first ring widths that are larger than the first ring widths of the oldest trees. Ring width generally decreases as the tree gets older (Cook et al. 1995) and this was simulated by setting the final ring width of each tree to half the value of the initial ring width. The theoretical

shape of the decay of ring widths (a mixture of specific tree geometry and local forcing) is not known with any confidence (Briffa et al. 1996) and although this decay is generally curvilinear, a linear decay is used in the artificial data because this form of decay is simple to apply and to interpret and most standardisation methods are able to handle trees that have a linear decay.

Trees tend to vary in their growth patterns and to obtain “random” trees, where the youngest trees tend to grow faster and tend to have steeper rates of ring-width decay than older trees, random numbers are used to vary the initial starting conditions. A random increment with mean zero is imposed (by multiplication) to the first and final rings of each tree to give some variation in both growth rates and ring-width decay rates. Intermediate ring widths are set by linear interpolation between the initial and final values and random variations are added (by multiplication) to all rings. In tree measures, the noise to be reduced by averaging consists of both medium and high-frequency variance. The medium-frequency noise cancels more slowly and thus requires larger numbers of samples, relative to the high-frequency noise and only high-frequency noise is used in this study. The multiplicative method is used to preserve the roughly linear relationship between local mean and local variance (Cook et al. 1990). A brief description of each series of randomly generated tree measures is given in the text describing their use.

### **3.4. Data Comparisons and Relationships**

#### **3.4.1. Meteorological Data Comparisons**

Mean seasonal temperatures are plotted in Figure. 3.4.1, to enable comparison of data from the three meteorological sites: Sodankyla (red), Bödö (blue) and Tornedalen (black). The three plots show summer temperature as the arithmetic mean of June, July and August (a), winter temperature as the arithmetic mean of previous December, current January, and current February (b) and annual temperature as the arithmetic mean of all 12 calendar months (c). There were several cold summers between 1890-1910 at Bödö and Tornadalen, a period which is not included in the shorter meteorological record from Sodankyla. At these three sites, in the summer, the magnitude of the medium-frequency variance (century long trends) is less than the magnitude of the high-frequency variance: in every decade there is at least one temperature value above the mean and one temperature value below the mean. Higher temperatures in the last decade, markedly so in the winter series, are sufficient to





Figure 3.4.1 Means of mean monthly temperatures for Sodankyla, Bodo and Tornedalen. (a) Summer (June, July & August), (b) Winter (December, January & February), (c) Annual mean (All months), and (d) Normalised summer temperatures.

Sodankyla (1908–2000)						Common Period (1908–2000)					
SodTJan	SodTFeb	SodTMar	SodTApr	SodTMay	SodTJun	SodTJul	SodTAug	SodTSep	SodTOct	SodTNov	SodTDec
SodTJan		.29					.22				.22
SodTFeb	.29		.42	.38							
SodTMar		.42									.23
SodTApr		.38			.28						
SodTMay				.28		.21			.27		
SodTJun					.21						
SodTJul	.22							.21			
SodTAug							.21				
SodTSep					.27					.25	
SodTOct									.25		.27
SodTNov										.27	.26
SodTDec	.22		.23								.26

Bodo (1869–2000)						Common Period (1908–2000)					
BodTJan	BodTFeb	BodTMar	BodTApr	BodTMay	BodTJun	BodTJul	BodTAug	BodTSep	BodTOct	BodTNov	BodTDec
BodTJan		.23		.18					.34		-.18
BodTFeb			.40	.31							.18
BodTMar		.47		.21							.18
BodTApr		.27			.34						.19
BodTMay				.25		.27	.18				.20
BodTJun					.22		.33	.21			
BodTJul						.28		.45			
BodTAug						.22	.44		.40		
BodTSep	.32							.30		.19	
BodTOct									.24		.24
BodTNov		.21	.25							.25	.27
BodTDec	.22	.21	.29			.22					.22

Tornedalen (1816–2000)						Common Period (1908–2000)					
SweTJan	SweTFeb	SweTMar	SweTApr	SweTMay	SweTJun	SweTJul	SweTAug	SweTSep	SweTOct	SweTNov	SweTDec
SweTJan		.28					.18		.29		
SweTFeb	.37		.45	.37	.23						
SweTMar		.42		.37	.27	.22		.22			.16
SweTApr		.35			.48	.24					.16
SweTMay			.22	.42		.38	.15	.22			.21
SweTJun					.31		.32				.16
SweTJul	.21					.21		.23			
SweTAug							.25		.19		
SweTSep										.15	
SweTOct									.24		.30
SweTNov			.23							.30	.37
SweTDec	.21		.24								.28

(Only values significant at  $p < 0.05$  level are printed)

Table 3.4.1 Mean Monthly Temperature, within site correlations

produce an apparent overall trend in the century long data sets which becomes marginal if the last decade is removed. Mean monthly temperatures over the full period of measurement were compared at the three sites. Sodankyla winters are about 1.0°C lower and summers 2.0°C lower than at Tornedalen, reflecting the more northerly climate. Böö

winters are 9.0°C higher and summers 2.0°C lower than at Tornedalen, and the variance in winter temperature at Böö is only half that of Tornedalen reflecting the influence of the Atlantic Ocean. When the three sets of summer temperatures are normalised (mean = 0.0, standard deviation = 1.0) over their common period (1908 to 2000), the variance of the series is remarkably similar (Figure 3.4.1d).

### 3.4.2. Meteorological Data Correlations

No significant autocorrelation is apparent in the monthly meteorological data, i.e. the value of a monthly variable is not related to the value of that variable in the previous year of the same month. The sets of monthly temperature data for each site were correlated against each other and those results that are significant at the  $p < 0.05$  level are shown in Table 3.4.1. Correlations based on the full available length of record are shown in black and those for the common period of 1908 to 2000 are shown in red. For adjacent months at a site, correlations are generally about 0.25 reflecting some persistence in conditions. The consistent exception to this is that at all sites correlations between February and March are 0.4 and between February and April are 0.3 which may be due to the influence of snow cover. (Also possible because the NAO has more persistence at this time of year (Osborn et al. 1999)). At Böö, summer temperatures in adjacent months showed a higher correlation at 0.4.

Month	Sodankyla to Böö 1908 - 2000	Sodankyla to Tornedale 1908 - 2000	Böö to Tornedalen 1869 - 2000
January	0.86	0.96	0.88
February	0.83	0.95	0.87
March	0.86	0.95	0.86
April	0.78	0.91	0.76
May	0.72	0.87	0.79
June	0.73	0.92	0.79
July	0.76	0.94	0.78
August	0.65	0.95	0.73
September	0.78	0.95	0.82
October	0.87	0.97	0.90
November	0.82	0.96	0.86
December	0.88	0.98	0.89

Table 3.4.2 Correlations of mean monthly temperature between meteorological stations, over their common period (indicated) for each pair. (All correlations significant at the 99.9% level)

The sets of temperature data for each site were correlated against the same months' temperature at the other sites and the results, shown in Table 3.4.2, indicate the large-scale coherence in the pattern of temperature anomalies during the last century.

Correlations of mean monthly temperature between Sodankyla and Bødö are in the range 0.65 to 0.88, with the lower values in summer. Correlations between Sodankyla and Tornedalen are in the range 0.87 to 0.98. Correlations between Bødö and Tornedalen are in the range 0.73 to 0.83.

### 3.4.3. Tree ring data - Statistics

Tree count, mean tree age, mean tree radius, and mean ring width for each region are shown in Table 3.4.3. Standard deviations are shown in brackets and, with the exception of Rutajarvi, mean ring-widths are similar, with half a standard deviation separating the sites. Luosto and Helldalisen have larger mean tree age than the sub-fossil chronologies because it is possible to select older looking trees from the large choice available for modern chronologies. The trees from Rutajarvi, with low mean age and double the growth rate of the other trees are not used in the standardisation section of this thesis but are used to test the PBS model (Chapter 7).

Region Name	Number Trees	Mean Age (years)	Mean Radius (cm)	Mean Ring (micron)
Tornetrask AD	586	188 (84)*	13.4 (5.5)*	709 (455)
Finnish-Lapland AD	430	179 (60)*	11.6 (4.4)*	649 (445)
Tornetrask End Align	720	180 (75)*	12.6 (5.1)*	698 (467)
Finnish-Lapland End Align	1004	173 (56)*	10.5 (3.8)*	606 (428)
Luosto	100	291(109)	17.3(3.5)	596(403)
Helldalisen	89	306(110)	15.6(3.8)	490(326)
Rutajarvi	95	133(62)	15.0(2.8)	1157(742)

\* Note: Excludes any estimate of missing years or radius to the centre of the tree.

Table 3.4.3 Summary statistics for the seven chronologies of this study: Tree counts, mean age, mean radius, and mean ring width (means with standard deviations).

Tree counts and mean ring width (with standard deviation) for all chronologies are plotted in Figures 3.4.2 and 3.4.3. For the long chronologies of Tornetrask AD and Finnish-Lapland AD, both mean ring width and its standard deviation have been smoothed with a low-pass spline (with a 50% cut off frequency set at 5% of chronology length) for presentation purposes. Tree counts for the Tornetrask AD and Finnish-

Lapland AD sites vary considerably over time. Tree counts for the “modern”

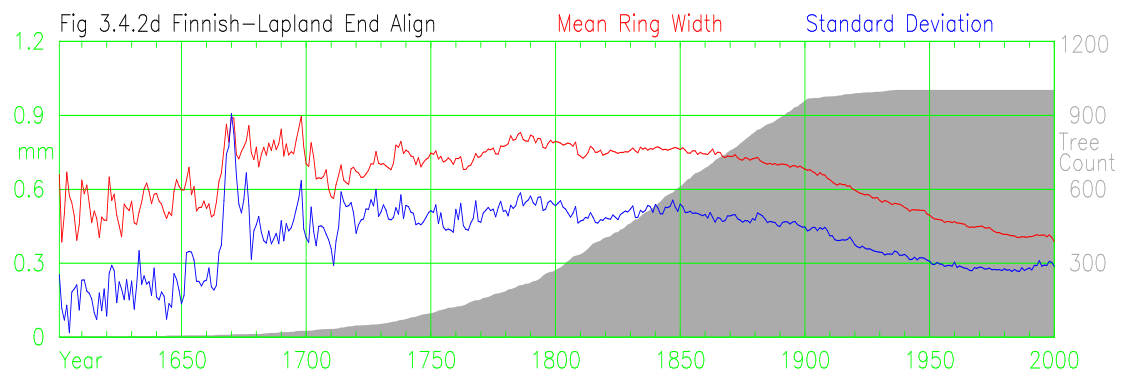
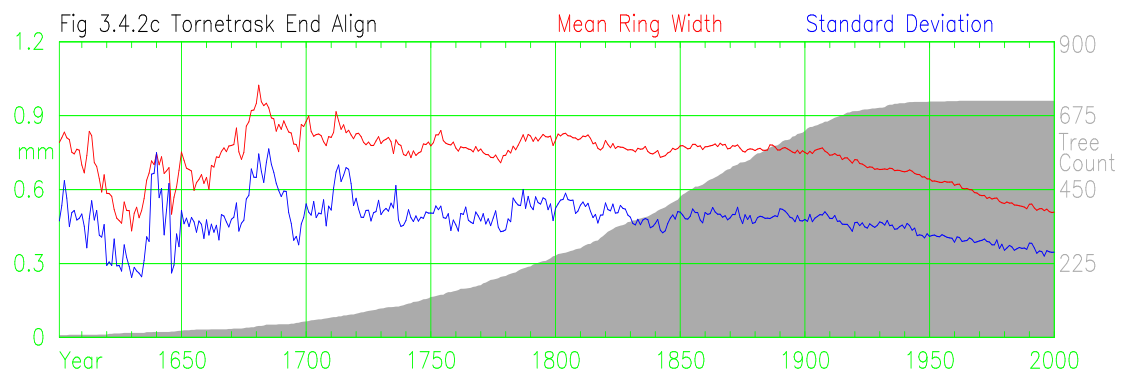
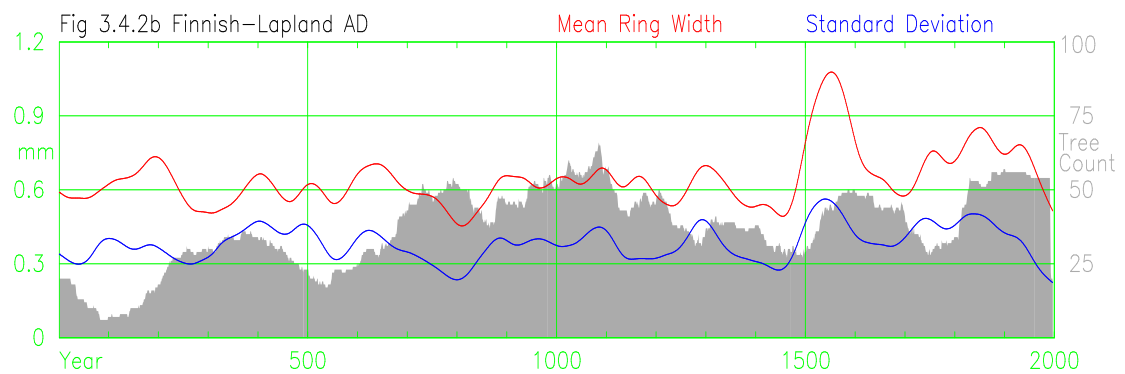
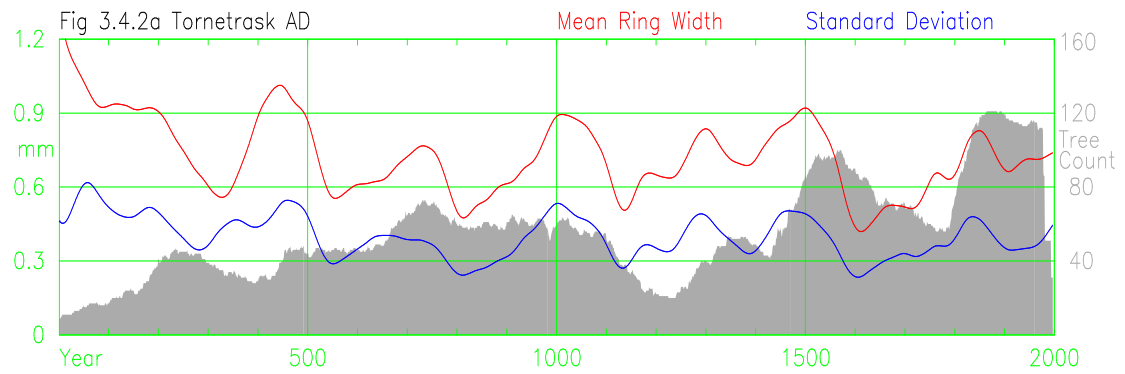


Figure 3.4.2 Mean ring widths, standard deviations (plotted from zero), and tree counts by calendar year (shaded area). (a) Torneutrask AD (smoothed), (b) Finnish-Lapland AD (smoothed), (c) Torneutrask End Align, (d) Finnish-Lapland End Align.

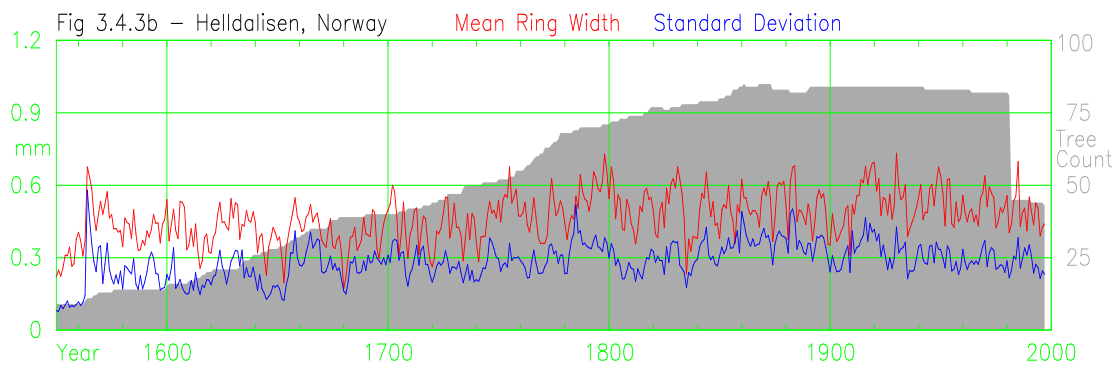
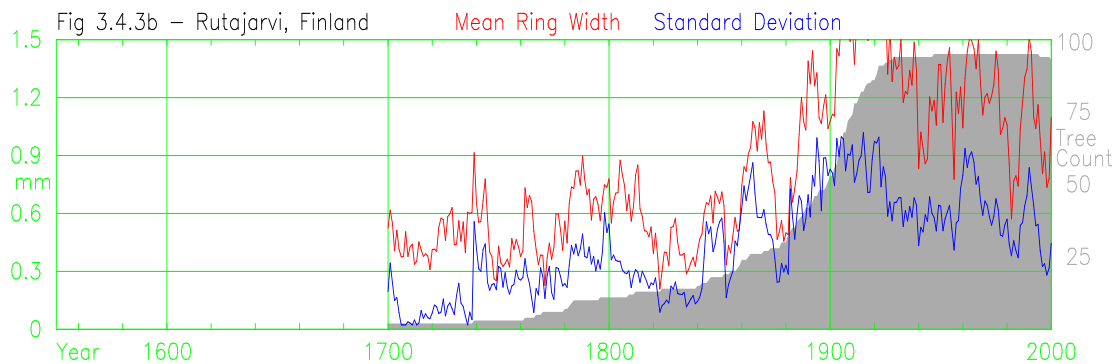
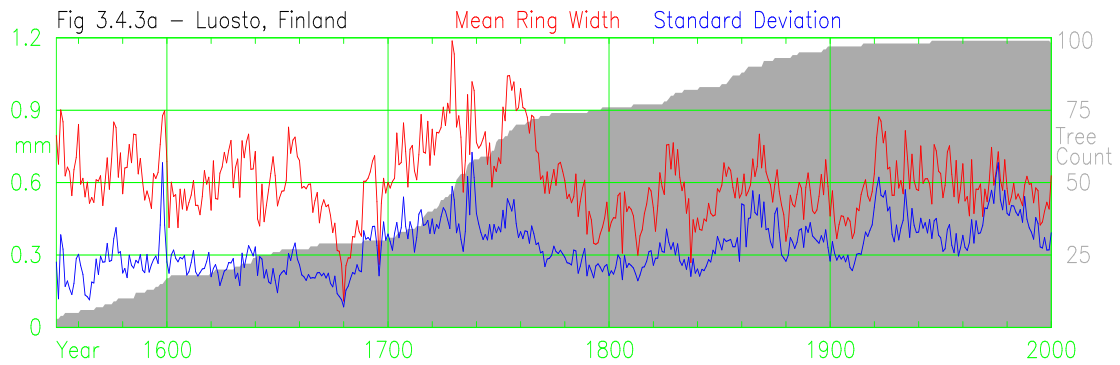


Figure 3.4.3 Mean ring widths, standard deviations (plotted from zero), and tree counts by calendar year (shaded area) for (a) Luosto, Finland, (b) Rutajarvi, Finland, (c) Helldalisen, Norway.

chronologies of Helldalisen, Luosto, Rutajarvi and both end aligned chronologies increase steadily over time. In Figure 3.4.3 the Helldalisen trees (a) have a slightly higher rate of growth than the Luosto trees (b) which may well reflect the higher summer temperatures away from the maritime influence. At all sites and through time the standard deviations of ring-width have similar relative magnitudes to their mean values suggesting the presence of variation in growth rates which is not “common” to a specific year. At all sites there is an increase in mean ring width, relative to the expected decay, after 1920.

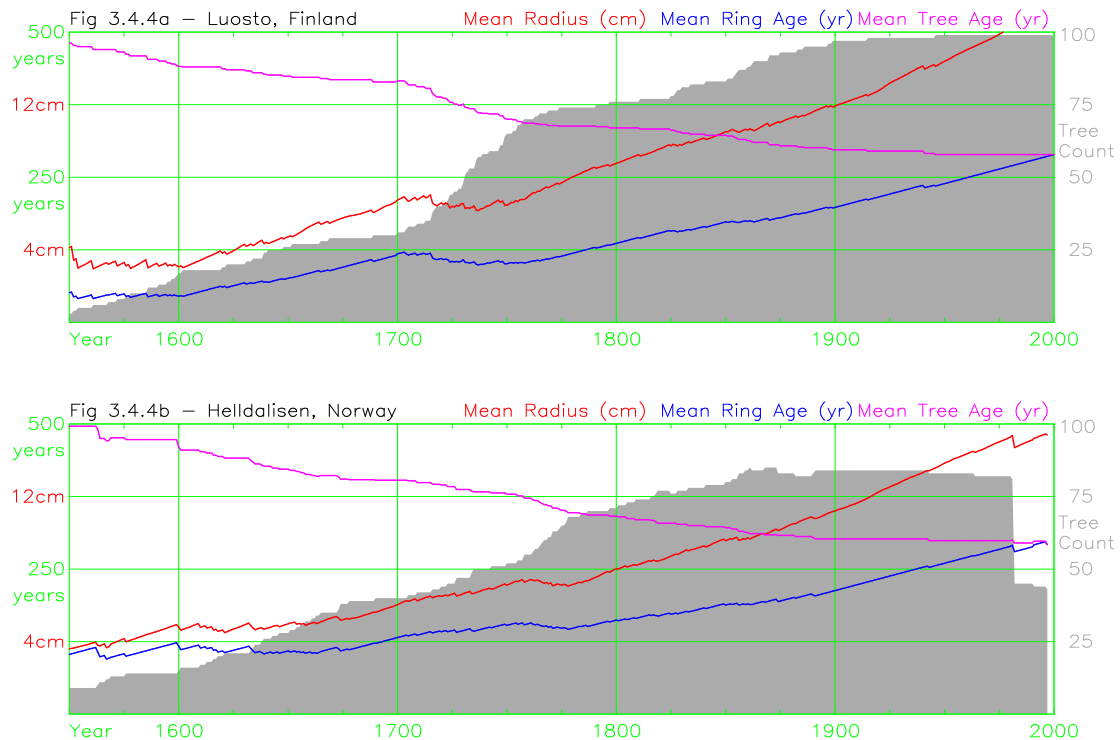


Figure 3.4.4 Means of current tree radius, current ring age, and final tree age for rings and trees contributing to each calendar year at (a) Luosto, (b) Helldalisen.

In Figure 3.4.4 tree counts for each year show the addition of trees to the Luosto and Helldalisen chronologies from 1550 to the 20th century. Mean current tree radius of trees in each calendar year rises steadily with time because existing trees get larger, moderated by the addition of new (smaller) trees, until the 20th century when few new trees are added and the curve of mean tree radius becomes steeper. The mean ring age in a calendar year increases steadily because existing trees get older, moderated by the addition of new trees with young rings, and increases sharply over the final century in which no new trees are added. The mean age of trees in each calendar year starts high, because only the oldest trees are represented, decreases steadily in the period when younger trees are added, and does not change during the final period when no trees are added. All these plots show that chronologies made from samples at these sites are not constant over time with respect to mean tree age, mean ring age and mean tree radius, a direct result of selecting samples from living trees of differing ages and differing growth rates from one time period. Importantly, the early parts of both chronologies consist of the youngest rings from the oldest trees.

### 3.4.4. Tree-ring data - Correlations

The chronologies and statistics reported in Tables 3.4.4 and 3.4.5 are based on the use of mean ring widths for each tree, i.e. the average of individual radii for each tree, and all the correlations are calculated for the common period of data overlap between the specific series being compared. The requirement at this stage is to demonstrate a common high-frequency signal between trees and sites. Detrending curves were created as the values of a 30-year low-pass spline (Cook & Peters 1981). High-pass filtered series of tree indices were created by the division of measured values by the low-pass detrending curves. Chronologies were created as the arithmetic mean of tree indices (Holmes 1986).

Region Name	Tree Counts	Mean Between Tree correlation	Mean Tree to Site correlation
Tornetrask AD	586	0.37(0.15)	0.59(0.10)
Finnish-Lapland AD	430	0.38(0.16)	0.61(0.10)
Luosto	100	0.41(0.12)	0.62(0.10)
Helldalisen	89	0.34(0.12)	0.57(0.08)
Rutajarvi	95	0.41(0.14)	0.61(0.10)

Table 3.4.4 Mean between tree and mean tree to chronology correlations, with standard deviations, for each region, based on high-pass filtered series of tree indices.

Table 3.4.4 lists the mean of between tree correlations and the mean of tree to chronology correlations, with standard deviations, for each region, based on high-pass filtered series of tree indices. The mean inter-tree correlations (Briffa & Jones 1990) of tree indices show that all regions contain a clear common within-site signal. The means of the within-site correlations, each tree to the chronology developed from all other trees, have values above 0.5 and these also demonstrate that there is a clear common signal. Table 3.4.5 lists the region-to-region chronology correlations, with standard deviations and common period lengths, based on high-pass filtered chronologies. The comparisons shown here indicate that the temperature measures have more variance in common over distance than the high pass filtered tree measures. The temperature comparisons (Table 3.4.2) include medium-frequency variance, which matches well, and are over shorter common periods of less than two centuries. The Rutajarvi region of south Finland has little high-frequency variance in common with the other regions despite this region, internally, having a clear common signal. The presence of a medium-frequency increase in growth rate after 1920 would improve correlation statistics.



Site	Site	Common Period (yr)	Between Site Correlation
Tornetrask AD	Finnish-Lapland AD	2049	0.69
Tornetrask AD	Luosto	448	0.60
Tornetrask AD	Helldalisen	448	0.53
Tornetrask AD	Rutajarvi	298	0.13
Finnish-Lapland AD	Luosto	448	0.77
Finnish-Lapland AD	Helldalisen	448	0.45
Finnish-Lapland AD	Rutajarvi	298	0.14
Luosto	Helldalisen	448	0.39
Luosto	Rutajarvi	301	0.25
Helldalisen	Rutajarvi	298	0.08

Table 3.4.5 Region to region correlations between each region, based on high-pass filtered chronologies.

### 3.5. Summary

Three well-replicated chronologies of ring-width measures (Luosto, Rutajarvi and Helldalisen) have been produced as part of this study by sampling trees and measuring ring-widths. Series of mean monthly temperature measures have been chosen from the sites of Bødö in Norway, Sodankyla in Finland, and Tornedalen in Sweden. Data from two chronologies of ring-width measures covering the last two millennia, (Tornetrask AD and Finnish-Lapland AD) have been selected for testing purposes. Two “end aligned” chronologies with no apparent common forcing signal (Tornetrask end-aligned and Finnish-Lapland end-aligned) have been developed for testing purposes. Some principles and methods required to generate series of simulated trees have been established for use later. Trees from the Rutajarvi region of south Finland are only used in the PBS model.

## **Chapter 4. Tree Growth**

The objective in this Chapter is to develop some tools that can assist with the standardisation process. This Chapter contains four separate sections with the theme of separating the common, climate-related forcing of tree growth from the age-related growth trends seen in series of ring-width measurements. Section 4.1 examines and distinguishes two aspects of tree growth; the parts of tree growth for which climate forcing is common to all trees and the parts of tree growth which are not common, i.e. specific to individual trees. Processes from tree-growth models are examined and these set specific constraints on the methods that may be used both to develop expected growth rate curves and to generate chronologies. The extent to which curve-fitting and RCS methods of removing the age-related growth trend from trees conform to these constraints is discussed. Section 4.2 provides a mathematical chronology model consisting of a set of mathematical procedures that conform to the principles set out in Section 4.1 and also provides the necessary mathematical tools for tree and chronology index manipulation. Section 4.3 sets out a novel method of capturing long-timescale variance in a chronology in the form of a mathematical procedure BFM, which calculates the “best fit means” of series of indices. Section 4.4 examines the problem that arises when curve-fitting methods are used to estimate age-related growth curves from series of measurements that contain the effects of the common, climate-related forcing on tree growth.

### **4.1. Growth Rate and Amount of Growth**

#### **4.1.1. Introduction**

This section examines the way climate controls tree growth, assessed from tree-growth models, and the implications that this has on standardisation methods. It is a lengthy process and a summary description is presented here. Two specific tree-growth models are examined, HYBRID (Friend et al. 1997) and GUESS (Smith et al. 2001), and procedures from within these models are used to develop a “tree-growth model” based representation of tree growth. At the start of each year, these tree-growth models accumulate the foliage of all trees and distribute this foliage into a number of layers forming a description of the canopy. The mass of carbon generated by the canopy in small time steps, e.g. days or hours, is calculated using climatic variables of interest to dendroclimatologists, such as temperature, precipitation, cloud cover, light intensity and CO<sub>2</sub> concentrations. The carbon produced in each time step is accumulated over a year.

The common effect of climate control on tree growth is shown to be on this carbon production process. At the end of the year the carbon generated by a tree's foliage is allocated to that tree and, because trees have differing amounts of foliage, this results in trees receiving differing amounts of carbon in a specific year. Each tree then allocates the carbon received to growth and, via an allocation strategy which uses records of the tree's current size (including diameter), the size of the annual ring increment is calculated. Because trees have different diameters, ring increments will vary. Dendroclimatic methods seek to isolate the "climate" forcing common to all trees using two basic methods; detrending and averaging. These two methods must, between them, remove the effects of variation in foliage mass, allocation strategy, and diameter in order to isolate the common "climate" signal. After a detailed discussion of these processes, this section concludes that curve-fitting methods succeed in this task while, although in theory the RCS method should succeed, the detrending process of the RCS method is so poor that in practice there are never enough samples in each year for the averaging process to complete the task.

#### 4.1.2. Climate controls photosynthesis

The expertise of foresters and ecologists concerning the effects of climate on tree growth has been collected, refined and built into tree-growth models (Shugart & Smith 1996). Tree-growth models are designed to predict the rates of growth of trees in varying climatic conditions (Dale & Rauscher 1994). An examination of two tree-growth models, HYBRID and GUESS, finds that the primary control on tree growth by environmental variables is via the instantaneous rate of photosynthesis in foliage. Calculations of the rate of photosynthesis are made using a number of variables, some of which are climate related. The results are accumulated to estimate the mass of photosynthate (growth material or carbon) that is generated by the canopy at chosen timescales. The annually accumulated effects of temperature, moisture availability, cloudiness and other climatically-varying parameters on tree growth are contained within these photosynthesis calculations. Respiration rate is temperature-dependent over short periods. The net amount of respiration in any year can be largely explained by the temperature effects on photosynthesis (Dewar et al. 1999) and at annual timescales the effect of variation of temperature on respiration can be ignored. The assumption is made here that common control by climatic conditions on tree growth is in the amount of photosynthate (carbon) generated in the canopy each year.

#### 4.1.3. Expected Growth Rate is proportional to Foliage Mass

Dendrochronologists have noted a somewhat noisy, common forcing effect on tree growth (Fritts 1976c) and some “mechanism” must transfer the climate control of the canopy to individual trees. An assumption made here that the canopy can be considered to be comprised of a number of “units” of foliage which, at a site level, all produce the same amount of photosynthate in a specific year. The “common” effect of climate control on tree growth could be measured as the mass of carbon produced by an “average” unit of foliage in each year. If measurements of the annual production of carbon by units of foliage were available then the fractional deviation in growth rate for each year could be obtained by dividing these measured values by the mean rate of production of carbon by unit foliage over the time span of the chronology. This mean carbon production rate by unit foliage is a constant applicable to all years of all trees and in dendroclimatic terms will be the expected growth rate for all trees and all years. If a tree-growth model is asked to produce an “expected growth rate” value for a specific tree then average climate, canopy conditions, and environmental conditions will be used to calculate the rate of production of photosynthate. The tree-growth model will need to know the tree’s foliage mass and current dimensions, and can then calculate a ring increment which will be the “expected growth rate” because average climate conditions were used.

Foliage is a permanent part of a tree’s structure while leaves (needles) are continuously lost and re-grown in a maintenance process. Variation in the rate of production of photosynthate by foliage due to the age of leaves is removed by considering units of foliage consisting of representative samples of leaves of all ages. Foliage at the top of the canopy has a higher production rate than foliage near the base of the canopy due to shading (Mäkelä & Vanninen 1998) but “units” of foliage would consist of representative samples of foliage from all heights in the canopy. Trees that are not tall enough to have foliage near the top of the canopy are unlikely to survive the competitive struggle for light (Dewar 1993), and will thus not be sampled by dendroclimatologists. Each tree has units of foliage and the assumption made here is that, at a site, units of foliage of fast growing trees, slow growing trees, large trees, small trees, old trees, and young trees will all have “similar” average production rates of carbon per unit of foliage in a given climate year. This is a sweeping assumption but, because many of the differences found in individual trees will be removed by the averaging process, only needs to be an approximation.

Growth is normally measured on a per tree basis for each year. Scaling production in the form of carbon produced per unit foliage to that of carbon produced by an individual tree is achieved simply through multiplication by foliage mass. Where growth measures are of the mass of carbon produced by each tree in each year, then the expected growth rate would be the product of the mean carbon production rate by foliage and the current foliage mass of the tree. The only variation in the expected growth values at a site across all years and all trees is in foliage mass and the expected growth rate for every tree ring will be proportional to the current foliage mass of that tree. The crucial point is that current foliage mass is an important factor in the estimation of expected growth values.

#### 4.1.4. Foliage mass increases while trees get bigger

The foliage mass of a tree varies as the tree becomes older and larger. In trees with circumferential growth, foliage mass is generally constrained by mechanical strength and thus diameter. As diameter increases foliage mass increases leading to increasing growth rates (carbon production) despite decreasing ring increments. This variation in foliage mass is not common to all trees and is not the signal of interest i.e. must be factored out of tree growth measures using the expected growth curve. There is a need to investigate the development of foliage over the life of trees in order to evaluate methods of predicting expected growth curves which account for foliage mass changes. To increase foliage mass a tree must increase the size of many other structures such as crown height, branch length, sapwood area, fine root mass and stem strength (Mäkelä 1986). All these increases require carbon. The only source of carbon in a tree is via the foliage which leads to production of carbon (growth) being exponential (Mäkelä 1986), simply because foliage begets foliage. As the tree gets larger the proportion of available carbon that can be used to increase foliage mass reduces (Magnani et al. 2000) leading to a decay in the exponential rate of increase in foliage mass.

Respiration by consuming carbon is a major contributor to this reducing exponential rate of foliage increase, with growth respiration proportional to the mass of new structure and maintenance respiration proportional to the mass of living structure (Mäkelä 1986). The mass of carbon added to a tree each year increases over most of the life of a tree (Hamilton & Christie 1971). Foliage mass also increases over most of the life of a tree (Stoll et al. 1994), even though it fluctuates annually within this long-term growth pattern

(Mäkelä & Albrekson 1992). The rate of increase of foliage reduces as the tree gets larger and in the oldest trees (Kaufmann 1996) the foliage mass may decrease. Foliage mass is approximately proportional to sapwood area (Mäkelä 1986) but increasing tree height increases the cost of sapwood per unit foliage, both in the proportion of new wood needed and in the maintenance overhead. The rate of “compound interest” of foliage increase reduces as the tree gets larger.

#### 4.1.5. Variation in Growth Rates

Natural variations in the growth rates of trees (Fritts 1976d) occur because of differences in growing conditions during a tree’s life. For open canopy trees on poor sites, root proportion is higher and foliage density is lower than on good sites (Mäkelä & Albrekson 1992). If a tree is growing in a hollow where the water table is nearer the surface rooting depth can be limited (Nicoll & Ray 1996). In an area where soil mechanical strength varies, trees adjust their growth to meet local requirements (Matthegek 1991c). These “microsite” variations will lead to small differences in the proportion of carbon allocated to the rate of increase of foliage. Small differences in sapling size (foliage mass) result in large differences in growth rates (Friend et al. 1997) and growth rates control the foliage mass leading to persistence in the rate of increase of growth rates.

Carbon dioxide concentration directly affects photosynthesis and the rate of production of growth material per unit foliage per year (Gunderson & Wullschleger 1994) because the “cost” of absorbing carbon changes. Norby et al. (1999) notes "*an acceleration of ontogeny in increased CO<sub>2</sub>*" and that "*large growth responses to elevated CO<sub>2</sub> resulted from the compound interest associated with an increasing leaf area*". Extra growth in the second year was due to increased CO<sub>2</sub> in the second year and the extra foliage in the second year that was generated because of increased CO<sub>2</sub> in the first year. Ideally the growth increase due to increased CO<sub>2</sub> concentration should be detected while the growth increase due to additional foliage should be factored out by the expected growth curve.

In stands of even-aged trees stem diameter can vary considerably (Stoll et al. 1994) and generally the trees with the largest stem diameters will have most foliage. Trees with higher foliage mass have faster growth rates. In a closed canopy the mass of foliage each tree may have is limited by space (Vanninen & Mäkelä 2000) and the rates of growth of trees can depend on the distance to nearest neighbours. The average growth rate of trees

will depend on stem density per unit area of forest (Biondi et al. 1994) and stem density will vary with average stem size, average tree age, and over time with the results of thinning due to competition (Dewar 1993). In uneven aged, naturally sown forests there will be large differences in growth rates which are not dependent on the common forcing (Mateu et al. 1998).

The rate of increase of foliage mass in trees depends on foliage mass with the result that small variations in foliage mass produce persistent differences in the rate at which trees progress through their lifecycle (ontogeny) and it is this persistence which must be accounted for by expected growth curves. In addition to within site variations, each year of common forcing (climate) changes the tree for the rest of its life. If a tree-growth model is asked to predict the expected growth rates of a tree based on average climate conditions then it would produce a series of ring increments based on steadily changing foliage mass, tree diameter, etc. If an above average climate year were to occur then the tree, at the end of that year, would have a larger ring, more sapwood, and more foliage (both relative to an average year) and the tree-growth model would predict a higher rate of expected growth for the rest of the tree's life. A single poor climate year would induce the tree-growth model to produce a lower expected growth rate for the rest of the tree's life. The amount of growth material produced in any year depends on the climatic forcing in that year. **The expected growth rate in any year is independent of that year's common forcing but is dependent on the history of growth forcing to date.**

The conclusion here is that any method of predicting the expected growth rate of a tree without reference to the history of growth of that tree will be producing tree indices which are dependent on both the history of common forcing and the current year's common forcing. The rate of growth of trees in a specific year will not be a direct measure of that year's common forcing. The average growth rate of trees will not be dependent on a specific year's climate forcing because last year's climate forcing will have preconditioned the trees. To find a value for common forcing in a specific year as a fractional deviation, the measured growth of each tree must be compared to an estimate of the expected growth rate of that tree.

#### 4.1.6. Tree Measures Demonstrate Variation in Growth Rates

The rate of growth of a tree is defined here by the time taken for that tree to reach a specified diameter leading to the relative references of “faster growing trees” and “slower growing trees”. The previous paragraphs suggest that at any one time the rates of growth of trees at a typical dendroclimatic site will vary considerably and there will be faster and slower growing trees growing contemporaneously. This is shown in Figure 4.1.1. At the Tornetrask (a) and Finnish-Lapland (c) sites the mean ring-width, plotted by ring age, for the fastest growing third of trees (red) is more than twice that of the slowest growing third of trees (blue) in the first century of growth. After the first century, although ring-widths converge, the diameter of the fastest growing trees is much larger than the diameter of the slowest growing trees and the fast growing trees are gaining carbon at a rate four times that of the slow growing trees ( $\text{area} \propto \text{diameter}^2$ ). The decay in ring-width disguises the steady increase in the annual carbon gain. Plots by calendar year for the Tornetrask (b) and Finnish-Lapland (d) sites show that over the last two millennia there have been both fast growing trees (red) and slow growing trees (blue) in every calendar year. The counts of fast growing trees (magenta) and slow growing trees (cyan) are shown in Figures (b) and (d) and these counts vary over time.

There are fast and slow growing trees growing in all periods represented by these two chronologies. The effects of common forcing may alter the ratio of fast and slow growing trees in different periods but the expected magnitude change at any time in these chronologies due to the randomness of sampling is also significant e.g. with a sample of only 20 trees then replacing a fast growing tree with slow growing tree will change chronology indices by a few percent. The count of trees needed to reduce the random sampling effects by averaging, when using mean growth rates, will be large (Briffa et al. 1996). The “local” mean growth rate at any one time will be the result of the previous decades of common forcing and will not depend on the current year’s common forcing. A measure of the current year’s common forcing can be obtained by dividing the current year’s growth by the expected growth (local mean of growth rate). Using the average growth rate over all time (applied by ring age) as the expected growth rate will produce indices which are measures of both previous decades of common forcing and the effects of current year’s growth.



Fig 4.1.1a Mean rings by ring age – Tornetrask AD Chronology

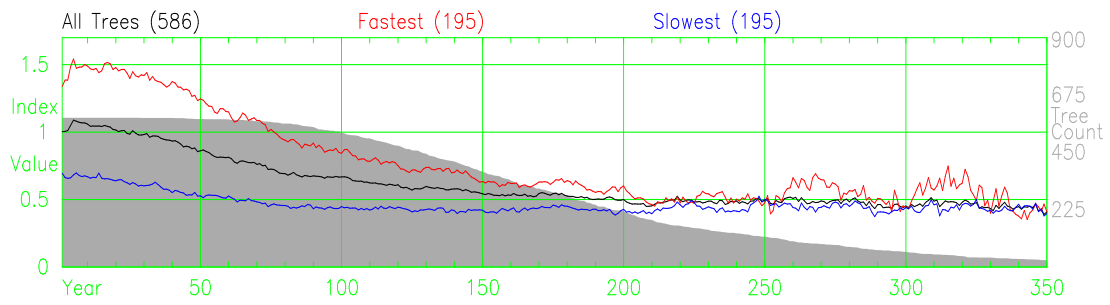


Fig 4.1.1b Mean rings by calendar age – Tornetrask AD Chronology

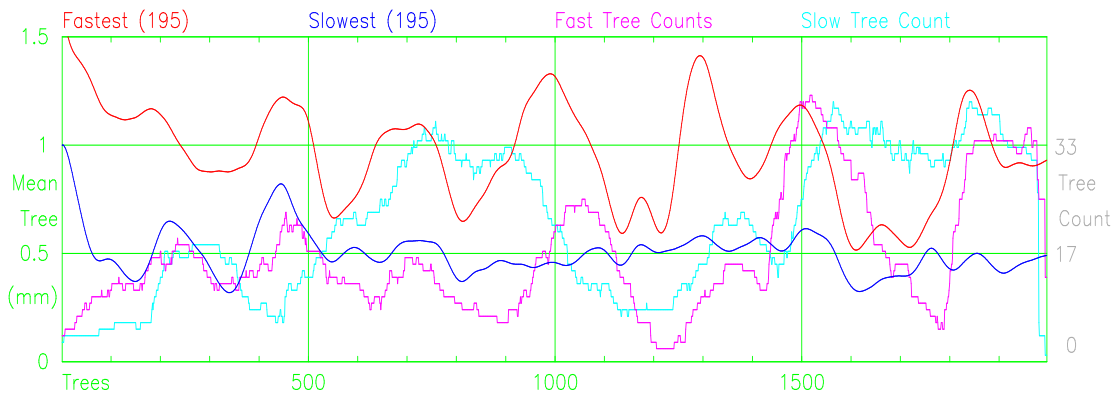


Fig 4.1.1c Mean rings by ring age – Finnish–Lapland AD Chronology

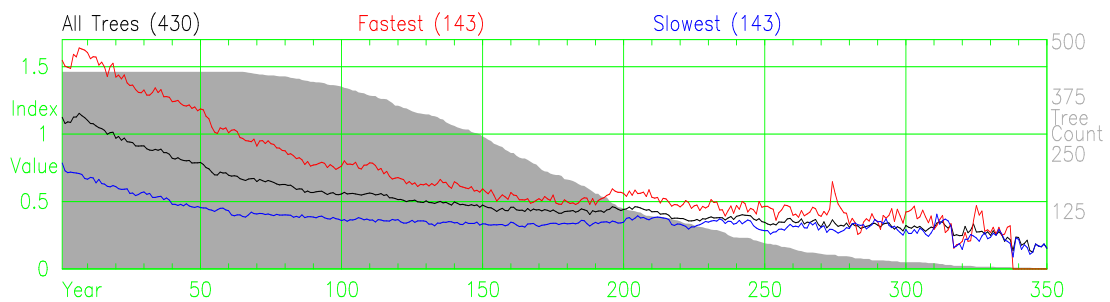


Fig 4.1.1d Mean rings by calendar age – Finnish–Lapland AD Chronology

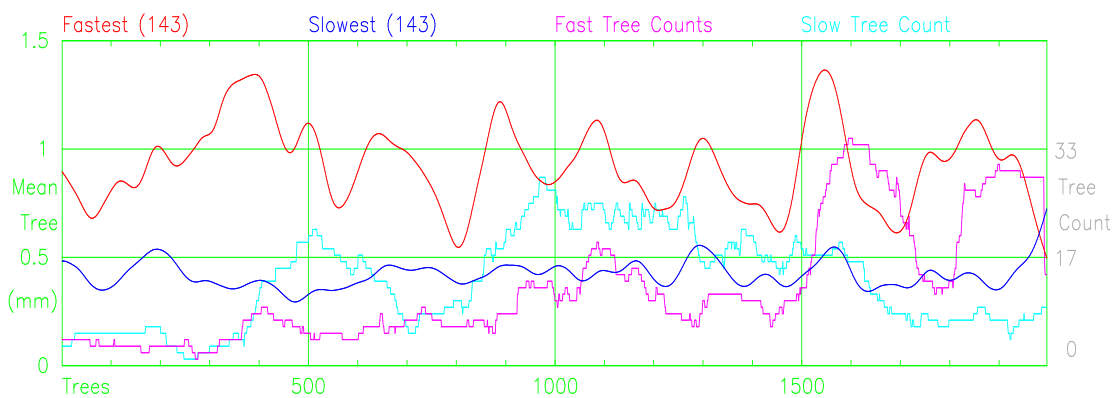


Figure 4.1.1 (a) Tornetrask AD mean ring-width of the fastest, slowest and all trees by ring age. (b) Tornetrask AD mean ring-width of fastest and slowest trees by calendar year with tree counts. (c) and (d) as (a) and (b) but for the Finnish–Lapland AD trees.

#### 4.1.7. Predicting Ring Width Decay

In the “real world” the availability of tree measures from previous periods is limited to those which are preserved naturally. The orbit of the Earth controls the strong seasonal cycle experienced by most extra-tropical trees and produces a continuous series of annual rings which form a record of growth through time leading to the use of various ring parameters. The growth material available to each tree is distributed among various compartments including ring increments of the stem. Variation of expected ring-widths over time will be proportional to changing foliage mass and the evolving non-linear relationships, over the life of the tree, between available growth material and diameter increments.

The plots of mean ring-width by ring age (RCS curves) shown in Figure 4.1.1 (a) and (c) demonstrate that the magnitude of ring widths tends to fall because trees get older and larger. This growth trend in series of ring-widths is the result of a number of complex interacting processes. Each year a volume of wood is distributed around the surface area of a three dimensional stem. The mechanical strength requirements lead to the need for the stem to taper (Dean & Long 1986) and proportionately more wood is added to the lower parts of the stem as the tree gets larger. The rate of height growth decreases with age and in some trees competition can lead to rapid initial height growth (Mäkelä & Sievanen 1992). The mechanical strength of the stem is a constraint on foliage mass (Morgan & Cannell 1994a) and the lifelong increase in stem diameter leads to increases in foliage mass and carbon production over most of the life of a tree (Hamilton & Christie 1971). The rate of growth of trees measured as diameter increments decays over the life of a tree, while other measures of tree growth rates such as diameter, basal area, foliage mass, living wood mass, and annual carbon production all tend to increase over the life of the tree (Vanninen et al. 1996). Generally, tree growth rates steadily increase while ring-widths get smaller. There is no generally acceptable equation of ring-width decay to describe these complex relationships (Briffa et al. 1996) which leads to empirical methods of generating expected growth curves.

Time does not control plant growth described by Landsberg (1986b, p7) “... *time is not a driving variable, i.e. the change of state of a plant is not dependent on time per se but upon some condition, associated with time, which causes the change*”. The existence of large differences in the growth rates of trees leads to ring age being a “poor” predictor of

ring-width. Ring age does not distinguish between the red and blue curves of Figure 4.1.1 (a) and (c). The reduction of ring-width due to diameter increase, leads to some dependence of ring-width on the average rate of growth of the tree. The slope of decay of ring-width measured in length per unit time will be larger in fast growing trees than in slow growing trees because diameter increase is spread over fewer years. The existence of diameter measures allows the use of diameter as an explanatory variable in the derivation of expected growth curves. Diameter on its own is a “poor” predictor of ring-width and diameter as the area beneath the curves of Figure 4.1.1 (a) and (c), will not distinguish between the red and blue curves.

The tendency for fast growing trees to continue growing quickly and for slow growing trees to continue growing slowly implies that **a combination of age and diameter** (average rate of growth to date) will be a reasonable predictor of ring-width compared to age or diameter on their own. The diameter reached in a given time is a measure of growth rate. Tree-growth models calculate the annual mass of photosynthate available for growth and add this material to the existing structure in a balanced way (maintaining empirically-measured structural relationships) to generate a stem diameter increment. A simplified view of this process envisages tree-growth models predicting ring-width increments from the available mass of growth material and the accumulated history of the tree (current sizes of the tree’s structures). For trees of the same species and site, the dendroclimatic equivalent to similar history is of trees that have reached the same diameter in the same amount of time. Trees of the same diameter and age are likely to have had similar foliage masses over their life to date and similarity of foliage mass and diameter leads to the expectation of similar ring widths. Tree-growth models use the history of tree growth whereas most dendroclimatic curve-fitting methods use both history and future of growth i.e. the curve fit at any ring is constrained by both earlier and later ring widths. As trees cannot foresee the future the predisposition to grow at a certain rate must come from the past (Cook et al. 1990) and leads to the use of one-sided or causal filters. This “past only” idea is not pursued in this project and both history and future are used in the generation of expected growth curves. (The RCS method does not use either and the newly proposed methods MRCS and SARCS of Chapter 5 use both.)

#### 4.1.8. Discussion

Common forcing controls the rate of photosynthesis and the “climatically” controlled rate of carbon production by foliage in a year is expected to be common to all trees. Trees present foliage to the atmosphere at the start of the growing season and this foliage gives them the potential to generate growth material during the growing season. The mass of foliage sets the expected growth rate for a tree in a specific year independently of the amount of “climatic forcing” in that year. Differences in the foliage mass of trees will lead to different expected growth rates for each tree. The foliage mass and expected growth rates of a tree are dependent on the history of growth of that tree and both age and diameter are needed to estimate expected growth. This reasoning applies to curve-fitting standardisation methods where the expected growth curve is fitted through all growth measures representing the growth history (and future) of the tree and the measured ring width is divided by the expected value to produce fractional deviations (Cook et al. 1990). When curve-fitting methods are used to create expected growth curves, the area under the series of measures and the area under the expected growth curve are equal and over time the accumulated areas to date will be similar. The area under both curves, the sum of ring widths, is radius and this leads to the conclusion that curve-fitting methods of creating expected growth curves use both age and diameter as explanatory variables in their predictions of expected ring width. A novel part of this study is an attempt to apply this set of assumptions to the RCS method whilst retaining the ability to preserve a life-span trend in series of tree indices.

Examination of Figure 4.1.1 (a) and (c) shows faster growing and slower growing trees having similar ring-widths in the 3<sup>rd</sup> century of growth. The RCS method will generate similar values of growth indices for both sets of trees suggesting similar growth rates. A tree-growth model, which allows for fast growing trees to have diameters twice the size of the slow growing trees, will predict that the faster growing trees are growing (producing carbon) four times faster than the slower growing trees. The RCS method of generating expected growth values does not use diameter and as a result produces poor estimates of tree growth rates. Persistence in the growth rates of trees is not considered and the RCS method tries to overcome this problem, created by mean growth rates, by using larger numbers of trees in each year. Problems which arise in the RCS method from the use of mean ring width at a specific ring age to estimate the growth rates of trees are discussed in detail in Chapter 5.

## **4.2. Mathematical Chronology Model**

### 4.2.1. Introduction

The objective of setting out a mathematical chronology model is to have a consistent set of definitions, relationships, and processes for the development, from tree measures, of series of tree indices and chronology indices. This chronology model forms a set of rules and some useful tools. The model is based on “traditional” methods with the addition of a number of novel features.

### 4.2.2. Creating Chronology Indices

The magnitude of the common forcing on tree growth is assumed to be a fractional deviation and an average growth year will produce an index value of 1.0. Values of the age-related growth curve represent the amount of growth expected in an average growth year and for this reason they are called “expected growth values”. Series of ring measures are presumed to be a composite of the age-related growth curve, the effects of common forcing, and high-frequency noise. In section 4.1 it was established that the common effect of climate forcing on tree growth is on the production rate of foliage. Because tree growth measures are made for a tree, the effect of common forcing on a tree will be proportional to the size (mass of foliage) of that tree which dictates the use of a multiplicative model for the manipulation of tree growth measurements and indices. In order to relate each ring width to each expected growth value and chronology index an error term is introduced. The error term represents the high-frequency noise that needs to be removed from tree measures by the averaging process of chronology creation. In this multiplicative model, error is considered as a fractional deviation and zero error has a value of 1.0.

$$\text{Ring width} = \text{Expected growth} * \text{Chronology index} * \text{Error} \quad (1)$$

Chronology indices are the arithmetic mean of tree indices for a year so:

$$\text{Chronology index} = \text{SUM (Tree index)} / \text{Count (Tree index)}$$

The values of tree indices in any year will vary and the differences between tree indices and a chronology index for a year is considered as “error” and an error factor is used where a value of 1.0 represents zero error.

$$\text{Tree index} * \text{Error} = \text{Chronology index}$$

The sum of errors in any year is zero as chronology indices are the mean of tree indices for the year so:

$$\text{SUM (Tree index} * (\text{Error} - 1.0)) = 0.0$$

Creating chronology indices, which are fractional deviations, from the arithmetic average of tree indices for a calendar year requires tree indices to be fractional deviations. To create tree indices as fractional deviations then the measured values must be divided by expected values so:

$$\text{Tree index} = \text{Ring width} / \text{Expected growth}$$

Up to this stage the chronology model follows “traditional” methods (Fritts 1976d; Cook et al. 1990) in that tree indices are created as fractional deviations by dividing measured growth by expected growth and chronology indices are the mean values of tree indices for each year, thus setting the sum of errors for each year to zero. In traditional methods, the mean value of chronology indices is usually rescaled to a value of 1.0. In this study, the mean value of tree indices is rescaled to 1.0 which sets the count-weighted mean value of chronology indices to 1.0 which deviates from traditional methods. The reason for this is that the “best fit means” (Section 4.3) method uses this definition of chronology index mean and this change, from traditional methods, has no other significant effects.

#### 4.2.3. Signal-free Measures

The objective here is to remove the effects of the common forcing signal from a series of ring-width measures. There appears no justification for fitting expected growth curves to series of measures that contain the effects of common forcing because the “expectation” is based on average values of the common forcing signal on tree growth. Chronology indices are fractional deviations and it is appropriate to remove the effects of common forcing from ring measures by division.

Re-arranging equation (1) above produces:

$$\text{Expected growth} = \text{Ring width} / (\text{Chronology index} * \text{Error})$$

This allows expected growth values to be described as signal-free, noise-free ring measures. A new measure is defined here, called the “signal-free” measure, with a value for each ring measure. Signal-free measures contain noise but do not contain the effects of common forcing.

$$\text{Signal-free measure} = \text{Ring width} / \text{Chronology index}$$

In Section 4.1 it was noted that each year of common forcing preconditions a tree’s growth for the rest of that tree’s life so the signal-free measures created here will only be

an approximation of the ring widths likely to be produced in an average climate, i.e. a sequence of years with no variation in the common forcing on tree growth. That the magnitude of the age-related growth curve is usually larger than the magnitude of the common forcing, is relevant to assessing the net effect of this preconditioning. The existence of unwanted noise in ring-width measures sets practical limits on the use of signal-free measures to the consideration of the average effect on many trees. This concept of signal-free measures is used in Section 4.4 to reduce distortion when using curve-fitting methods and in Chapter 5 to reduce the distortion found in RCS curves.

#### 4.2.4. Resetting Means or Rescaling

Some standardisation methods produce series of tree indices with a mean value of 1.0. There is no reason to accept this arbitrary mean value and the mean values of series of tree indices (or series of chronology indices) may need to be reset. The variance of series of tree indices is generally proportional to the local mean of the indices (Cook et al. 1990). In this study manipulation of the means of a series of tree indices is performed by the multiplication of all indices in a series by a common factor and the process is referred to as rescaling (Briffa et al. 1996). This is consistent with indices being fractional deviations with standard deviations proportional to the local mean values. This model does not allow the use of subtraction processes to generate tree indices or the resetting of variance without reference to the mean. Rescaling the variance of series of indices, performed in the normalisation process, is not allowed in the processes of chronology production. In Section 4.3 this rescaling is used to set the mean value of all series of tree indices to the mean values of chronology indices over their common period within the BFM method.

#### 4.2.5. Resetting the Slope

Some standardisation methods produce series of tree indices with a slope of zero. Dendroclimatologists generally leave the slope of a series of tree indices and chronology indices at the value of slope produced by standardisation. If standardisation produces series with an arbitrary slope and there is no reason to accept this arbitrary slope, the conclusion reached here is that “sensible decisions” might be used to adjust the slope of series of tree indices (or series of chronology indices). Matching the slope of a predominately temperature-controlled chronology to fit the slope of temperature measures over a common period might be valid. Matching the slope of a chronology to fit a “known” past temperature value derived from another proxy measure might be an

alternative approach. The variance of series of tree indices is generally proportional to the local mean of the indices (Cook et al. 1990). In this study manipulation of the slope of a series of tree indices is accomplished through the division of all indices in a series by the corresponding values of a straight line passing through the centre (or count-weighted centre for chronology indices) of the series.

Curve-fitting methods set the slope of each series of tree indices to zero. The only readily reversible method of adjusting slope appears to be by using a straight line through the centre of a tree (or count-weighted centre for a chronology). The only curve-fitting methods that remove slope in a “reversible” manner are those that use sloping straight lines because the other functions use curves that can “bend” to fit a tree. The RCS method uses the RCS curve which, although not straight, is completely inflexible, i.e. the values are fixed permanently by the tree measures used to build the RCS curve. Any slope adjustment caused by the division of ring-widths by the values of the RCS curve will be about the centre of the tree (as the mean values of either can be rescaled to fit). The effect will be similar to the slope adjustment created using a straight line because the “expected” curvature of the series of measures should exactly match the curvature of the RCS curve. The curvatures should cancel to leave the approximate effect of rotation using a straight line about the centre of rotation. This may not be an exact method but if, in practice, this method produces a good approximation then it has value.

The method of slope adjustment used here differs from the normal method of detrending with a straight line fitted by least squares methods because lines are constrained to pass through the count weighted centre of the series being rotated. The removal of slope is achieved by rotation about the count-weighted centre and is by the division of all values of the series by the corresponding values of a sloping line, a method which will maintain the relationship between mean and variance. The calculation shown below is for chronology indices. For tree indices the counts are set to 1.0 for each year, the change of slope “a” needs to be known, and the final equation resets the mean to 1.0.

Year(1:n) = Chronology year numbers  
Count(1:n) = Counts of rings for each year of the chronology  
Index(1:n) = Chronology index values  
Z = Count-weighted centre of rotation (year)  
a = Slope change required



$$Z = \text{SUM} (\text{Count} (1:n) * \text{Year}(1:n)) / \text{SUM} (\text{Count}(1:n))$$

$$\text{Index} (1:n) = \text{Index}(1:n) * (1.0 + a * (Z - \text{Year}(1:n) ) )$$

$$\text{Index}(1:n) = \text{Index}(1:n) * \text{SUM} (\text{Count}(1:n)) / \text{SUM} (\text{Index}(1:n) * \text{Count}(1:n))$$

This rotation is easily reversed because the count-weighted centre remains fixed and the only variable is “a”. If index values are allowed to “weight” the position of the centre the rotation the centre of rotation may move and reversal is difficult. The need to rotate chronology indices arises because some standardisation methods (both existing and those introduced within this study) create chronologies with arbitrary slope of zero or worse i.e. some unwanted value of slope. That the slope is “undetermined” allows the pragmatic decision to impose or prescribe a specified slope.

#### 4.2.6. Summary

Chronology indices are presumed to be fractional deviations and tree indices are presumed to be fractional deviations with noise. Division and multiplication are used to manipulate the values of measurements and indices and a number of addition or subtraction processes are not allowed. The concept of signal-free measures is introduced. Count weighting is set as a standard when dealing with chronology means and slopes. Series of tree indices and chronologies that have arbitrary slopes may be rotated.

### 4.3. *Best Fit Means (BFM)*

#### 4.3.1. Introduction

This section deals with long-timescale trends at or beyond the length of a series of tree indices so that the variables of interest are the mean values of each series of tree indices. Creating a chronology from overlapping series of tree indices is traditionally performed by calculating arithmetic means (Fritts 1976d). When each series of tree indices has the same mean value as the chronology indices over their common period the series of tree indices are described here as having their “best fit means”. Chronologies are created from the arithmetic mean of tree indices and procedure BFM is developed to rescale each series of tree indices to have “best fit means”. An explanation follows as to why “best fit means” are needed, how they are calculated and their value in dendroclimatology.

#### 4.3.2. Trend in Mean

Trends (periods of above or below average chronology indices) for periods longer than the length of a series of tree indices are contained in the mean value of the series. If a 200-year long chronology is created by joining two 100-year long trees end on, then, if the mean values of indices for each tree are the same, there will be no variance at periods beyond 200-year frequency and if the mean values of indices of each tree are different there can be variance at periods beyond 200-years. Manipulation of the values of tree indices that does not change the series means will not change the long-timescale trends of the resulting chronology at periods longer than those of the life-span of the trees. The assumption is made in this study that these statements concerning the limits of the preservation of low-frequency variance apply to chronologies developed by averaging multiple overlapping series of tree indices of varying lengths.

#### 4.3.3. Overlapping Trees

The assumption is made that the values of tree indices are fractional deviations of measured growth from expected growth and that the common forcing of a specific year will produce similar tree index values for all trees. The division process used to remove the age-related growth trend (medium-frequency noise) leaves tree-indices which are, by definition, identical in value apart from the existence of unwanted high-frequency noise, referred to as “errors”. The expected mean value of random noise for the same year is zero, because of averaging, and the assumption is made here that the noise in a series of tree indices will be normal. The possibility of bi-modal or other distributions is ignored. (Both the effects of mechanical wind stress with consistent differences in tree cores taken pointing in different compass directions and the presence of trees with light/heavy seed production in the same year (Tappeiner 1969) could create bi-modal distributions). Overlapping sections of series of tree indices ought to have similar mean values, because growth forcing is common and the indices represent this growth forcing. The mean value of any series of tree indices would then be the same as the mean value of chronology indices over their common period, consistent with a zero sum of errors for each series. If detrending methods produce series of tree indices that are consistent with the chronology (the mean value of tree indices equals mean value of chronology indices over the common period) then BFM is not needed. If detrending methods cannot establish the “correctly fitting” mean value of a series of tree indices then the mean value of the series of tree indices should be left “floating” until the chronology indices are created. The

assumption is made that if the mean value of a series of tree indices is not consistent with the chronology then, consistent with a multiplicative model, the mean values should be “corrected” by rescaling. This assumption implies that a series of tree indices can only provide information about the common forcing signal during the period of growth and that information concerning growth trends at periods beyond the length of the series is absent.

#### 4.3.4. Best Fit Examples

An example is discussed to illustrate the overlapping of tree indices over a common period. Presume there is a 400-year long chronology to be made from two overlapping 300-year series. Each has a linear life-span trend with a 10% growth increase each century and some random noise. Both index series have means of 1.0. If they are averaged (as shown in Figure 4.3.1) the mean series (blue line Fig. 4.3.1b) is created with off-set or biased ends. Rather than use simple arithmetic averaging, a method of fitting these trees to form a more valid chronology is to set the mean values of the period common to both trees to the same value by rescaling all the indices of one tree. The chronology indices, created by averaging, can then be rescaled to a mean of 1.0. This will produce a 400-year long chronology with a 10% growth increase each century (red line Fig. 4.3.1b) and results in finding the “best fit mean” values for each series of tree indices; in this case the means will be 0.92 and 1.08 respectively. The trees do not contain trends at periods beyond 300 years and yet the chronology contains a trend of period 400 years. Low-frequency variance has been introduced by resetting the mean values of tree indices. The assumption behind this procedure is that the common forcing continued for 400 years and trees growing in a common period will have experienced similar “fractional deviations” from their expected growth.

The second example uses a simulated “modern” chronology with all series of tree indices ending on the same year. The 51 series, with ages ranging from 100 to 300 years, have been created artificially to simulate a standardisation method that can preserve a life-span trend and produces series of tree indices with means of 1.0. The chronology indices are known and the values are 0.97 for the first 250 years and 1.16 for the last 50 years and each series of indices has the same value as the chronology indices, but with their values of each series rescaled to a mean of 1.0. Averaging these series of tree indices, each with a mean of 1.0, produces a chronology with the expected common signal but with an

Fig 4.3.1a Two generated series of tree indices.

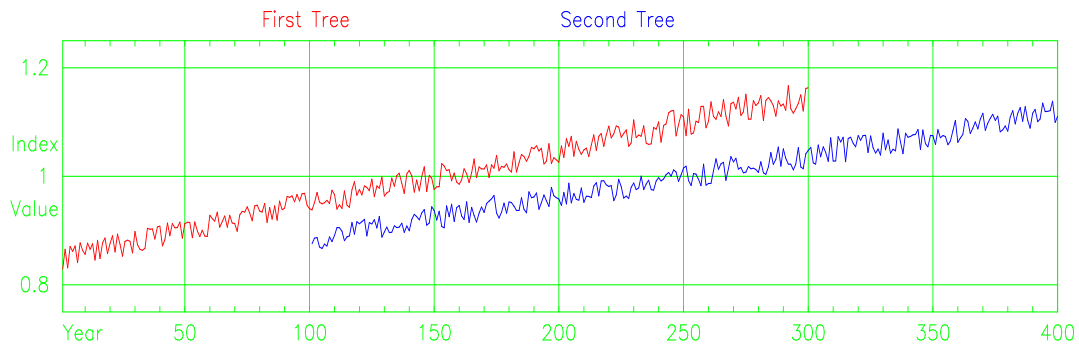


Fig 4.3.1b Chronologies from first and second tree by arithmetic and BFM methods.

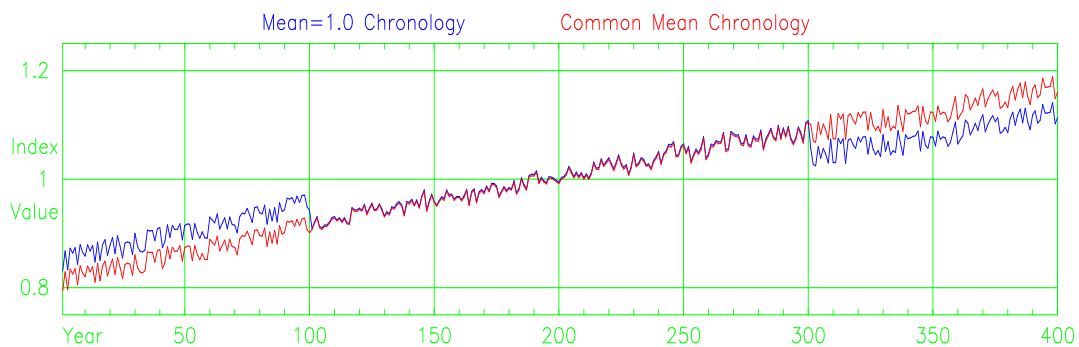


Fig 4.3.1c Chronologies from indices with means of 1.0 by arithmetic and BFM methods

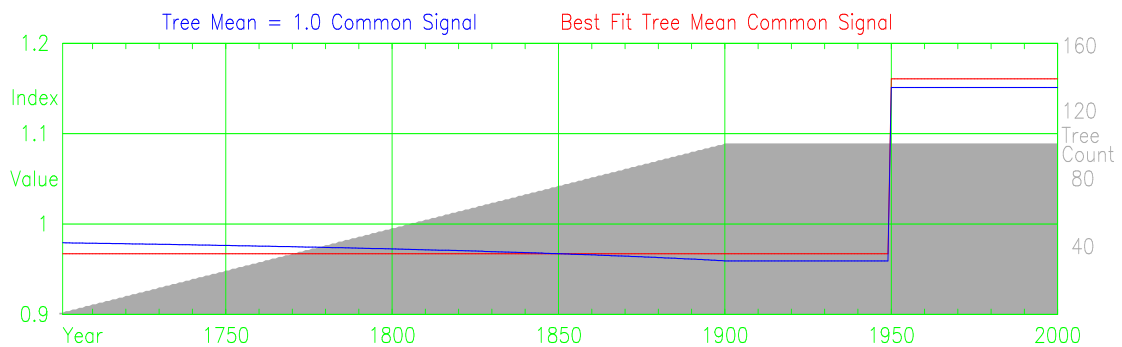


Figure 4.3.1 (a) Two generated series of tree indices, (b) chronologies from these by arithmetic mean and by BFM method, and (c) chronologies from series of indices with a mean of 1.0 by arithmetic mean and by BFM method.

apparent downward trend in the first two centuries (blue line Fig. 4.3.1c). The trend represents a 2% slope over the first century, when tree counts are changing due to differences in tree ages. The chronology index values are known and “best fit means” can be calculated for each series of tree indices over the common period of the chronology. The mean value of tree indices of the 100-year-old tree will be 1.07 and the mean value of tree indices of the 300-year-old tree will be 1.00 and other trees will have values between these. After averaging all trees the chronology indices can be rescaled to have a mean of 1.0. The chronology created as the arithmetic mean of tree indices, after “best fit means” are set, contains the common signal that is wanted (red line Fig. 4.3.1c). The

importance of this example is that if the method of detrending can preserve a life-span trend in series of tree indices then leaving the mean value of series of tree indices at a value of 1.0 will introduce a bias into the resultant chronology. It would be possible in this example to use the last 100 years as a common period and set the means of all trees to a common mean but in many chronologies there may not be a suitable common period so the BFM method becomes necessary.

In both these examples the original values of the means of series of tree indices are unimportant because they are changed and, given the specified mean value of chronology indices, there is only one positive value of the mean of each series of tree indices that will achieve a best fit value. If a detrending method cannot retain a life-span trend in series of tree indices there will be no benefit in using the BFM method. Series of tree indices created using data adaptive standardisation methods do not have an overall trend, a best fit straight line to these series would be approximately horizontal, and overlapping such series is unlikely to produce an overall trend in a long chronology. If a detrending method can retain a life-span trend in series of tree indices but cannot retain variance at frequencies lower than that of the length of individual series, then the BFM method should be used. If the mean values of series of indices are not set to their “best fit” values, then averaging of these series will generate low-frequency variance that is inconsistent with the assumption that indices are fractional deviations. If a detrending method can produce series of tree indices which have a life-span trend and mean values which are consistent with the low-frequency variance in the chronology then these means will already be the best fit means and no further action is necessary.

#### 4.3.5. Best Fit Means Procedure

The procedure must find a mean value for each series of tree indices such that this mean is identical to the mean value of chronology indices over their common period. The inputs are dated series of tree indices. Indices are all positive and are assumed to be fractional deviations, which can be rescaled by the multiplication of all indices in a series by a constant. Series must be continuous, and series must overlap in time with at least one other series. Any missing or aberrant sections in series, i.e. segments with null values, can be removed by splitting a series into separate series of at least two years length. The resulting chronology must be continuous and all years must be connected to a neighbouring year by a series with indices for both years, series that butt up against each

other without any overlap are considered unconnected. Floating sections of chronologies can be treated as separate chronologies. The overall mean value of indices from all series will be set to 1.0.

The mathematics is described using a hypothetical chronology made from four trees (A, B, C and D) each with a series of indices ( $x_A(1:n_a)$ ,  $x_B(1:n_b)$ ,  $x_C(1:n_c)$  and  $x_D(1:n_d)$ ). Each series of indices is rescaled to have a mean of 1.0 and the means ( $m_A$ ,  $m_B$ ,  $m_C$  and  $m_D$ ) need to be found to create a BFM chronology. A chronology index is the sum of all indices for that year divided by the number of indices in that year and an array of tree counts by year,  $N(1:r)$ , is created for the chronology. The following illustrates setting the mean value of each tree's indices to the mean value of chronology indices, excluding that tree, so one is subtracted from each value of  $N(1:r)$ . For the means to be equal, the sum of chronology indices equals the sum of tree indices over the period of overlap between tree and chronology years which have more than one tree. The periods (p:q), (r:s) and (u:v) for trees A, B and C are used to form sets of simultaneous equations relating the means of all trees to each other (Table 4.3.1).

	$m_A$	$m_B$	$m_C$		$m_D$
1	$+\sum(x_A(p:q))$	$-\sum(x_B(p:q)/N(p:q))$	$-\sum(x_C(p:q)/N(p:q))$	=	$+\sum(x_D(p:q)/N(p:q))$
2	$-\sum(x_A(r:s)/N(r:s))$	$+\sum(x_A(r:s))$	$-\sum(x_C(r:s)/N(r:s))$	=	$+\sum(x_D(r:s)/N(r:s))$
3	$-\sum(x_A(u:v)/N(u:v))$	$-\sum(x_B(u:v)/N(u:v))$	$+\sum(x_A(u:v))$	=	$+\sum(x_D(u:v)/N(u:v))$

Table 4.3.1 Simultaneous equations relating the mean values of tree indices.

All the Table entries are derived from the known values of indices and counts. Elimination and back-substitution result in our being able to describe all tree means in terms of tree D.

$$m_A = x * m_D, \quad m_B = y * m_D, \quad m_C = z * m_D$$

Assuming the sum of all indices equals the count of indices (mean = 1.0) then the value of  $m_D$  can be found from:

$$m_D = (x * n_a + y * n_b + z * n_c + n_d) / (n_a + n_b + n_c + n_d)$$

The values of all other means can then be found.

The above finds best fit means for tree to chronology excluding the tree but adding an extra term, for the current tree, to the chronology index mean allows a similar calculation to find the best fit means where the chronology includes the tree. The sequence of series

was found to be immaterial for all chronologies tested in this study. The BFM procedure uses series of dated tree indices and is independent of the method of standardisation used to create the tree indices. The relative sizes of indices within a series are not changed because rescaling is by the multiplication of all indices of a tree by a constant. This procedure is implemented as a FORTRAN subroutine.

#### 4.3.6. Evaluation – Best Fit Means

Testing the BFM procedure was a simple check that the mean values of series of tree indices were equal to the mean values of chronology indices and the procedure passed this test. Series of tree indices with a life-span trend are needed to evaluate the BFM procedure which leads to using tree indices created using the RCS method. Strictly speaking, indices created by the RCS method are not fractional deviations (Section 4.1) but this is ignored for now. Long chronologies of overlapping trees, the Tornetrask AD and Finnish-Lapland AD chronologies are used to evaluate the BFM procedure. The tests devised are repeated on both these chronologies. For presentation purposes graphs are smoothed, with a low-pass spline with a 50% magnitude cut-off set at 5% of chronology length). Where relevant, tree counts are displayed on the graphs.

The BFM method initially sets the mean value of all series of tree indices to 1.0, thus discarding variance at timescales beyond that of the length of constituent series. In Figures 4.3.2 the differences between chronologies and the differences between the means of series of tree indices are shown for chronologies developed using arithmetic means and BFM methods. The chronologies created using arithmetic means and BFM are surprisingly similar (Figure. 4.3.2 (a) and (c)) considering that the mean values of series of tree indices are so different. Sorting trees by rising value of RCS generated “mean value of indices” for each tree, highlights the difference and in general the values generated by BFM (red line Figure. 4.3.2 (b) and (d)) appear random with regard to the RCS generated series of indices (blue line Figure. 4.3.2 (b) and (d)). The slow growing and fast growing trees are allocated smaller and larger mean values respectively using the RCS method whilst the means generated by BFM appear to be independent of the growth rates of these trees. That series of tree indices with such different mean values create such similar chronologies when index values are averaged by calendar year demonstrates that the BFM method generates low-frequency variance independently of mean growth rate.

Fig 4.3.2a Chronology comparisons – Tornetrask AD Chronology

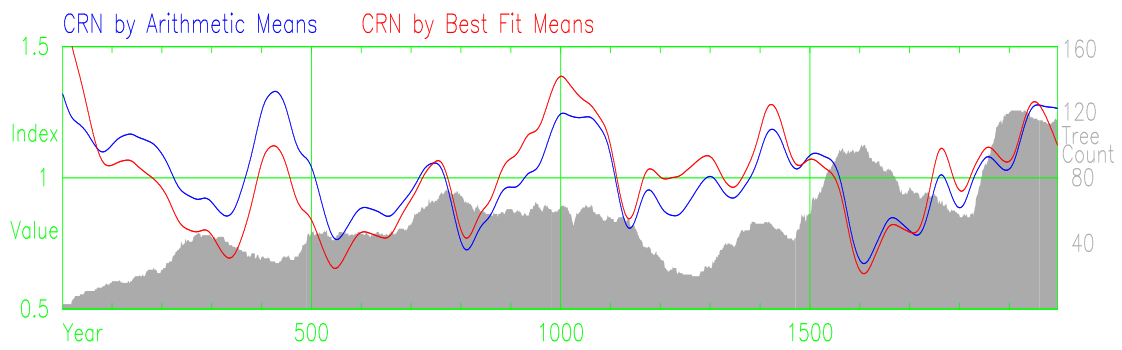


Fig 4.3.2b Means of tree indices comparison – Tornetrask AD Chronology

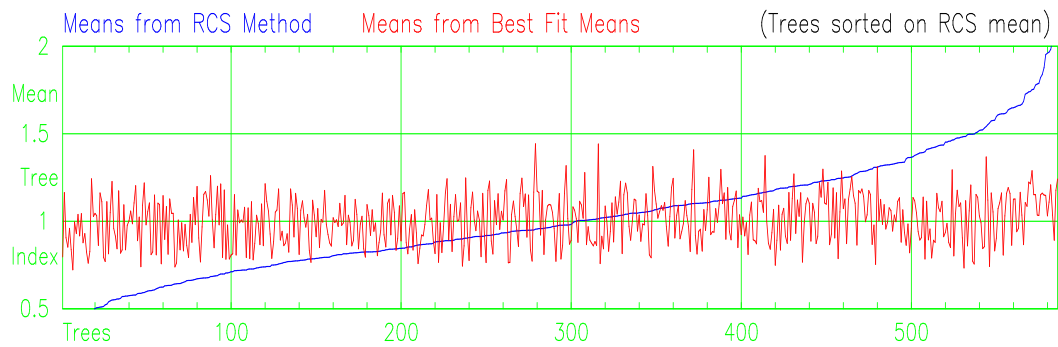


Fig 4.3.2c Chronology comparisons – Finnish-Lapland AD Chronology

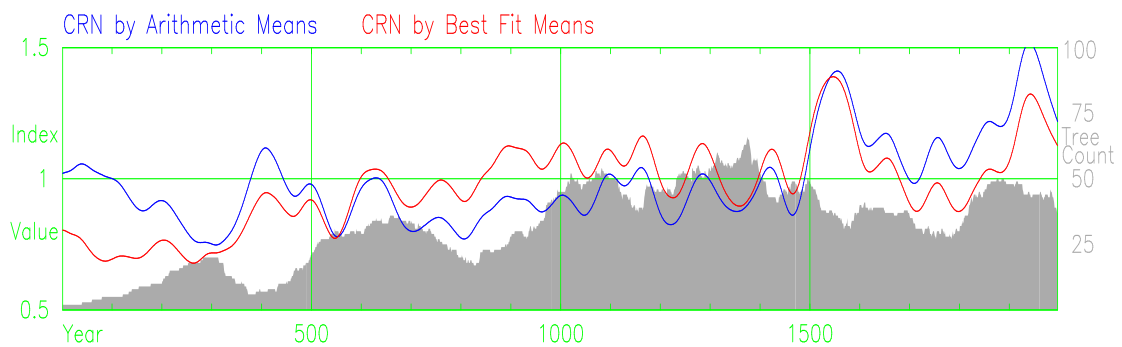


Fig 4.3.2d Means of tree indices comparison – Finnish-Lapland AD Chronology

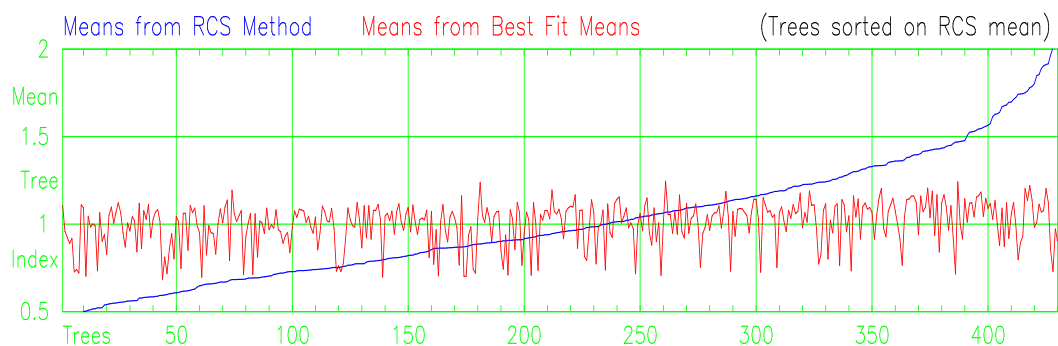


Figure 4.3.2 (a) and (c) Chronologies created using arithmetic and BFM methods. (b) and (d) The mean values of series of tree indices created using the RCS and BFM methods, both sorted on the RCS method mean.



The measurement series are categorised as “faster” or “slower” growing trees according to the time taken to reach 10cm radius. The RCS method produces series of tree indices with mean values that are larger for faster growing trees than for slower growing trees. The BFM method calculates the mean values of series of tree indices to fit the chronology. The question here is how different are the arithmetic means of faster and slower growing trees using tree indices created by the RCS and BFM methods. Figure 4.3.3 (a) and (c) show the RCS mean value chronologies separately for faster and for slower growing trees and plots (b) and (d) show the BFM mean value chronologies for faster and slower growing trees. Tree counts are shown for the fastest growing trees (a) and (c) and the slowest growing trees (b) and (d). The large differences in the RCS generated mean value of tree indices for faster and slower growing trees is expected, because the RCS method uses the growth rates of trees to establish low-frequency variance in chronologies. This magnitude difference will result in the RCS method placing more “weight” on faster growing trees in the final chronology. The RCS generated chronology will be sensitive to random variations, such as microsite differences, in the rates of growth of trees and will require a lack of bias in tree selection. The BFM method produces similar chronologies for both rates of growth over most of the length of the chronologies. The BFM method will be more robust in the presence of varying growth rates. The disadvantage of the BFM method is that it is unable to distinguish between the fastest and slowest growing trees and variations created by latitudinal or altitudinal differences cannot be studied using the BFM method.

The overlapping procedure in BFM is similar to recreating original values from a series of first differences and a known constant. Errors will propagate along the series (in either direction) and the mean levels either side of any weak points, such as small numbers of trees, will be uncertain relative to each other. If a series of tree indices is considered as having an overall slope with superimposed high-frequency noise, then the magnitude of the noise and the length of the series will be factors in establishing the amount of “error” that can be imparted on this slope by the noise. The longer the series the smaller is the potential for slope error due to noise. Increasing the number of series (sample depth) will decrease error but this depth will need to be “overlapped depth”. If 20 trees are joined in a situation where ten trees end on year 1901 and the other 10 trees start on year 1900 the overlap at 2 years is small despite the sample depth being large.

Fig 4.3.3a Chronologies by averaging RCS indices – Tornetrask AD Chronology

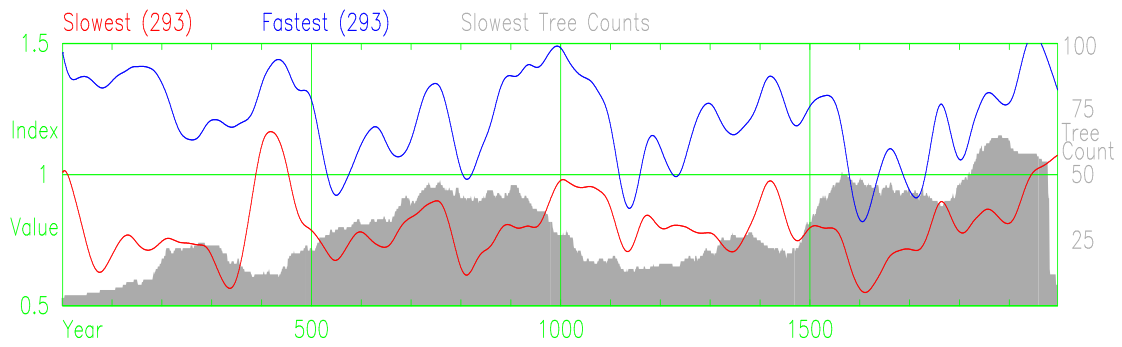


Fig 4.3.3b Chronologies by BFM method – Tornetrask AD Chronology

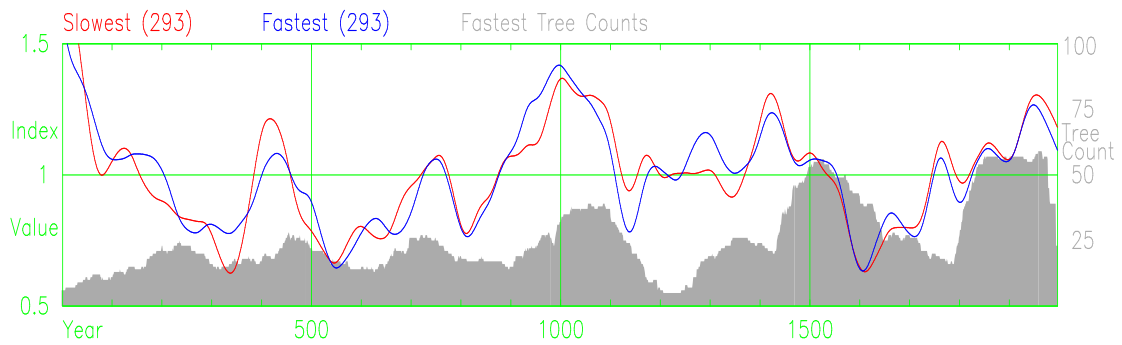


Fig 4.3.3c Chronologies by averaging RCS indices – Finnish–Lapland AD Chronology

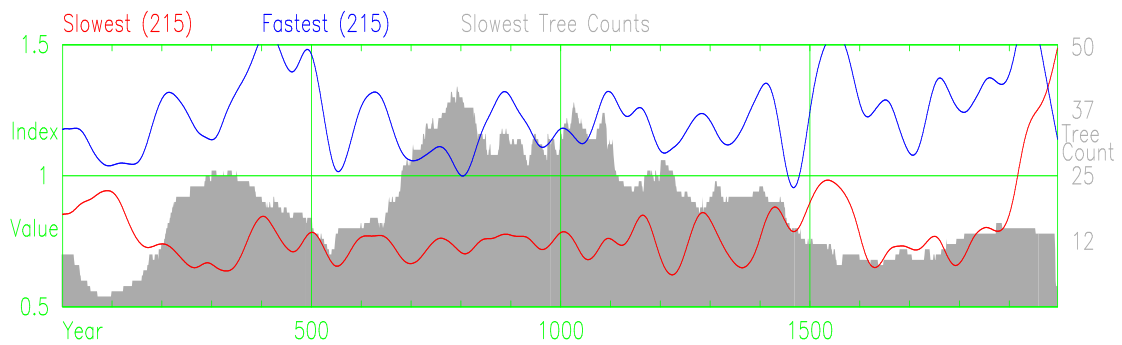


Fig 4.3.3d Chronologies by BFM method – Finnish–Lapland AD Chronology

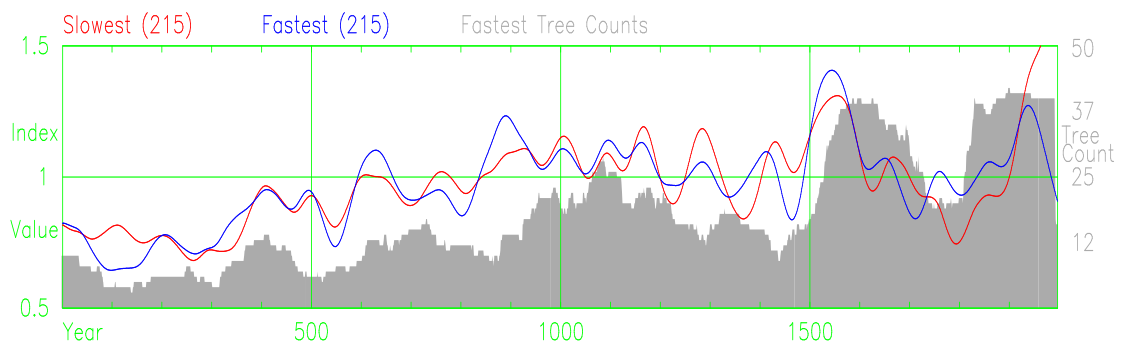


Figure 4.3.3 Comparison of chronologies made using indices created by the RCS method, (a) and (c) chronologies by arithmetic means and (b) and (d) chronologies created by the BFM method. Fastest and slowest trees based on time to reach 10cm radius.

The series of indices generated by the RCS method contain life-span trends with noise and the effect of reducing the mean length of series of tree indices is tested using the BFM method. The BFM method discards variance beyond the length of the series of tree indices by setting the mean values of all series to 1.0 before proceeding and the question being asked is how much variance can be discarded without inducing major changes to the resulting chronology indices? Series of trees indices were sub-divided into maximum lengths of 150, 100 and 50 years and the original and resulting series of indices were used to create chronologies by BFM methods. The amount of variance discarded by these subdivisions is progressively increased. Tree counts reduce in the first few centuries and in order that the variability in this time period should not unduly influence the more well replicated sections the slopes of all chronologies was set to zero and the means of chronology indices set to 1.0 for the period 600 to 1600 A.D. in order to highlight the differences between chronologies at periods of 1000 years and below. The results are shown in Figure 4.3.4 where the chronology corresponding to each mean length of series is shown by a different colour: with full series (black), maximum length 150 years (blue), maximum length 100 years (red), and maximum length 50 years (cyan). Differences are greater in the first few centuries for both sites and differences are larger for the 50 year length limit (cyan) than the other chronologies. Where the sample depth drops to ten trees at 400 A.D. the Tornetrask chronologies diverge considerably. The Finnish-Lapland chronologies appear “unstable” at around 540 A.D. where sample depth is 15, a sample depth that causes no apparent problem for the Tornetrask trees at 800 A.D. There was a severe environmental anomaly around AD 540 (Baillie 1994) shown by narrow rings at Tornetrask in AD 536 and AD 542. This event may have reduced the “overlapping depth” (trees died and trees germinated around this period) despite the sample depth, a problem shown in Figure 5.8.3 and discussed in Sections 5.8 and 6.3.

The long-timescale variance preserved by both RCS and BFM methods is preserved in the mean values of series from theoretical considerations. Simply replacing each index in a series by its mean value should allow the long-timescale variance to be isolated. This long-timescale variance is compared in Figure 4.3.5. Each value of a series was replaced by the mean value of the series and the resulting mean-value series were averaged to create “mean-tree” chronologies. The two methods produce roughly similar mean-tree chronologies using the Tornetrask trees (Figure. 4.3.5a) for the central parts of the

chronologies. (The trees used to extend this chronology from mid 1980s to late 1990s appear to be faster growing than the trees used earlier which is not a significant problem

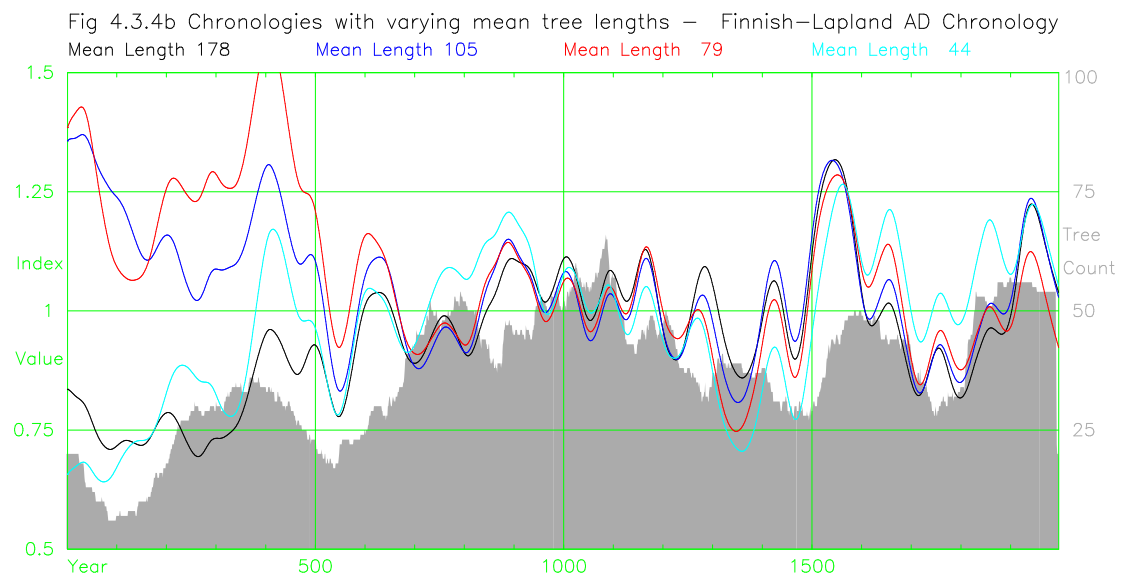
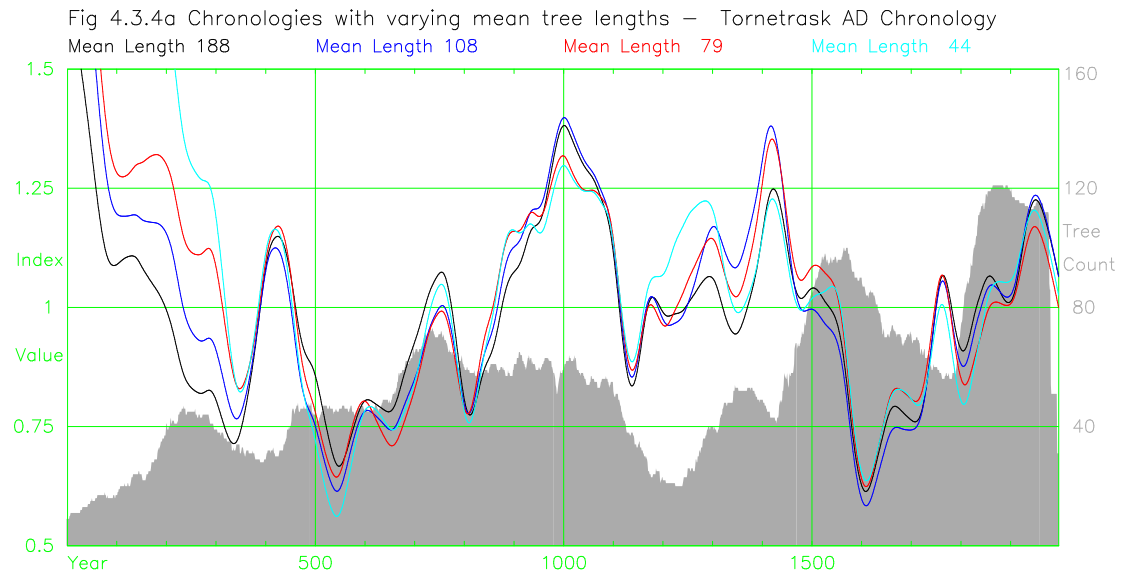


Figure 4.3.4 Chronologies made from indices created by the RCS method and averaged using BFM method. Series of differing maximum lengths subdivided to obtain each chronology. Slopes set to zero and means to 1.0 for period 600 to 1600.

for the BFM method which does not use growth rates.) The two methods produce differing “mean-tree” chronologies using the Finnish-Lapland trees (Figure. 4.3.5b) even after allowing for the difference in the overall slope of the chronologies. The BFM mean-tree chronologies are smoother than the RCS mean-tree chronologies because each series “fits the chronology” over their common period. There is a small phase shift between RCS and BFM mean-tree chronologies. The problems with indices generated by the RCS method (Section 5.2 to 5.5) severely restrict conclusions from mean-tree chronologies.

Fig 4.3.5a Mean Tree Chronologies – Tornetrask AD Chronology

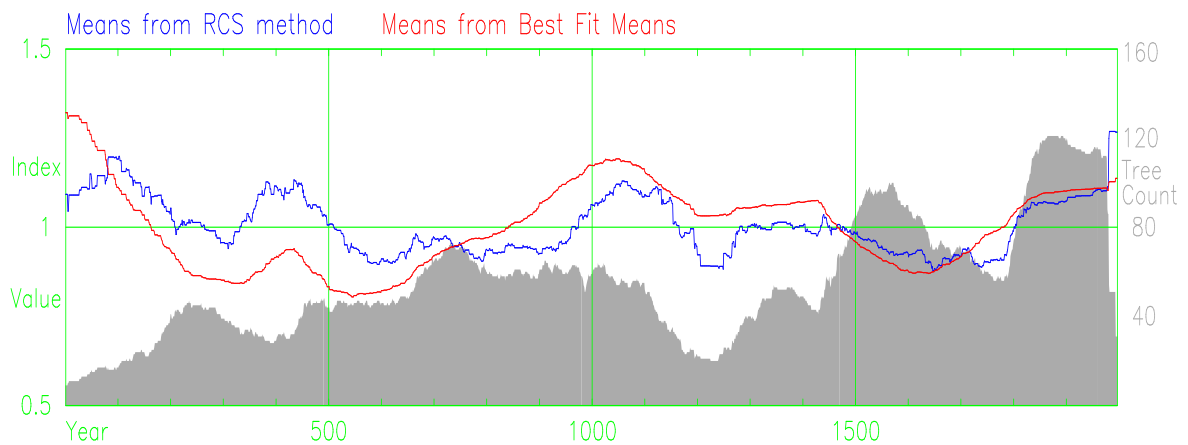


Fig 4.3.5b Mean Tree Chronologies – Finnish–Lapland AD Chronology

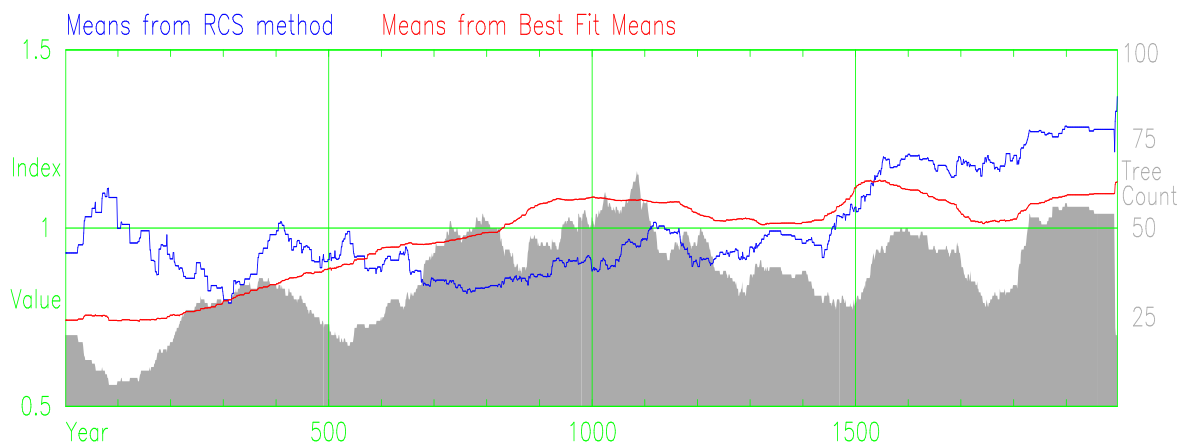


Figure 4.3.5 Comparison of mean tree chronologies by RCS and BFM methods. All indices of each tree replaced by the series mean.

#### 4.3.7. Discussion

The BFM method is a tool for averaging series of tree indices and only addresses a part of the standardisation procedure. It is restricted to processing series of indices that are fractional deviations and have a meaningful overall slope. It could be used to “average” a number of separate chronologies to form a regional mean but not to average series of temperature measures (variance not proportional to mean) over a region. There is potential to examine alternative “best fit means” applications such as resetting the slope (as well as mean) of tree indices to fit the slope of chronology indices or using additive methods which do not presume a relationship between mean and variance. There is an “overlapping” problem which might be quantified using a theoretical approach but, because the variability in series of tree indices is unpredictable, no attempt at quantification has been made here. The first decades of series of tree indices often contain larger proportions of error, because of the large variance in the growth rates of saplings,

which may cause a problem for the BFM method. The RCS method is not suitable for a detailed evaluation of this procedure and further evaluation is left to later stages of this study where the BFM method is built into alternative standardisation methods which are evaluated. Evaluation of the BFM method is as part of a standardisation method and not in isolation. The conclusion, at this stage, is that the “best fit means” method is a credible alternative to the use of mean growth rates for the capture of variance at periods beyond the length of the constituent series of tree indices. What this low-frequency variance “is”, remains to be tested. The BFM method is a mathematical procedure for finding the mean values of series of indices such that these means will have the same value as their arithmetic mean over the common period.

The main benefit of the BFM method to standardisation procedures is that it enables long-timescale variance to be established from tree growth measures without the need to use mean tree growth rates. The generation of expected growth curves can proceed free from the distortion created by the need to retain the mean growth rates of a tree in a series of tree indices.

#### **4.4. Trend distortion**

##### **4.4.1. Introduction**

The problem being addressed here is that the existence of medium-frequency common climate-related variance in series of ring-width measures can cause a serious problem when using curve-fitting methods of standardisation. Because the fitted curves are not able to distinguish between climatic and non-climatic variance in measured ring-width series, data adaptive standardisation methods remove some of or distort the climate signal of the resulting chronology. The approach taken here to illustrate this is to use “artificially” created signals and show how well these are represented in the chronologies generated using a representative curve-fitting method. The Hegershoff Curve (Warren 1980) method of standardisation is selected for exploration of this problem because this method is a commonly used example of “curve-fitting” techniques. It was also used to demonstrate the sensitivity problem (Briffa et al. 1998b). The implementation of the Hegershoff method used here is taken from program ARSTND (Cook 1985). It consists of the selection of an age-related growth curve for each tree from a hierarchical series of *a priori* mathematical models; a Hegershoff curve, a modified exponential curve, a negatively sloping line, and a horizontal line (Section 2.5.4). The extreme case of a step

increase in tree growth rates is chosen because such an event appears to have occurred in the European boreal forest in the 20th century. A ubiquitous increase in tree growth rates was reported (Briffa et al. 1998a) and foresters have noted a large increase in tree growth rates in the boreal forest across most of Europe (Spiecker 1996), in Finland (Mielikainen & Timonen 1996), in Denmark (Skovsgaard & Henriksen 1996), in Sweden (Elfving & Nystrom 1996), in France (Badeau et al. 1996) and in Germany (Wenk & Vogel 1996).

The problem is demonstrated in Section 4.4.2. In Section 4.4.3 the problem is named and the effects of detrending a randomly generated series of tree measures with an added “common signal” are used to show the source of the problem. The extent of the problem is discussed in Section 4.4.4 and in Section 4.4.5 simulated chronologies are used to show the effects of this problem on selected artificially generated medium-frequency common forcing signals. In Section 4.4.6 the methods developed later (Section 5.5.8) are used to show that the problem can be avoided in the specific examples used here and these results are then summarised and discussed.

#### 4.4.2. Demonstration of the Problem

The series of ring-width measures forming the Luosto and Helldalisen chronologies (Section 3.3.3) are used for this demonstration. The trees from these two sites form a well-replicated body of measurements covering the last four centuries. Different growth regimes are simulated for the period from 1920 to 2000 by changing the values of ring-width measures for this period. Three artificial chronologies of ring-width measures were created from the series of measures by the multiplication of measured values, from 1920 onwards, by a constant factor for each generated chronology. The chronologies are colour coded (Figures 4.4.1 and 4.4.4) for display purposes. The chronology derived from the original unmodified measured values is plotted in black; the results of a 30% increase and a 30% decrease in ring widths after 1920 are shown by the red and blue lines respectively while a much larger decrease of 60% to all series is shown by the magenta line. The mean ring-widths of each chronology are plotted by calendar year from 1750 to 2000 in Figure 4.4.1(a) and the magnitude of the changes to mean ring width from 1920 are clearly visible. The chronology indices generated by standardising these four sets of tree measures using the Hegershoff method are plotted in Figure 4.4.1(b). In the last 3 decades Figure 4.4.1(a) shows a 3 fold difference in mean ring-width while over the same period there is little difference in the magnitude of chronology indices created by the

Hugershoff method. The high-frequency signal is preserved in all chronologies whilst at decadal-plus frequencies the chronology indices do not represent the known differences in the magnitude of the series of ring-widths. These graphs show that chronologies created using the Hugershoff method are liable to distort any evidence of a ubiquitous recent step increase in tree growth.

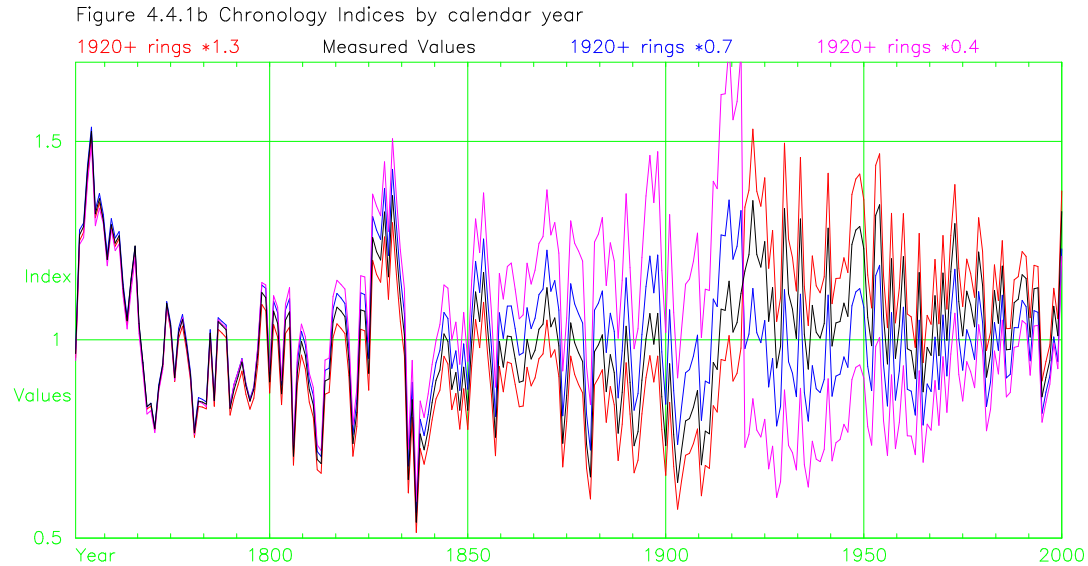
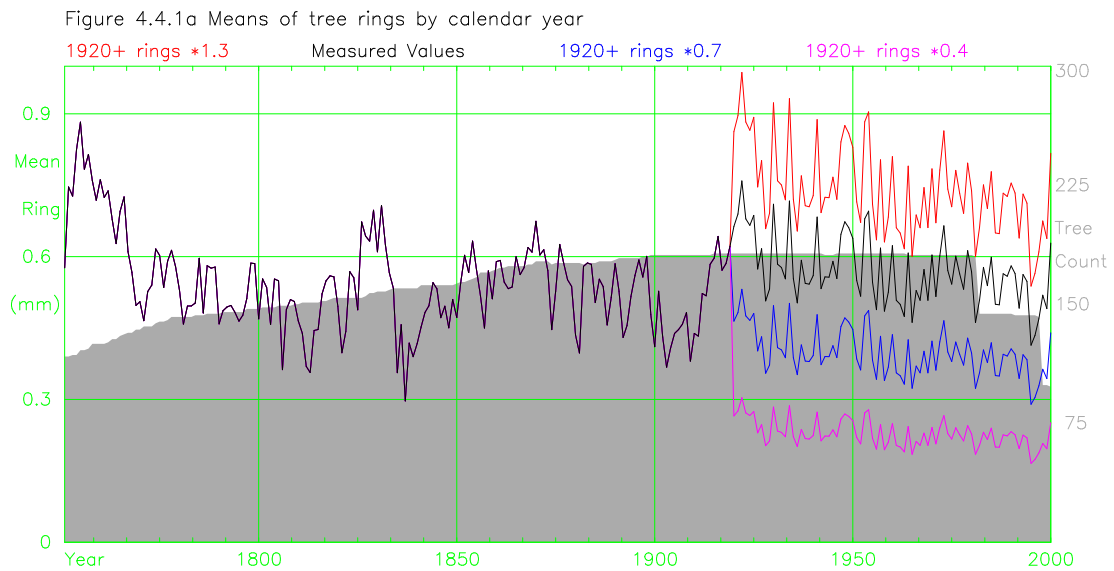


Figure 4.4.1 Hugershoff standardisation of chronologies created using the Luosto and Helldalisen trees. Ring width values from 1920 onward adjusted by factors of 1.3, 1.0, 0.7 and 0.4.

The plotted curves in Figure 4.4.1 show clearly the relationship between high-frequency variance and the local mean of values for both mean ring-widths and chronology indices, a result of assuming that the common signal is a fractional deviation and the use of multiplication. High-frequency variability is not affected but clear medium-term



distortion occurs. Index values from 1850 to 1920 are unduly raised, in comparison with the timing of simulated growth change because of lower ring-widths after 1920 and are depressed in response to the increase in all ring-widths after 1920. Indices relating to the 30% increase (red) and measured values (black) decay after 1920 indicating a step increase in ring-width after 1920 whilst indices for the 60% decrease (cyan) increase after 1920 indicating a step decrease in ring-width after 1920. Indices with a 30% decrease (blue) after 1920 have values around 1.0 without any slope which is indicative of no step change from 1920 onwards. The increase of 40% in ring-width is consistent with reports of foresters in Fennoscandia.

#### 4.4.3. Trend distortion

In this study the name “trend distortion” is used to describe this problem because the “assumed” cause of this problem is the existence of medium-frequency variance in the common forcing signal (trend) which distorts the resulting series of tree and chronology indices. “Ideally” the effects of common forcing should be removed from series of measures prior to estimating the expected growth curve because short term increases or decreases in growth rates are not “expected” from general tree ageing. When using curve-fitting methods to estimate expected growth curves, tree measures which contain the effects of common forcing are used and the values of tree and chronology indices created can hence differ from the “ideal”, i.e. distortion can occur. An example is used here to demonstrate trend distortion in a simple hypothetical ring-width series. A series of measures (cyan line, Figure 4.4.2a), with a two decade long growth increase near the recent end, are used to simulate a known temporary change in common forcing. A visually estimated detrending line (blue line, Figure 4.4.2a) has been fitted by ignoring the known common forcing and fitting a smooth line to the series of measures that would be “expected” if the known growth increase had not occurred. A negative exponential detrending line (red line, Figure 4.4.2a) is fitted by the least squares method to the series of measures including the growth increase. The difference between the two expected growth curves is created by “detrending” the known common forcing signal. The indices produced by division are displayed in Figure 4.4.2.b and the difference between indices created using the visually estimated detrending curve (blue) and indices created using the negative exponential detrending curve (red) are plotted as a grey wedge. This grey wedge, as the difference between the signal generated by detrending series of tree measures both with and without the common forcing signal, is trend distortion.

Figure 4.4.2a – Alternative expected growth curves for a tree with a short growth increase.



Figure 4.4.2b – Alternative series of indices and the difference as trend distortion.

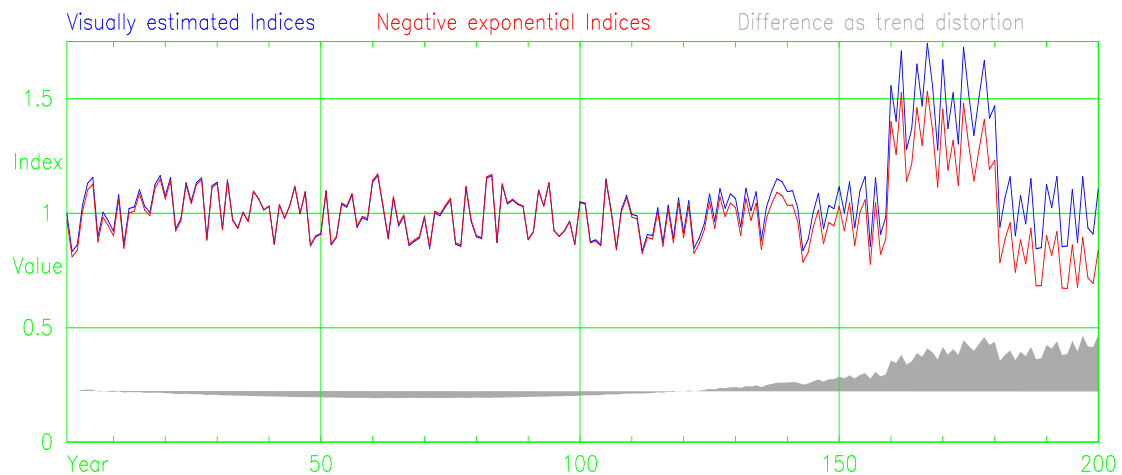


Figure 4.4.2 Illustration of trend–distortion using alternative expected growth curves on a randomly generated tree with a two decade long growth increase.

#### 4.4.4. Why and When a Problem

The simplest form of trend distortion occurs when a series of measures is detrended by calculating a least squares fitted straight line and indices are then created by the division of the measured values by the values of the straight line. The resulting indices will have the property that the sum of the product of index value and distance from the centre of the straight line (units of value \* years) will be zero. Distance to the left is positive, distance to the right is negative, and the “moments” of two halves of the series of tree indices will balance. The straight line detrending and division process sets the sum of the product of index value and distance from the centre to zero by varying every index by an amount proportional to that index’s distance from the centre of the line. The “excess moment”

created by a medium-frequency trend such as a step increase near the end of a series can only be “balanced” by adjusting every index value. A straight line detrend will produce symmetrical wedges of trend distortion about the centre with magnitudes of opposite signs. For detrending curves that are more flexible than a straight line the trend distortion will be of limited extent. The negative exponential curve (which can “bend to fit”) used on the randomly generated tree shown in Figure 4.4.2(a) has “balanced” the growth increase over a period of two decades (years 160 to 180) by reducing the values of all indices from years 100 to 200 by an amount proportional to the distance from year 100, producing the wedge shaped trend distortion shown in Figure 4.4.2(b). A curve-fitting detrending line is constrained to remove all slope over a specified interval in the creation of indices and can only remove the slope by adjusting the values of all indices over a period (number of years) defined by the flexibility of the detrending curve. The length of the “wedge” of trend distortion is set by the period of “rotation” of the detrending curve. The magnitude of the distortion of each index value will be proportional to the distance of the index from the centre of rotation. The overall magnitude of the “wedge” will be such that the “sum of the product of distance and magnitude” of the “wedge” and of the growth increase will be similar, where magnitudes are measured from the mean value of 1.0 and distances are measured from the centre of rotation. Trend distortion will always be greater in magnitude at the end of a series than at points near the centre of rotation.

High-frequency variance in the common signal will average out and will not produce trend distortion. Variance in the common signal at frequencies lower than that of the flexibility of the detrending curve will be removed because the detrending curve can “follow” the series of measures. When the common forcing has medium-frequency variance and the detrending line is inflexible then trend distortion can occur. When the medium-frequency change in measured values is near the end of a series the magnitude of the distortion is larger and growth increases or decreases near the end of a tree will produce larger amounts of distortion. To get a “common” effect in a chronology the distortion needs to be at the same end of each tree i.e. start or finish. In the central portions of long chronologies trees will start and end on different dates and averaging will reduce the magnitude of trend distortion. Distortion in a chronology will be maximum at the modern end of a chronology, where many trees end on similar dates, in a situation where there has been a distinct increase or decrease in tree growth rates over a period of decades to half the frequency of response of the detrending curve. A step

change in tree growth contains variance at all frequencies and can create a large amount of distortion.

The examples selected to demonstrate the segment length curse (Cook et al. 1995) show the wedge shaped end effects of trend distortion quite clearly. Examination of Figures 1C and 2C in Cook et al (1995) shows that the amplitude of the difference between the known signal and the signal produced by detrending with a sloping line is progressively larger when the ends of the series are approached. In these examples the detrending process has reversed the sign of the chronology indices relative to the series mean in the initial and final decades of the chronologies when compared to the signs of the known signals. (This sign reversal relative to the mean would result in a large reduction in the values of correlation of the decadal means of the known signal against the decadal means of the chronology indices near the ends of the chronology and could create an “apparent” change in sensitivity.)

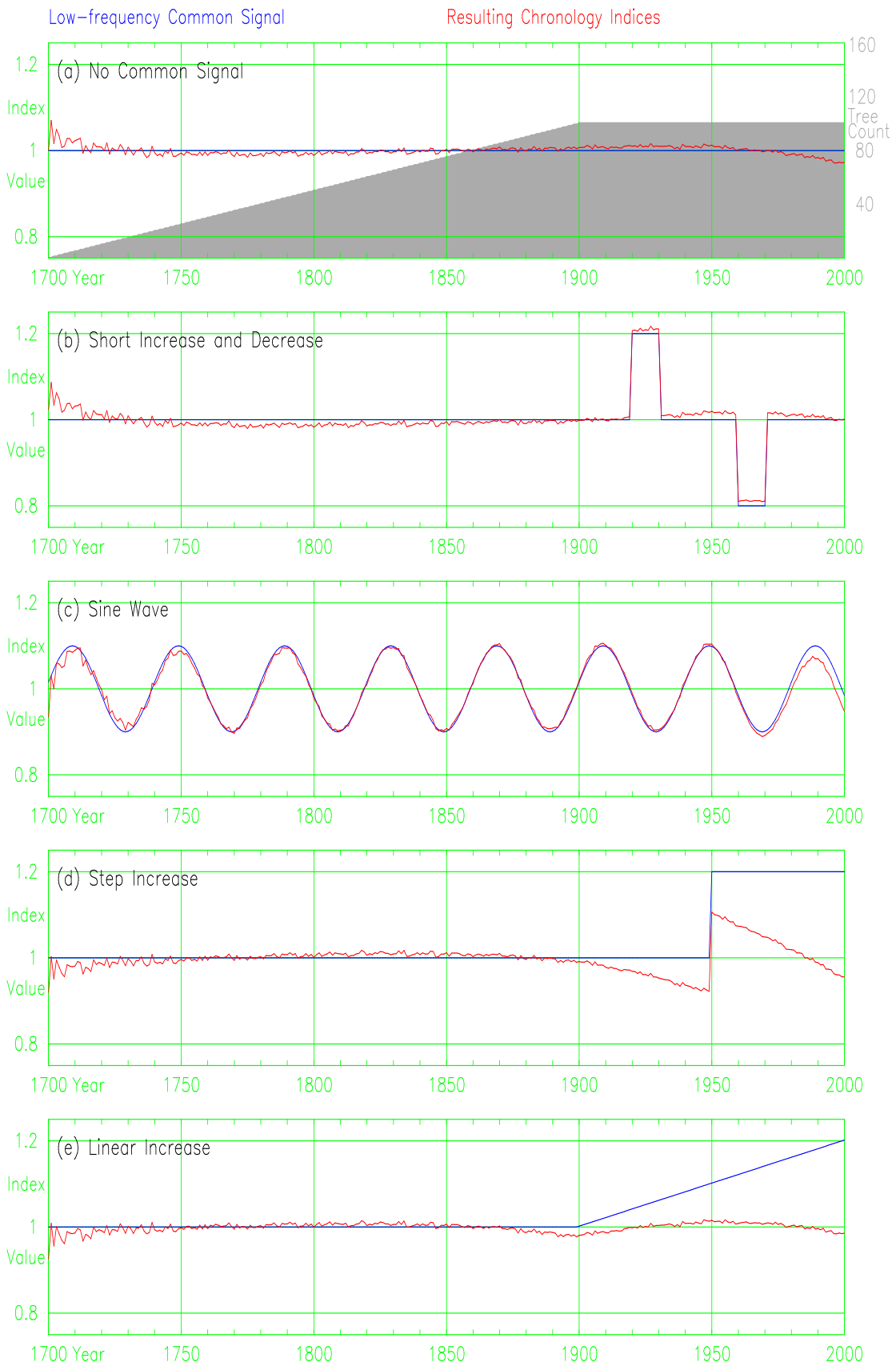
#### 4.4.5. Simulated Trees with Known Signals

The assumption that low-frequency chronology signals can be added to series of tree measures by multiplication (Section 4.2.2) is used to develop series of simulated tree measures that contain known low-frequency trends. Series of tree measures are created to simulate a dendroclimatic sample extracted from uneven aged, naturally grown, living trees. This was achieved by generating 51 trees starting on every even year from 1800 to 1900 with all trees finishing at year 2000. The youngest tree was given a first ring width of 2.0 mm, the oldest tree a first ring width of 1.0 mm, and the other trees linearly interpolated values based on tree age. The final ring width of each tree was set to half the value of the initial ring width. A random increment with mean 1.0 and standard deviation 0.1 was added (by multiplication) to these first rings and final rings to give some variation in decay rates. Intermediate ring widths were set by linear interpolation between the initial and final values. Series of random numbers with mean of 1.0 and standard deviation of 0.1 were generated to represent noise which was added to all rings by multiplication.

Chronology signals were generated that contain known low-frequency common forcing, some with a life-span trend and some without a life-span trend, to examine the ability of the Hugesshoff method to extract signals from the simulated trees. The random trees

generated above are used to represent a series of trees with no low-frequency common signal. A short increase and decrease chronology was created by increasing rings for the period 1920 to 1930 by 20% and decreasing rings for the period 1960 to 1970 by 20%. A sine wave of period 40 years and magnitude  $\pm 20\%$  was applied to the whole calendar period to produce a sine wave chronology. A step increase chronology was created by increasing the value of all rings from 1950 to 2000 by 20%. A linear increase chronology was created by increasing the values of tree rings from 1900 to 2000 by linearly increasing values from 0% to 20% in steps of 0.2%. These simple chronology signals were generated to represent common forcing and the ring widths of each random tree were multiplied by the corresponding annual index value to generate the effects of the specified medium-frequency common forcing on the ring widths of the random trees.

These low-frequency signals are plotted as blue lines in the five separate plots (a-e) of Fig. 4.4.3 and the chronologies generated using the Hegershoff method are plotted as red lines. There is a small “end effect” bias at both ends of all chronologies (red lines) which is likely to be the result of all trees having a linear decay instead of an exponential decay. These are ignored in the following discussion. The “no common signal” plot (Figure 4.4.3a) shows that standardisation accurately produces a chronology with no common signal. The “short increase and decrease” plot (Figure 4.4.3b) shows that this signal is clearly reproduced. The decrease is nearer the end of the chronology and trend distortion is produced with indices from 1930 onwards having values above 1.0 whilst indices before 1920 have values below 1.0. The amplitude of this trend distortion is small because the effects of step increases and step decrease at different dates nearly cancel out and the problem caused by trend distortion is minor in this case. The “sine wave” plot (Figure 4.4.3c) shows that this sine wave is clearly reproduced in phase and amplitude. The mean of the first two decades of the sine wave is above 1.0 and the mean of the last two decades is below 1.0 leading to a small false overall trend in the series. The amplitude of this trend distortion is small. In Figure 4.4.3d the “step increase” signal (blue) is not recognisable in the generated chronology indices (red). Indices prior to 1900 are approximately 1.0 and are not distorted. The trend introduced by the step increase has been removed by reducing the values of chronology indices leaving a series of chronology indices with no life-span trend as expected. The high-frequency step increase has been reproduced accurately. The difference between the low-frequency signal and the chronology indices from 1900 becomes progressively larger demonstrating that the



4.4.3 Randomly generated chronologies with a variety of common signals, standardised using the Hughschoff method, and used to demonstrate the effects of trend-distortion.

magnitude of the distortion is roughly proportional to distance from the centre (of rotation) of the series. The last two decades of indices have values below the average and have been distorted the most. Correlations of decadal means of the “step increase” signal against decadal means of the chronology indices will be smaller after 1980 because of the change of sign of indices relative to the mean. The low-frequency “linear increase” signal (Figure 4.4.3e) is virtually removed leaving chronology indices which are approximately 1.0 for the full length of the chronology, demonstrating that this linear increase over 100 years is at a frequency sufficiently low to be beyond detection by this detrending method when using up to 200 year old trees.

The results of testing the random series are in agreement with the expectations developed earlier. The Hegershoff method reproduces the common signal in the random trees provided there is little or no life-span trend in the common forcing signal. The Hegershoff method removes trend with trend distortion if the common signal has frequency characteristics higher than those that the detrending curve can follow but low enough to create a life-span trend. The Hegershoff method removes trend without significant distortion provided the life-span trend is of lower frequency than the frequency that the detrending curve can follow.

#### 4.4.6. Avoidance of Trend distortion

The assumption that trend distortion is caused by detrending the “common signal” is tested by removing the common signal from series of tree measures. A chronology created by the Hegershoff method is assumed to be an estimate of the values of the common forcing. The assumption that the values of chronology indices are fractional deviations allows the common signal to be removed from a series of measures by division which leaves a series of signal-free measures. If the resulting series of signal-free measures are standardised using the Hegershoff method the resulting chronology will be substantially signal-free with the exception that the signal-free chronology will contain some residual trend distortion. The product of the original chronology and the distortion free chronology will produce a more accurate estimate of the values of common forcing. Repeating this process a few times (iterating) results in a signal-free chronology with very little signal and a reasonably stable estimate of the values of common forcing. There is a need, in iterative methods, to prevent any “runaway” effects and this is achieved here

by resetting the mean values of signal-free measures for each tree after iteration to their starting means. The process can be summarised as follows:

Variables used:

Tree(fy:ly) = Series of dated tree measures

CRN(fy:ly) = Series of dated chronology indices

SFTree(fy:ly) = Series of dated signal-free tree measures

SFCRN(fy:ly) = Series of dated signal-free chronology indices

Procedure used:

1. Create CRN from all Tree(fy:ly) using Hugershoff method.

2. For each tree remove the currently estimated common signal:

$SFTree(fy:ly) = Tree(fy:ly) / CRN(fy:ly)$

3. For each tree reset the means of signal-free measures:

$SFTree(fy:ly) = SFTree(fy:ly) * SUM(Tree(fy:ly)) / SUM(SFTree(fy:ly))$

4. Create SFCRN from all SFTree(fy:ly) using Hugershoff method.

5. The “net” chronology is the product of all signal-free chronologies:

$CRN(fy:ly) = CRN(fy:ly) * SFCRN(fy:ly)$

6. Repeat (2) through (5) five more times then stop.

This procedure was followed using data for the four chronologies described in Section 4.4.2 and the resulting chronologies are displayed in Figure 4.4.4b. The means of ring-widths by calendar year are plotted in Figure 4.4.4a for comparison. The trend distortion has been removed from the trees used to create these four chronologies and although these chronologies are “trend distortion free”, because the chronologies have no overall slope, the early sections of all four chronologies have differing slopes. Each series of tree indices created by curve-fitting methods are constrained to have a slope of zero (Cook et al. 1995) and consequently chronologies created using curve-fitting methods are approximately horizontal, i.e. a best fitting straight line will have zero slope. Examination of the 30% increase in mean-ring chronology, red line of Figure 4.4.4a, suggests that the slope of the chronology indices created from these trees should be positive and examination of the 60% decrease mean-ring chronology, magenta line of Figure 4.4.6a, suggests that the slope of the final chronology indices created from these trees should be negative. The standardisation method used has produced four chronologies with chronologies are “known” and this allows the arbitrary decision to be made that the slope



Figure 4.4.4a Means of tree rings by calendar year

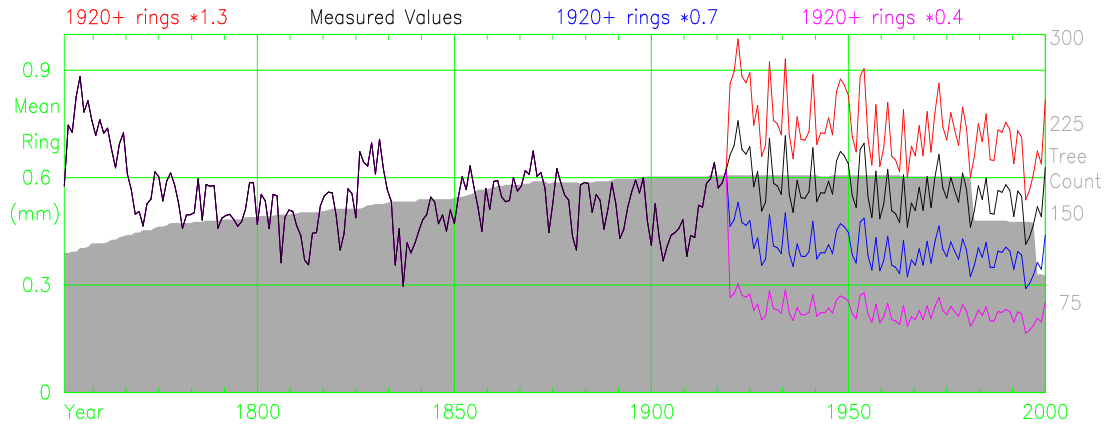


Figure 4.4.4b Chronology Indices by calendar year

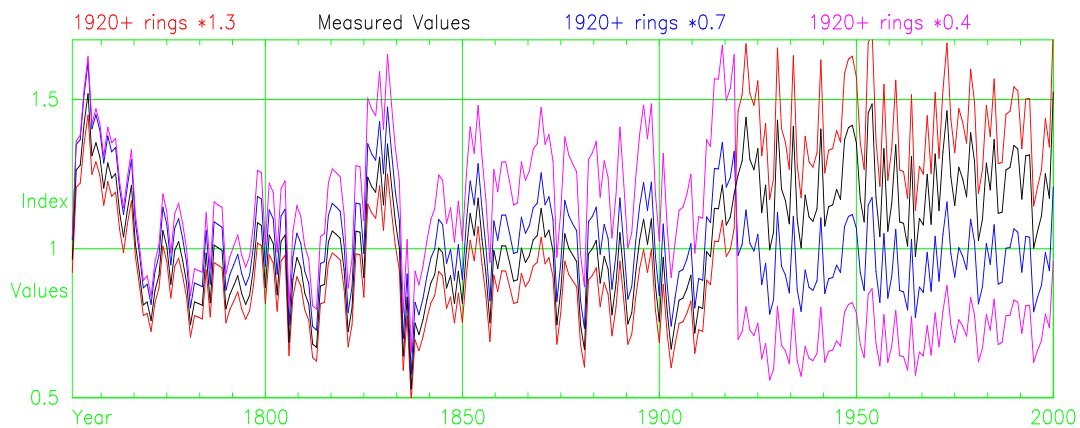


Figure 4.4.4c Chronology Indices by calendar year

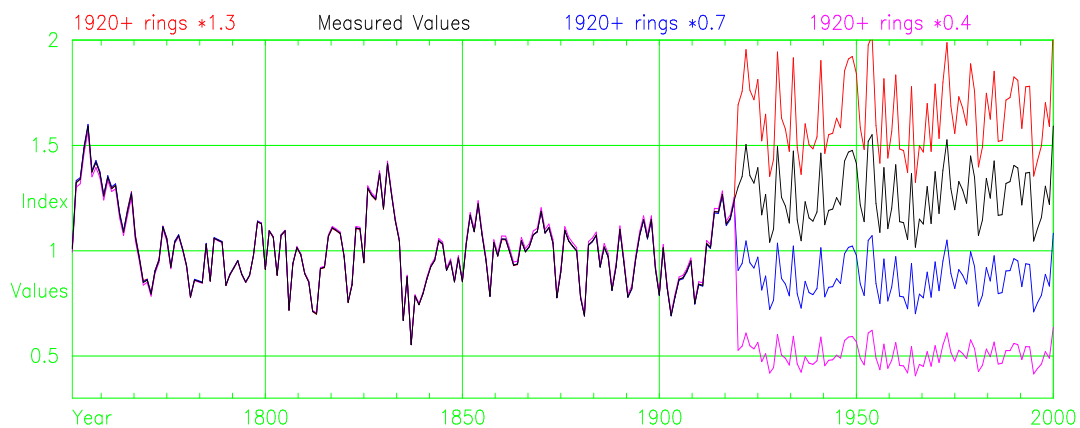


Figure 4.4.4 Demonstration of the effects of removing the common forcing signal from raw measures. Measures (a), signal-free chronologies (b), and rotated (over period to 1900) chronologies (c)

approximately zero overall slope. The characteristics of the trees used to create these (count-weighted) of the 1550-1900 portions of these chronologies will be zero and the count-weighted mean values of the indices from 1550 to 1900 will be 1.0. The “rotation” to adjust slope and resetting of means was achieved using the procedure described in Section 5.5.6 and the resulting slope and mean corrected chronologies are displayed in Figure 4.4.4c. The removal of trend distortion is clearly demonstrated by comparing the

Figures 4.4.1b and rotated chronologies of Figure 4.4.4c. The common forcing signals recovered are consistent with the magnitude changes made to the tree measures for the years 1920 to 2000.

A warning is necessary here however. The Hugesshoff method uses a hierarchical choice of detrending curves whilst iterative procedures need “smoothly” changing functions to achieve convergence. The six iterations used here only partially converge. Because 200 trees are used the effects of changes in the selection of detrending curves, used for individual trees, between iterations are minimised and convergence is approximate in the well replicated sections of the chronology. (The early part of the chronology with only 15 trees is not displayed). This problem could be overcome by using smoothly changing curve-fitting methods such as fixed length (for each tree) smoothing splines. Caution is also warranted in another respect. The rotation to correct the slope of the chronology should be performed on each individual tree (series of tree indices) because series of tree indices are different lengths. The large overlap (common period) in most of these trees enables reasonable results to be achieved by rotating the chronology by the average slope. In the presence of sub-fossil trees this rotation would fail because the pre-1550 sub-fossil section of the chronology, with a mean index value of 1.0, would set the slope of the pre-1900 period to zero even though the 1550 to 1900 periods had varying slopes.

#### 4.4.7. Discussion

Given that the geographic focus of this project is Fennoscandia, the evidence from instrumental climate records of anomalous increases in mean temperatures in recent decades justifies a strong expectation of increased tree growth. The evidence of these simulations points to the need for caution in the use of similar “curve-fitting” approaches to the standardisation of chronologies intended to provide a long-term context for measuring the relative magnitude of this warming. Trend distortion was identified as being the result of detrending the common, climate-related forcing signal and, by using the property of chronology indices as fractional deviations, an iterative method of removing this distortion was demonstrated although this method is severely limited in the scope of its application. Even if the trend distortion problem of “curve-fitting” detrending methods could be reduced or solved, the “tree length” limits to the resolution of low-frequency variance from series of tree measures rules out the use of such curve-fitting detrending methods in this project. Later, further exploration is made of how signal-free

measures can be used in the recovery of long-timescale temperature variability in the Fennoscandian area using RCS based standardisation methods.

#### **4.5. Conclusions**

This chapter dealt with the separation of the commonly expressed forcing, over the lifetime of a group of trees, on growth from the age-related (expected) growth trend upon which it is superimposed. The common forcing is considered to represent the climatic control of photosynthesis in foliage. The expected growth trend for a series of ring-width measurements was found to be dependant on the history of growth of the tree, and both ring age and diameter are needed to generate estimates of expected growth values for a specific tree. Ring width does not measure growth rate unless diameter is known and, although ring-age and diameter both increase over time, ring age on its own can be a poor predictor of diameter. It is an important aspect of this work that chronology and tree indices are assumed to be fractional deviations and this leads to the requirement that multiplication and division be used to manipulate index values. A consistent model is developed with some tools needed to manipulate tree measures, tree indices and chronology indices.

The “Best fit means”, or BFM method, which resets the mean values of series of tree indices to equal the mean values of the chronology over their common period, is presented. The BFM method enables long-timescale variance to be established without a dependence on preserving mean tree growth rates, and thus allows the generation of expected growth curves that are not dependent on the mean growth rates of trees.

The effects of climatic control on tree growth were shown to influence the development of expected growth curves and this problem is called trend distortion. The assumption that chronology indices are fractional deviations allows the use of division, for removing the effects of common forcing from series of ring measurements, in the creation of signal-free measures that can be used to produce expected growth curves that are substantially unbiased by external common (e.g. climate) forcing. This technique is limited in its scope of application as is discussed in Section 5.5.8. The conclusion is reached that curve-fitting methods are unsuitable for the task of isolating medium and low-frequency variance from the Scandinavian trees sampled and explored for this project and hence effort is concentrated on examining and resolving problems found in the RCS method.

## **Chapter 5. RCS Method – Problems and Improvements**

### **5.1. Introduction**

This chapter is about problems with the RCS method, the causes of these problems, the development of tools and techniques to overcome these problems, and finishes with a discussion of residual problems. The viewpoint and tools developed in Chapter 4 are used along with some additional techniques to modify the existing RCS method and create alternative methods of standardisation.

If all ages of trees were well represented at all times throughout the span of a chronology then simply averaging the raw ring-width measurement data would remove the “age-related bias” in the final chronology (LaMarche 1974a). This averaging will give a measure of the mean growth rate of trees in terms of the mean ring width for each year. The RCS method is an improvement on simple averaging because, by removing the mean age-related growth trend from trees, the RCS method reduces the numbers of trees needed to estimate the mean growth rate of trees. Where sufficient numbers of trees are available for simple averaging the RCS method produces a chronology whose variance is similar to that of the measured mean ring width for each year. The RCS method scales ring width by the mean ring width, for that ring age, and averages the resulting tree indices to produce a chronology.

The need to preserve low-frequency variance in chronologies led to the development of the RCS method (Briffa et al. 1992a). This preservation requirement is overriding in that any alternatives or improvements to the RCS method must retain this ability to preserve variance at frequencies beyond those of the length of individual trees. The “best fit means” (BFM) method (Section 4.3) can preserve variance at frequencies beyond those of the length of individual trees provided the detrending method used can preserve a life-span trend in individual trees. The preservation of long-timescale variance by the BFM method is achieved by overlapping the variance in series of tree indices. The BFM method reduces the requirement placed on detrending from preserving low-frequency variance over the chronology length to preserving variance over the tree length and it is this reduced requirement on detrending which opens up the possibility of alternative methods of standardisation in order solve some of the existing problems. Existing problems with the RCS method and suggested ways of overcoming or mitigating these,

along with new problems associated with the suggested “improvements”, are now discussed.

## **5.2. Variation of Mean Growth Rate**

In the boreal forest, the mean value of temperature varies with altitude and latitude whilst the temporal variance in series of temperature measures (as represented by anomaly time series) is more consistent over altitudinal and latitudinal gradients but variance becomes larger the more continental as opposed to oceanic the location. At Bödö (Figure 3.2.1) winters are 10.0°C warmer and summers 2.0°C colder than at Sodankyla (Figure 3.4.1a), while correlations between the 12 series of mean monthly temperatures (1908 to 1999) at these sites produced values in the range 0.65 to 0.88 (Table 3.4.2). The variability in temperature measures (correlation) is consistent over geographical regions while mean values vary considerably from site to site. The rates of growth of trees, measured by the mean time to reach a given diameter, at the four sites used in this project are roughly proportional to mean summer temperature: the warmer sites produce faster growing trees. The dependence of tree growth on the measured value of temperature implies that measuring the long timescale variability in tree growth rates will be more spatially robust than measuring the mean growth rates of trees.

The RCS method uses the mean growth rate of trees to establish the long timescale variance in chronologies. In the boreal forest trees growing on a south facing slope tend to grow faster than trees growing on a north facing slope. If one RCS curve is built using combined sets of trees from north and south facing slopes, this RCS curve could be used to produce separate chronologies for each site, north and south facing sites, that clearly show the difference in growth rates. This ability of the RCS method to compare mean growth rates necessitates / implies that samples must be homogeneous over time and application of the RCS method to provide long sub-fossil chronologies assumes no bias due to clustering of samples (in time) derived from systematically different mean conditions (Briffa et al. 1996). Using the RCS method may require latitudinal and altitudinal adjustments in the form of rescaling (Briffa et al. 1996). If RCS generated chronologies from separate sites are averaged to create regional chronologies then this averaging results in rescaling (mean value of each series of chronology indices set to 1.0 before averaging) and removes the effects of site to site variation in overall growth rates, i.e. latitudinal and altitudinal variations can be removed. Meteorological measuring

stations are not always placed at the altitudes and latitudes of the trees used to build chronologies and matching the variance in chronologies with the variance in measured climate variables, using correlations and response functions, effectively rescales the chronologies.

The RCS method rescales at a site level, by setting the mean value of chronology indices to 1.0, whilst the BFM rescales each tree. The BFM method assumes that each series of tree indices records the variations in growth rate over the life of the tree without reference to the overall magnitude of growth rate that tree experienced. Each individual tree is automatically “rescaled” and this removes some of the requirement to “ensure no bias due to clustering in time” and allows more flexibility in tree sampling procedures. The requirement for continuous multiple “overlapping” of trees is introduced by the BFM method.

### **5.3. RCS Indices are Larger and Slope**

In any year the units of foliage of fast growing trees, slow growing trees, young trees, old trees, big trees and small trees are all assumed here to produce carbon at the same climate controlled rate (Section 4.1.2/3). When the rate of growth of trees is measured as the time taken to reach a specified diameter then series of tree indices created by the RCS method are larger for the faster growing trees than for the slower growing trees. This is shown for the Tornetrask AD and Finnish-Lapland AD chronologies in Figure 5.3.1 (b) and (d).

When plotted by ring age, series of tree indices for the fastest growing trees have a downward slope and series of tree indices created for the slowest growing trees have an upward slope (Figure 5.3.1 (b) and (d)). At each site, the division of tree measures by the RCS curve values to create series of tree indices preserves the magnitude of a tree’s growth rate relative to the mean growth rate (at that ring age) represented by the RCS curve. The overall growth rate of a tree, relative to the mean growth rate of all trees, is preserved in the mean value of each series of tree indices and in the RCS method the overall growth rate is used to assess the low-frequency variance of common forcing.

The expected growth rate of the 50th year’s ring, as estimated by the RCS curve, is a constant for a chronology. If the minor differences created by smoothing are ignored then the RCS derived tree indices are created without reference to previous or subsequent growth years of a tree. The 50th year ring measures of all trees can be averaged and each

Fig 5.3.1a Mean rings by ring age – Tornetrask AD Chronology

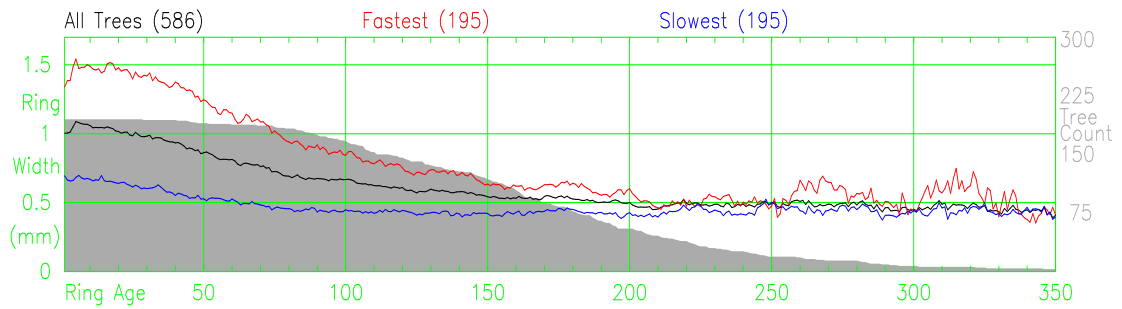


Fig 5.3.1b Mean indices by ring age – Tornetrask AD Chronology

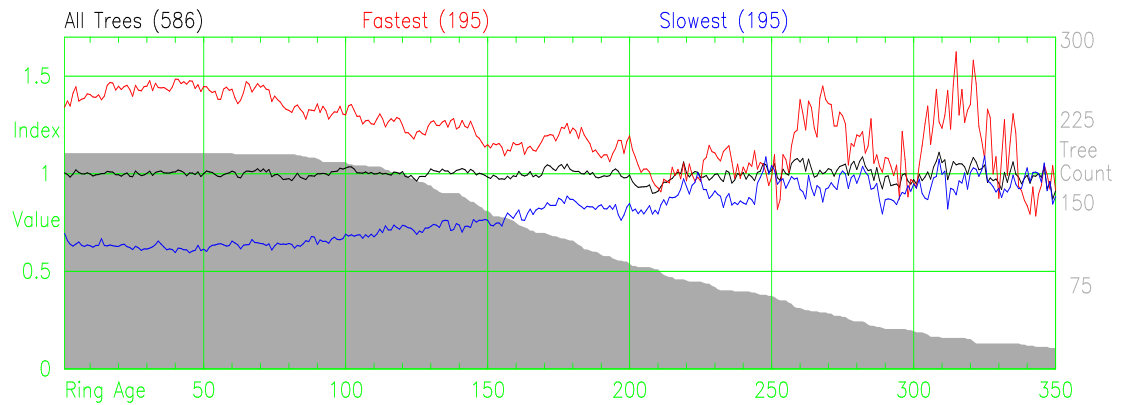


Fig 5.3.1c Mean rings by ring age – Finnish–Lapland AD Chronology

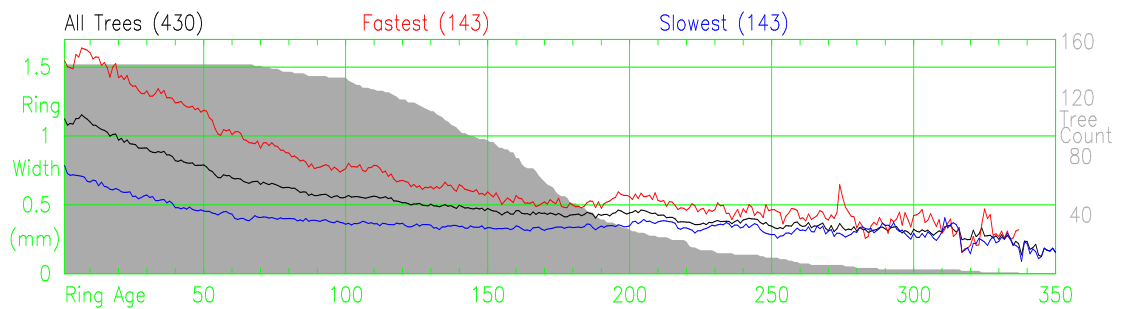


Fig 5.3.1d Mean indices by ring age – Finnish–Lapland AD Chronology

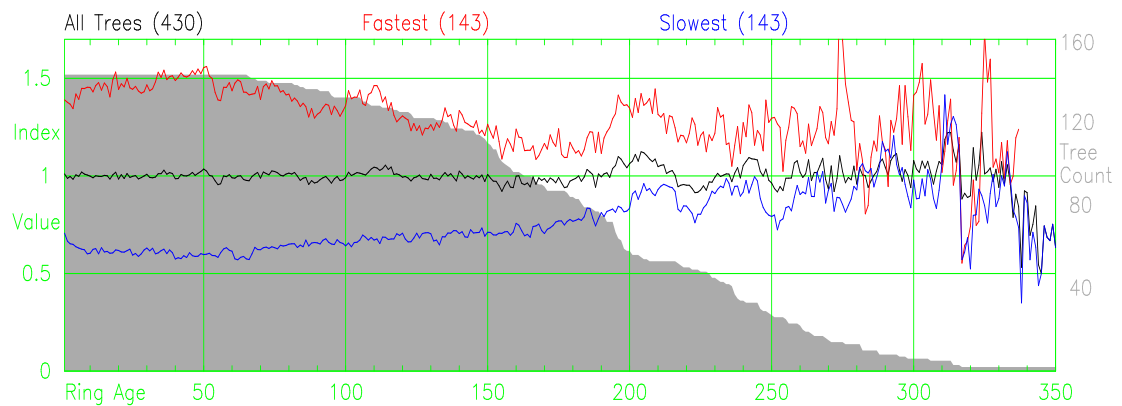


Figure 5.3.1 Mean ring-width (a and c) and mean tree indices (b and d) using the RCS method at the Tornetrask AD (a and b) and Finnish–Lapland AD sites plotted by ring age separately for the fastest and slowest growing thirds of trees.

tree's 50th year index created by dividing by the mean of all 50th rings independently of any other year of growth. The RCS method does not use previous growth history of a tree in the production of expected growth curves and this causes the accumulated history of common forcing to be preserved in values of tree indices i.e. any preconditioning by decades of favourable or unfavourable climate forcing. In Fig 5.3.1 (b) the average 50th ring index value for the fastest growing trees is 1.4 and for the slowest growing trees is 0.6 and these values are the results of the steady progress through time of the growth of faster and slower growing trees. The cause of the different rates of growth could be microsite variations, or the accumulated history of common forcing, or unidentified causes and combinations of the above. Persistence in the rate of growth of each tree leads to slow changes in the accumulated history of growth and the difference between the 50th and 51<sup>st</sup> year will reflect the change in common forcing of the 51<sup>st</sup> year relative to the 50<sup>th</sup> year. The values of 0.6 and 1.4 are not fractional deviations due to the climate factor of the 51<sup>st</sup> year and for these two sets of trees alternative expected growth curves can be inferred from their previous growth history.

At 250 years of age the mean values of ring width of the fastest growing trees and the slowest growing trees are similar (Figure 5.3.1 (b)). The separate average values of the 250th year indices for fast and slow growing trees generated by the RCS method for these trees would be approximately 1.0 at around 250 years of age. The area under these curves (sum of radial increments) is a measure of diameter and it can be seen that the fastest growing trees (red curve) have approximately twice the diameter of the slowest growing trees (blue curve) by this age. If height differences are ignored, the rate of growth of the fastest trees (expressed by carbon gain per year) will be four times that of the slowest trees at 250 years of age. An example of a site that might produce such trees could be site in the boreal forest with the fastest growing trees growing on a south facing slope and the slowest growing trees growing on a north facing slope.

The RCS method, by producing similar sized tree indices, shows both sets of trees at age 250 to be growing at the same rate. These trees grew over a time period of more than 50 centuries and it is possible that the fastest growing trees grew in periods during which common forcing produced fast growth and the slowest growing trees grew in periods during which common forcing produced slow growth. Half way through the 3<sup>rd</sup> century of growth the RCS method is unable to distinguish a four fold difference in "growth"



rates. Even if the overall growth rates of these trees were controlled completely by common forcing the RCS method is unable to isolate the magnitude of that forcing in series of tree indices at 250 years of age. Esper et al (2002) noted this with their trees “...young non-linear trees grow 2-3 times faster than the linear trees up until 200 years of age.” This is a predictable result because the average growth of the RCS curve must underestimate the accumulating diameter of faster growing trees and overestimate the accumulating diameter of slower growing trees. The comparison of fast and slow growing trees is somewhat unfair in the light of the definition of growth rate in terms of “mean ring increment” and the RCS presumption that there are sufficient trees for the averaging process to remove differences. The decay from 1.4 to 1.0, over 250 years, of the values of indices of faster growing trees is a function of standardisation and unrelated to common forcing. This point highlights the need for careful control of sample distribution over time when using the mean growth rate of trees. Variation in the mean growth rate of trees will not cause a problem for the BFM method but a consistent “age-related” bias in the slope of series of tree indices at one point in time will cause a problem for the BFM method. If series of indices of the faster growing trees of the current century slope downwards whilst the final century of series of indices from slower growing trees are roughly horizontal then there could be an “artificially” induced downward slope in the most recent century of a chronology.

#### **5.4. Modern sample bias**

##### **5.4.1. Introduction**

Methods of standardisation that use the average growth rate of trees to generate chronology indices, such as the RCS method, require samples of trees that are roughly homogeneous over time. In the boreal forest, trees from lower elevations and lower latitudes generally grow faster than trees from higher elevations and higher latitudes. If the growth rates of trees from different periods are used care needs to be taken to ensure that the samples for each period are taken from sites with similar distributions of altitude and latitude. If similar sampling strategies are used to take samples from each year of interest then these samples are expected to be homogeneous over time (assuming, of course, that no other time-dependent change in common forcing exerts an influence). Chronologies developed from living trees sampled at one point in time or within one epoch (a modern chronology) are generally not homogeneous with respect to time and the phrase “modern sample bias” is used to describe the bias that can be created by this lack

of homogeneity. The potential for modern sample bias occurs because the fastest growing trees of the earliest centuries and the young slower growing trees of the most recent centuries are generally missing from dendroclimatic samples taken from living trees at one point in time.

#### 5.4.2. Random variations in growth rates

Figure 4.1.1 showed that the growth rates of trees vary and there were fast and slow growing trees in all calendar years over the last two millennia at the Tornetrask and Finnish-Lapland sites. Variation in growth rates between different trees growing at any specific point in time appears to be the normal situation and it is this variation which leads to modern sample bias. Consider building a tree-ring chronology from trees sampled at one point in time from a large, naturally grown forest with unvarying common forcing (mean climate). Presume that the maximum tree size in this forest is limited by the probability of mortality being high for the largest trees. If samples are restricted to trees whose radius is 10cm at breast height, the samples will be from trees of varying ages (Enquist 1999). Presume, for this example, that the youngest tree is 100 years old, representing the minimum time required to reach 10cm radius and the oldest tree is 300 years, being the maximum time to reach 10cm radius. There are many samples from trees of each age, and many 50th rings for each chronology year from year 100 to year 300. A graph of the growth rate of the 50th ring of each tree against calendar year will show a steady increase in growth rate over a 200-year period. The youngest tree must have been growing three times faster than the oldest trees in order to reach the same size in one third of the time. For samples taken at one point in time the earliest calendar years are represented by the oldest trees and most recent calendar years by the youngest trees. This result for the 50th ring of 10cm radius trees will apply equally to other larger tree radii and other ring ages. This is independent of any variation in the common climate forcing on tree growth. Figure 5.4.1 is used to demonstrate this effect. The two “End Aligned” chronologies are used to represent large samples of trees taken in the year 2001 from a forest that has no net common forcing signal. The removal of all trees with rings which grew after 1725 excludes any modern “anthropogenic” effects from these chronologies. The mean ring widths of all tree rings with cambial ages between the ages of 40 and 60 from trees whose final radius was between 12 and 14 cm are plotted (red lines, Figure 5.4.1 (a) and (b)). The plots show a steady increase in mean ring-width over time. The mean growth rate of the trees from this specific age range appears to have increased over

Fig 5.4.1a Plots of mean ring width from the Tornetrask End Align Chronology

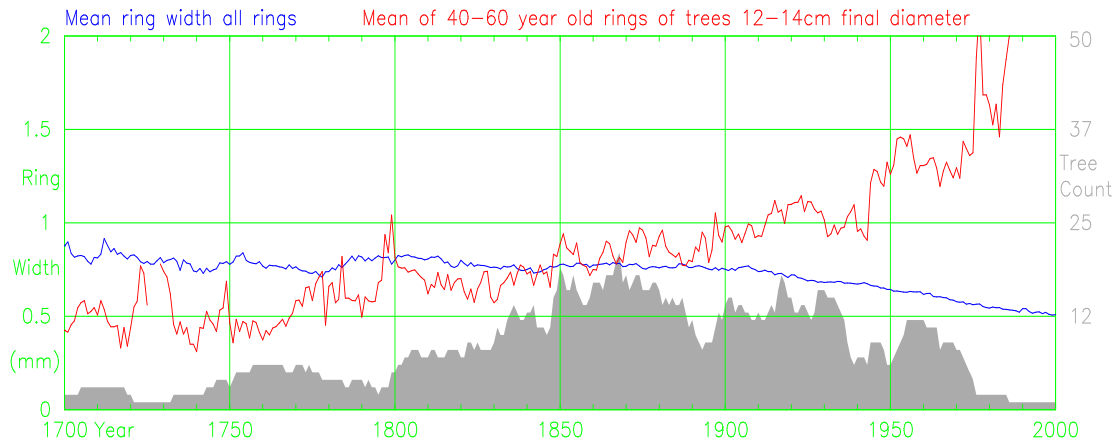


Fig 5.4.1b Plots of mean ring width from the Finnish-Lapland End Align Chronology

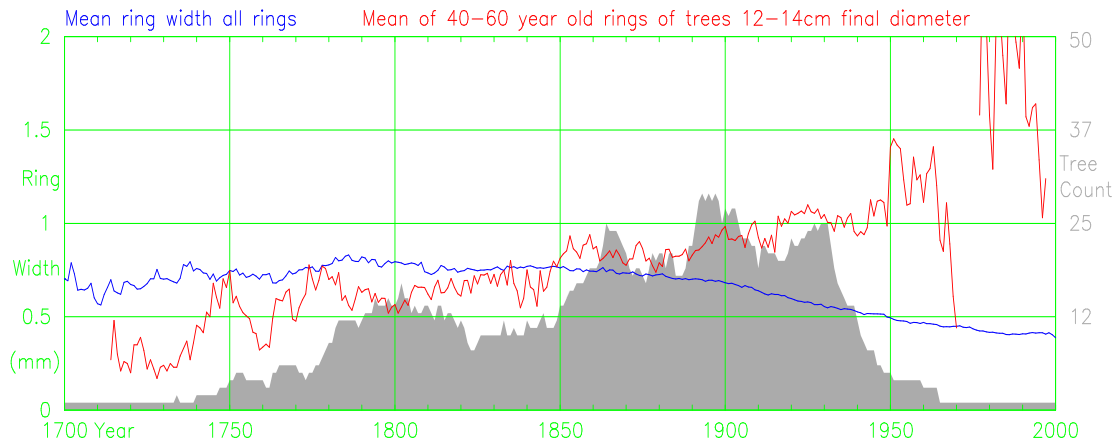


Figure 5.4.1 Plots of mean ring width of rings aged between 40 and 60 years from trees of final radius between 12cm and 14cm. Ring counts shown along with the mean ring width of all trees. Trees from the Tornetrask and Finnish-Lapland end aligned chronologies.

time. Random variations in growth rates will generate this effect in a sample, taken at one point in time, of trees whose final diameters are similar. Any limit on maximum tree size will result in an equivalent situation because the removal (by mortality) of the fastest growing trees of earlier periods will produce an inevitable bias towards the slower growing trees in the early part of a modern chronology, those that survive to be included in the modern cores.

### 5.4.3. Modern chronologies

A dendroclimatic sample of cores from naturally grown, living trees generally contains the largest and oldest trees available and some smaller or apparently younger and “healthier” looking trees are included to assist in crossdating (old trees with suppressed recent rings can be more problematic for confirming ring boundaries and crossdating).

Samples will be from trees above some minimum radius, small trees are not generally sampled because they may suffer excessive damage from coring, and short ring sequences may be difficult to crossdate. Table 5.4.1 lists the statistics relating to the two sites from which new chronologies were developed for this project. The sampling strategy was to select trees of various ages and sizes (much more than has been usual in dendroclimatology) to allow comparisons of growth rates. The oldest trees are roughly 75% of the radius of the largest trees despite being 50% older. The radial growth rate (over the first century of growth) of the youngest trees was three times greater than that of the oldest trees. The oldest trees did not reach the minimum sampling size until they were two centuries old. The minimum size of samples was 8cm radius and the largest tree sampled was 27cm radius. Modern chronologies will have samples from trees at varying stages in their life cycle. Comparisons of the dimensions of mean statistics for young and old trees are complicated by the decay of ring-width as the trees get older.

Site	Luosto	Helldalisen
Number of Trees	100	89
Mean Tree Radius (cm)	17.2 (3.5)	15.7 (3.8)
Mean Tree Age (year)	291 (109)	306 (110)
Mean Ring Width* (micron)	596 (403)	490 (326)
<b>Youngest 15 Trees</b>		
Mean Radius (cm)	14.8 (2.2)	14.8 (3.1)
Mean Age (year)	127 (35)	158 (22)
Mean Ring Width* (micron)	1177 (663)	898 (439)
<b>Oldest 15 Trees</b>		
Mean Radius (cm)	18.3 (3.5)	16.3 (3.8)
Mean Age (year)	460 (38)	478 (65)
Mean Ring Width* (micron)	389 (220)	333 (207)
<b>Smallest 15 Trees</b>		
Mean Radius (cm)	12.3 (1.0)	10.4 (1.1)
Mean Age (year)	229 (141)	274 (96)
Mean Ring Width* (micron)	561 (555)	339 (212)
<b>Largest 15 Trees</b>		
Mean Radius (cm)	23.4 (1.5)	21.7 (1.6)
Mean Age (year)	364 (79)	346 (96)
Mean Ring Width* (micron)	634 (360)	610 (349)

\* - of rings that grew in first century of growth

Table 5.4.1 Site statistics, all radii and ages include pith estimates and standard deviations are shown in brackets.

The trees from the Luosto and Helldalisen chronologies are used (Figure 5.4.2) to demonstrate some properties of these “modern” chronologies. The blue and red dots of Figure 5.4.2 show final tree age plotted against final tree diameter. There is a large spread

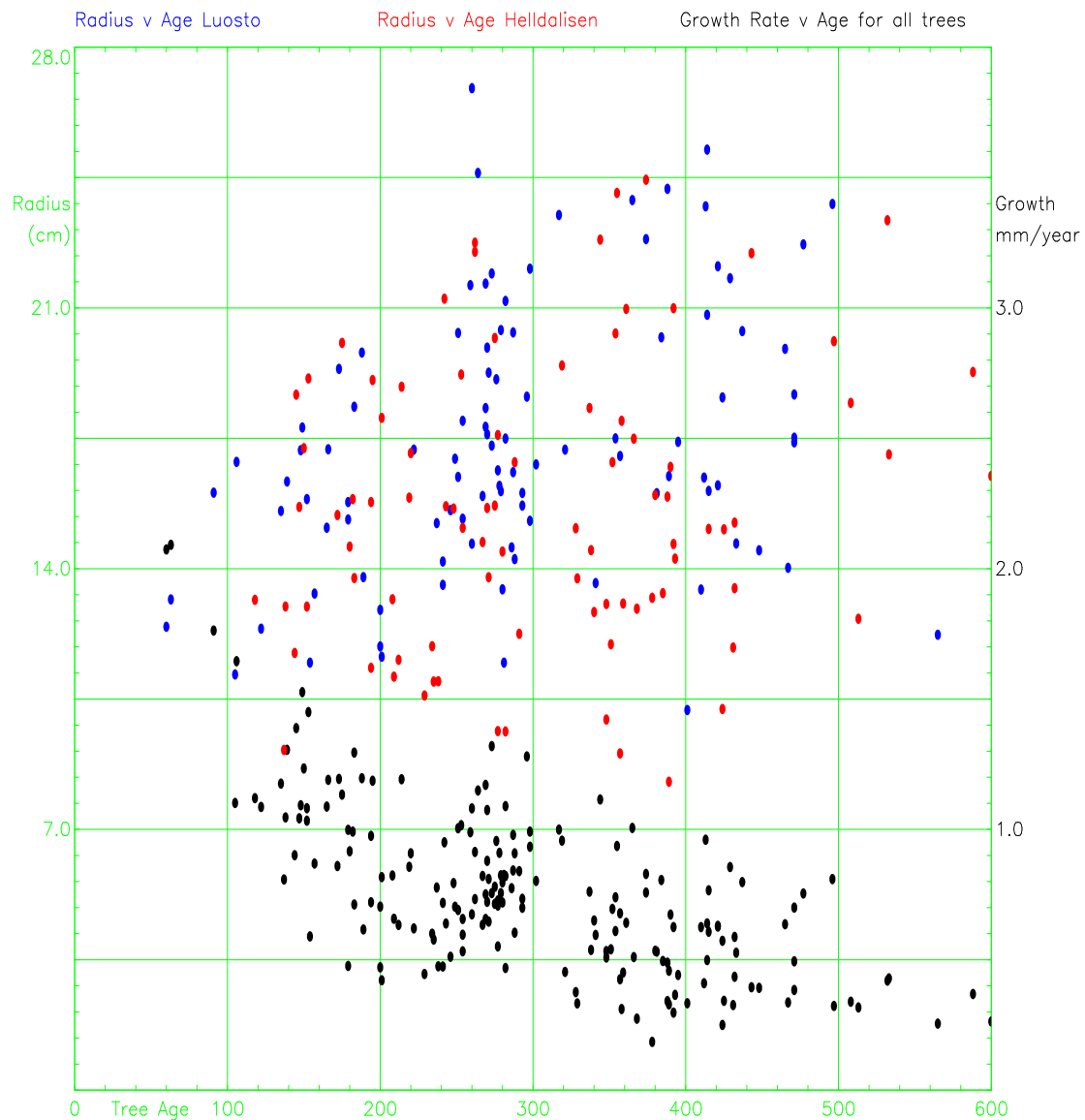


Figure 5.4.2 Scatter plot of final radius against final age and growth rate (mean during first 100 years) against final tree age for trees from Luosto and Helldalisen.

of tree ages for each final diameter range and the relationship between tree radius and tree age looks to be effectively random. The spread of ages (200 to 550 years) of the largest radius class (21cm – 27cm) is consistent with size related mortality. The trees that reached 25cm in 300 years or less all died, because there are no trees greater than 25cm and above 300 years old. The black dots show a scatter plot of the mean growth rate during the first century of growth of each tree, against final tree age. These display a clear systematic pattern. Young trees had to have high growth rates to attain the minimum radius, whereas to survive into old age the old trees grew slowly. Sampling gaps appear, such as in the bottom left hand portion of the plot, where there are no young slow growing trees and the top right hand portion, that contains no fast growing old trees. This pattern illustrates real potential for modern sample bias.

#### 5.4.4. Incomplete Samples

The assumption here is that the fastest growing trees of earlier centuries became large, died and were therefore not available for inclusion in any modern chronology of living trees. The slowest growing trees of the most recent century had not reached the “minimum sample size” and were not available to a modern chronology. The apparent increase in the growth rates of trees is the result of comparing the mean growth rates of the slowest growing trees of previous centuries with the mean growth rates of the fastest growing trees of the current century. The RCS method provides a constant expected growth rate for each ring age. The arguments that there may not have been any fast growing trees in the earliest periods of a chronology and that there may not have been any young, slow growing trees in the latest period of a chronology may be correct for specific sites. Figure 5.4.3 also demonstrates how simulated “modern” samples taken from sub-fossil chronologies have the property that they produce chronologies with a more positive slope than the slope of the chronologies from which they are taken.

The RCS method was used to generate series of tree indices for the Tornetrask AD and Finnish-Lapland AD sites. Seven pseudo “sampling” dates were selected from 1980 backwards in steps of 200 years for the creation of simulated “modern” chronologies. All trees with radius above 7cm on the sampling date were chosen. The tree indices of those trees up to and including the sampling date were extracted from the full chronology of tree indices and averaged to build a mean index chronology for the chosen sampling date. All chronologies were smoothed with a 100 year smoothing spline. The seven short chronologies are plotted on top of the full chronology in Figure 5.4.3. For both the Tornetrask and Finnish-Lapland sites six of the seven simulated “modern” chronologies have more positive slopes than the corresponding sections of the full chronology. The chronologies ending at 1980 match the full chronology in the last two centuries because both have modern sample bias (i.e. no slow growing young trees are present). Observation of the other simulated chronologies suggests that the full chronology is probably 10% higher in the last two centuries than it ought to be, a result of not having young slow growing trees from the modern period. This has implications for climate reconstruction.

These simulated chronologies differ from the full sub-fossil chronology because the simulated sampling excludes trees that have not yet reached the minimum sampling size

and excludes trees that died before the year in which the simulated chronology was “sampled”. These exclusions lower chronology index values in the earliest period of the simulated chronologies and raise chronology index values in the most recent period of the simulated chronology, all relative to the full sub-fossil chronology. All the tree indices used here have the same values for the full chronology and “modern” chronologies and the differences are produced by the sampling procedure.

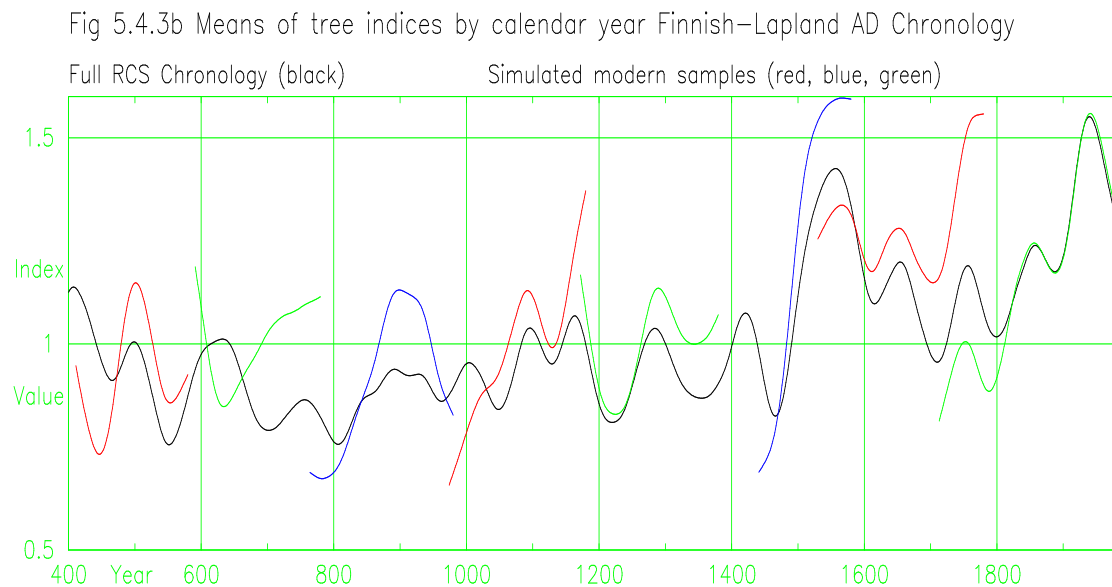
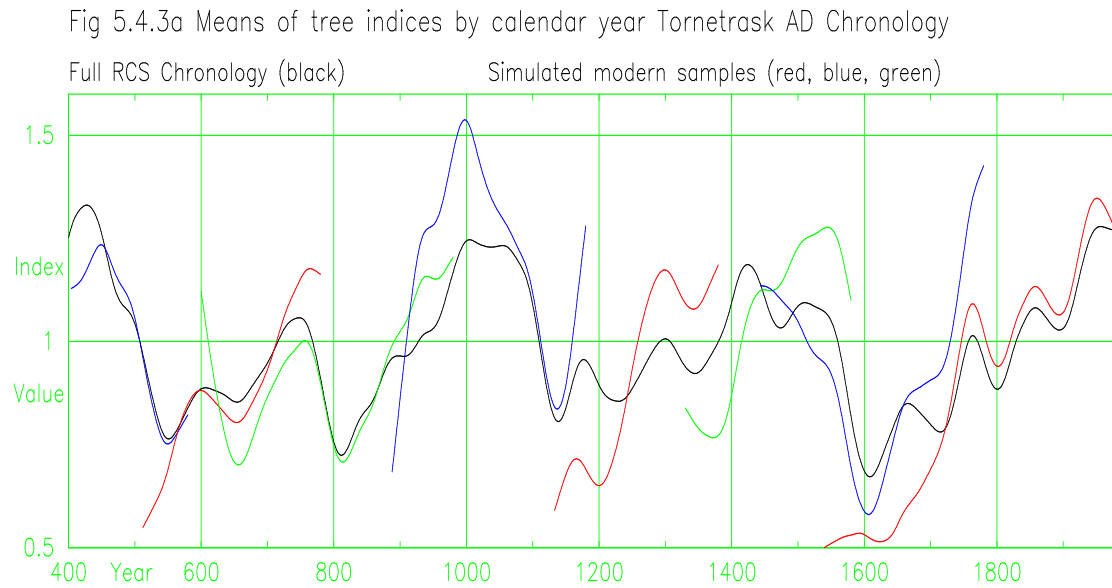


Figure 5.4.3 Simulated modern samples extracted from sub-fossil chronologies at 200 year intervals. Demonstrating that chronologies developed from modern samples have a more positive slope than chronologies built from overlapping trees.

#### 5.4.5. Real and Apparent Problems

Examination of individual trees from Luosto and Helldalisen shows growth increases in the 20th century. Eighty percent of trees have a step like increase of ring width around 1920, and in many cases this increase was maintained in a situation where ring increments were expected to decline according to the generally accepted form of ring/age model (Figure. 5.4.4c). Trees from the Fennoscandian boreal forest are growing faster in the 20th century than would be expected from the previous growth history of those trees. Demonstrating the existence of a sample bias using modern chronologies is problematical due to this general increase in growth rates over the 20th century with a magnitude larger than that of the supposed bias. There is a large amount of published data which, using the cambial age of tree rings from samples taken in the modern period, conclude that there has been a large growth increase over the past few centuries. Spiecker (1996) includes growth trends studies across Europe. In Sweden, Elfving & Nystrom (1996) show a steady increase in the estimated productivity of forest land but note that "*... trees of the same age and diameter had the same growth rate in 1953 as in 1992*" and "*The combination of age and tree size as explanatory variables must be avoided in studies of growth trends*". In Germany, Wenk & Vogel (1996) show large increases in height growth rates when comparing young stands with old stands. In France, Badeau et al. (1996) found growth increase trends all above 50% over the last century, but note that "*The oldest sampled trees may still be alive because they were not big enough to be harvested. Conversely, the trees of the same age but with higher productivity may have been harvested already*". Comparisons of ring width increments of the same cambial age from modern chronologies find large growth increases in the modern period. The rates of growth of existing trees show increases in this century above that expected for steadily ageing trees.

Modern sample bias can be shown using chronologies with a wide spread of tree ages and the Luosto and Helldalisen chronologies are combined into a "northern" chronology for this purpose. Series of tree indices were created using the RCS method. The oldest and youngest 25% of trees were used to create mean ring-width and mean tree indices by ring age and calendar age and these series are plotted in Figure. 5.4.4. The mean ring-widths of the youngest trees are larger than those of the oldest trees (Figure. 5.4.4a). The mean indices of the oldest trees (blue line, Figure. 5.4.4b) slope upward when plotted by age (as expected) with the RCS method. The mean indices of the youngest trees (red line, Figure.



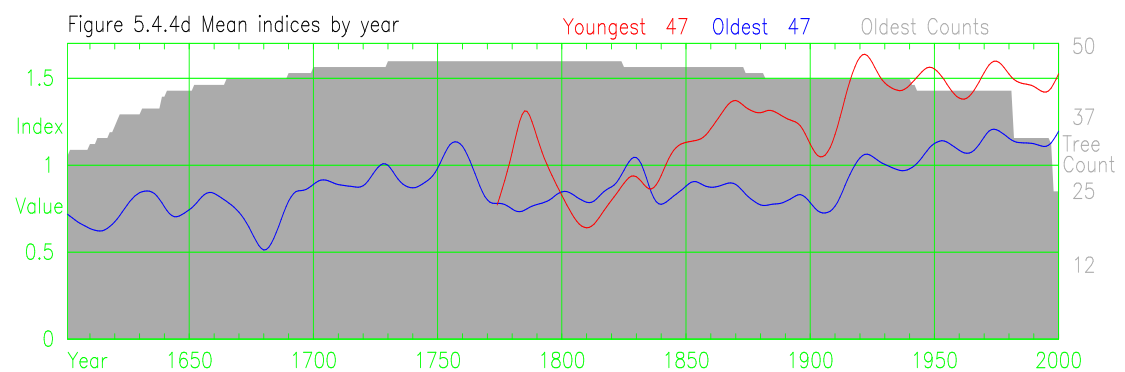
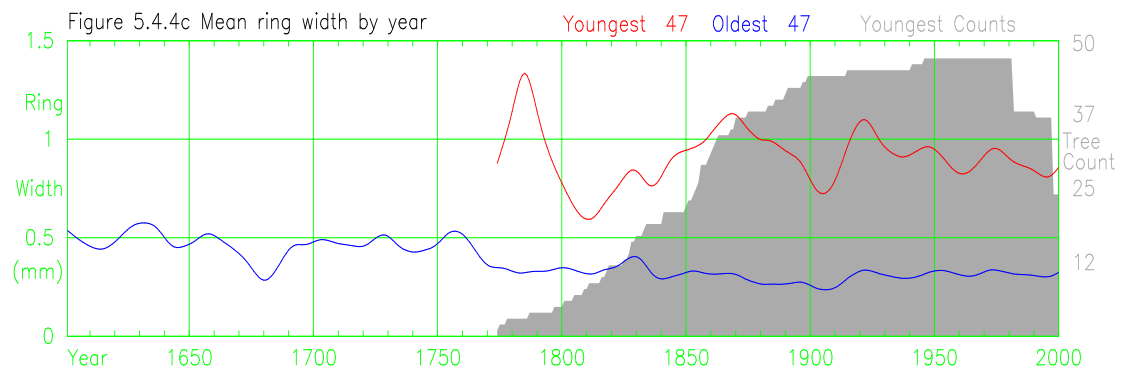
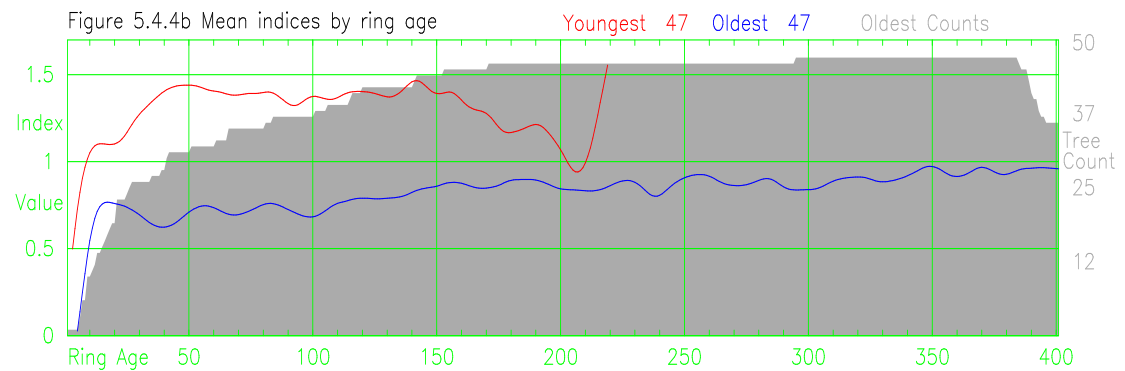
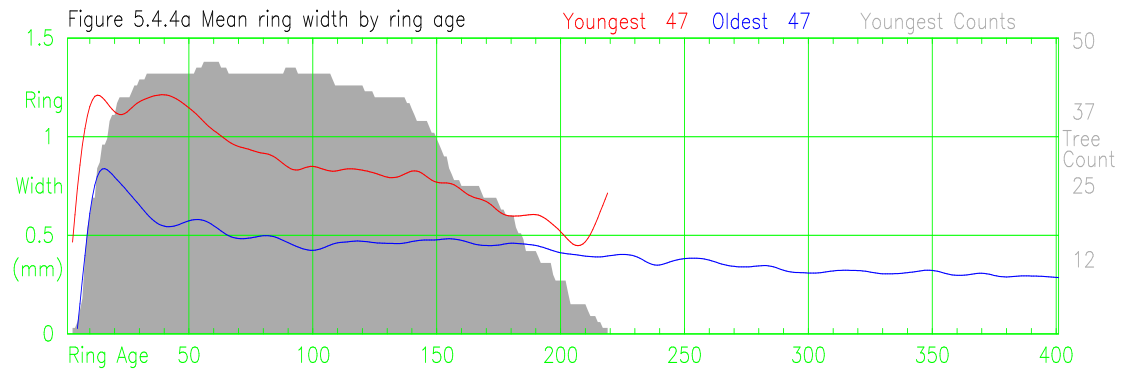


Figure 5.4.4 Plots of mean ring-width and mean indices showing the differences between the youngest and oldest trees in a modern sample. Trees from the Luosto and Helldalisen sites were combined and plots were smoothed with a 20 year spline.

5.4.4b) are expected to slope down but do not slope down because of the large growth increase after 1920. The plot of mean ring-widths by calendar year (Figure. 5.4.4c) show both the larger measures of the younger trees (red) and the smaller measures of the older trees (blue) in the recent centuries whilst only the smaller measures of the older trees cover the earliest centuries. The plots of indices (Figure. 5.4.4d) slope upwards. The growth increase since 1920 shows up in both the youngest and oldest tree indices and is superimposed on the bias.

The RCS method will preserve “apparent” growth changes due to the effects of modern sample bias. Real growth changes that might have occurred could be related to effects such as rising atmospheric carbon dioxide concentration, fertilisation from nitrogen deposition, and increased temperatures (Woodward 1987; Briffa et al. 1998a). All these effects will be superimposed on normal tree growth and represent a single direction change (rise or fall) over a period of a century or two. Any investigation of one of these effects will be dependent on being able to exclude the other effects contributing to low-frequency growth changes (Wigley et al. 1987). Modern sample bias will vary from site to site but because the slope of a chronology is always increased this will enhance site to site and wider region cross correlations at medium-frequencies. Regional means of chronologies will, therefore, retain this bias.

#### 5.4.6. Discussion

Modern sample bias will only apply to trees whose normal growth is in the form of concentric rings, such as the *Pinus sylvestris* used in this project. If between-tree comparisons within even aged stands are excluded, then these statements apply to the comparison of growth rates between stands, where harvesting limits maximum size and the time taken to reach this size varies. The sub-fossil sections of chronologies should suffer less from the size related mortality problem because only dead trees are sampled and mortality by natural causes can be presumed more random in time. Sub-fossil chronologies do not suffer a time related bias from a minimum sampling size because all trees used must have reached a diameter large enough to be preserved, sampled and crossdated and these processes set a minimum sampling size for all time. However, the modern end of sub-fossil chronologies will suffer from the modern sample bias problem. Standardisation methods that create tree indices which are independent of tree growth rates (e.g. curve-fitting methods) will not have problems with modern sample bias.

Modern sample bias might be avoided by taking samples in each year (or decade or century) of interest to preserve homogeneity through time. Modern sample bias is avoided in this study by ignoring the “growth rates” of trees in assessing the common variability of tree growth. Samples from living trees taken in a single year are not suitable for assessing time-dependent changes in the rate of growth of trees (individual trees can be growing faster than they used to but modern sample bias can obscure the differences ). The reliability of the recent end of chronologies that use mean growth rates will be lower than the reliability of the central portion of these chronologies. Without any form of correction, the RCS method (Briffa 1992) and the Age Band Decomposition method (Briffa 2000) will be suspect if used on modern chronologies.

## **5.5. The Slope of the RCS Curve**

### 5.5.1. Introduction

RCS curves set a “natural” limit to the resolution of low-frequency variance in series of tree indices which is the length of the chronology. The RCS method avoids this limit by using the growth rate of trees to set the magnitude of low-frequency variance in the final chronology while the BFM method is limited to using the slope in series of tree indices. This section is concerned with the problem caused by the “slope” of the RCS curve being incompatible with the slope of the chronology and methods of avoiding the problem.

### 5.5.2. Low-frequency limits of RCS Curves

The theory of why any overall trend in a chronology is removed from series of tree indices by the RCS curve is discussed and this is followed by a demonstration of the effects on chronologies of introducing an artificial trend to series of tree indices created using the RCS and BFM methods. A hypothetical example is used to show that using a “site based” RCS curve introduces a limit in the retention of long-timescale variance in series of tree indices. (If the set of trees used to create the RCS curve is not the set of trees used to create the chronology then this constraint need not apply.) If a 1000 year long chronology which should have a 10% slope over the full period of the chronology is created from 200 year old trees then the average extra slope of each tree will be 2%. As every tree has this 2% slope an RCS curve created from these trees will contain this 2% slope, this 2% slope will be removed from each tree during the detrending process, and the 10% overall slope of the chronology will be removed from every series of tree

indices. The average slope of all trees is removed because this forms a part of the age-related growth trend within the RCS curve

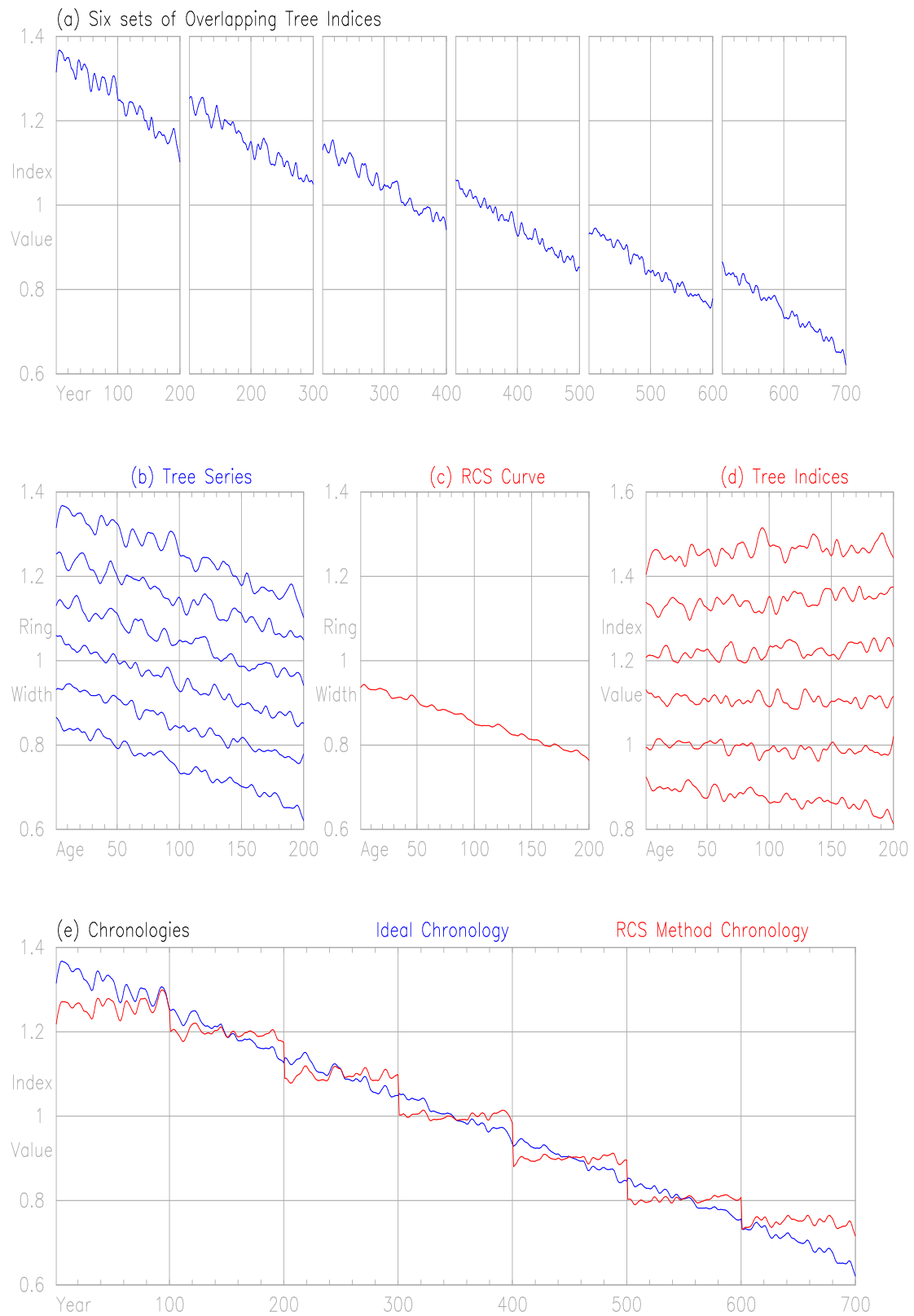


Figure 5.5.1 Demonstration of the incorporation of the mean slope of series into the RCS curve and the removal of this mean slope from resultant tree indices.

This is demonstrated in Figure 5.5.1. Simulated series from trees with a downward slope (a) are aligned by ring age (b) and averaged to create an RCS curve (c) which contains the average downward slope of all trees. The series of indices created (d) by dividing by the RCS curve have lost their overall slope and are (very) roughly horizontal. Figure 5.5.1e shows that the RCS method chronology (red) retains variance beyond the length of the series, derived from the differing mean values of each series of tree indices, but the medium-frequency variance, over the length of each tree, is lost completely relative to the ideal chronology (blue). There may be variation depending on changing tree distribution and tree ages over the life of a chronology but the general conclusion is that detrending with an RCS curve cannot preserve the life-span trend of a chronology in the slope of series of tree indices, despite the RCS method being able to preserve low-frequency variance.

The RCS method uses the mean values of series of tree indices to generate long timescale variance in chronology indices, independent of the slope of individual series of tree indices. The averaging process to create an RCS chronology will be mixing trees with “the wrong slope” (the slope of the chronology having been removed by the RCS curve) with the low-frequency signal generated by the mean value of each series of indices and some distortion can occur. The problem of using arithmetic means to average series of tree indices whose means and slopes do not match is shown in Figure 4.3.1. If the slope of a chronology is not preserved in series of tree indices then the BFM method cannot “generate” this slope from the series of tree indices. If there is no slope over the length of the chronology, the mean values of indices from the first half and second half of the chronology will be approximately equal and in practice demonstrable levels of preserved low-frequency variance will be restricted to frequencies of the chronology length and below. If the BFM method is used on RCS generated indices and there is a significant overall trend in the resultant chronology then this indicates a “theoretical” problem because the above theory precludes a significant overall trend.

The sensitivities of the RCS and BFM methods to the “slope” of the RCS curve are demonstrated by artificially adjusting the slope of an RCS curve and comparing results. An RCS curve was created using the Tornetrask AD chronology and separate “versions” of the RCS curve were created by tilting the initial RCS curve around its “count-weighted centre”, calculated using the procedure described in Section 4.2.3. The RCS

Figure 5.5.2 (a) Varying RCS curve slope RCS curves – Tornetrask AD Chronology

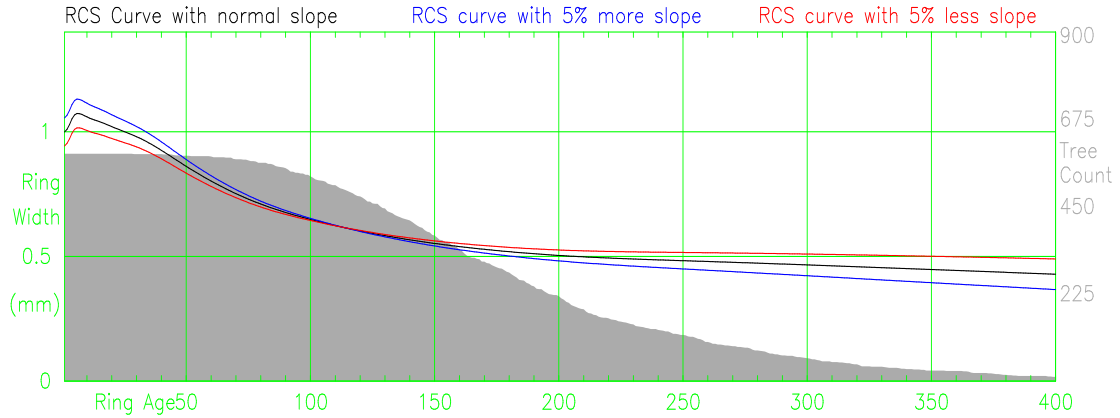


Figure 5.5.2 (b) Varying RCS curve slope RCS chronologies – Tornetrask AD Chronology

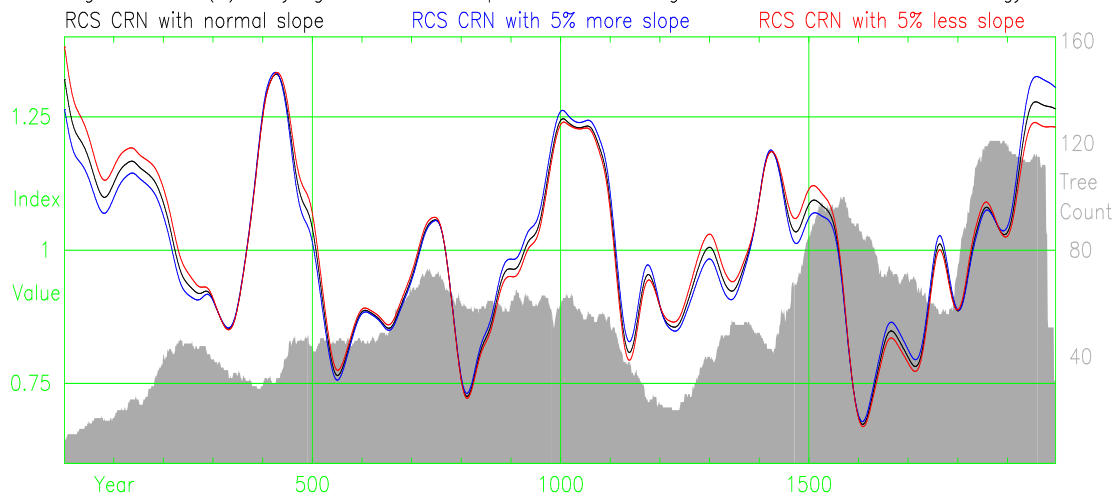


Figure 5.5.2 (c) Varying RCS curve slope Best Fit Chronologies – Tornetrask AD Chronology

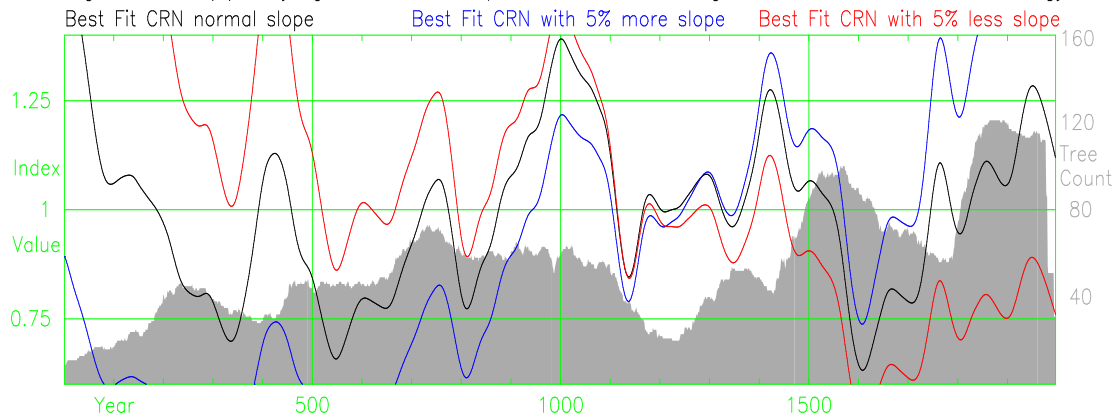


Figure 5.5.2 Sensitivity of RCS and BFM methods to the slope of the RCS curve, (a) RCS curves, (b) RCS created chronologies, and (c) BFM created chronologies.

curve values were increased or decreased by 5% per century based on distance from the centre and the three RCS curves (original, plus 5%, and -5%) are plotted in Figure 5.5.2a. These three RCS curves were used to produce expected growth curves and create tree indices using the RCS method applied to the Tornetrask AD trees. Separate chronologies

were then generated using the RCS method of arithmetic means (Figure 5.5.2b) and BFM method (Figure 5.5.2c). The low-frequency component of the three RCS chronologies are very similar over most of their length where the increases and decreases created by the change of slope balance because of the spread of tree germination dates. The earliest centuries, where the front ends of many trees coincide, and the most recent centuries, where the tail ends of many trees coincide, are sensitive to the slope of the RCS curve. The rotation of the RCS curve about the “110 year centre point” will increase (or decrease) the mean value of series of tree indices that are less than 100 years in length which explains some of the 20th century difference in the RCS chronologies. A “wrongly sloping” RCS curve will create problems in the final century of a chronology because of the subsequent scaling against temperature records involved in creating temperature reconstructions from the chronology.

The three best fit means chronologies vary consistently because the slopes of each tree overlap to form a long chronology and the  $\pm 5\%$  slopes per century are transferred to the chronologies. A “wrongly sloping” RCS curve is disastrous for the BFM method. The BFM method is a mathematical procedure and always arrives at the correct answer (to given precision) although this answer may not be the intended result. The main point here is that the RCS method is not sensitive to the slope of the RCS curve whereas the BFM method is very sensitive to the slope of the RCS curve.

### 5.5.3. Randomly Generated Chronologies

Three large sets of randomly generated trees were created, using the principles set out in Section 3.3.6, to examine some of the problems and solutions discussed in the following sections. The three sets all use the same trees which consist of a simulated sub-fossil chronology and a simulated modern chronology joined together. The sub-fossil section consists of 600 trees with randomly selected ages between 100 and 300 years and each tree starts on a different date between 1100 and 1699. The modern chronology consists of 200 trees each starting on a separate year between 1700 and 1899 and all finishing in the year 2000. Figure 5.5.4 shows ring counts by calendar year for all trees (a), the modern trees (b), and the sub-fossil trees (c). The ring-widths of all trees decay linearly to half their starting value over the life of the tree. The younger trees have larger starting growth values than the older trees, and white noise is added to all simulated tree measures. This large set of randomly generated trees is used to represent a chronology with no common

forcing: called “random no signal”. A 50% step growth increase was added (through multiplying by 1.5) to all tree rings for the period from 1950 to 2000 and this chronology with a step increase is called “random step up”. A 50% step growth decrease was also simulated by division of all rings by 2.0 for the period from 1950 to 2000 and this chronology is called “Random step down”. The step increase and decrease may seem large but the step found in the Luosto and Helldalisen chronologies: 40% over 80 years (Section 4.4.6) is of similar magnitude.

#### 5.5.4. Problems with the Slopes

The sensitivity of standardisation methods to the slope of the RCS curve is only relevant if the slope of the RCS curve can be “wrong”. Three ways in which the slope of the RCS curve can be “distorted” are identified. The first is that the presence of a medium-frequency “common signal” in trees can distort the RCS curve and this is discussed in detail in Section 5.5.8. The second could occur because the RCS curve is created using trees of different ages and this can impart a ring-age-related bias to the RCS curve. The third is a result of building the RCS curve from trees with substantially different growth rates.

If there is a relationship between the rate of growth of trees and the final age of trees then this can alter the slope of the RCS curve. The “random no signal” chronology is used to demonstrate this. All the trees in this artificially generated chronology have a linear slope and the RCS curve for this chronology should be a straight line. Examination of the black line of Figure 5.5.3a shows that the RCS curve is linear for the first 100 years, the period with constant tree count, but is curved in the period during which tree counts are reducing. This curvature is produced here because the older trees are given slower growth rates than the younger trees. The values of the RCS curve at each ring age are the mean size of tree-rings at that ring age. As the younger trees only contribute to the earlier sections of the RCS curve, the mean rate of growth represented by the RCS curve decreases in part because the faster growing (younger) trees are not old enough. Where the rate of growth of trees is measured in terms of the time taken for trees to reach a specified diameter, then the rate of growth of older trees was found to be lower than the rate of growth of younger trees in all the chronologies used in this project. (The implication is that there is a cause of mortality in which the probability of mortality increases with size more than it increases with age.)



The slope of the RCS curve will be greater than the slope found in an “average” tree i.e. the general reduction of ring width with age found in trees. To capture the reduction of ring width with age the RCS curve would need to be built using some form of “first difference” between rings or “average fractional deviations” and in the absence of a suitable alternative the problem remains. This reduction in growth rate by tree age was deliberately built into the random trees because it appeared in the measured trees. The larger magnitude reduction of ring width with ring age in individual trees obscures the effect of mean growth rate reduction by tree age in RCS curves developed from series of measures. The RCS method is insensitive to the excess slope of the RCS curve whereas the BFM method, devised here, is sensitive to the slope of the RCS curve and this problem becomes more significant. From theoretical considerations, the problem must be present in any situation where there is a propensity for slower growing trees to live longer than faster growing trees.

The final slope problem of the RCS curve is that, in practice, trees with substantially different growth rates are used to build the RCS curve. Examination of Figure 5.5.3 (b) and (c) which shows separate RCS curves for the fastest two-thirds (red lines) of trees, the slowest two-thirds of trees (blue lines), and for all trees (black lines) shows that the slopes of the RCS curves vary systematically with tree growth rates. The end-aligned chronologies (Section 3.3.5) are used in this example to avoid the effects of any recent growth increase or modern sample bias and still use all available trees. The slope of these RCS curves will not “fit” the “average” slope of the trees of any particular growth rate. These systematic misfits generate series of tree indices with slopes, which can capture the slope of variation in the “common forcing signal” over their life, but also contain a slope which is a function of the overall growth rate of the tree and the mean growth rate of all trees. The RCS method uses the averaging process to smooth away these distortions but the BFM method, which generates low-frequency variance from the slopes of series of tree indices, has problems with this distortion. When using the BFM method, one solution is to create a series of RCS curves for each “growth rate class” (Section 5.7).

#### 5.5.5. Slope Removal and Trend-free Chronologies

The uneven distribution of upward sloping slow growing tree indices and downward sloping fast growing tree indices can influence the slope of a chronology (Section 5.3).

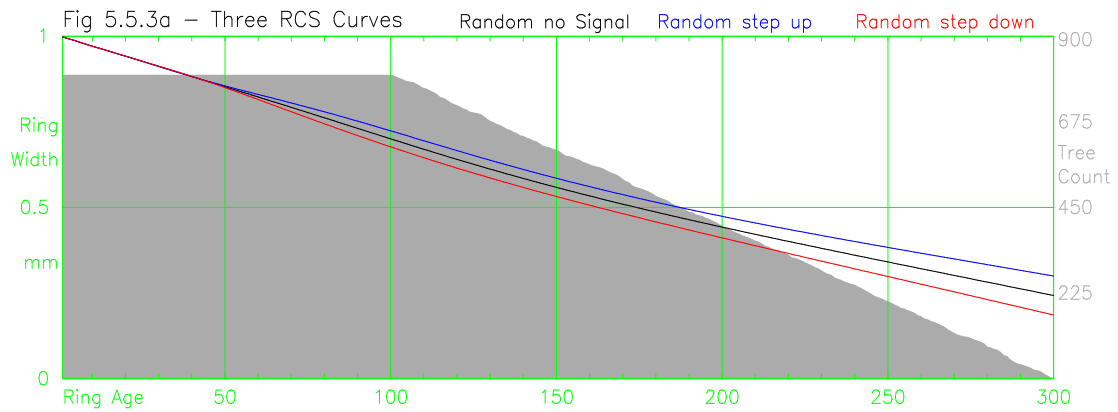


Fig 5.5.3b Mean rings by ring age – Tornetrask End Align Chronology

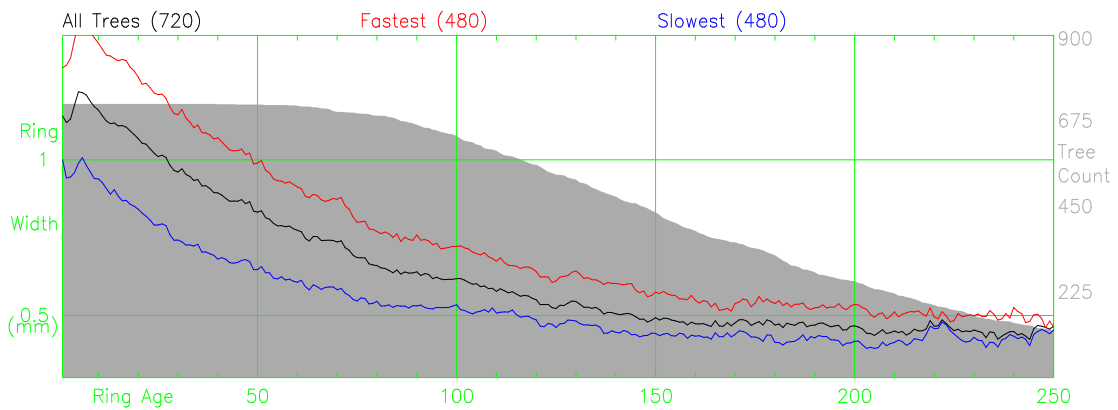


Fig 5.5.3c Mean rings by ring age – Finnish–Lapland End Align Chronology

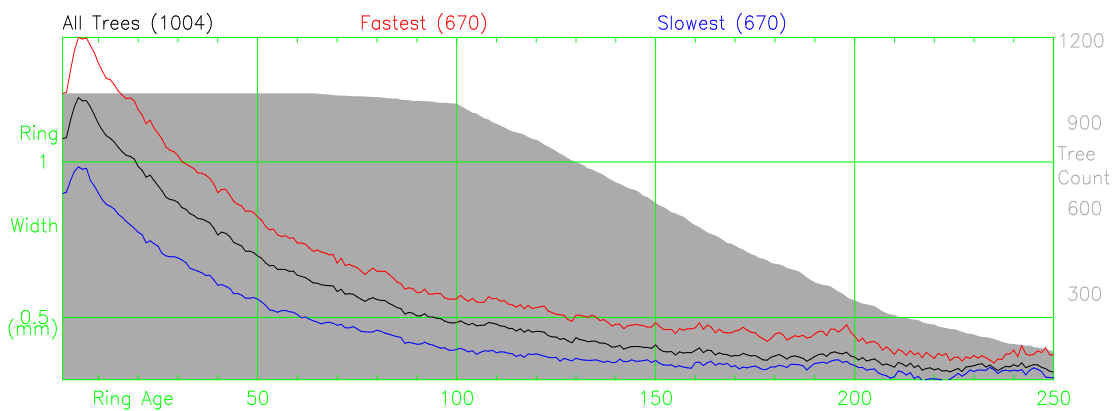


Figure 5.5.3 RCS curves for (a) random no signal, step up, and step down chronologies and (b and c) RCS curves for all, fastest and slowest growing trees from the Tornetrask (b) and Finnish–Lapland (c) end align chronologies.

Modern sample bias can also affect the slope of a chronology (Section 5.5). The tree-age bias can influence the slope of the RCS curve (Section 5.5.4). The “common signal” can influence the slope of the RCS curve (Section 5.5.8). Theory predicts that if the RCS curve has the same slope as the average slope of the trees then the overall chronology created by the BFM method cannot have a significant trend but in practice the BFM generated chronologies can have a significant slope. Solutions to overcome each of these

problems might become available but until they do the pragmatic approach of correcting any “error” in the overall slope of a chronology is adopted here. The method used in this study is to rotate the chronology about its count-weighted centre. The term “trend-free” is used to describe the resulting chronology. The assumption that the BFM method limits the resulting chronology to be “trend-free” allows these “problems” to be minimised by the simple expedient of rotating the chronology to be “trend-free”.

The following calculations rotate a chronology, such that a “count-weighted” best fitting straight line will be horizontal, and the final calculation resets the count-weighted mean of chronology indices to 1.0:

### Data Definitions

Year(1:n)	= Chronology year numbers
Count(1:n)	= Counts of rings for each year of the chronology
Index(1:n)	= Chronology index values
Z	= Count-weighted centre of rotation
Distance(1:n)	= Z – Year(1:n)
a	= Slope change required

### Calculations

$$Z = \text{SUM}(\text{Count} * \text{Year}) / \text{SUM}(\text{Count})$$

$$A = - \text{SUM}(\text{Index} * \text{Count} * \text{Distance}) / \text{SUM}(\text{Index} * \text{Count} * \text{Distance}^2)$$

$$\text{Index} = \text{Index} * (1.0 + a * \text{Distance})$$

$$\text{Index} = \text{Index} * \text{SUM}(\text{Count}) / \text{SUM}(\text{Index} * \text{Count})$$

The flexibility of this rotation is over the full length of the chronology and in practice this will limit the retention of long-timescale variance to frequencies of the length of the chronology and below.

#### 5.5.6. Rotation of Chronologies

Figure 5.5.4 is used to show the effects of rotation on the random chronologies but, before these effects can be seen, other problems need to be explained. In all the chronologies the chronology indices in the final century become progressively smaller, referred to here as “20th century dip”. The cause is that series of tree indices generated by the RCS method slope when plotted by age (Figure 5.3.1b). Faster growing trees produce index series that slope down and slower growing trees indices that slope up. The upward slope of the slower growing trees is concentrated in the first half of the series of indices

while the last centuries of slower growing trees have indices without any slope. The faster growing trees have indices with a larger magnitude (in the RCS method but not the BFM method) and a steeper slope (in both RCS and BFM methods). In the central portion of the chronologies of overlapping trees, when indices from the first section of a tree are too high and indices from the last section of a tree are too low, the effects cancel because each year of the central parts of a chronology is composed of indices from the first and last sections of different trees. In the final century of the chronology there are no “first section of tree indices” and the chronology indices of the final century become progressively smaller because of the downward slope of indices from faster growing trees, a manifestation of modern sample bias discussed in Section 5.5.4.

The RCS method was used to create chronologies from the three sets of random trees described in Section 5.5.3. Modern sample bias is shown clearly in Figure 5.5.4 (a), (b), and (c) with indices created by the normal RCS method (black lines). The indices in the 18th century are low due to the shortage of fast growing trees and the indices for the 20th century are high due to the shortage of slow growing trees (Section 5.4). (The magnitude of this effect in these generated trees is  $\pm 10\%$  or about one quarter of the magnitude normally found in chronology indices.) The indices show the “20th century dip” described above and this “reduces” the apparent magnitude of modern sample bias in the 20th century. The series of tree indices created using the RCS method were used to create “best fit means RCS” chronologies which are plotted in blue (Figures 5.5.4). These chronologies slope upward because the slopes of the decay of the RCS curves are smaller than the slopes of decay of series of tree indices and the RCS curve does not decay linearly as do the series of tree measures. The effects of modern sample bias are reduced by the BFM method and this reduction accentuates the “20th century dip” in the blue and red lines. The AD 1100 to 1700 sections of all three blue lines curve gently where the line approaches zero which is a result of the division method and of approaching the “division by zero” limit (Cook & Peters 1997). The BFM method finds the “natural” slope of these series of tree indices as the blue lines. This “natural” slope has been “averaged” away by the arithmetic means of the RCS method (black lines).

The overall trends were removed from these three chronologies (blue lines) by rotation to create “trend-free” chronologies using the method described in Section 5.5.5 and the resulting chronologies are plotted in red. The “20th century dip” shows up in all three

chronologies. In the “random no signal” trend-free chronology the values in earliest centuries slope up showing trend distortion to balance the down slope of values in the final century (Fig 5.5.4a, red line). In the “random step up” trend-free chronology the earliest centuries’ values slope down to balance the step up of the final century (Fig 5.5.4b, red line). In the “random step down” trend-free chronology the values of earliest centuries slope up to balance the step down of the final century (Fig 5.5.4c, red line). The three chronologies (red lines) are “trend-free” in that a best-fit straight line calculated for each chronology will have a slope of zero.

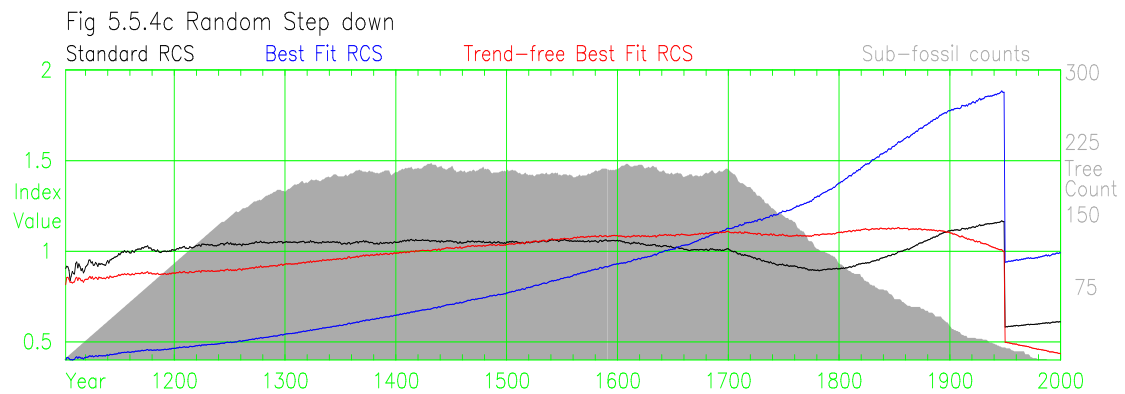
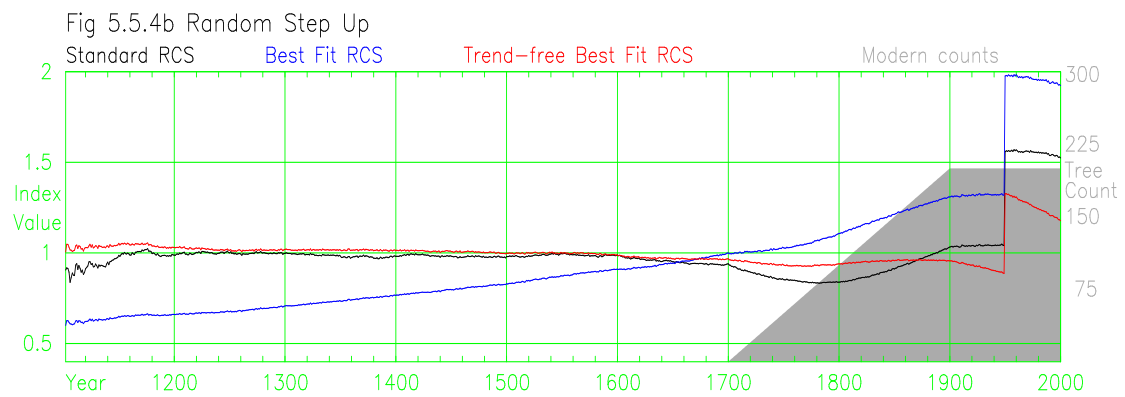
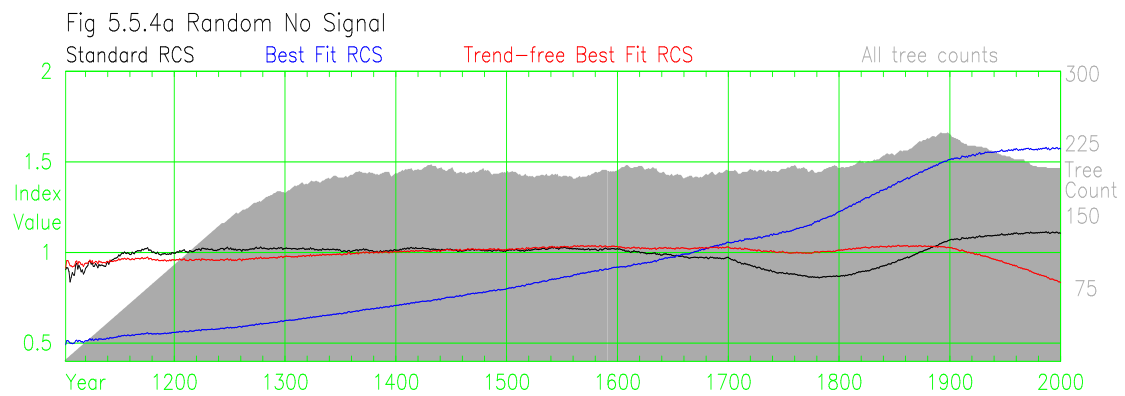


Figure 5.5.4 Comparison of chronologies created with RCS, "best fit means RCS", and "trend-free best fit means RCS" methods using the (a) random no signal, (b) random step up, and (c) random step down chronologies.

This discussion highlights the underlying difficulties inherent in the application of RCS standardisation, with multiple potential biases being superimposed in the final chronology. Their individual effects are virtually impossible to isolate and quantify, even when using randomly generated chronologies with known common signals. Using series of tree measures where the shorter, steeply sloping indices of the faster growing trees are added, by count-weighted means, to the longer, shallowly sloping indices of the slower growing trees and the resulting curve is “adjusted” by progressively removing slower growing trees in recent centuries leads to a chronology whose bias is difficult to describe.

### 5.5.7. Chronology Slope Correction

The chosen method of rotation to remove unwanted “slope” from a chronology was selected because it is readily “reversible”. The three chronologies (Figure 5.5.4, red lines) should be horizontal prior to the 20th century but can be seen to have the “wrong” slope. The slope that is “removed” from a chronology can be reinstated by finding a suitable value for “a” (the slope), which only requires one assumption (one equation for each unknown). Making this assumption requires a means of judging success and it would be possible to select a value of “a” which “maximises” the relationship with measured climate because the manipulation involved (rotation) is at a frequency lower than the lowest frequency at which variance can be retained. An “exact” method was not found but a series of empirical trials found an approximation which is used. The assumption is that the slope of these chronologies is not known and the only information available from which to develop a “correction” is in the chronology indices. Distortion in a chronology is created by having a medium-frequency feature like a step increase near either end of the chronology, as described in trend distortion (Section 4.4.4).

The terminology of Section 5.5.5 is used here. In a trend-free chronology indices to the left of the centre (Z) and indices to the right of the centre will have the same “moment”. This is expressed as follows:

$$\text{SUM left (Index * Count * Distance)} = -\text{SUM right (Index * Count * Distance)}$$

A step increase (decrease) near one end of the chronology will cause the count-weighted mean value of indices of that end to be lower (higher) than the count-weighted mean value of indices from the other end. By rotation, the mean values of indices of the right and left sides can be set equal, a state described as “means-equal”. The gradient “a” of the rotated slope is found by:

$$\begin{aligned}
a = & \quad ( \text{SUM} (\text{Count right} ) * \text{SUM} (\text{Index left} * \text{Count left} ) \\
& - \text{SUM} (\text{Count left} ) * \text{SUM} (\text{Index right} * \text{Count right} ) ) / \\
& ( \text{SUM} (\text{Count left} ) * \text{SUM} (\text{Index right} * \text{Count right} * \text{Distance right} ) \\
& - \text{SUM} (\text{Count right} ) * \text{SUM} (\text{Index left} * \text{Count left} * \text{Distance left} ) ) \\
\text{Index} = & \quad \text{Index} * (1.0 + a * \text{Distance}) \\
\text{Index} = & \quad \text{Index} * \text{SUM} (\text{Count}) / \text{SUM} (\text{Index} * \text{Count})
\end{aligned}$$

This rotation creates an imbalance in the “moment” and the “net moment” gives an estimate of the “trend-correction” required to reinstate the wedge created by trend distortion. Another rotation is used to reduce the “moment” of the “lightest” side by an amount equivalent to the “excess” moment of the “heaviest” side when in the “means-equal” state. The count-weighted mean value of all chronology indices is set to 1.0 after this rotation, in the following manner:

$$\begin{aligned}
a = & \quad \text{SUM} (\text{Index} * \text{Count} * \text{Distance}) / \\
& \quad \text{SUM} (\text{Index lightest} * \text{Count lightest} * (\text{Distance lightest} **2) ) \\
\text{Index} = & \quad \text{Index} * (1.0 + a * \text{Distance}) \\
\text{Index} = & \quad \text{Index} * \text{SUM} (\text{Count}) / \text{SUM} (\text{Index} * \text{Count})
\end{aligned}$$

These three “rotations”, creating a “trend-free” chronology, setting the left and right side means to produce a “means-equal” chronology, and the adjustment to create a “trend-corrected” chronology, are demonstrated in Figure 5.5.5. This is demonstrated using series of tree indices whose slope matches the slope of the final chronology and, because the RCS method is not suitable, the Multiple RCS method (MRCS) described in Section 5.7 is used. The MRCS method was used to generate all series of tree indices and the chronologies were created using the three steps described above to adjust the slope of chronologies. All three methods are achieved by rotating the chronology about its count-weighted centre (Z). It should be stressed that this limits the retention of low-frequency variance to frequencies higher than those of the length of the chronology. The trend-free chronologies (black lines) of Figure 5.5.5 (a) and (b) show the distortion created by setting the slope of these chronologies to be horizontal. The early parts of the “random step up” and “random step down” chronologies should be horizontal but the step up and step down at the modern end of these chronologies creates an overall trend. Setting the

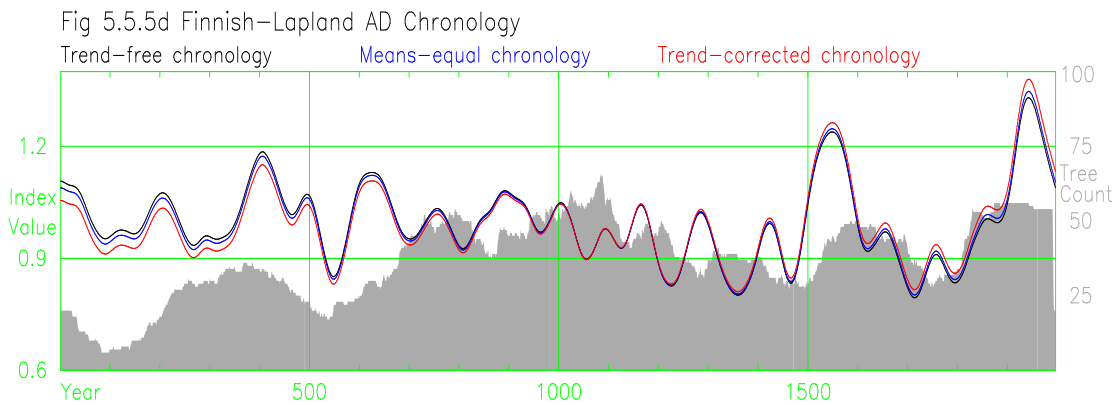
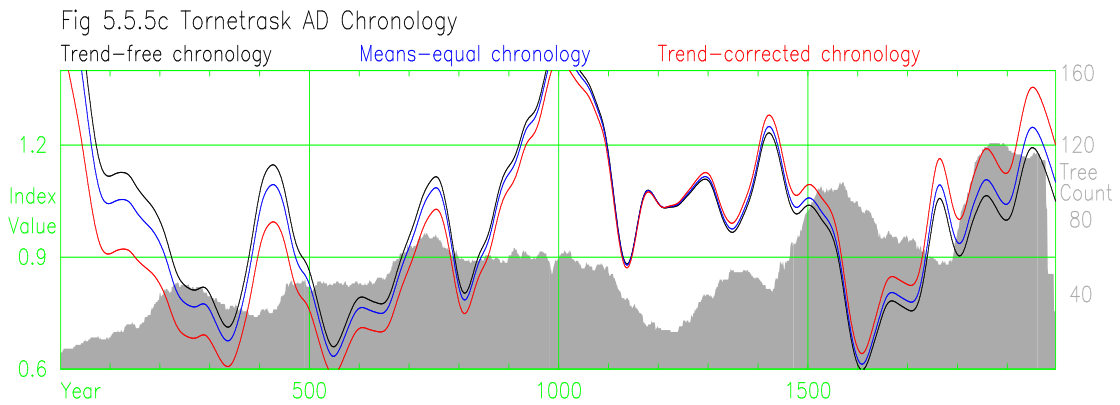
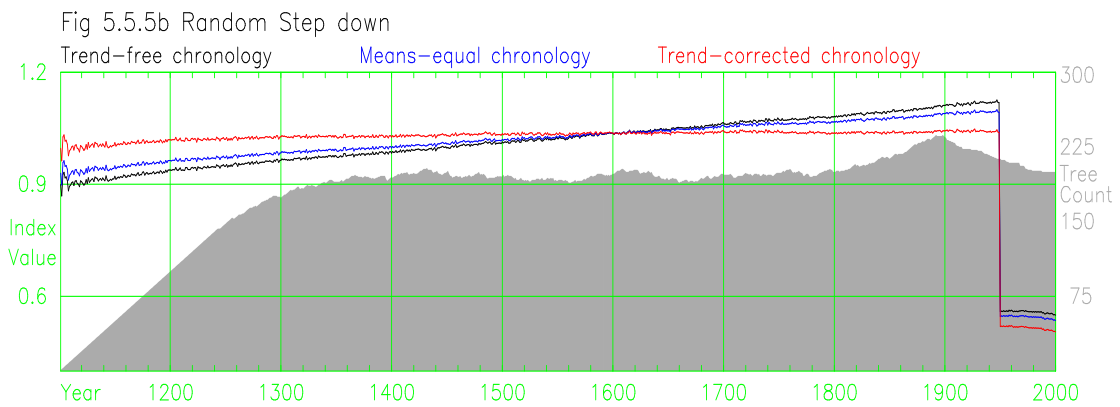
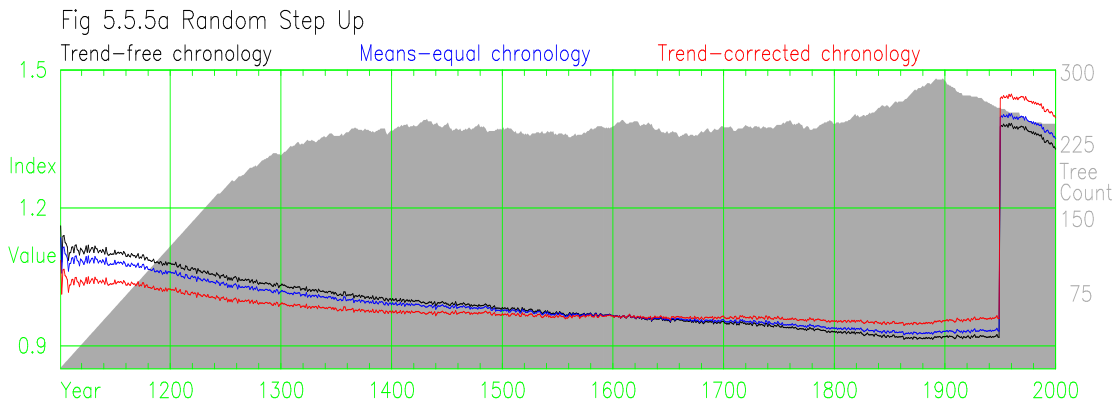


Figure 5.5.5 "Trend-free", "means-equal", and "trend corrected" chronologies for (a) random step up, (b) random step down, (c) Torneatrask AD, and (d) Finnish-Lapland AD chronologies.



means of both left and right halves to the same values reduces the problem slightly as can be seen in the blue lines of Figures 5.5.5 (a) and (b). Though not perfect, the “trend-correction” reduces the distortion in the random chronologies to minor and acceptable levels, as can be seen in the red lines of Figures 5.5.5 (a) and (b). The “trend-correction” in the step up chronology (a) is achieved by “depressing” the left hand side of the chronology by an amount required to counteract the “depression” caused by the step increase in the right hand side of the chronology.

Figure 5.5.5 (c) illustrates the differences in the effects of these methods when applied to ring-width measures from the Tornetrask AD chronology. The “trend-free” black line does not look unbalanced until account is taken of the larger number of trees in the 20th century compared with the 1<sup>st</sup> century. The amount of rotation of the “trend-corrected” chronology seems reasonable but there does not appear to be any way to verify this approximation. The differences between the three chronologies created using the Finnish-Lapland AD trees are small (Figure 5.5.5(d)) and the final chronology from 0 to 1800 appears to slope downward which may indicate an “incorrect slope” but again there does not appear to be any way to verify this approximation. There is no need to retain any particular “slope” when using the MRCS method because all chronologies are generated with an arbitrary slope.

#### 5.5.8. Expected Growth and Common Forcing

The effects of common forcing on trees are to produce variance in the growth measures of a year that is common to many trees and this variance is referred to as the “common signal”. An expected growth value is an estimate of how much growth would have occurred in an average growth year. Ideally an expected growth curve should be derived using series of tree measures which are free from the effects of the common signal because dividing by expected growth values must not remove the common signal. The difference between the “ideal” RCS curve and one that contains the effects of the common signal found in tree measures is considered here to be unwanted distortion.

The RCS curve is usually developed from tree measures that contain the common signal of the period in which the trees grew and if all trees are of the same age and from the same calendar period then the common signal will be exactly preserved in the RCS curve (Briffa 1992). This common signal will be removed from the chronology by the division

process used to produce tree indices (with the exception that the effect of “smoothing” the RCS curve leads to the retention of some variance). If all trees contain the same common signal but are of different ages then the common signal of each year will be contained in different parts (ring ages) of the RCS curve and the high-frequency component of the common signal will be removed by the averaging and smoothing processes used to create RCS curves. The magnitude of the distortion created by the medium-frequency component of the common signal will be reduced by using trees of different ages while the extent of this distortion will be increased and the overall slope of the RCS curve may be changed. The magnitude of this distortion can be reduced to minor levels by using trees from a wide range of time periods (Briffa 1992) and the avoidance of this distortion leads to a requirement for large numbers of sub-fossil trees when using the RCS method. Minor levels of distortion to the slope of the RCS curve are acceptable using the RCS method but because the BFM method is sensitive to the slope of the RCS curve, minor distortion can create a problem (Section 5.5.4).

The three artificially generated random chronologies (random no signal, random step up, and random step down described in Section 5.5.3) are similar in all respects except for the presence of different artificially generated common signals in the last century. These common signals lead to three different RCS curves which are plotted in Figure 5.5.3a. The differences in the slopes of the RCS curves created by the “step up” (blue) and “step down” (red) common signals relative to the “no signal” (black) are a few percent per century. The magnitude of the distortion caused by a step increase (50% increase over 50 years) even when diluted 3:1 by sub-fossil trees and distributed over 250 years still creates a significant change in the slope of the RCS curve. In an “ideal” world the RCS curve created from the trees with no common signal should be used to detrend all three sets of randomly generated trees. The task here is to find a way of removing this “distortion” from the RCS curve.

If chronology indices are fractional deviations and their values are known the effects of the common signal could be removed from individual series of tree measures by division. The term signal-free (Section 4.4.6) is used to describe the results of this division and a signal-free RCS curve could be created using signal-free series of measures. An RCS curve created from a modern chronology with a wide spread of tree ages may be distorted due to medium-frequency variance of the common signal but this distortion will be

spread over centuries and the magnitude of this distortion at any single ring age will be a small proportion of the magnitude of the medium-frequency variance of the common signal that created the distortion. The approach used here assumes that a chronology created using a “distorted” RCS curve will be a rough estimate of the chronology being sought and that this rough estimate can be used to generate a signal-free RCS curve with less distortion.

Division of series of tree measures by chronology indices is the method chosen here. Iterative methods should be able to produce a signal-free RCS curve and more importantly this will partially reduce the need for large numbers of sub-fossil trees. The distortion to the slope of the RCS curve, a few percent per century, will create a chronology with this slope over its full length when using the BFM method. A problem exists in that if there is an overall trend in the chronology (Section 5.5.8) then iterative methods to remove the chronology signal from the RCS curve do not converge (practical observation not theoretical) and the chronology simply rotates. The theoretical idea that the use of an RCS curve removes any overall trend (Section 5.5) allows the chronology to be rotated until there is no overall trend without loss of any of the low-frequency information that is considered recoverable.

Some stages during the removal of the “common signal” from the “random step up” series of tree measures, in the creation of signal-free RCS curves, are displayed in Figure 5.5.6. The Multiple RCS method (Section 5.7) is used to generate eight RCS curves, to create series of tree indices, and to generate a chronology using the BFM method in this example. To simplify the display, the means of the resulting RCS curves (count-weighted sum of the MRCS curves) are used and these are shown in Figure 5.5.6a, the mean values of tree measures by calendar year are displayed in Figure 5.5.6b, and the chronologies are displayed in Figure 5.5.6c. The “1<sup>st</sup> pass” versions plotted in black show the RCS curve with distortion due to the “step up” common signal (a), the effect of this “step up” on the mean ring-widths (b) and the distortion of the chronology due to the presence of the “step up” in the RCS curve. This 1<sup>st</sup> pass chronology is removed from the series of tree measures by division and the signal-free trees used to create a new chronology. These processes were repeated six times and the “3<sup>rd</sup> pass” (blue) and “6<sup>th</sup> pass” (red) versions are displayed. The RCS curve becomes progressively steeper because the effects of the step-up are removed. The “step up” after 1950 could also be described as a “step down”

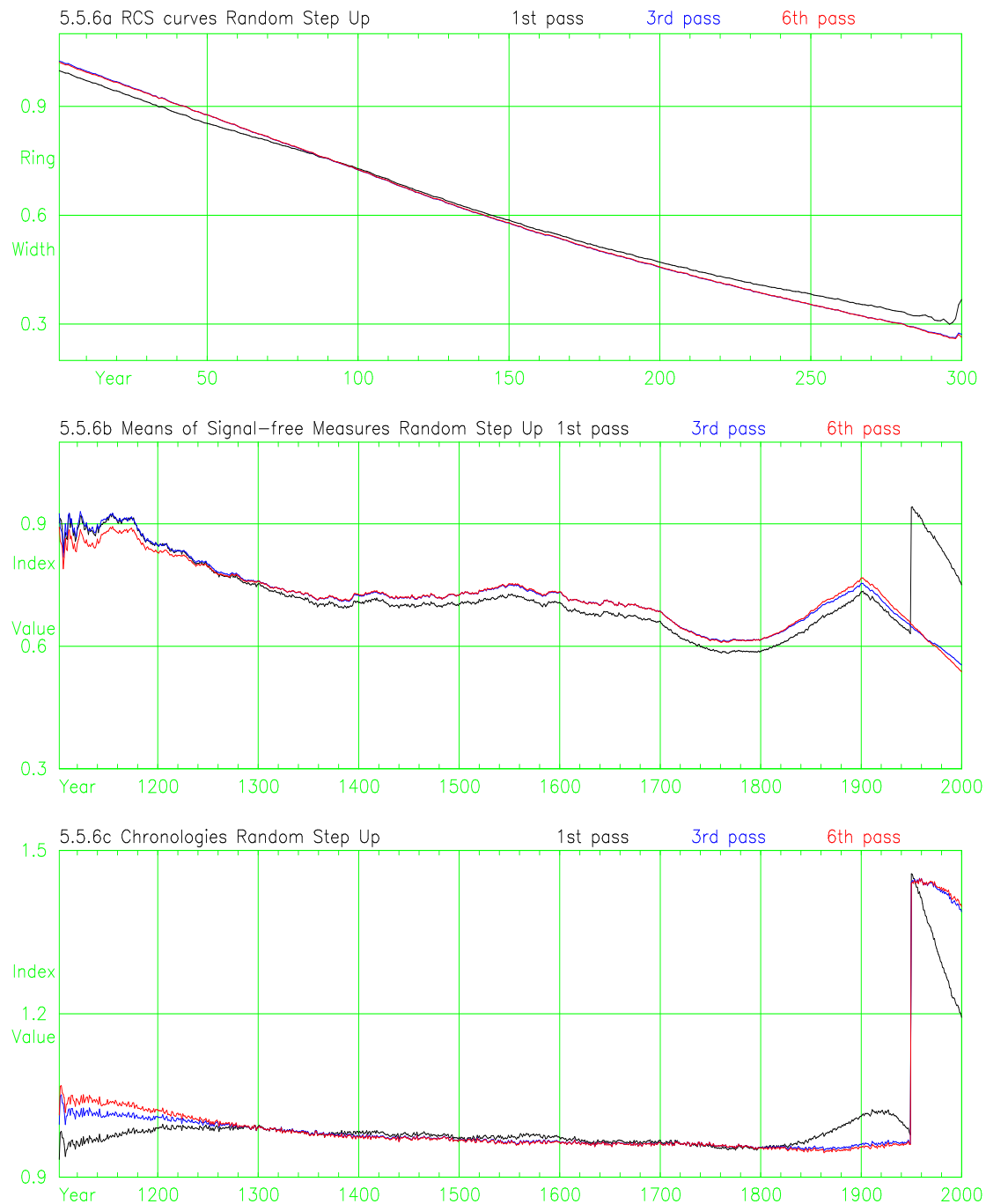


Figure 5.5.6 The 1st, 3rd and 6th stages of the iterative removal of a "common signal" from the random step up trees. (a) RCS curves, (b) means of signal-free tree indices, and (c) the resulting chronologies

prior to 1950 and the procedure, unable to distinguish between these, both increases measured values before 1950 and reduces measured values after 1950. The “step up” from year 1950 to year 2000 in the mean value of signal-free tree indices (b) is removed, leaving all trees sloping down in the last century of growth, the built in linear decay of these random trees. The reduction of bias can be seen at both ends of the chronology in the mean values of tree indices. The presence of the step up signal causes chronology

index values after 1950 to decay rapidly (black line Figure 5.5.6c). This decay (distortion) is gradually reduced by successive iterations. The final result is not “perfect” because other problems still exist but the red chronology is a marked improvement on the black chronology and establishes the value of this iterative approach.

### **5.6. Smoothing the RCS Curve**

The experimentally derived curve of mean ring width by ring age for a site has high-frequency variance resulting from sample variability and is usually smoothed to create a more generally applicable RCS curve. Some form of least squares fitted line (Briffa 1992) such as negative exponential functions (Briffa 1996) has to date been used for the smoothing process. Observations of the data from the sites developed during this study, the red curves in Figure 5.6.1; show that the first few values of the mean ring width curves rise steeply and that maximum values occur in the first decade. The estimates of missing years to the centre of each tree for all these trees clarify the early parts of the mean ring width curves. The end portion of the mean ring width curves, where tree counts are small, have larger amplitude high-frequency variance than do the earlier sections. Smoothing these curves requires a method that can both follow the early rise and remove the high-frequency variance in later years.

A satisfactory method of smoothing mean ring width curves was developed for this project from a cubic smoothing spline (Cook and Peters 1981) by replacing the fixed frequency cut off value with an age dependent frequency cut off value. A cubic smoothing spline with a fixed frequency cut off is fitted by forming and solving a series of simultaneous equations, one for each year. The frequency cut off relates previous and following values to the current value and limits the rate of change of the smoothing curve by setting appropriate values in each equation. A modification of this approach has been developed here that incorporates a frequency cut off that is dependent on cambial ring-age, with a different value for each simultaneous equation, instead of the fixed frequency cut off used traditionally (Cook and Peters 1981). The 50% frequency dependent cut-off at any ring age is set to that ring age plus four for each simultaneous equation. The resulting spline is more flexible in early years and progressively stiffer in later years resulting in retention of the initial rise and removal of unwanted variance in the later years. The method is referred to as an “age dependent smoothing spline”. The resulting unsmoothed RCS curves (red) and smoothed RCS curves (blue) are shown in Figure

5.6.1. This age-dependent smoothing spline has been used here to smooth the RCS curves generated during this project. Although the unsmoothed RCS curves do not match “expectations” of a smoothly varying age-related growth curve the effects of these variations on the final chronology are reduced by averaging over calendar years and the benefits of smoothing are limited to those areas of the RCS curves with small tree counts. The need to “smooth” RCS curves is also reduced by using signal-free trees.

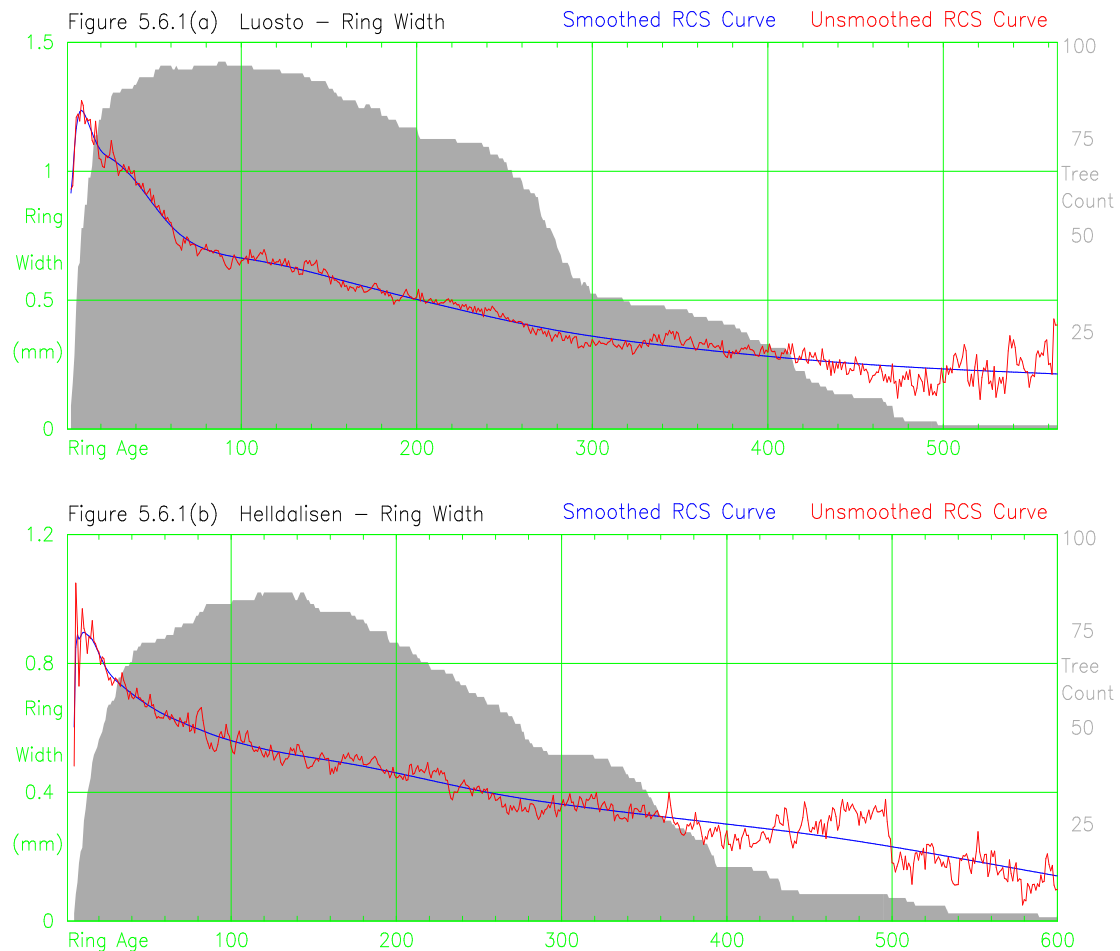


Figure 5.6.1 Smoothing RCS curves using an age-dependent smoothing spline

## 5.7. Multiple RCS Curve Method (MRCS)

### 5.7.1. Introduction

The existence of the BFM method removes the necessity to preserve overall growth rates in series of tree indices and the detrending method need only capture the variance in growth rates over the life of a tree. Earlier it was reasoned that trees that have reached the same diameter in the same amount of time will have similar foliage mass and expected growth rates will be the same. This might lead to the building of an “RCS surface” which

forms a two dimensional estimate of expected growth rates where age and diameter are used to define expected growth values. Hence the expected ring-width value of a 10cm diameter 100 year old tree can be evaluated from an RCS surface. Several thousand trees would be required to provide sufficient data to complete a table of ring-width measures for a variety of time periods for each age and size class of tree. An attempt to achieve this was made by creating a series of RCS curves for classes of growth rates and the method was called the “Multiple RCS method” or MRCS. Using the mean rate of growth of a tree to select a “better fitting” RCS curve would produce improved predictions of expected growth rates relative to the predictions made using a single RCS curve (Section 4.1.5). The slope of series of growth measures will be independent of the best fitting site-related expected growth curve and this method is able to preserve a life-span trend in individual series of tree indices. The decay of ring-width associated with diameter increase is expected to be similar for all trees of a specific growth-rate class and this decay is preserved in the RCS curve built from trees of that growth class, and is removed from the trees by the division process.

A disadvantage of this approach is that large numbers of trees are needed and, with fewer trees in each RCS curve, there will be an increasing probability that the medium-frequency common forcing of a period could distort the shape of the individual RCS curves. The latter problem is reduced by the use of signal-free RCS curves (Section 5.5.8). The mean growth rates of trees will be lost by the MRCS method and it is necessary to use the BFM method to obtain variance at timescales beyond the lengths of individual trees. (It would be possible to use the relative “growth rates” of the individual RCS curves to reinstate the mean value of each series of tree indices and then proceed with the standard RCS method.) The robustness of the low-frequency variance in the chronology becomes dependent on the depth of the overlap between trees (Section 4.3.6). The use of BFM method will limit the resolution of low-frequency variance in a chronology to the length of the chronology (Section 5.5.5). The advantages will be that means of the indices of fast and slow growing trees will have more similar values than produced using a single RCS curve and these indices will have smaller slopes when plotted by age (Section 5.5.4). The effects of both the modern sample bias problem and of microsite variation on tree growth rates will be reduced leading to more robust chronologies and the “modern” end of chronologies will be more stable using the MRCS method than when using the RCS method.

### 5.7.2. MRCS Method

A simple summary of the MRCS method:

1. Sort trees by growth rate and produce multiple RCS curves.
2. Divide original measures by RCS curve values to create tree indices
3. Use BFM method to create chronology indices.
4. Apply “trend-correction” to adjust the slope of chronology indices.
5. Divide measures by chronology indices producing signal-free measures
6. Re-create multiple RCS curves using signal-free tree measures
7. Repeat 2 through 6 until chronology index values settle down.

There are a range of options that could be used within the MRCS method and those selected and some alternatives are discussed. The method used to sort trees by “growth rate” is to compare each tree’s growth rate with the growth rate of a single RCS curve created using all trees. The final radius of each tree is divided by the radius of the single RCS curve at that final tree age to produce a “relative” growth rate for each tree. If the tree has a larger radius than the RCS curve then the tree’s radius at the final RCS curve age is used. Where estimates of missing radius and missing years (rings) to the centre of the trees are available these are used in the creation of the single RCS curve and the estimation of final tree radius and final tree age. Trees are sorted by “relative” growth rates and roughly equal numbers of trees are used to create each of a series of RCS curves representing increasing growth rate classes. The first set of MRCS curves are created using series of measures and all subsequent sorting of trees and creation of MRCS curves is based on series of signal-free measures.

The number of RCS curves and the number of trees used to create each RCS curve are constrained by the total number of trees available. There will be a “minimum requirement” to reduce noise in each RCS curve and diminishing returns in terms of growth rate matching from increasing the number of RCS curves. The use of eight separate RCS curves in this study was the result of limiting the minimum number of trees in any RCS curve to greater than 50 trees and 50 seems a reasonably robust number. In other applications this parameter might vary. (Where trees which are not part of the final chronology are used to create the RCS curves then the “range of growth rates” contributing to each RCS curve may be used in selection and equal numbers of trees in each RCS curve may not apply).



Tree ages vary leading to the oldest part of an RCS curve having a decreasing ring count and an increasing variance. With eight RCS curves the number of rings in the “poorly represented” sections of RCS curves becomes more significant than with a single RCS curve. The faster growing trees used in this study, tend to be younger than the slower growing trees and ring widths tend to similar values as faster and slower growing trees become older (Section 5.5.4). The decision was made here to “top up” the ring counts of faster growing RCS curves that fall below 15 trees to the level of 15 trees by adding in rings from progressively slower growing trees in order to stabilise the variance of the end sections of the RCS curves. The RCS curves are smoothed with an age-related spline (Section 5.6), where a smoothing option is required. It may be more appropriate to use a forward going smoothing mechanism which uses ring counts to weight the smoothing effect of each ring age, thus stabilising variance. RCS curves made from large numbers of signal-free tree measures are relatively smooth and, because the effects of this variance are reduced by averaging over calendar years, there is no necessity to remove this residual high-frequency variance.

Expected growth values for each tree are created by selecting a section of the RCS curve for that tree’s growth rate using the tree’s first and last year. The model selected for this study (Section 4.2) is of the common forcing on tree growth being a “fractional deviation” and this model dictates the division of tree measures by expected growth values to create series of tree indices. Division of tree measures by the values of chronology indices is used to create signal-free series of tree measures (Section 5.5.8). There are two (and maybe more) distinct options to iteratively remove the distortion created by common forcing in the development of chronology indices. The first option is to estimate the common signal, and repeatedly remove this common signal from the trees, develop a residual signal, and accumulate these residual signals with the initial signal to create chronology indices. The second option is to estimate the common signal, remove the common signal from the RCS curves, and create chronology indices using the original series of measures. Both were tried and they produced similar results. The second option was chosen here because this method separates the development of RCS curves from the production of chronology indices and may allow the production of a set of “regional” RCS curves which can be applied to the trees of individual sites to create individual “site” based chronologies. The common signal removed from each tree in the creation of signal-

free RCS curves will be the “site” common signal rather than the “regional” common signal.

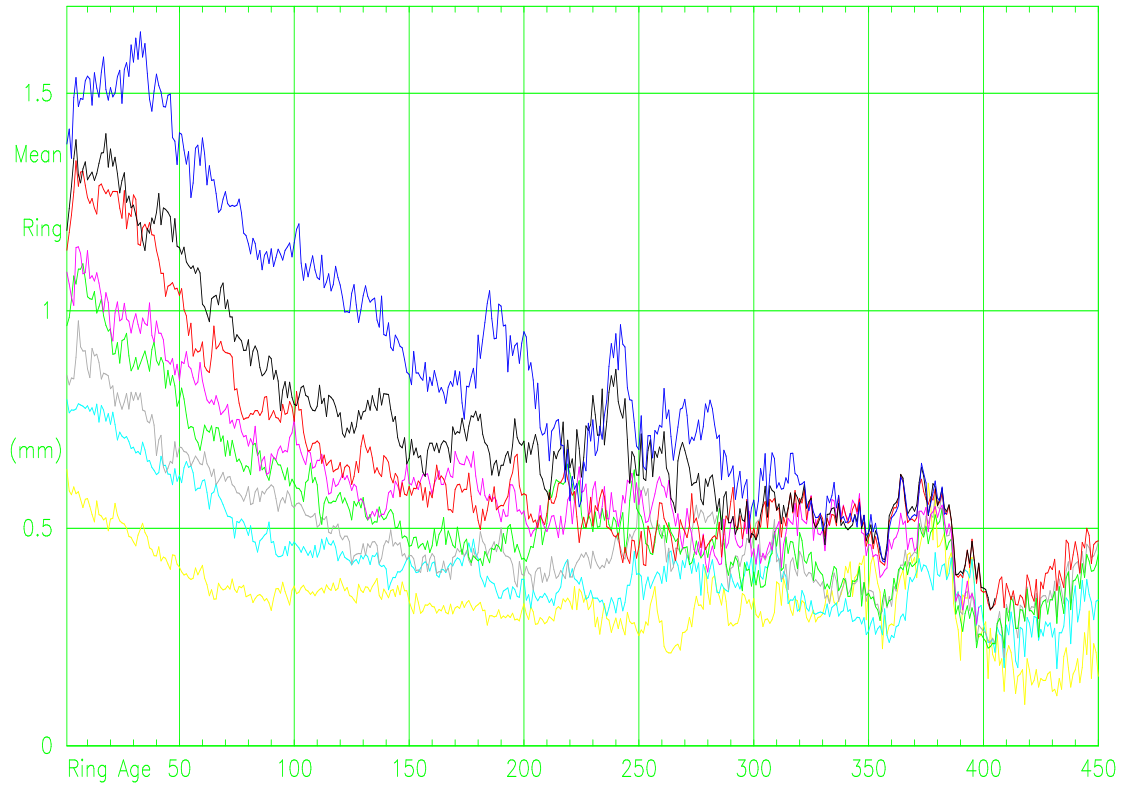
Trend-correction is applied in this study. The overall slope of the chronology and the slope of the RCS curves are matched by the division of each series of measures by the values of chronology indices. If chronology indices form a sloping line then this slope is removed from every tree leading to the slope being removed from the RCS curve(s). Using either a “trend-corrected” or a “trend-free” chronology will have little difference on the final chronology provided the same method is used throughout. The slope of the final chronology being arbitrary i.e. can be set to any value. A detailed description of the implementation of the method used here is contained in the annotated code of the FORTRAN program.

### 5.7.3. MRCS Method - Examples

Sets of multiple RCS curves are shown in Figure 5.7.1 for the Tornetrask AD site and in Figure 5.7.2 for the Finnish-Lapland AD site. The multiple RCS curves created during the first iteration (i.e. from trees that contain the common signal) are shown in figures 5.7.1 (a) and 5.7.2 (a). These RCS curves have intrinsically “different” rates of growth and these different rates of growth tend to reduce to similar mean ring width values in the final centuries. The reduction of “noise“, caused by removing the common signal (signal-free RCS curves from series of signal-free tree measures) can be seen in figures 5.7.1 (b) and 5.7.2 (b). The smoothed RCS curves are plotted on top of the unsmoothed curves (figures 5.7.1 (b) and 5.7.2 (b)) and these curves generally remain separate for the first two centuries after which they converge and sometimes cross.

Examination of figures 5.7.1b and 5.7.2b shows that the smoothed multiple RCS curves look similar for the Tornetrask and Finnish-Lapland sites. The largest growth rate curve at the Finnish- Lapland site is larger than that of the Tornetrask site but the differences do not appear to be excessive and the best fitting RCS curve for each individual tree can be selected on the basis of overall growth rate. Trees from different sites have been used to create single RCS curves (Esper et al. 2002) and this was tried here. The RCS curves were built using signal-free trees and the series of signal-free trees from these two sites were saved and used to generate multiple RCS curves to detrend the trees from the other site. The results of generating chronologies using the BFM method were disastrous and

5.7.1a 1st iteration unsmoothed RCS Curves – Tornetrask AD Chronology



5.7.1b Unsmoothed and smoothed signal-free RCS Curves – Tornetrask AD Chronology

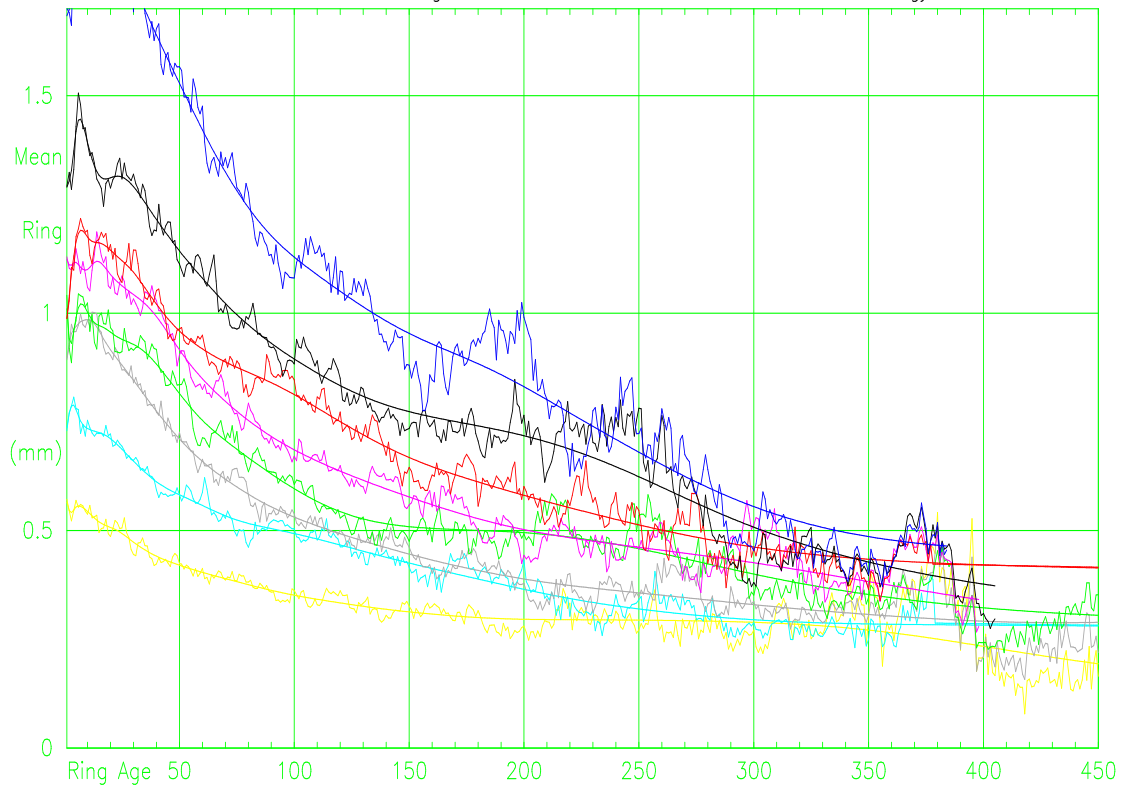
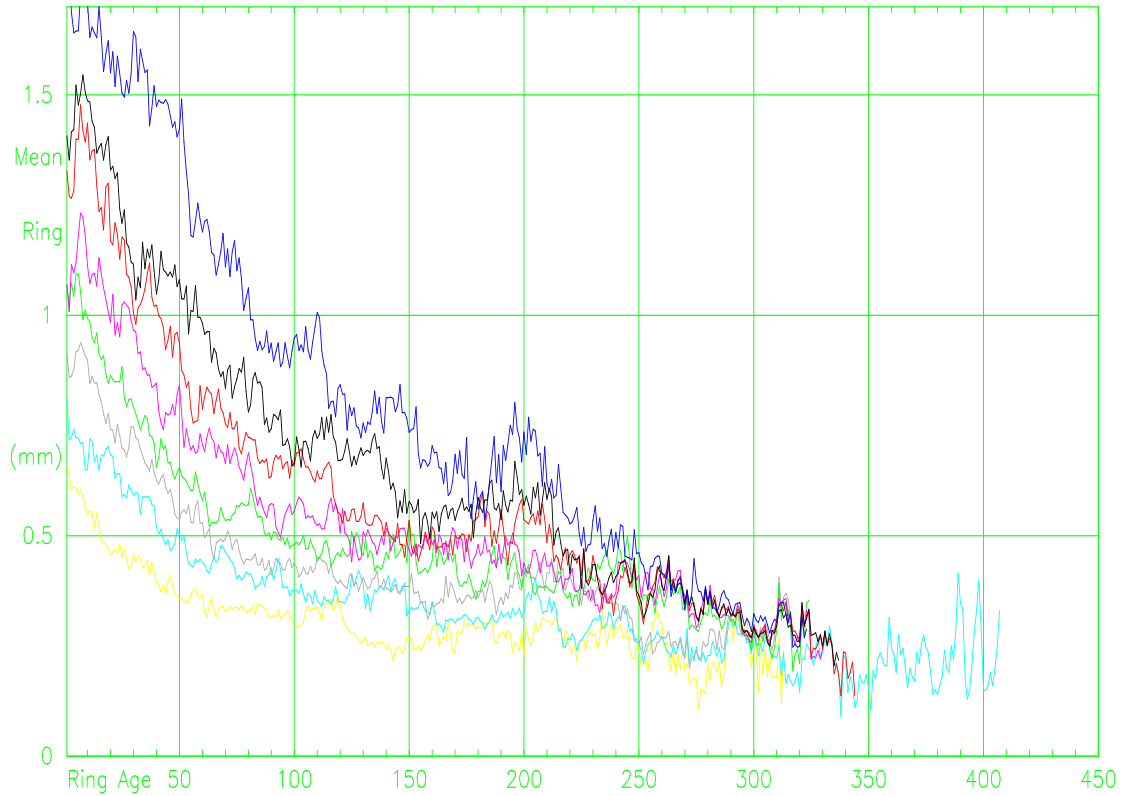


Figure 5.7.1 Multiple RCS curves for Tornetrask AD site. (a) First iteration RCS curves, (b) final signal-free RCS curves and age-dependent spline smoothed RCS curves.

5.7.2a 1st iteration unsmoothed RCS Curves – Finnish–Lapland AD Chronology



5.7.2b Unsmoothed and smoothed signal-free RCS Curves – Finnish–Lapland AD Chronology

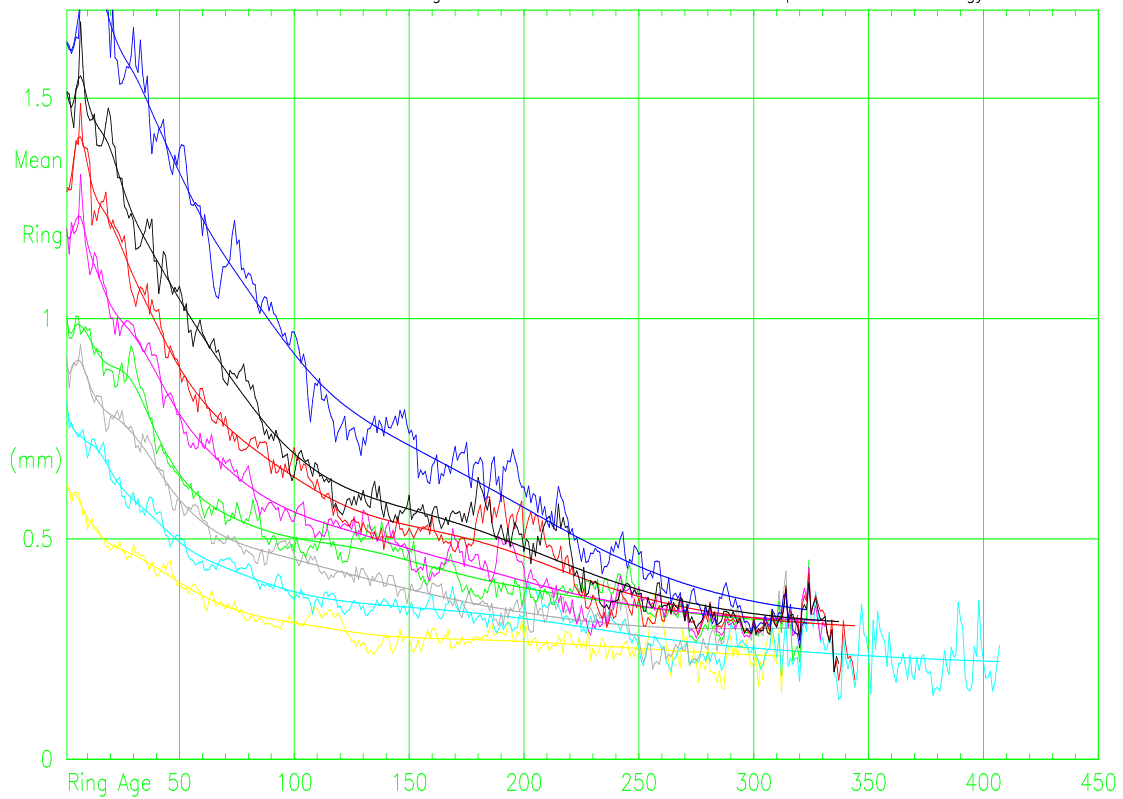


Figure 5.7.2 Multiple RCS curves for Finnish–Lapland AD. (a) First iteration RCS curves, (b) final signal-free RCS curves and age-dependent spline smoothed RCS curves.

Figure 5.7.3 is used to explain why. The single RCS curves for the Tornetrask site (blue) and Finnish-Lapland site (red) have distinctly different slopes. Each site RCS curve is the count-weighted sum of the eight MRCS curves and all are plotted together with Tornetrask MRCS curves in cyan and Finnish-Lapland MRCS curves in grey. The slopes of these MRCS curves are distinctly different in the first century for the two different sites. For a given age and diameter the MRCS curves of the Tornetrask and Finnish-Lapland sites have differing curvatures and using simple rotation will not make up the difference. The Tornetrask trees appear to have a shallower decay in ring-width than the Finnish-Lapland trees in the first century of growth. The RCS method is insensitive to the slope of the RCS curves and chronologies could be produced using the RCS method but the BFM method produces strongly curving chronologies (middle up or down relative to ends) when using the RCS curves from one site to detrend trees from the other site.

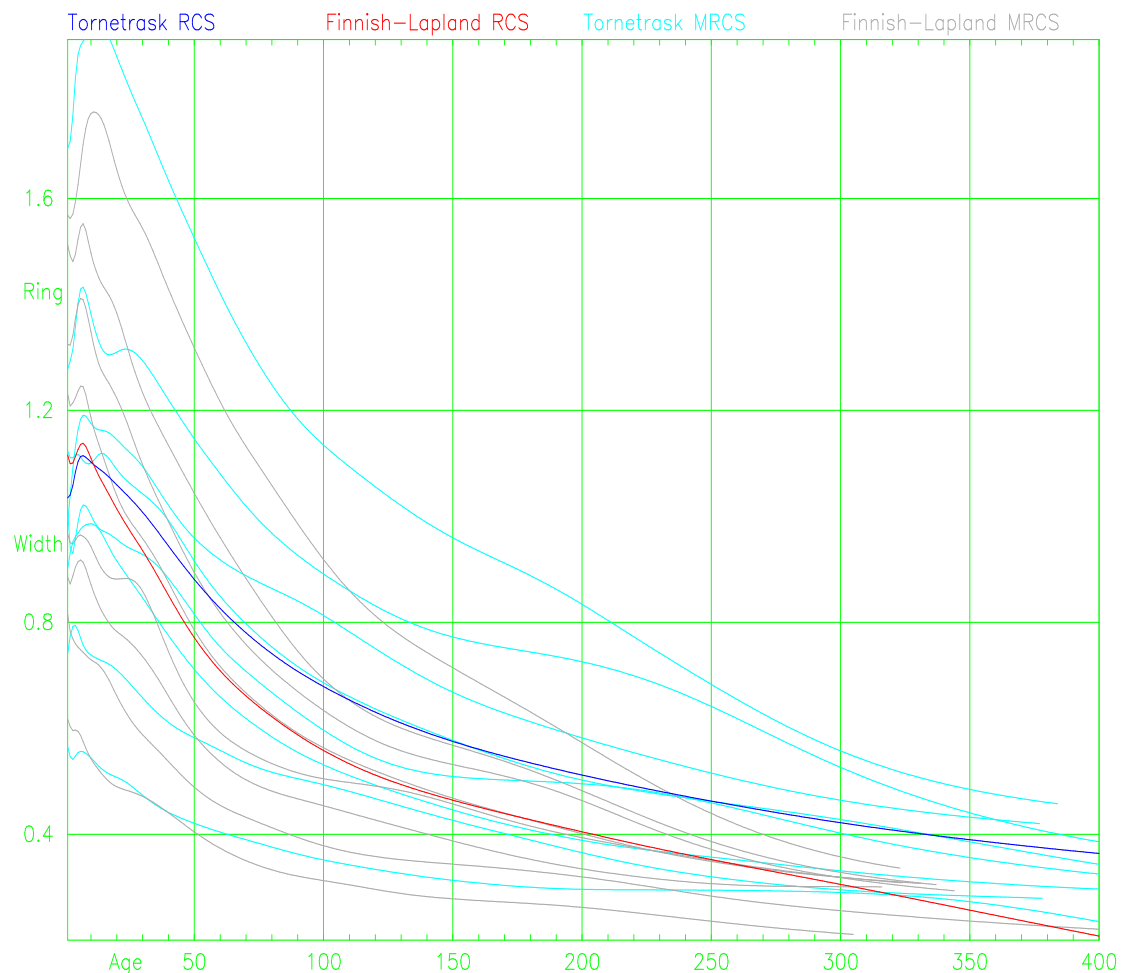


Figure 5.7.3 RCS and MRCS curves for the Tornetrask and Finnish-Lapland sites

Attempts to use RCS curves built of trees from distant sites were abandoned because a solution to the problem was not found in this study. The use of multiple RCS curves

cannot be tested in isolation because the techniques represented by the BFM method, the use of signal-free RCS curves, and the results of chronologies with arbitrary slope are all bundled together in the MRCS method. Testing of the MRCS method and a comparison with other methods is described in Chapter 6.

## **5.8. Size adjusted RCS Method (SARCS)**

### **5.8.1. Introduction**

The RCS and MRCS method require several hundreds of trees and the Size Adjusted RCS method (SARCS) is developed to deal with situations where the number of trees available is limited. The existence of the BFM method allows alternative methods of developing expected growth curves from an RCS curve. The SARCS method is an adjusted version of the RCS method in which a tree's radius is used to obtain a "better fitting" series of expected growth values from the RCS curve than can be obtained using ring age alone. When using the RCS method, ring age is used to select a portion of the RCS curve to form the expected growth values of a tree. Because diameter increase leads to ring-width decay it would be reasonable to use diameter instead of age to estimate expected growth. A diameter based regional curve was tried in which, for all trees, the average time in years to grow through each millimetre of diameter from zero to the largest diameter reached was plotted. The "expected growth rate" of any tree ring could be evaluated using the tree's current diameter to "look up" the mean growth rate of all trees at that diameter. The results (not shown) were similar to those of the standard age based RCS method suggesting that either age or diameter can be used to predict expected growth values. The model of expected growth rate (Section 4.1) developed from tree-growth models, suggests that both age and diameter need to be used in the prediction of expected growth values. This raises the possibility that if an age-based RCS curve is created and expected growth values are selected on the basis of tree diameter then both age and diameter are being used to develop expected growth values. Both "size adjusted age" and "age adjusted size" methods were investigated in this study. Both produced similar results but because the "size adjusted age" or SARCS method is a simple modification of the existing RCS method of selecting expected growth values, the SARCS method was selected for use in this study.

In the RCS method the expected growth curve for an individual tree is the series of values selected from the RCS curve using that tree's first and last ring age. A portion of the

change of ring width in trees that have circumferential growth is due to radial increase. The accumulating (over time) area beneath the RCS curve represents increasing radius and a different segment of the RCS curve could be selected for an expected growth curve using a tree's initial and final radius. This segment of the RCS curve will represent some form of the average rate of ring width decay of all trees when progressing from the initial to the final radius, but split into the average number of time steps. The presumption that time is not a driving factor in tree growth (Landsberg 1986b) and knowledge that the RCS curve is smooth allows the RCS curve to be linearly partitioned into an arbitrary number of equal time steps. (The choice of linear partitioning is for simplicity, in the absence of justification for more complex methods.) It is necessary to divide this segment of radial growth into the same number of time steps (one for each tree ring) that correspond to the time taken for the individual tree to grow in order to obtain an expected growth value for each measured ring-width. The underlying presumption is that the RCS curve captures the average rate of decay of ring-width in trees over the selected diameter range. Faster growing trees will achieve this decay in less time than the "average" time taken by the RCS curve and slower growing trees will take more time to achieve this decay. By dividing the selected segment of the RCS curve into an appropriate number of steps the RCS curve is "fitted" to the individual tree.

Because the expected growth curve and the series of measures have the same number of years and the same radial increment both will have the same mean value. Indices created by division will have a mean of approximately 1.0 and a roughly homogeneous variance. This method does not preserve variance at frequencies beyond that of the length of the tree because the mean values of series of tree indices are set to 1.0 (Section 4.3.2). If a series of measures started with small rings and ended with large rings (relative to the average tree over the same radial increment) then this life-span trend is preserved in the resulting series of tree indices. Consistent with the model of "fractional deviations" tree indices are created by division. The chronology is created using the BFM procedure in order to obtain variance at timescales beyond those of the length of individual trees and the frequency limit of half the length of the chronology will apply. The method of slope adjustment used with the SARCS method is "trend-correction", as for the MRCS method. To reduce the effects of low-frequency variance of the common signal, signal-free series of tree indices are used to create a signal-free RCS curve.

### 5.8.2. SARCS Method

1. Build age based RCS curve(s) from tree measures.
2. Extend the RCS curve(s) to fit the largest diameter tree.
3. Select expected growth values from the RCS curve using tree radius.
4. Divide original measures by expected growth values to create tree indices.
5. Use BFM procedure to create chronology indices.
6. Apply “trend-correction” to adjust the slope of chronology indices.
7. Divide measures by chronology indices producing signal-free measures.
8. Re-create the RCS curve(s) using signal-free tree measures.
9. Repeat 2 through 8 until chronology index values settle down.

There are a number of alternative methods that could be used to build the RCS curve and to select expected growth values. The choices made in the SARCS method are empirical in that reasonable results ensue. The important features are that both age and radius are used in the development of expected growth values and that the method chosen can preserve a trend over the life of a tree. The minimum number of trees needed will be a subjective decision. Sufficient trees are needed to remove the high-frequency noise found in series of tree measures aligned by calendar year. Sufficient trees are needed to estimate the age-related growth trend (RCS curve). Sufficient overlap of tree series is needed to produce acceptable limits to confidence levels when using the BFM method. The option to use a signal-free RCS curve rather than signal-free trees was selected following the same reasoning used in the MRCS method (Section 5.7.2). The SARCS method uses ring age and tree diameter and, where available, estimates of missing pith years and radius are used. In the absence of these estimates then the first ring of each tree is assumed to start at zero diameter and to be the first year of growth.

A problem with the SARCS method is that the radial increment of the RCS curve (the average of all trees) will be less than the radial increment of the largest trees and it is necessary to extend the RCS curve in order to produce expected growth values for the later rings of the larger trees. The extension of the RCS curve can be achieved in many ways; the extrapolation of a smooth curve, linear extension, and the expected decay due to diameter increase were all tried with no method being particularly successful. It would be possible to discard rings near the end of larger trees but because the method is designed for use with limited tree numbers this is not considered a practical option for



this study. A further option arises with the SARCS method in that if 100 trees were available then two separate RCS curves of 50 trees each (faster and slower growing trees) could be used thus combining the MRCS and SARCS methods where tree numbers are sufficient. The reliance on extended RCS curve values and the amount of stretching and shrinking of timescales would both be reduced by using two RCS curves leading to less scope for error. A decision was made for this project to set the SARCS method to use one RCS curve for less than 80 trees, two RCS curves for 80 to 150 trees, and three RCS curves for more than 150 trees. A detailed description of the implementation of this method used here is contained in the annotated code of the FORTRAN program.

The difference, created by using multiple RCS curves with the SARCS method, in the reduction of ring age-related bias in series of tree indices is shown in Figures 5.8.1. The Finnish-Lapland AD chronology was used and series of tree indices created using one RCS curve (a), two RCS curves (b), and three RCS curves (c) are plotted by ring age for fast and slow growth rate classes. Rates of growth were established by the time taken (or projected to be taken) for each tree to reach 10cm radius. The mean values of tree indices for the fastest growing trees (red) and the slowest growing trees (blue) are plotted in Figures 5.8.1. Using one RCS curve (a) the age-related bias is less than half the magnitude of that created by the RCS method (Figure 5.3.1d) but the index values of the first three decades slope steeply, slow growing trees slope down and fast growing trees slope up. Using two RCS curves (b) and three RCS curves (c) reduces the magnitude of the bias and the slope in the first 30 years demonstrating the improvement achieved by using more than one RCS curve in the SARCS method. The series of tree indices were sorted by final tree size and mean index values by ring age for the smallest trees (blue) and largest trees (red) are plotted in Figure 5.8.2. The results are similar to those for the faster and slower growing trees except that the excessive slopes in the first three decades are more consistent. Similar results (not shown) can be produced using the Tornetrask chronology suggesting a consistent pattern of “ring age-related bias” when using the SARCS method. This bias is probably caused by the decision to use linear partitioning of the RCS curve in the creation of expected growth curves. That the end portions of the largest trees all dip downwards suggests a problem with the RCS curve extension method. Using two curves in the SARCS method produces less than one quarter of the ring-age-related bias found in the RCS method. The steep slopes of the first few decades of series of indices can lead to an “overlapping” problem. The Finnish-Lapland trees

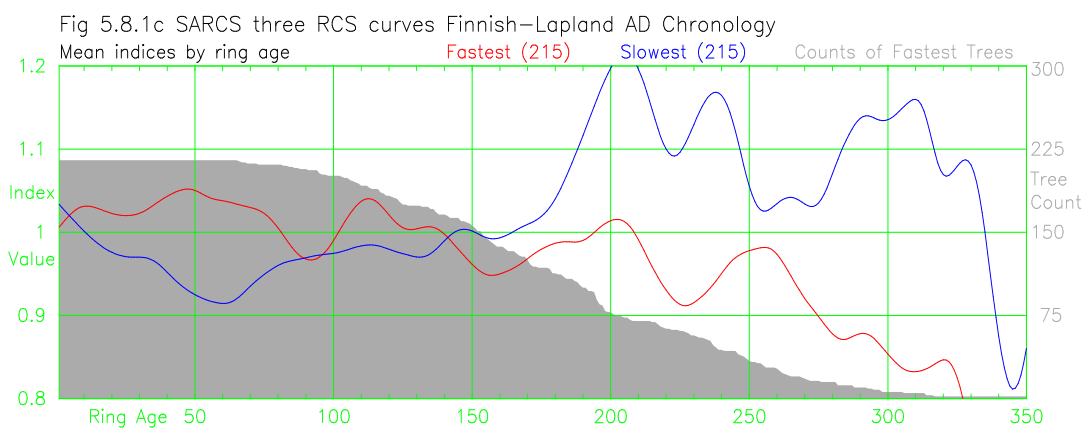
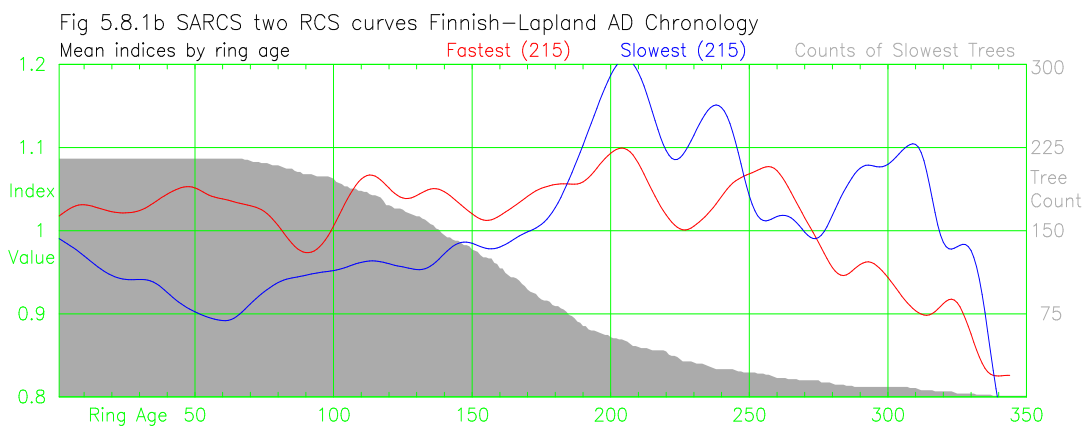
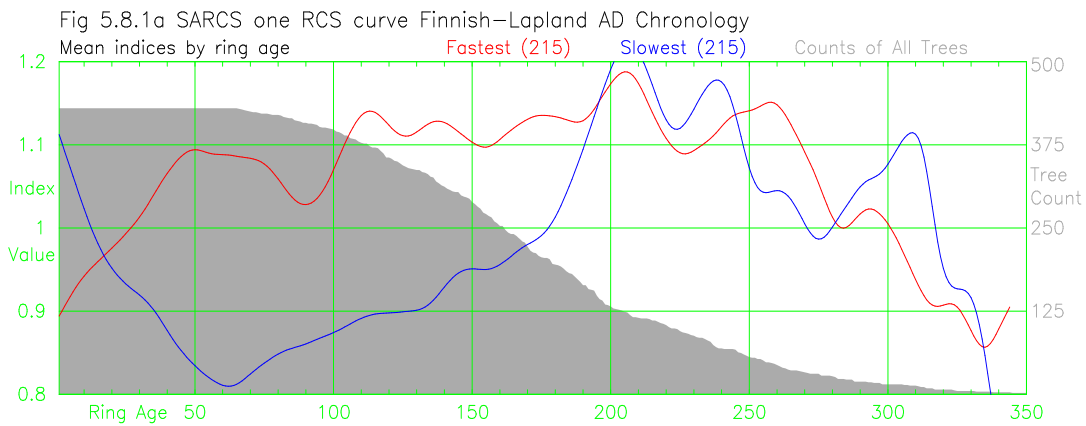


Figure 5.8.1 Comparison of mean indices by ring age of the fastest and slowest growing trees at the Finnish–Lapland AD site using the SARCS method with (a) one RCS curve, (b) two RCS curves (c) and three RCS curves.

which were growing during the period AD 530 to 550 are used to demonstrate how this problem can occur. Figure 5.8.3 shows that four trees end and eight trees start between AD 510 and 540. The BFM method is sensitive to the level of overlap. The demonstration using the BFM method with shortened series of tree indices shows how this sixth century period in the Finnish-Lapland chronology (Figure 4.3.4b) and the AD 400 period in the Tornetrask chronology (Figure 4.3.4a) become “unstable” if some of the long series are

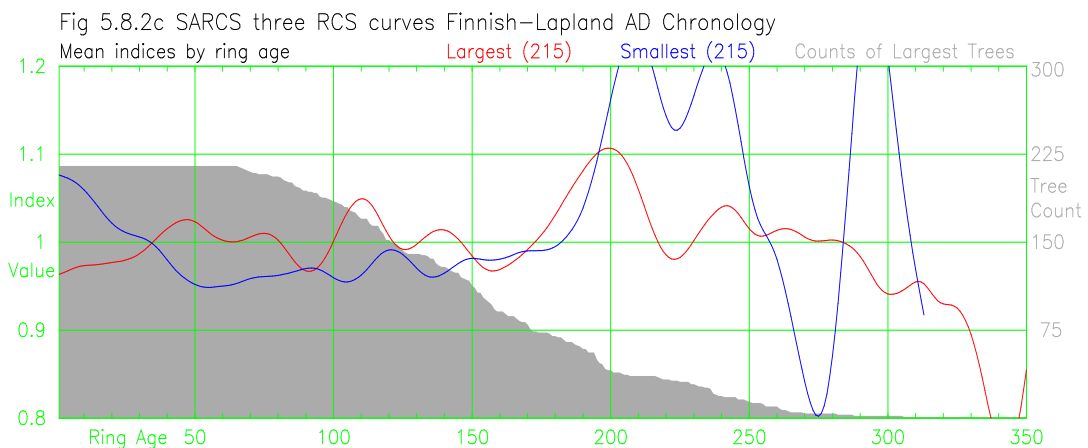
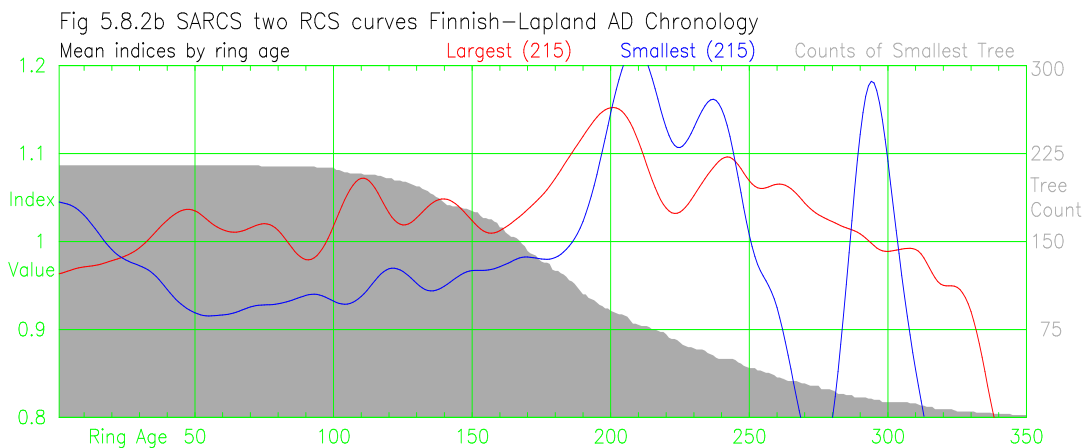
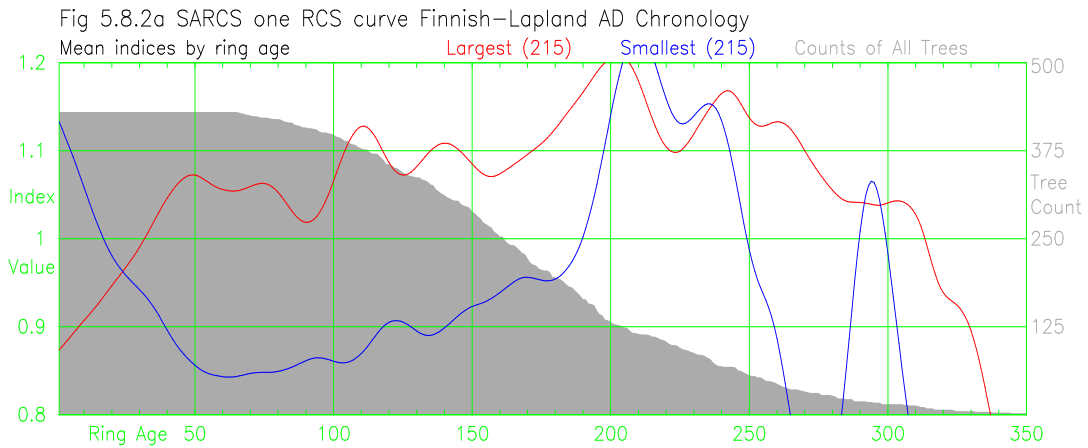


Figure 5.8.2 Comparison of mean indices by ring age of the smallest and largest trees at the Finnish–Lapland AD site using the SARCS method with (a) one RCS curve, (b) two RCS curves (c) and three RCS curves.

split into shorter sequences of tree indices. The SARCS method will be more sensitive to the depth of overlap of trees than the MRCS method due to the larger slopes of series of tree indices in the first few decades but, in practice, the SARCS method is less likely to be used on long chronologies.

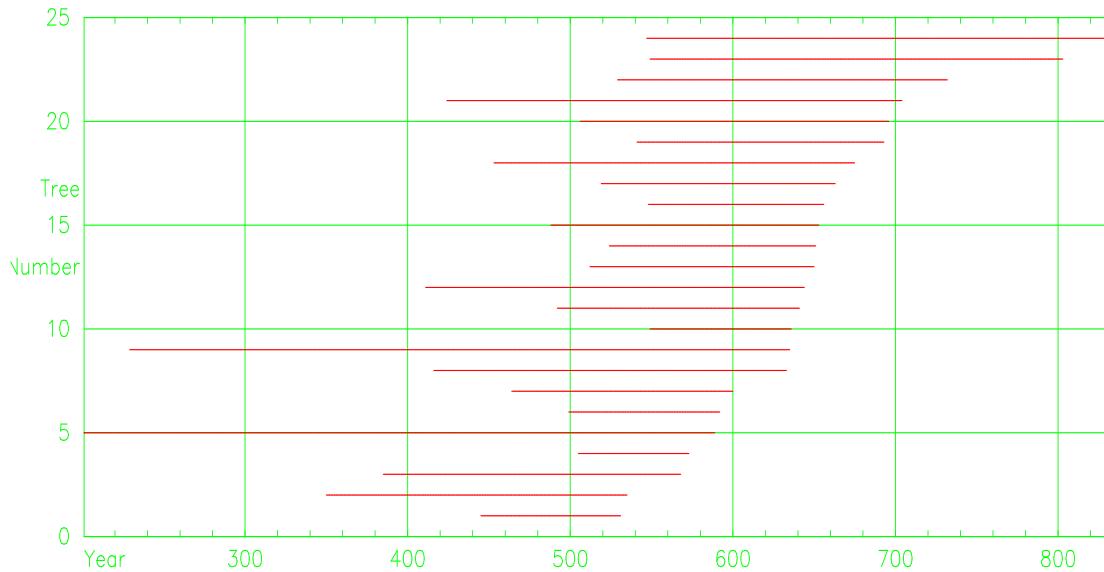


Figure 5.8.3 The overlap of trees from the Finnish-Lapland site in the AD 530 to 550 period.

The “stretching” of RCS curves to fit individual trees cannot be tested in isolation because the techniques represented by the BFM method, the use of signal-free RCS curves, and the problems of chronologies with arbitrary slope are all bundled together in the SARCS method. Testing of the SARCS method and a comparison with other methods is described in Chapter 6.

### 5.9. Conclusions

Expressing the RCS curve in terms of mean ring width against ring age for a sample population of trees does provide the opportunity to preserve long-timescale tree-growth forcing in chronologies, but this work has identified several problems and potential biases in its application. The wider significance of these in different ecological situations needs further exploration but the specific aspects of the operation of the RCS approach that required investigation in this further research were identified. A list of these problems is as follows:

1. Faster growing trees make larger contributions to the chronology than do slower growing trees.
2. Series of indices from faster growing trees slope downwards and those from slower growing trees slope upwards.
3. The method is unable to distinguish between the rate of growth of fast and slow growing trees in the later stages of growth i.e. in the 3<sup>rd</sup> century of the examples.
4. The average slope of the chronology is removed from each series of tree indices resulting in the potential loss of some *medium-frequency* variance.

5. *Modern sample bias* will occur in chronologies if there is a tree age-related growth bias. The age related bias is a ubiquitous feature of trees with circumferential growth.
6. The RCS curve slope is not the same as the average slope of the decay of ring width if there is a tree age-related growth bias in the samples used to construct the RCS curve.
7. The shape of the RCS curve can be biased by the presence of a trend in the common forcing of the modern period (*trend distortion*).

The BFM method rescales each tree to preserve long-timescale variance. This rescaling solves some of the problems of the RCS method and, in addition, allows alternative methods of developing expected growth curves which can solve further problems.

New tools and techniques have been introduced to overcome specific problems. The problem that faster growing trees make a larger contribution to the chronology than do slower growing trees i.e. problem (1) is removed by the BFM method which rescales each series of tree indices. The problems that series of indices slope (2) and converge in the 3<sup>rd</sup> century (3) are reduced by using diameter in the generation of expected growth curves; the MRCS method uses diameter to select from eight RCS curves and the SARCS method uses diameter to stretch the RCS curve to fit each tree. The RCS, MRCS and SARCS methods can still lose some medium-frequency variance (4) from the chronology, though this effect is likely to be significant only at the “ends” of a chronology. The MRCS and SARCS methods, by limiting the retention of long-timescale variance to that of the length of the chronology, impose long-timescale variance limits, of the slope of series of tree indices and of the mean values of series of tree indices, with consistent values. However, this consistency allows the overall slope of MRCS and SARCS generated chronologies to be adjusted whereas RCS (and curve-fitting) chronologies cannot be “rotated”. The problem of modern sample bias (5) is removed by the BFM method which rescales each series of tree indices.

The RCS method is not sensitive to the slope of the RCS curve (6) but the BFM method suffers from this problem, which is transferred to the MRCS and SARCS methods. The solution adopted here is to assume that chronologies created using the BFM method have an arbitrary overall slope and an approximate method of resetting the slopes of chronologies is proposed and used in the MRCS and SARCS methods. This solution to

the problem of chronologies having the wrong slope (i.e. of rotating the chronologies) is a preliminary expedient. A better solution would be to find a method of building RCS curves without an age-related bias. This option warrants further investigation.

The problem created by the effects of trend distortion (7) can be minimised by using iterative procedures to implement the use of signal-free measures in the generation of RCS curves. Signal-free methods are applied to the RCS curves used in the MRCS and SARCS methods but could also be applied when using the RCS method. The use of signal-free measures adopts the concept that a group of trees contain a common signal, which can be estimated by the mean of between tree correlations. The use of RCS curves and signal-free methods presume a spread of ring ages in each calendar year and should not be used with even-aged stands.

Identification of problems inherent in the RCS method and the development of techniques for overcoming them, has effectively led to the production of new methods of standardisation. Of the many possible combinations of multiple techniques that could have been selected, for practical purposes, two specific methods have been chosen. MRCS and SARCS, both based on the concept of RCS but both using diameter and ring age to produce more relevant and generally applicable expected growth values. Both methods incorporate the use of signal-free measures and the BFM method. They produce chronologies with an arbitrary slope, but can be applied to the development of modern chronologies without the need for sub-fossil trees. The MRCS method uses multiple RCS curves and requires several hundred trees. Situations where this number of trees will be available are limited. The SARCS method stretches/shrinks the RCS curve to fit each tree and is specifically designed to be used with as few as 50 trees.

The MRCS and SARCS methods of standardisation represent significant improvements of the existing RCS method and the main innovations are the use of the BFM method to retain long-timescale variance, the use of both ring age and diameter in the generation of expected growth curves, and the use of signal-free measures. Comparisons of chronologies generated using the new and old methods along are made along with comparison with climate data in the following chapter.

## Chapter 6. RCS, MRCS and SARCS Comparisons

### 6.1. Introduction

Chapter 5 was about theoretical problems and solutions and this chapter concerns the application of the methods discussed to series of tree measures in order to assess the value to dendroclimatology of these new methods. Existing and new methods of standardisation are compared both with each other and with measured temperatures using artificial and measured ring width data in order to test the ability of the new methods to resolve the identified problems.

### 6.2. Comparison of RCS, MRCS and SARCS Methods

#### 6.2.1. Expected growth curves and tree indices

Expected growth curves created by the RCS method have the tasks of removing the age-related growth trend, preserving the non-age-related variance in each series of measures, and of retaining the magnitude of tree growth relative to the average rate of growth of all trees. Expected growth curves created by the MRCS and SARCS methods only have to remove the age-related growth trend and preserve the non-age-related variance in each series of measures. The difference between expected growth curves generated for sample individual trees by the RCS, MRCS and SARCS methods are shown in Figure 6.2.1. The RCS method expected growth curves (blue) will have the same values at each ring age for all trees and are constrained to be below the growth measures (black) for the two fast growing trees (a & b) and above the growth measures for the slow growing tree (d). The MRCS method, by using a series of RCS curves representing differing tree growth rates, produces expected growth curves (red) which fit the measures more closely than do RCS expected growth curves. Expected growth curves generated by the “SARCS” method (cyan) are fitted to signal-free trees and have a far better fit to the growth measures than the expected growth curves produced by the RCS and MRCS methods. Because the SARCS expected growth curves can follow the “change in diameter” there can be marked changes in the slope of SARCS generated expected growth curves where the ring-width has a marked change in size, e.g. in figure 6.2.1c there is a change of slope in the SARCS generated expected growth curve at AD 650. That all three sets of expected growth curves can be used to preserve long-timescale variance in the resulting chronologies is of overriding importance.

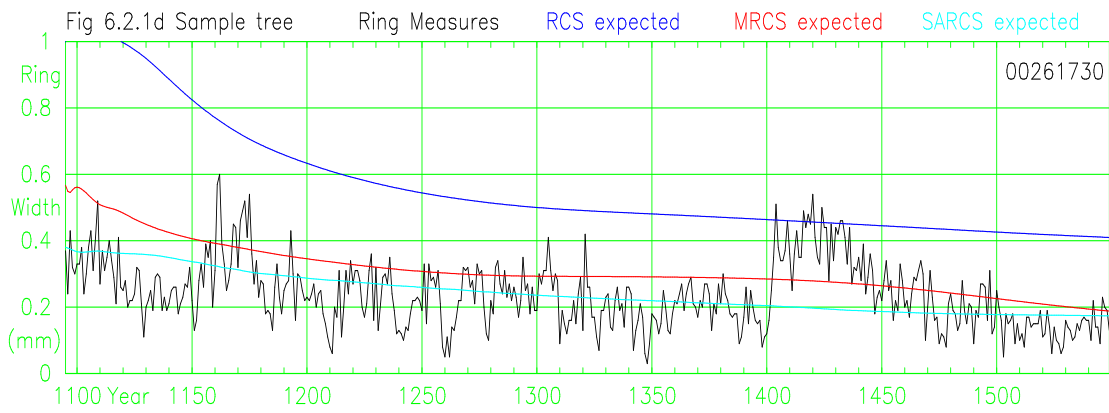
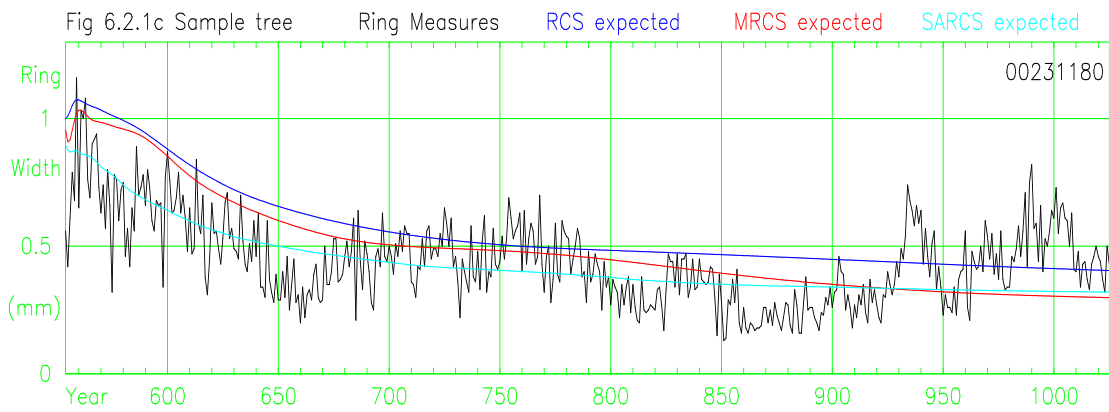
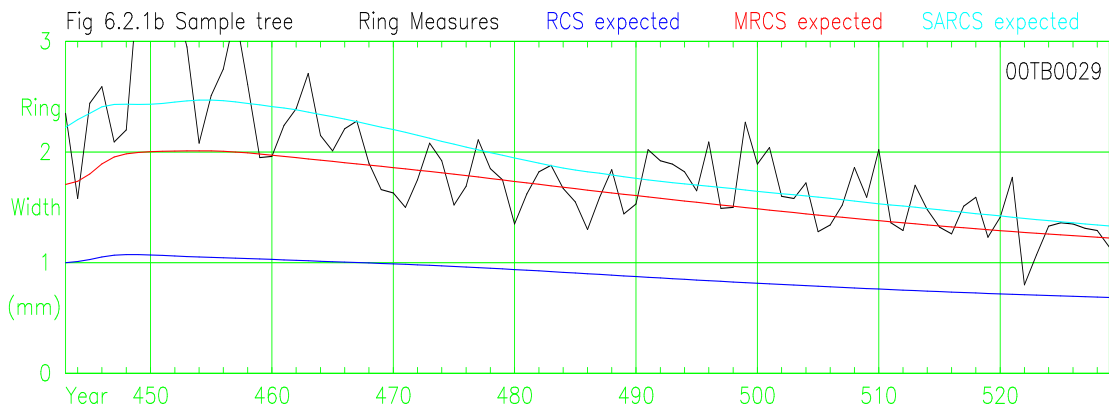
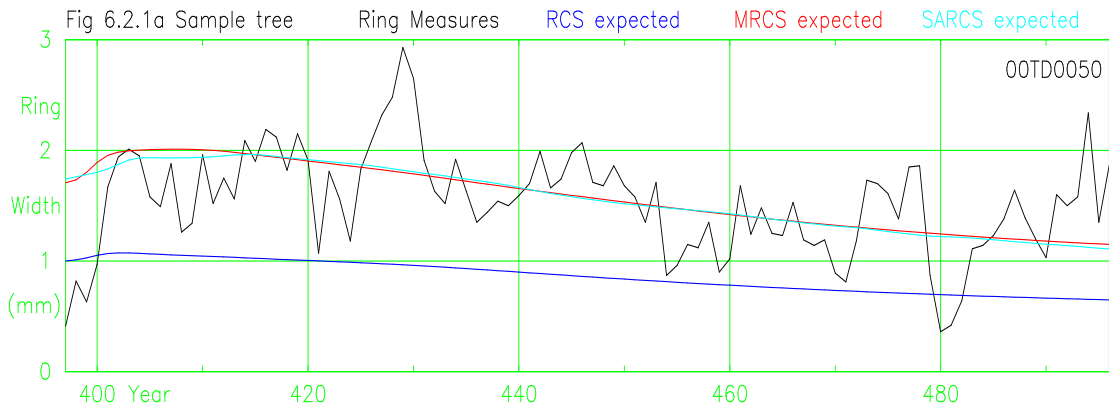


Figure 6.2.1 Sample series of measurements and expected growth curves using RCS, MRCS, and SARCS methods for fast (a & b), medium (c), and slow (d) growing trees from the Tornetrask AD site.



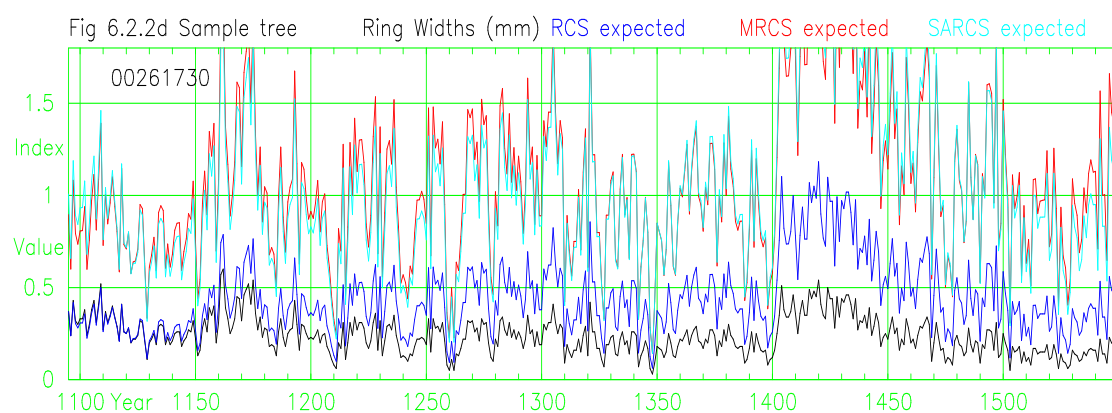
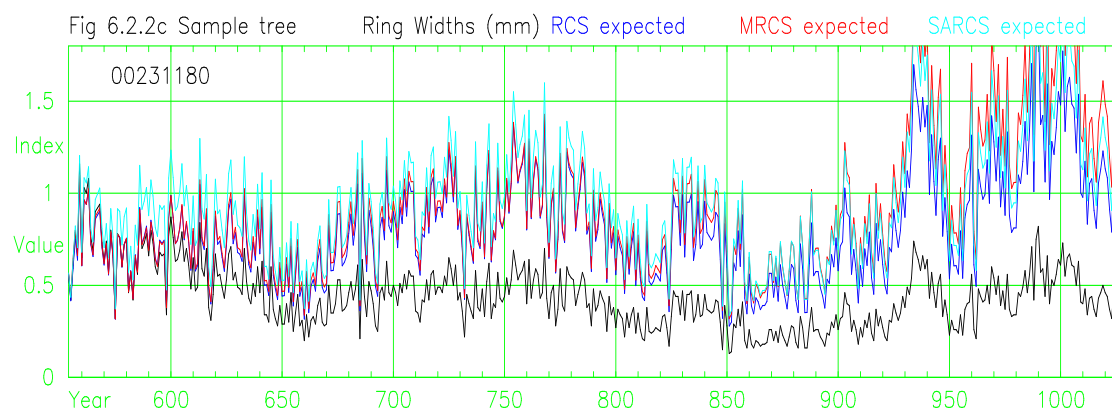
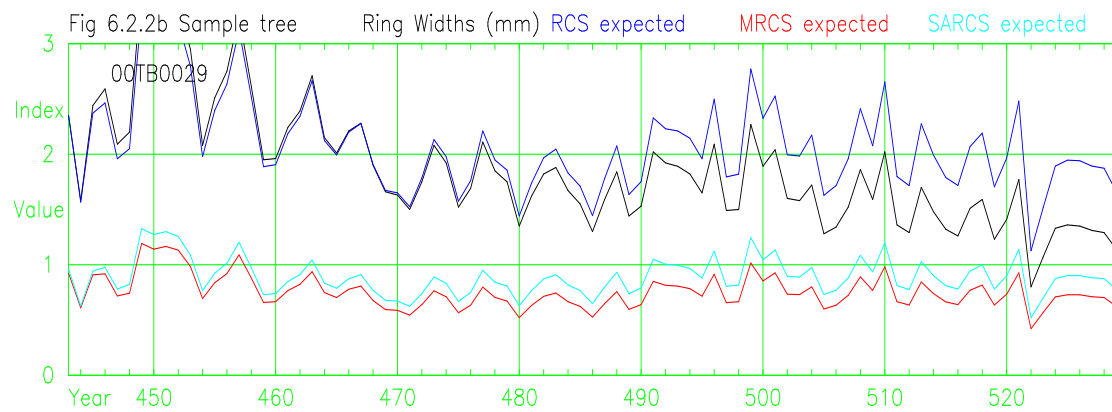
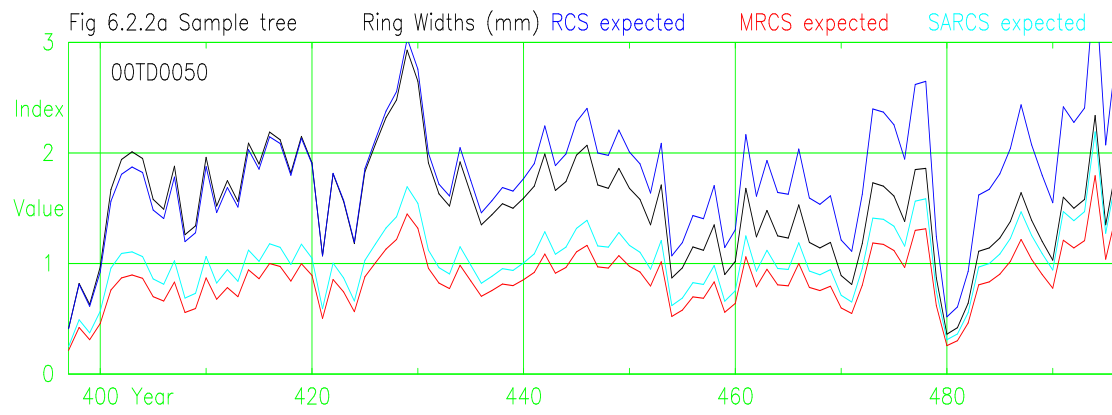


Figure 6.2.2 Sample series of measurements and tree indices created using the RCS, MRCS, and SARCS methods for fast (a & b), medium (c), and slow (d) growing trees from the Tornetrask AD site.

The difference between series of tree indices generated for the sample trees (Figure 6.2.1) by the RCS, MRCS and SARCS methods are shown in Figure 6.2.2. Tree indices generated by the RCS method (blue) have a wide range of values; being larger for the two fast growing trees (a & b) and smaller for the slow growing tree (d). The averaging to create a chronology will give four times more weight to the faster growing trees (a and b) than to the slowest growing tree (d). Series of tree indices created using the MRCS (red) and SARCS (cyan) methods are very similar to each other in magnitude because the BFM procedure has rescaled the mean values of tree indices to fit the mean values of chronology indices over their common period. The MRCS and SARCS methods give each tree equal weight in the chronology because each tree is forced to have a mean index value which is the same value as the mean of chronology indices. A significant proportion of the variation in tree growth rates is due to site factors which are not climate related and, in order to average out the difference due to the randomness of sampling, the RCS method will require more trees than do the MRC and SARCS methods. The indices generated by the division of measured values by RCS generated expected growth values will contain low-frequency variance due to the relative, to the RCS curve, growth rate of the tree but will not be fractional deviations due to the current year's common forcing signal (Section 4.1). The series of tree indices generated by division in the MRCS and SARCS method and rescaled using the BFM procedure will approximate "fractional deviations" due to the current year's common forcing signal.

#### 6.2.2. Means of tree indices by ring age

Removal of the age-related growth trend from series of ring measures should leave tree indices whose values are random with respect to ring age because this process should remove all age-related growth trends. In figure 6.2.3 the mean values of series of indices for the slowest (blue) and fastest (red) growing trees at the Finnish-Lapland site are displayed for indices created using the RCS (a), MRCS (b), and SARCS (c) methods. The rates of growth were established by the time taken (or projected to be taken) for each tree to reach 10cm radius. The consistent differences between the mean values of indices of the fastest and slowest growing trees form an "age-related" bias and the bias generated by the RCS method (a) is larger in magnitude than those of the MRCS (b) and SARCS (c) methods. The problem of ring-age related bias is reduced (not removed) by the MRCS and SARCS methods. The MRCS method is generally better in this respect than the SARCS method because the SARCS method produces series of tree indices with more

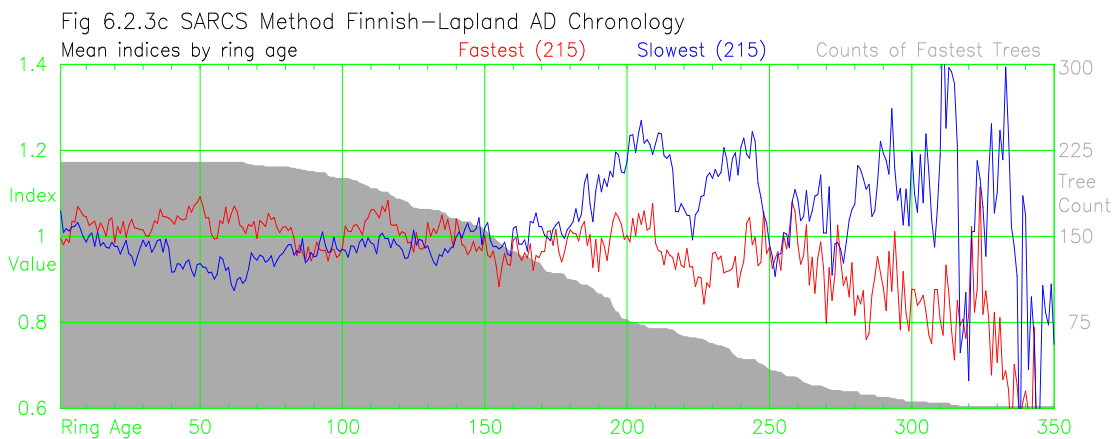
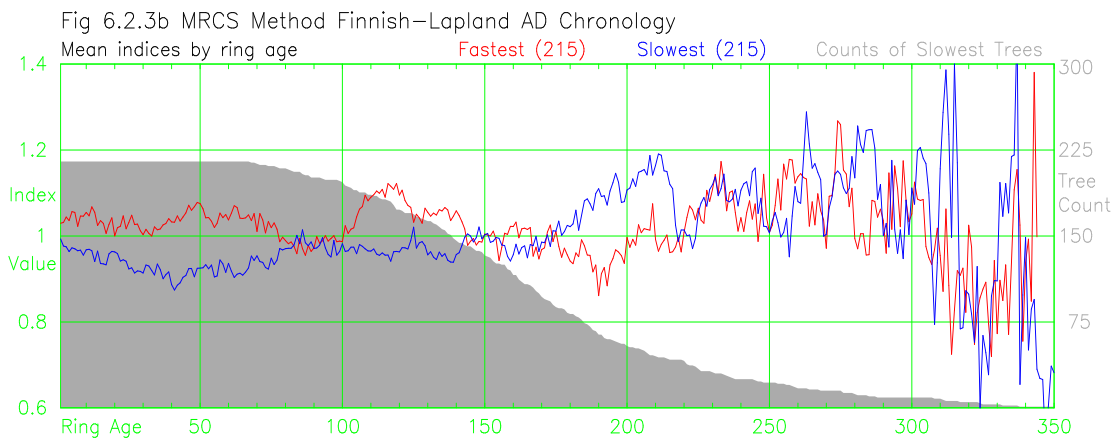
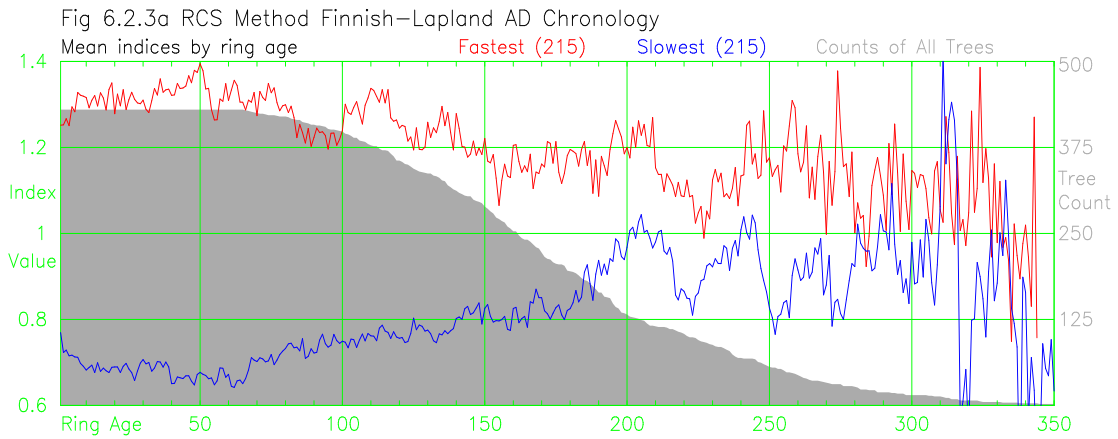


Figure 6.2.3 Comparison of mean indices by ring age of the fastest and slowest growing trees at the Finnish–Lapland site using the RCS (a), MRCS (b), and SARCS (c) methods.

slope in the first few decades, more clearly shown as a tree size-related bias (see Figure 5.8.2). The RCS, MRCS and SARCS methods leave the removal of this age-related bias to the averaging process used to create chronologies and this increases the number of trees (sample depth) needed for chronology generation. The MRCS and SARCS methods, with less magnitude of bias, will require fewer trees for bias removal than will be needed using the RCS method.

The reduction of slope, both upward and downward, in series of tree indices coupled with the rescaling of all indices of each series, within the BFM method, will ensure that the later indices of each tree (3<sup>rd</sup> century and beyond) are able to make a contribution to the long-timescale variance of the chronology. Subtle differences will be found between the RCS chronologies and MRCS and SARCS chronologies in the onset/offset and magnitudes of variance when viewed at medium-frequency i.e. smoothed chronologies.

### 6.2.3. Random Chronologies

Figure 6.2.4 shows chronologies created by the RCS, MRCS and SARCS methods from the random no signal (a), the random step up (b), and the random step down (c) sets of artificially generated trees (Section 5.5.3). Modern sample bias was built into the last three centuries of these random chronologies and this shows clearly in the RCS chronologies (black lines) whilst the magnitude of modern sample bias is reduced in the MRCS (blue) and SARCS (red) chronologies. Apart from the modern sample bias, the RCS method performs well in the central portions (AD 1200 to 1600) of all chronologies, with the first and last centuries having anomalous slopes because the age-related bias in the slopes of series of tree indices is not cancelled out by the averaging process (Section 5.5.4). The SARCS and MRCS methods create chronologies with an arbitrary slope and the chronologies shown here slope down (b) and up (c) because the trend-correction method (Section 5.5.7) does not fully counteract the effect on the slope of these chronologies of the step up and step down changes. The SARCS chronologies (red) have a slight curvature relative to the MRCS (blue) chronologies. This might be the result of the linear stretching, to fit RCS curve diameter to tree diameter, or the manner of RCS curve extension used within the SARCS method (Section 5.8). These random trees have a linear decay whilst the curve extension process used in the SARCS method is optimised for the “curved” decay of ring width found in series of measures. The slope of the SARCS generated chronologies (red lines of Figures 6.2.4 (b & c)) in the final century are particularly susceptible to the manner of RCS curve extension used within the SARCS method.

### 6.2.4. Chronology comparisons

The MRCS and SARCS methods produce chronologies with an arbitrary slope and for comparison purposes here the slopes of all chronologies (including RCS) are set to zero using the method of Section 4.2.5. Chronologies are smoothed to highlight the low-

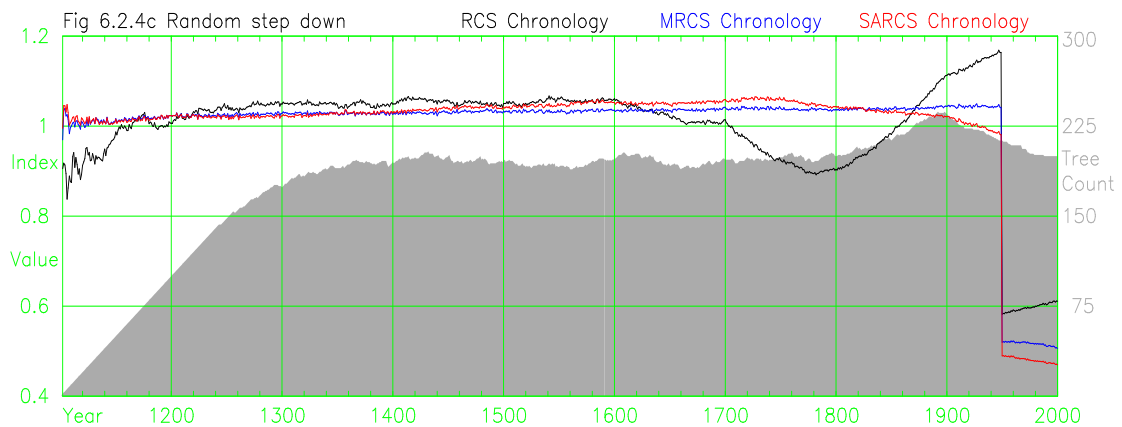
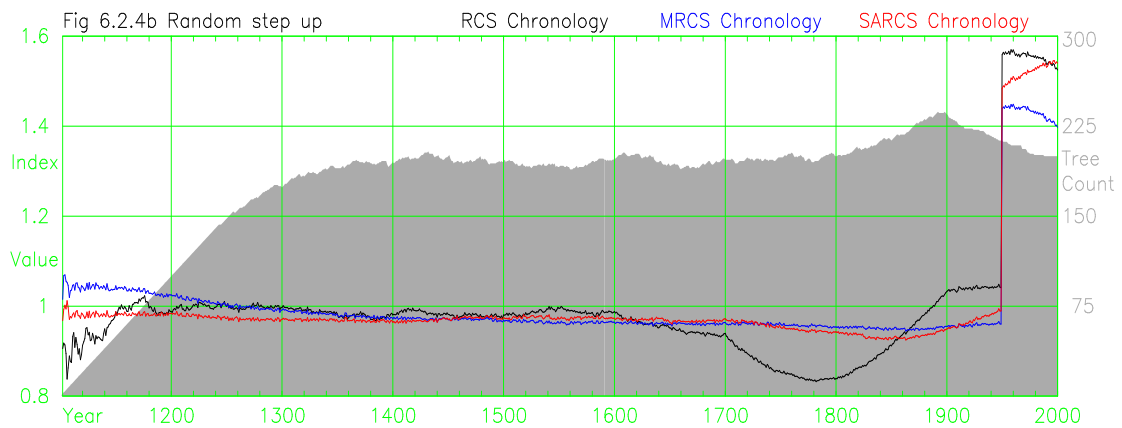
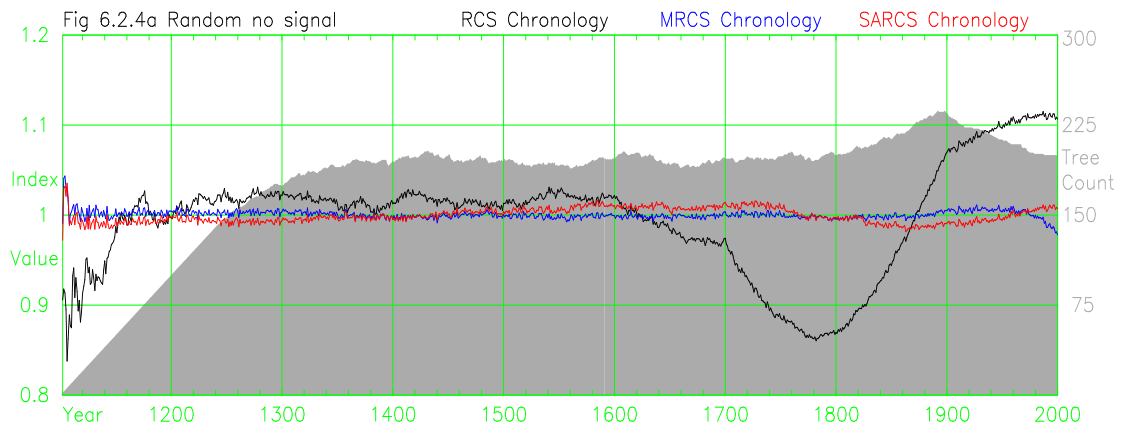


Figure 6.2.4 Chronologies from the RCS, MRCS, and SARCS methods using the random no signal (a), random step up (b), and random step down (c) trees.

frequency differences. Figure 6.2.5 shows chronologies created using the RCS, MRCS and SARCS methods on the Tornetrask AD (a) and Finnish-Lapland AD (b) sites. The MRCS (blue) and SARCS (red) methods at each site produce similar sets of results. These differ from the chronologies created by the RCS method at multi-century frequencies. The three Tornetrask chronologies (Figure 6.2.5a) are similar in the 8th and 18th centuries. The MRCS and SARCS methods have higher index values in the 10th and 11th centuries and in the most recent decades there is decay in index values in the MRCS

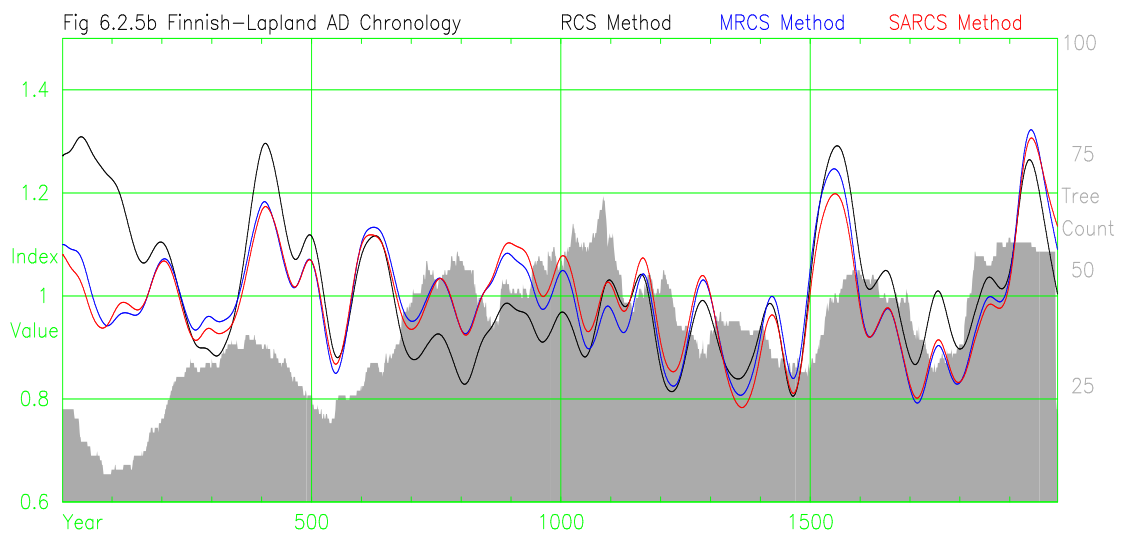
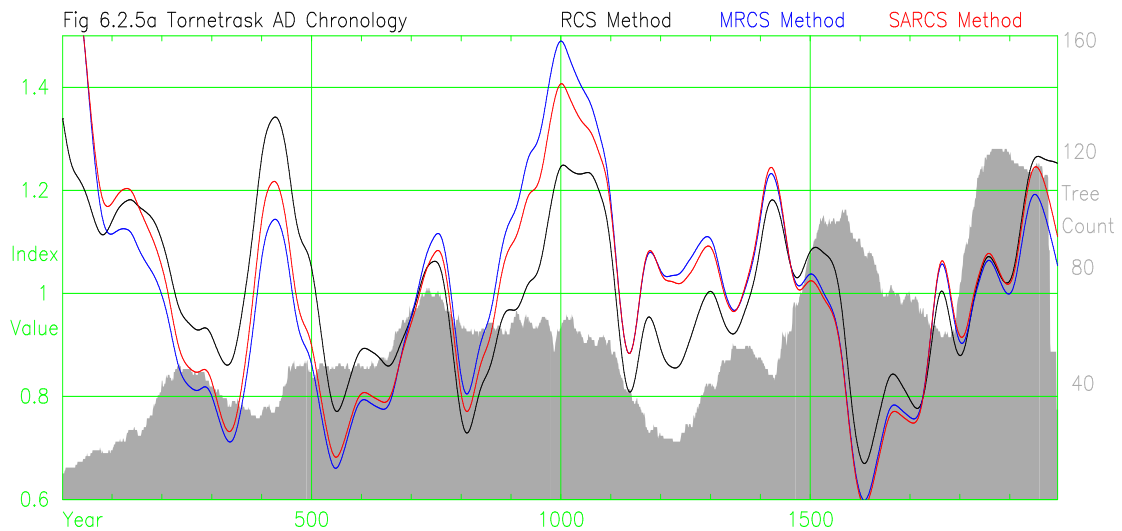


Figure 6.2.5 Chronologies created with the RCS, MRCS, and SARCS methods using the Tornetrask AD (a) and Finnish-Lapland AD (b) sites.

and SARCS chronologies not seen in the RCS chronology. The increased growth around AD 1000 is more marked and prolonged in the MRCS and SARCS chronologies, whilst the first five centuries have markedly lower index values in the MRCS and SARCS chronologies than in the RCS chronology. The MRCS and SARCS chronologies for the Finnish-Lapland site (Figure 6.2.5b) show the 7th to 11th century period has higher index values and the 16th to 20th centuries have lower index values relative to the RCS chronology. All the Finnish-Lapland chronologies are consistent in the last few decades of the chronologies whereas the variance at century timescales of the first two centuries of the RCS chronology has marked differences. The ability to arbitrarily “rotate” the MRCS and SARCS chronologies can change these results but will not remove the differences. The MRCS and SARCS method are producing similar results which differ from those of the RCS method.

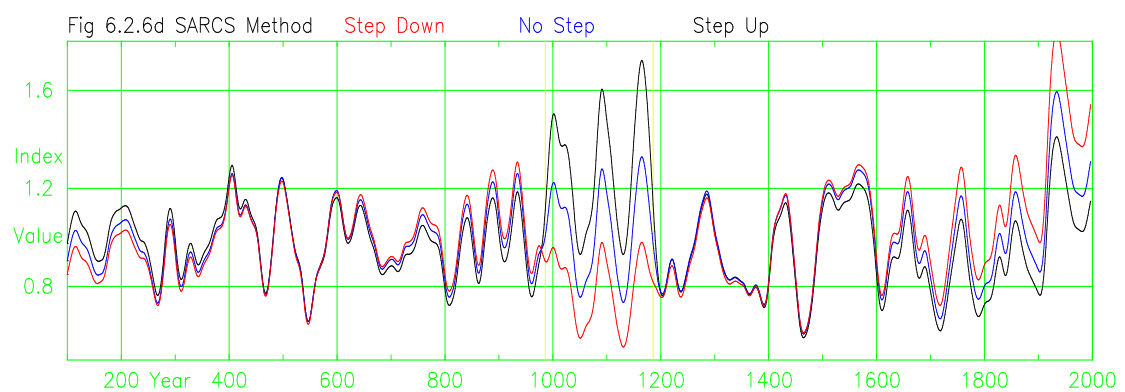
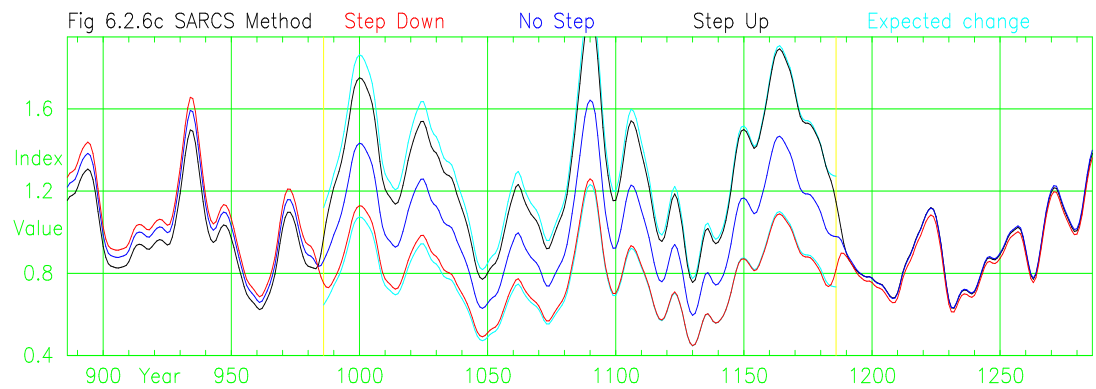
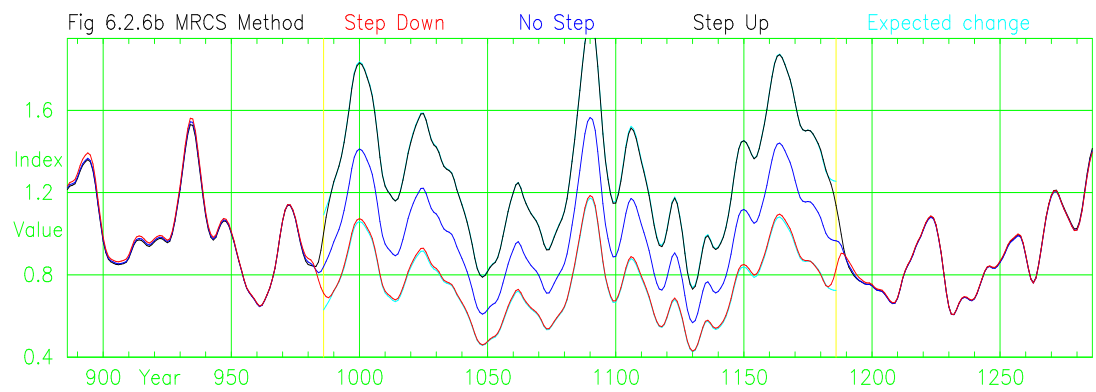
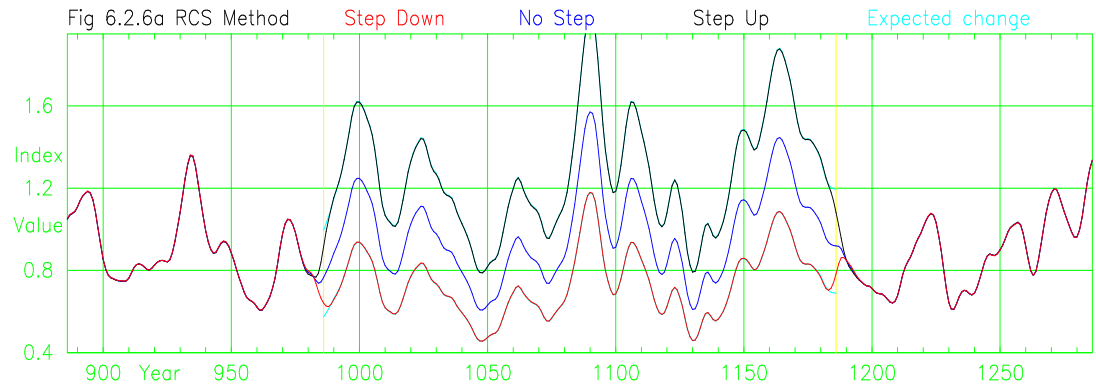


Figure 6.2.6 Test of the RCS (a), MRCS (b), and SARCS (c & d) methods ability to retain an artificial step increase or decrease in the middle of a chronology using trees from the Finnish–Lapland AD site.

### 6.2.5. Artificial step increase or decrease

The ability of these standardisation methods to preserve a step increase or decrease in series of tree indices is investigated by introducing changes to series of measures. For this purpose the Finnish-Lapland trees were used and two additional chronologies were created by firstly increasing the values of all tree measures for the years 986 to 1186 by 30% and secondly by decreasing the values of all tree measures for the years 986 to 1186 by 25%. The central centuries AD 986 to 1186 were chosen to reduce the need to change the slope of the chronologies generated by the MRCS and SARCS methods. The resulting chronologies are shown in Figure 6.2.6. The step up chronologies are black lines, the unchanged chronologies are blue lines, and the step down chronologies are red lines. For display purposes the mean values of the step up and step down chronologies were rescaled to the same mean values as the unchanged chronologies for the period excluding AD 986 to 1186, yellow vertical lines are used to highlight the period of change, and all chronologies have been smoothed with a 10 year, 50% cut-off, spline. Cyan lines, marking the plus 30% and minus 25% values relative to the unchanged chronology, are used to show the expected positions of the changed chronologies. The RCS (Figure 6.2.6a) and MRCS (Figure 6.2.6b) methods perform this task well confirming that both methods are able to distinguish step changes in the central portions of a long chronology without significant distortion. The SARCS method (Figure 6.2.6c) introduces some distortion at long timescales; the two century long increase and decrease are clear suggesting that individual trees are being detrended whilst the multi century variance is distorted suggesting there is a problem with the removal of the common signal in the production of signal-free RCS curves in the SARCS method. The two millennia long SARCS chronologies are plotted in Figure 6.2.6d showing that the SARCS method has distorted indices over periods of more than five centuries, with the 6th and 15th centuries having similar values.

The methods used above for a step increase and decrease in the centre of a chronology were repeated with a step increase of 40% and a step decrease of 40% from 1920 onwards to represent potential changes in the modern period. Trees measures from the Finnish-Lapland site are used. The slopes of the step up and step down chronologies created by the MRCS and SARCS methods were set to the same values as the slopes of the unchanged chronologies generated by these methods for the period up to AD 1900 for display purposes. The resulting chronologies are shown in Figure 6.2.7. The step up



chronologies are black lines, the unchanged chronologies are blue lines, and the step down chronologies are red lines. The cyan lines, showing the expected position of the changed chronologies, are more clearly visible than in Figure 6.2.5 showing some

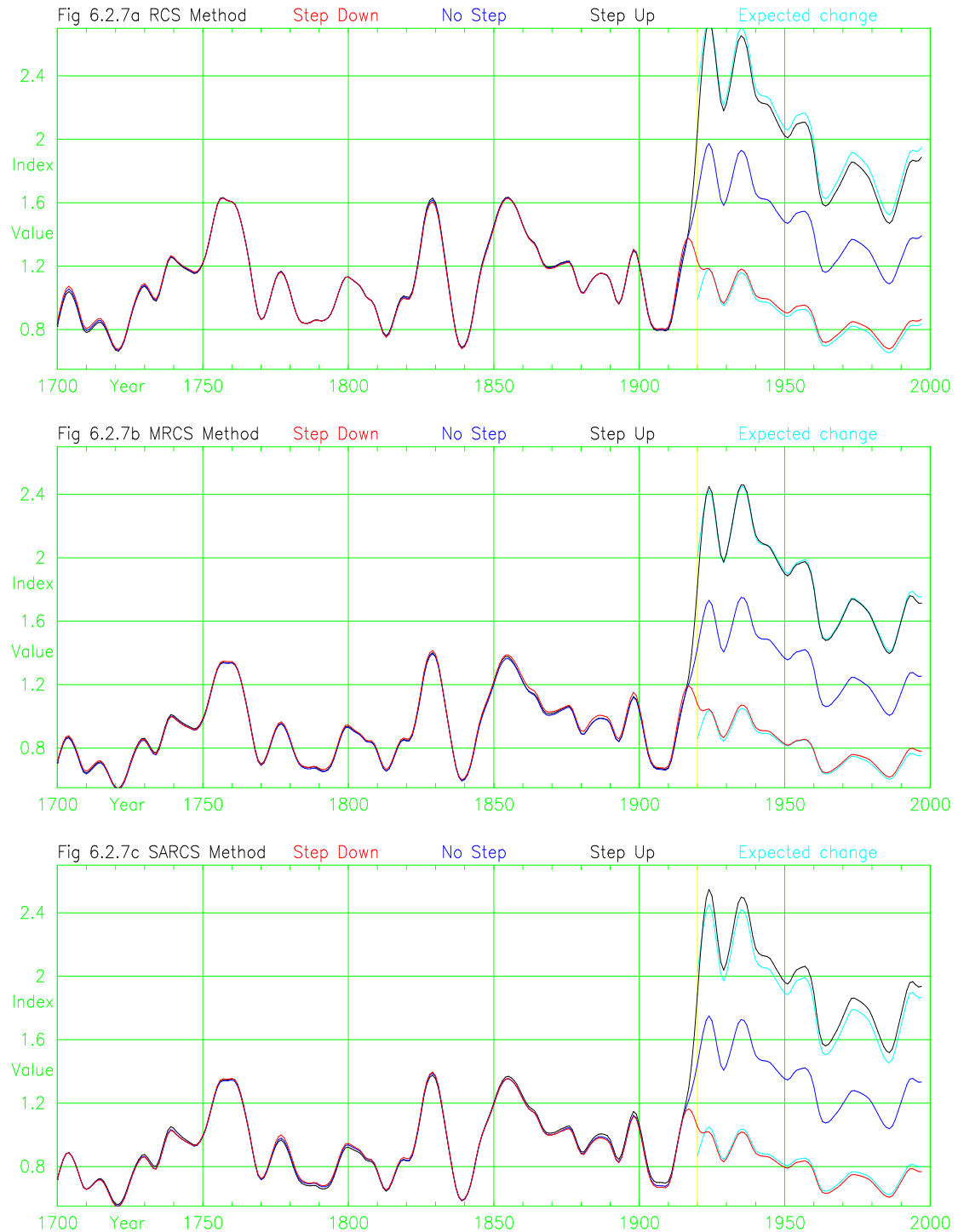


Figure 6.2.7 Test of the RCS (a), MRCS (b), and SARCS (c) methods ability to retain an artificial step increase or step decrease at the end of a chronology using trees from the Finnish–Lapland AD site.

distortion. The RCS (a), MRCS (b), and SARCS (c) all perform this test reasonably well. The distortion is greatest in the RCS chronology (about 5%) and least in the MRCS chronology. The SARCS method does not have a problem with the long timescale variance where the step up is at the modern end of the chronology. These tests are of the “relative” change in tree measures and confirm that the methods are consistent i.e. whatever bias exists is similar after the step increase or decrease. The negative slope of the RCS chronologies from 1920 to 2000 is greater than the negative slopes of the corresponding MRCS and SARCS chronologies over the same period.

### 6.2.6. Growth rate, Age and Size

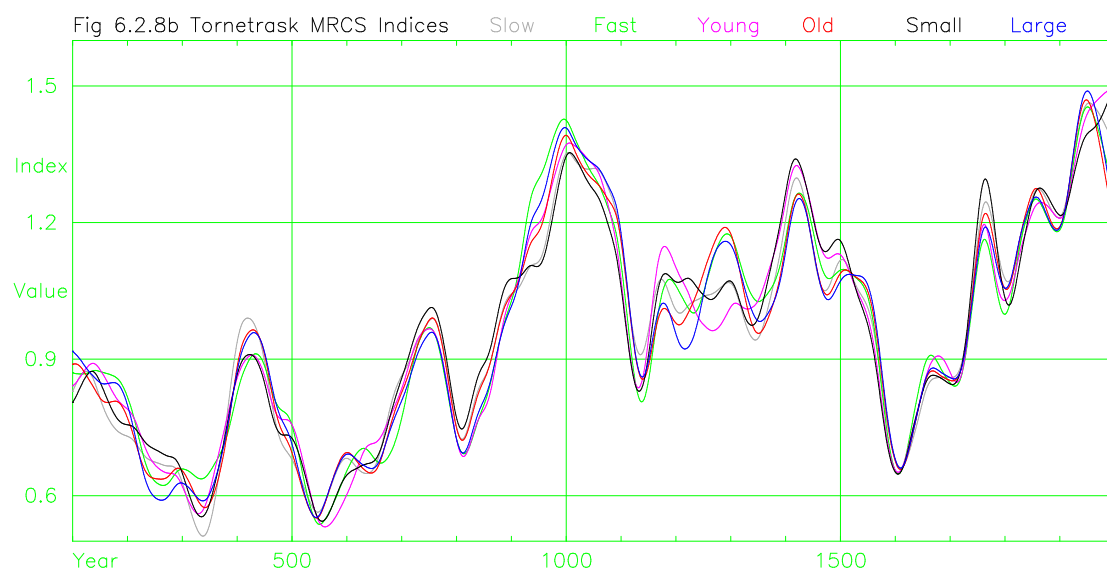
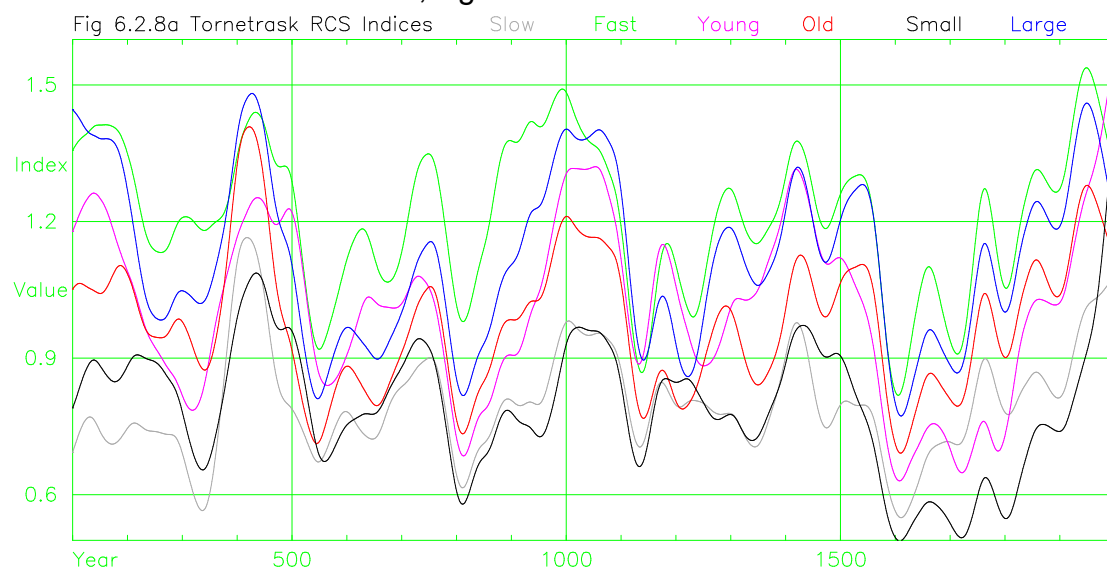


Figure 6.2.8 Tree indices created by (a) RCS and (b) MRCS methods. Mean values of tree indices by year for the 50% slowest, fastest, youngest, oldest, smallest and largest trees from the Tornetrask AD site.

One of the objectives of this project was to examine any differences in the common signal that might be created by trees of differing growth rates, ages and sizes. The Tornetrask AD trees were standardised using the RCS method and the MRCS method creating two sets of indices for all trees. The rate of growth of trees was assessed by the time taken (or projected time) to reach 10 cm diameter. Chronologies of the mean index values of all trees in a particular class are plotted in Figure 6.2.8. The chronologies have been smoothed with a 100 year, 50% cut-off smoothing spline for display purposes. Six classes, each using half the trees, were used: the slowest growing, fastest growing, youngest, oldest, smallest diameter and largest diameter trees. The separate chronologies created using indices derived from the RCS method (Figure 6.2.8a) vary considerably although the common signal, if scaled to fit, is reasonably similar. The separate chronologies using indices derived from the MRCS method (Figure 6.2.8b) are similar. This confirms that there is a similar signal in all these separate classes of trees and also that the BFM method, used within the MRCS method, has performed the rescaling action to produce “better fitting” series of indices. There is still a problem of the different classes of tree “disagreeing” in some periods such as AD 1150 to 1300 and, most importantly, AD 1950 to 2000.

A similar exercise to the above was repeated using a “modern” chronology, the Luosto trees from north Finland, and using the Hegershoff and SARCS methods to create tree indices. The RCS and MRCS methods are not suited to standardising modern chronologies with so few trees. Chronologies of the mean index values of all trees in each particular class are plotted in Figure 6.2.9 and the chronologies have been smoothed with a 20 year, 50% cut-off smoothing spline for display purposes. The mean index chronologies for separate classes, using both the Hegershoff (Figure 6.2.8a) and SARCS (Figure 6.2.9b) method created indices are remarkably similar, especially over the AD 1750 to 1920 period. The sequence from bottom to top (black, grey, red, blue and green) at AD 1700, where the mean index chronologies have a wide spread in values, is the same for both methods. Again, the different classes of tree “disagree” in some periods, such as AD 1690 to 1720 and AD 1920 to 2000. (Comparisons of Figures 6.2.8 and 6.2.9 need to allow for the different smoothing regimes, i.e. 100 and 20 years.) In Section 4.1 it was reasoned that curve-fitting methods, by using both age and diameter to produce expected growth curves, which follow the tree-growth model concept of using growth history. This demonstration implies that expected growth curves generated by the SARCS

method fit series of ring measures almost as well as expected growth curves generated by a sample curve-fitting method. The SARCS method's ability to preserve long-timescale variance in a chronology is an additional attribute.

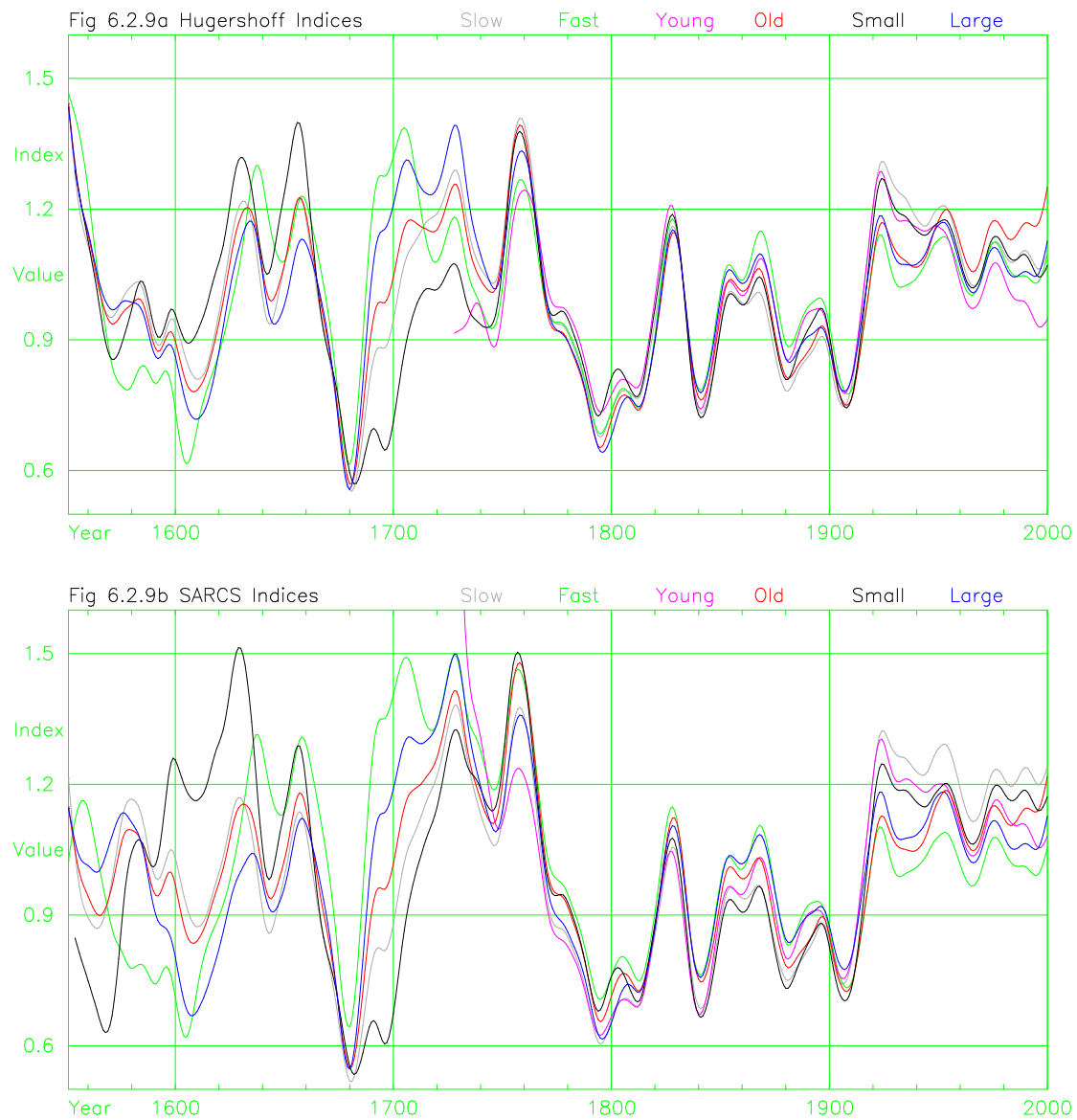


Figure 6.2.9 Tree indices created by (a) Hegershoff and (b) SARCS methods. Mean values of tree indices by year for the 50% slowest, fastest, youngest, oldest, smallest and largest trees from Luosto, Finland.

### 6.3. Errors and Uncertainty

#### 6.3.1. Introduction

The BFM method generates low-frequency variance in chronologies by “overlapping” series of indices from individual trees. The error involved in the overlapping process is a potential source of uncertainty which requires exploration. There is a need to estimate how the nature of the overlap at specific points in a chronology, in terms of the number of rings and their distribution between different trees, affects uncertainty

in the chronology when using the BFM method, in effect this is equivalent to identifying the weakest points in a given chronology. Bootstrapped confidence limits (Cook 1990) are used to estimate the potential error in chronologies focussing on specific areas of different sub-sample overlap. Variance of the error bars of the Tornetrask AD chronology, due to both the values of tree indices in a year and the count of trees in any year, is removed to show that the standard deviation of the difference between tree indices and chronology indices (standard deviation of absolute error) does not vary significantly over time and is thus a statistic that can be used to estimate error levels over the length of this chronology. The standard deviation of high-pass filtered tree indices is used to estimate errors associated with the overlapping of “noisy” tree indices and the effects this will have on uncertainty. The uncertainty created by variations in the slope of individual trees (the noise after low-pass filtering) is used to develop a method of assessing the number (sample depth) of trees needed to avoid excessive error. Sample chronologies are then examined and used to demonstrate how these concepts can be used to consider potential problem areas (of poor confidence).

### 6.3.2. Bootstrapped Confidence Limits

Chronology indices and their two tailed 95% confidence error limits, estimated using a bootstrap procedure (Cook 1990) on RCS and MRCS chronologies for Tornetrask AD and Finnish-Lapland AD, are shown in Figure 6.3.1. Confidence limits are plotted as a grey bar for each year and the chronologies are plotted as red lines. The error limits of the RCS chronologies are larger than those of the MRCS chronologies but the differences are difficult to see. In order to highlight low frequencies, each series of tree indices were low-pass filtered (using a 50-year spline) and averaged using the arithmetic mean (RCS) or BFM (MRCS) and bootstrapped error bars were calculated for chronologies built from “smoothed” series of tree indices (Figure 6.3.2). The MRCS method produces narrower confidence limits than the RCS method but, because bootstrapping calculates error about the mean value of chronology indices and BFM changes this mean, bootstrapped errors do not include error associated with the “overlapping” of BFM.

Error associated with the RCS curve, often several hundred samples deep, is usually small and can be overlooked. The MRCS and SARCS methods may have as few as 50 trees in each sub-RCS curve and thus have additional error. The use of multiple RCS

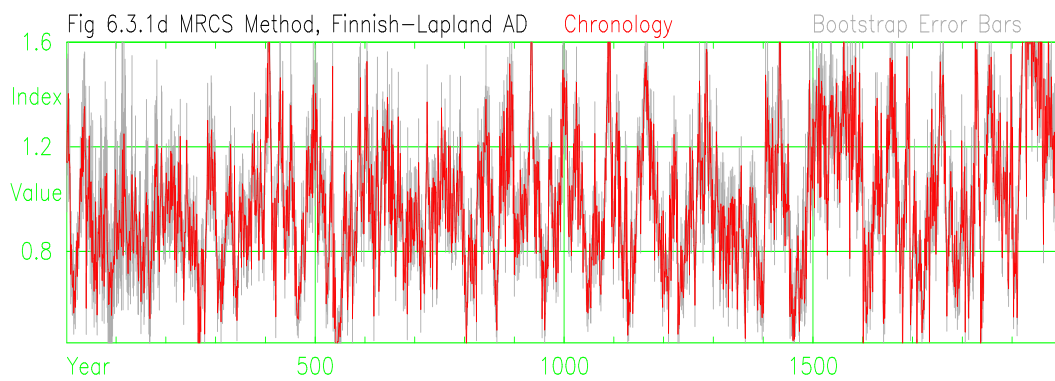
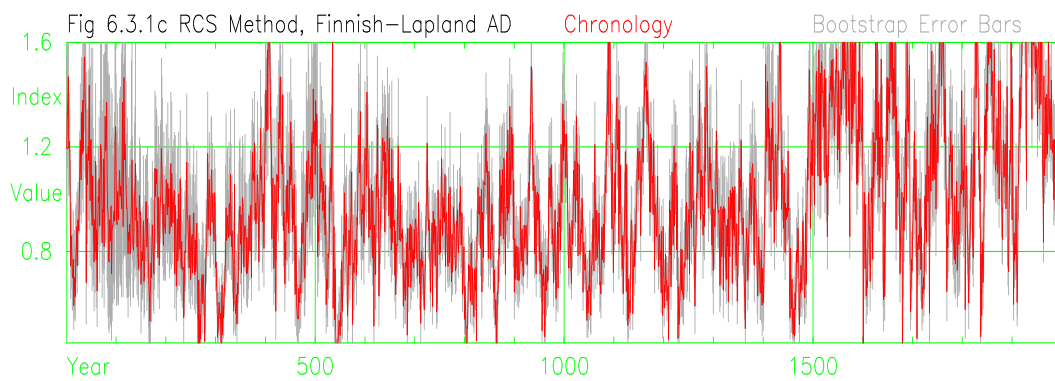
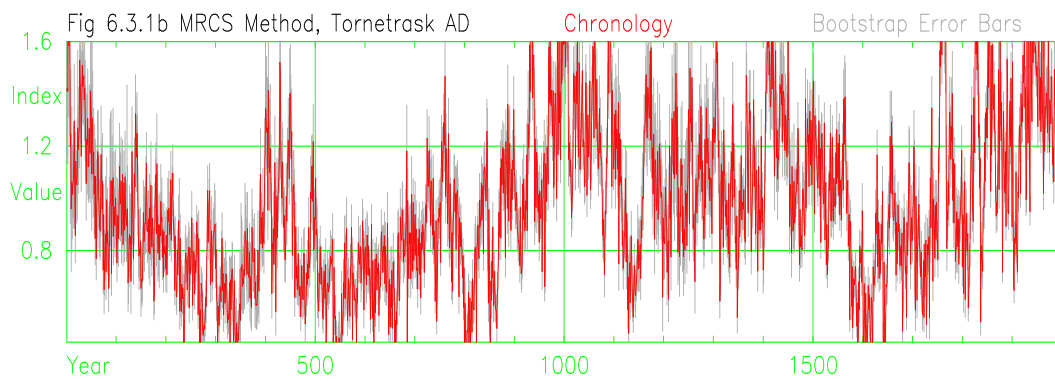
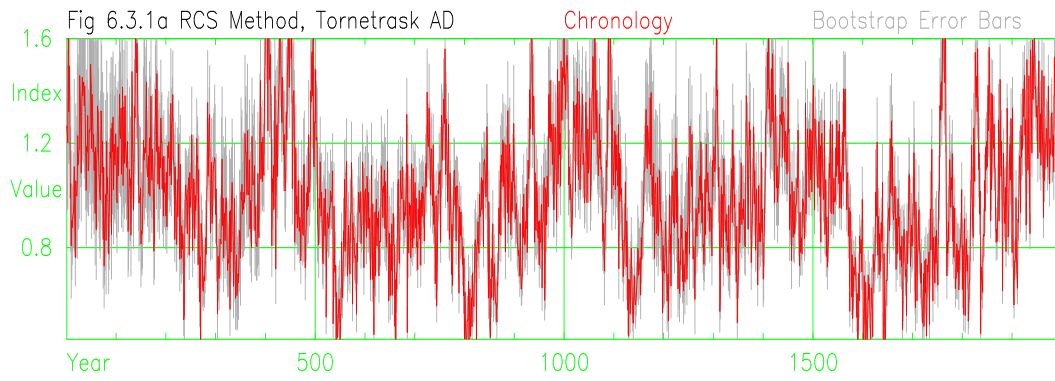


Figure 6.3.1 Chronology indices and 95% confidence error bars using (a & c) RCS and (b & d) MRCS methods on trees from (a & b) Tornetrask AD and (c & d) Finnish-Lapland AD.

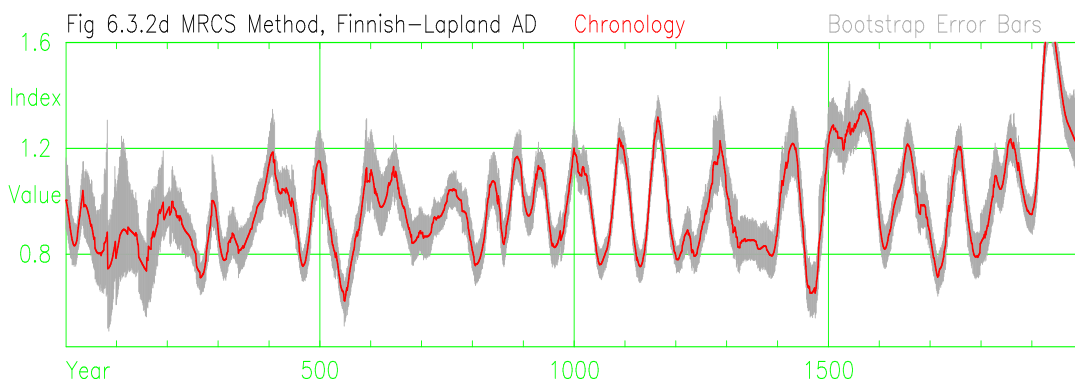
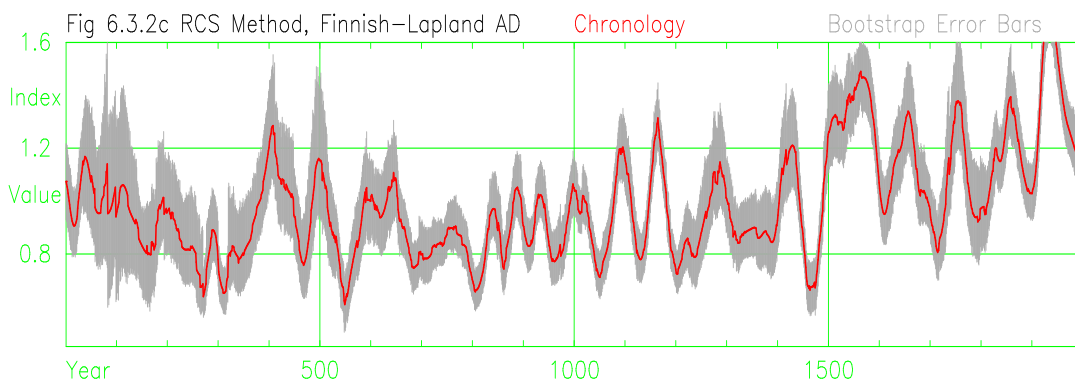
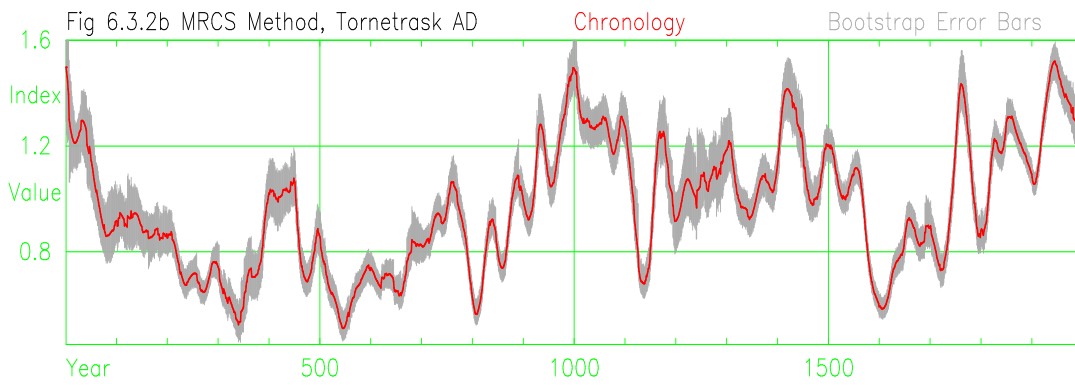
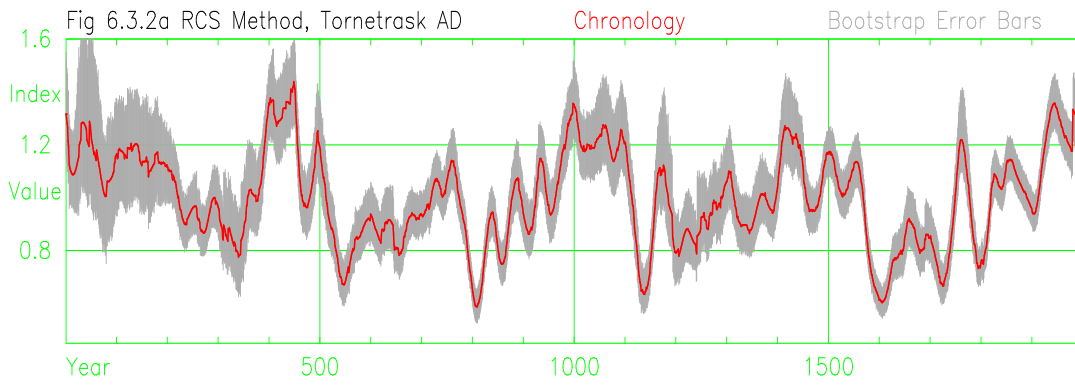


Figure 6.3.2 Bootstrapped 95% confidence error bars of chronologies created from low-pass filtered (50-year spline) series of tree indices derived from (a & c) RCS and (b & d) MRCS methods using trees from (a & b) Tornetrask AD and (c & d) Finnish-Lapland AD.

curves will improve the fit of each tree to its appropriate RCS curve and the use of “signal-free” measures will remove variance associated with the common signal, both of which tend to reduce the error associated with calculating the mean value of measures (RCS curve values) in the MRCS and, to a limited extent, SARCS methods.

Bootstrapped 95% confidence limits are shown in Figure 6.3.3 for 100-year Spline, RCS, MRCS and SARCS standardisation methods for (a) Tornetrask AD and (b) Finnish-Lapland AD. The confidence limits are plotted from zero to highlight the changes in magnitude over time and relative size of confidence limits derived from the different standardisation methods. The confidence limits vary over time and would not form a suitable statistic for examination of the ‘overlapping’ uncertainty. Varying tree counts over time are shown (grey shading) and wider confidence levels appear where tree counts are low. The variance of indices is expected to be proportional to the mean value because indices are fractional deviations. Figure 6.3.4 shows the progressive removal of these two effects from the bootstrapped confidence limits for indices created by the MRCS method using the Tornetrask AD trees.

The starting point is the bootstrapped 95% confidence limits plotted from zero, as red bars, by calendar year (Figure 6.3.4a). These were sorted by ascending value of chronology index (Figure 6.3.4b) to illustrate how the limits increase with increasing chronology index. Each value was then scaled by the chronology index value (Figure 6.3.4c) to remove most of the effect (on bootstrapped error variance) of chronology index size, i.e. the error bars are scaled to an index value of 1.0. There is, however, a discernable reduction in error magnitude with increase in chronology index size suggesting that the rescaling has not been completely successful. The residual values (error bars scaled to index of 1.0) were then sorted according to ascending value of tree count (Figure 6.3.4d) and the decreasing magnitude of the error bars with increasing tree count can be seen clearly. This was removed by scaling the error bars by the square root of tree count divided by the square root of maximum tree count, i.e. error bars are scaled to the value that would occur if all tree counts were the maximum occurring value (121 in this case). The residuals (Figure 6.3.4e) then show little relationship with tree count and, when resorted by calendar year (Figure 6.3.4f), show no low-frequency relationship with time. There is a discernable bias for the low tree counts in the steady increase of error magnitude in the first quarter of Figure 6.3.4e (tree counts < 30) but this is small.



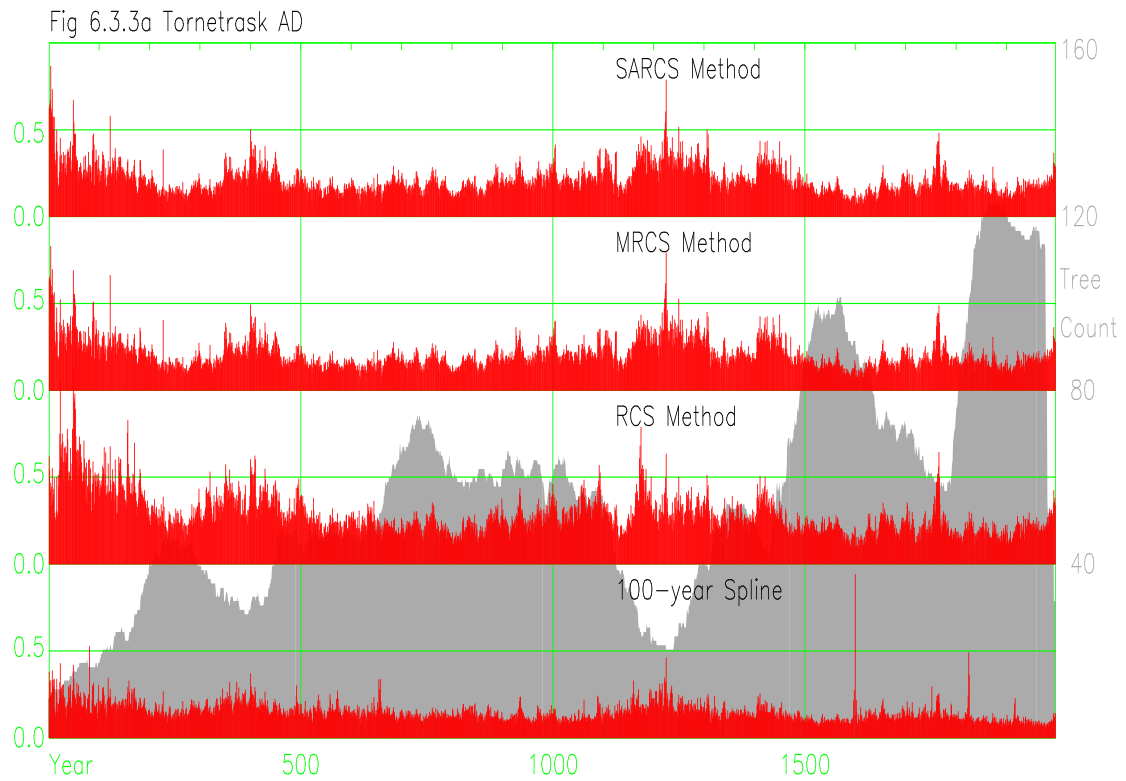


Figure 6.3.3 95% confidence bootstrapped errors plotted from zero for 100-year Spline, RCS, MRCS and SARCS chronologies using trees from (a) Tornetrask AD and (b) Finnish-Lapland AD.

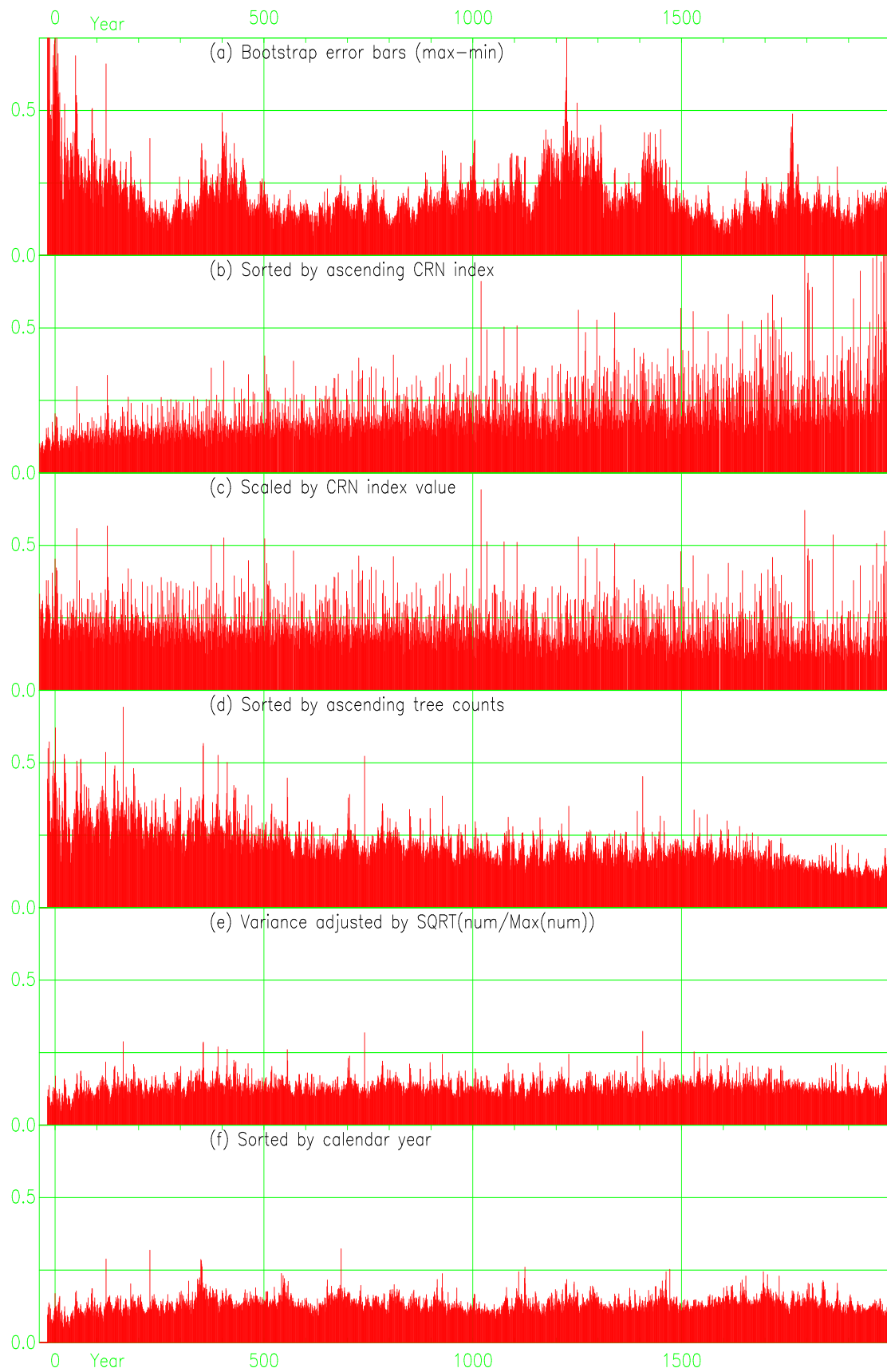


Figure 6.3.4 Bootstrap error bars from Tornetrask trees derived using the MRCS method showing a sequence of sorting and scaling processes.

### 6.3.3. Overlapping by BFM as a source of Error

To aid this discussion a hypothetical multi-millennial chronology, built from the Tornetrask AD trees, is used and two adjacent century-plus sections of chronology are considered, an early section and a later section (Figure 6.3.5). The BFM method sets the mean value of these chronology sections relative to each other using series of indices which “join” the two sections (overlapping trees). Sample series (from Tornetrask) are plotted, offset for clarity, in Figure 6.3.5. Uncertainty in the mean values of the indices of overlapping trees, from either side of the gap between chronology sections, will produce uncertainty in the mean values of the two chronology sections and thus uncertainty in the low-frequency variance of the overall chronology. It is convenient to separate the source of error into two types; error due to the overlapping series having differing slopes which is low-frequency error and shown by blue lines and high-frequency error due to noise arising out of differences in the values of individual indices (red lines) within the overlapping series. The mean value of all indices is set to 1.0 which distributes error over both halves of a chronology. There is a limit to the way low-frequency variance can propagate along the multi-millennial chronology because the overall slope is arbitrary (not knowable) and for practical purposes is set to zero.

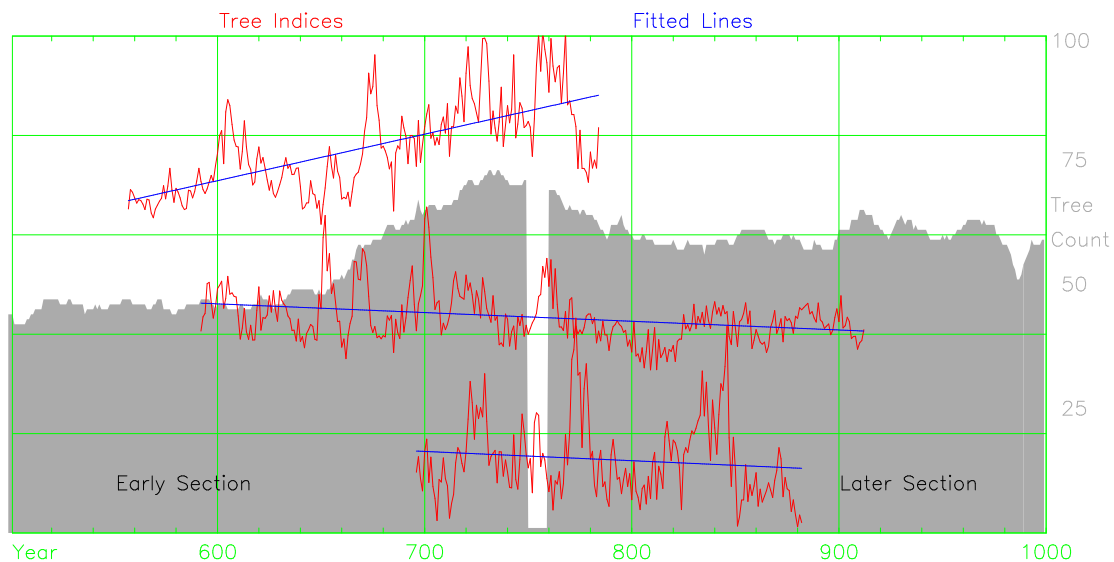


Figure 6.3.5 Tree counts by year for a hypothetical chronology with a gap and three sample series with least squares fitted lines, offset for clarity (counts and trees from Tornetrask).

The error created by medium and high-frequency noise can be estimated using the standard deviation of tree indices and the number of rings of overlap. The minimum count of rings in either direction for each tree is summed to produce the count of

overlapping rings which is used as a diagnostic measure here. If the two sections of chronology are joined by one 2-year old tree then the standard deviation of the means of the two sections will be the standard deviation of the tree indices. For practical purposes the number of rings (n) needed for the estimated mean of the early chronology section to be within  $\pm x$  of the actual mean with a probability of z% can be estimated (Mendenhall et al. 1990, page 305). For the Tornetrask and Finnish-Lapland chronologies, whose medium to high-frequency tree indices have a standard deviation of 0.35, the number of rings needed to achieve a 95% probability that the estimate is within  $\pm x$  of the required mean can be obtained using the following formulae:

$$n = [(1.96 * 0.35) / x ]^2$$

The value 1.96 is for 95% confidence levels and taken from Table 4 (Mendenhall et al. 1990, page 760). If the errors (differences between tree indices and chronology indices) are auto-correlated an adjustment needs to be made. An approximate adjustment factor (AF) can be derived (Osborn & Briffa 2000) using the one-year lag autocorrelation ( $r_1$ ) as follows:

$$AF = (1.0 - r_1) / (1.0 + r_1)$$

Individual errors from one tree usually have a high autocorrelation (for Tornetrask the mean of all trees is 0.81) whereas individual errors from different trees show no autocorrelation leading to the use here of both tree counts and overlapping ring counts.

The error created by low-frequency noise is estimated here using the variability of the slopes of series of tree indices (blue lines of Figure 6.3.5). At one point in time, with means set to common values, series will have varying slopes and the difference between the slope of a series and the slope of the chronology over their common period is considered error. The chronology slope at a point in time will be some form of average of the tree slopes. The effect of a slope error of one overlapping tree on the mean value of adjacent chronology sections will be the product of slope and half the series length (n/2).

$$\text{Error in Mean} = (\text{Chronology slope} - \text{Series Slope}) * n / 2$$

The standard deviation of the “slope error” for all trees in a chronology is used here to estimate the expected standard deviation of the mean of adjacent chronology sections for a given tree count and the magnitude of confidence levels that can be associated

with low-frequency variance. This error will change over time periods roughly equivalent to the length of trees, i.e. as trees enter and leave the chronology. In practice the low-frequency error will include the medium-to-high frequency error as the two are not independent.

	Tornetrask AD		Finnish-Lapland AD	
	Mean Absolute	Standard Deviation	Mean Absolute	Standard Deviation
All frequencies				
30-year Spline	0.15	0.20	0.15	0.20
100-year Spline	0.20	0.30	0.20	0.27
RCS	0.39	0.51	0.38	0.50
MRCS	0.29	0.39	0.29	0.38
SARCS	0.30	0.40	0.30	0.39
High-frequency (Mean=1.0, Slope=0.0)				
30-year Spline	0.16	0.20	0.16	0.21
100-year Spline	0.20	0.29	0.20	0.27
RCS	0.26	0.35	0.26	0.34
MRCS	0.26	0.34	0.25	0.34
SARCS	0.26	0.35	0.26	0.35
Low-frequency mean (Due to difference in mean)				
30-year Spline	0.01	0.01	0.01	0.01
100-year Spline	0.01	0.02	0.01	0.02
RCS	0.26	0.31	0.24	0.30
MRCS	0.00	0.00	0.00	0.00
SARCS	0.00	0.00	0.00	0.00
Low-frequency slope (Due to difference in slope)				
30-year Spline	0.00	0.01	0.01	0.01
100-year Spline	0.01	0.03	0.01	0.02
RCS	0.13	0.19	0.13	0.18
MRCS	0.13	0.18	0.12	0.17
SARCS	0.13	0.19	0.13	0.19
Ring Count	110,596		76,800	

Table 6.3.1 Means and standard deviations of the absolute error (chronology index – tree index) for Tornetrask AD and Finnish-Lapland AD chronologies developed using various standardisation methods and different filtering levels.

To demonstrate their application, these ideas are applied to the Tornetrask AD and Finnish-Lapland AD chronologies. The first stage is to estimate the standard deviation of error obtained as the absolute difference between index and chronology values. Selected filtering of tree indices was used and the results are included in Table 6.3.1. Indices created by the RCS, MRCS and SARCS method were used along with two alternative sets of high-frequency indices, (trees standardised using a 30-year high-pass spline and trees standardised using a 100-year high-pass Spline) for comparison purposes. The standard deviations at “All frequencies” were calculated using series

and chronologies generated by the five standardisation methods. The “High frequency” indices were generated from series by firstly rescaling both the series and chronology indices over their common period to have means of 1.0 and secondly by removing the slope from both sets of indices. The slope of each series of indices and the slope of the chronology indices over the common period were found by fitting straight lines to both sets of indices using least squares methods and the slopes were removed by dividing by the values of the fitted straight line. The “Low frequency mean” standard deviations use the difference in mean value of tree indices and mean value of chronology indices over the common period. The “Low-frequency slope” figures are calculated using the difference between the two sloping straight lines (series and chronology). In all cases the chronology indices were recalculated to exclude the tree being used in the calculation.

The first observation is that the Tornetrask AD and Finnish-Lapland AD chronologies have similar standard deviations in all categories. The number of samples needed for a given confidence limit is proportional to the square of the standard deviation. If indices from ten trees are averaged to generate each year of a high-frequency chronology from 30-year spline standardisation, then to create chronologies with similar magnitude confidence limits requires 18 trees if 100-year spline standardisation is used; 40 trees are needed by the MRCS and SARCS methods, and 62 trees are needed by the RCS method. The cost for the inclusion of low-frequency variance is a requirement for greater tree replication in order to maintain similar confidence levels.

The standard deviation of the medium-to-high-frequency variance is similar for RCS, MRCS and SARCS methods, i.e 0.35. This variance is used with to estimate how many rings of overlap are needed. For a 95% confidence level, within the limit of  $\pm 0.05$ , then 190 rings of overlap are needed if they are from one-year overlaps of 190 trees. If all the rings are from one tree (assuming the average value of autocorrelation of errors for the chronology) then 1700 overlapping rings are needed ( $r_1=0.81$ ,  $F=0.11$  in above equations).

For each year of a chronology the count of overlapping rings (minimum of either side) can be used to identify the “weakest” points and confidence levels due to the counts

of overlapping rings can be assessed. This is not independent of the other confidence levels and is not included in Bootstrap error estimates. The count of overlapping rings will change slowly (medium-frequency) over time as the trees comprising the chronology change. A major difference between RCS indices and MRCS/SARCS indices (that incorporate BFM) is that the RCS indices have values which differ much more from the local chronology mean and hence generate the extra “Low-frequency mean” variance shown in Table 6.3.1. The uncertainty associated with this variation in mean values is required by the RCS method in estimating the mean growth rate of trees i.e. the natural variation in tree growth rates must be removed to arrive at the mean of growth rate due to the effects of common forcing. The MRCS and SARCS methods do not need to remove the natural variability of growth rate of trees because the BFM method rescales each tree (with respect to the chronology) and thus removes most of the uncertainty arising from the natural variability of tree growth rates from MRCS and SARCS generated indices, but in doing so uncertainty due to overlapping is introduced.

#### 6.3.4. Overlapping Errors for Sample Chronologies

To assess the variability of the mean value of connected chronology sections all the Tornetrask AD trees with a ring between 500 and 1000 AD were selected. Tree counts (grey shading) and chronology indices (red line) generated by using the SARCS method on the selected trees are shown in Figure 6.3.6a. The count of overlapping rings for each year is shown in blue; calculated as the sum for all trees of the minimum of either the rings before or rings after the selected date. There are 71 trees and 4000 overlapping rings at 750 AD from which sub-samples are taken.

The minimum number of overlapping rings is reduced by deleting rings from the short end (relative to 750 AD) of each tree. The number of trees is systematically reduced by randomly selecting and then deleting trees with a ring at 750 AD. The BFM method is then used to rebuild the chronology with a weakened overlap at 750 AD and results compared. Figure 6.3.6(b) to (f) show the effect on the chronology indices, tree counts and counts of overlapping rings for the chronology, as the number of overlapping rings for each tree with rings at 750 AD is progressively reduced. Where the maximum overlap at 750 AD is set to two years this means that all trees with a ring at 750 AD either start with year 748 AD or end on year 752 AD, a tree starting at

748 AD has 5 years of overlap with each tree finishing at 752 AD and contributes two year to the “overlapping” ring count. With 71 trees, each with a 5 years overlap period, the chronology is robust and varies little from the full chronology.

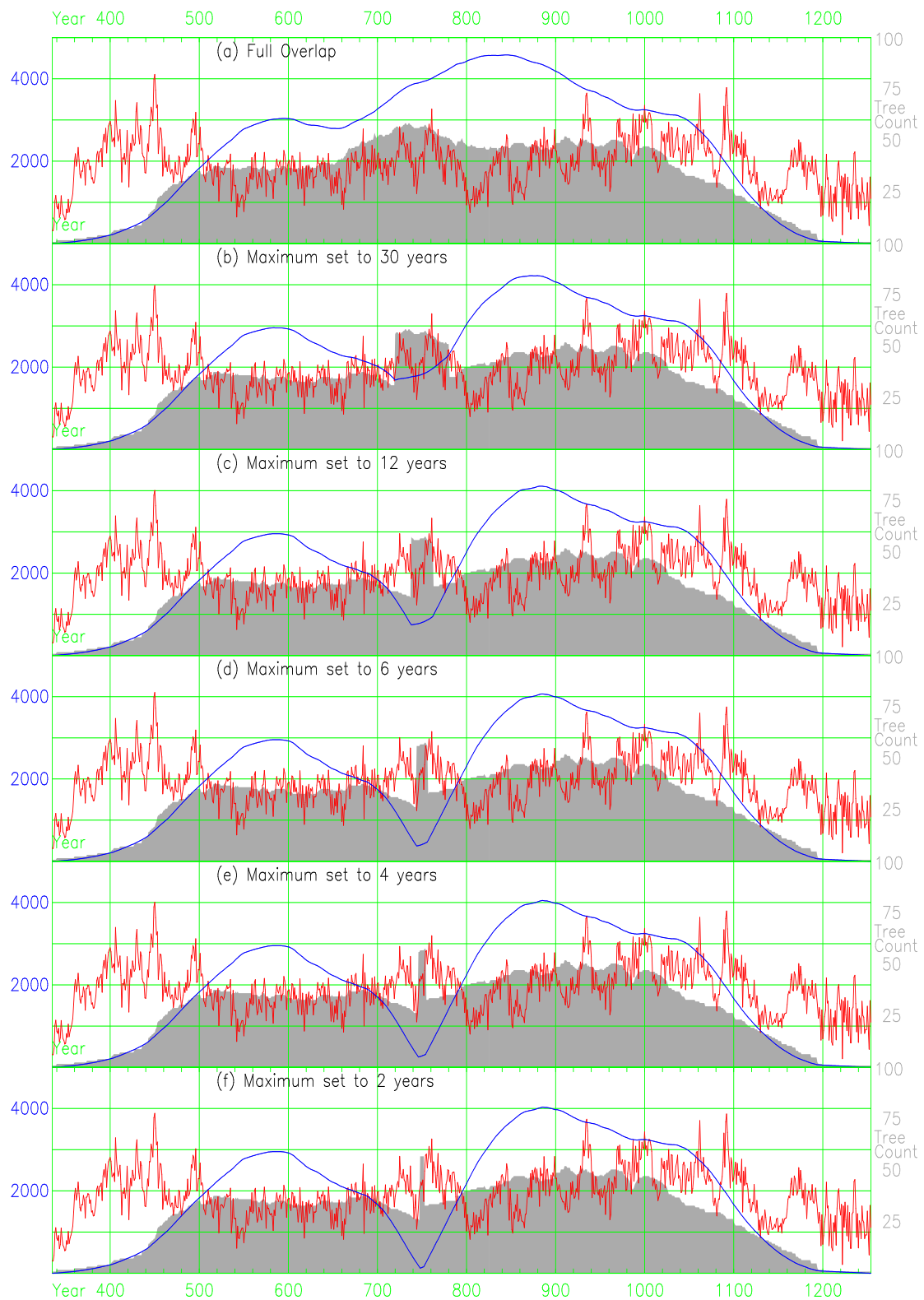


Figure 6.3.6 Progressively reduced overlap at 750 AD using all Tornetrask AD trees with rings from between 500 to 1000 AD, showing the strength of overlap, tree counts, and chronology indices (red).



To test the robustness of the overlapping, the methods above were used to reduce the overlap length, either side of 750 AD, to between sixty and two indices for each tree and the number of trees was limited to between sixty and five by random sampling from the 71 original trees. The chronology was built using BFM and the mean value of chronology indices before 700 AD relative to the mean value of chronology indices after 800 AD was computed. These dates were selected to remove the effects of deleting specific indices. One hundred random samples (realisations of a potential chronology) were taken for each selected tree count and set of overlapping segment lengths and the standard deviation of the relative change of the mean value of chronology sections was assessed. The results are shown in and plotted in Figure 6.3.7 as a pseudo-contour plot of the square root of tree count against number of rings of overlap with colour coded values indicating the range of the resulting standard deviation.

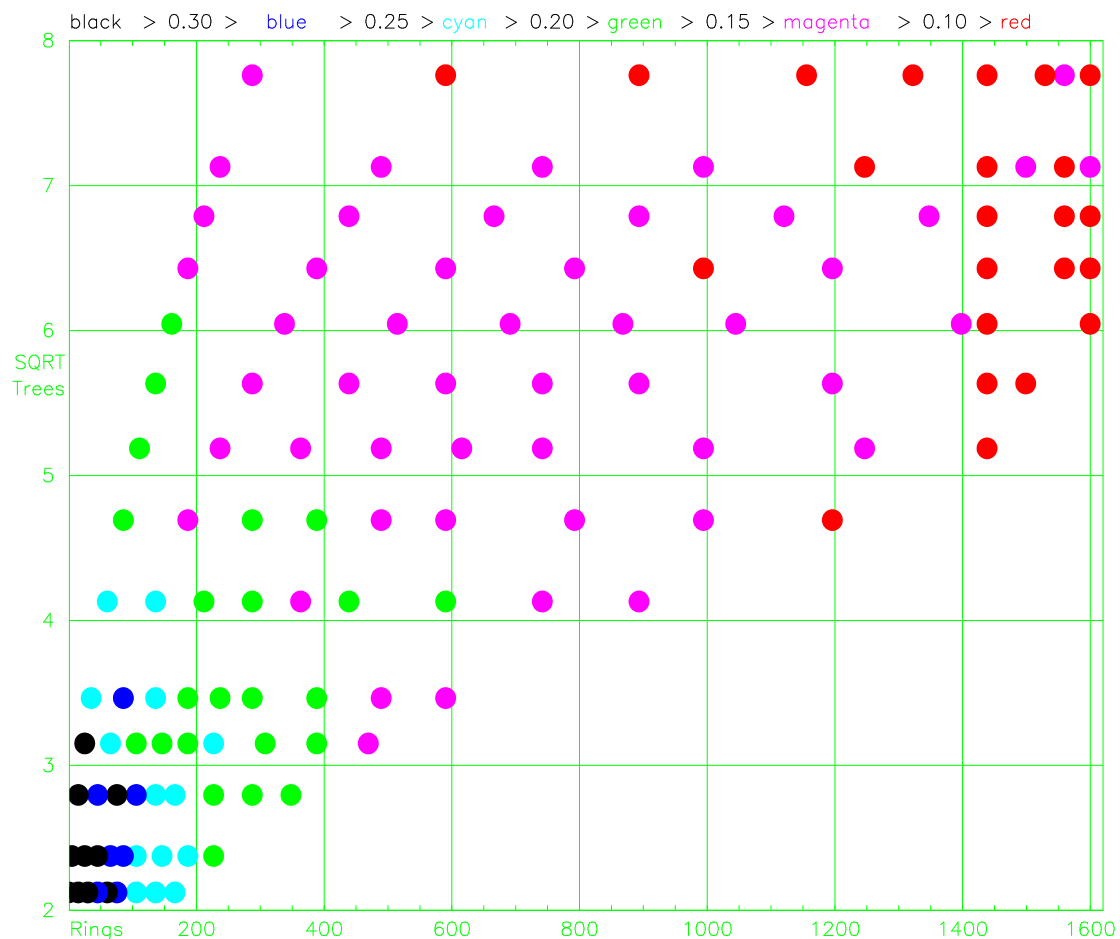


Figure 6.3.7 Standard deviation of chronology section means derived from 100 samples and plotted by overlapping ring count and square root of tree count.

There is a progressive reduction in standard deviation from left to right (increasing count of overlapping rings) and from bottom to top (increasing tree count). Given the

tree count and overlapping ring count at any point in a chronology and presuming stability in the scaled bootstrap error bars over time (Figure 6.3.4f) and table of values (not shown) used to create Figure 6.3.7 can be used to estimate the confidence levels of the chronology mean about that point in time. In Section 4.3.6, chronologies were shown to become “unstable” when the lengths of series of indices making up the chronology were progressively reduced. Figure 4.3.4 is reproduced along with plots of the count of overlapping rings in Figure 6.3.8 to demonstrate how the weak points of these chronologies can be identified by extrapolating data points from Figure 6.3.7. The Tornetrask AD and Lapland AD chronologies both have more than 20 trees (grey shading) and more than 800 overlapping trees for the period from AD 200 to the present (Black lines in Figure 6.3.8b and 6.3.8d) and the standard deviations of Figure 6.3.7 are expected to be less than 1.5 for this period. As the chronologies are progressively weakened overlapping ring counts reduce and ring counts drop below 400 for Tornetrask at AD 1200 and AD 400 and for Finnish-Lapland in the sixth century. The cyan chronology (Tornetrask with mean segment length 44), and to a lesser extent the red and blue chronologies, diverge from the black chronology after AD 1200. The shift at this date is translated to a slope change for later indices, because the slopes of these chronologies have been set to zero over the 600 to 1600 period by rotation.

In practice there is only one realisation of a chronology which may or not be correct. Being able to identify parts of a chronology which may have large error bars is crucial to the use of BFM. Chronologies created using the RCS method appear to degrade steadily as the number of samples is reduced. BFM chronologies have less error where there are sufficient trees but as tree and overlapping ring counts reduce below some critical limit then the local trends in BFM chronologies behave chaotically. The ability of the BFM method to preserve variance at frequencies equal to the length of the chronology is dependent on having sufficient samples over the length of the chronology. A 5000-year chronology with a weak point in the middle can be treated as one chronology using MRCS and SARCS methods to generate tree indices but each half needs to be processed separately by the BFM method, i.e. given a mean of 1.0 and zero slope. The two halves can be joined using arithmetic means but need an appropriate statement concerning the loss of long-timescale variance.

Fig 6.3.8a Chronologies with varying mean tree lengths – Tornetrask AD Chronology  
 Mean Length 188      Mean Length 108      Mean Length 79      Mean Length 44

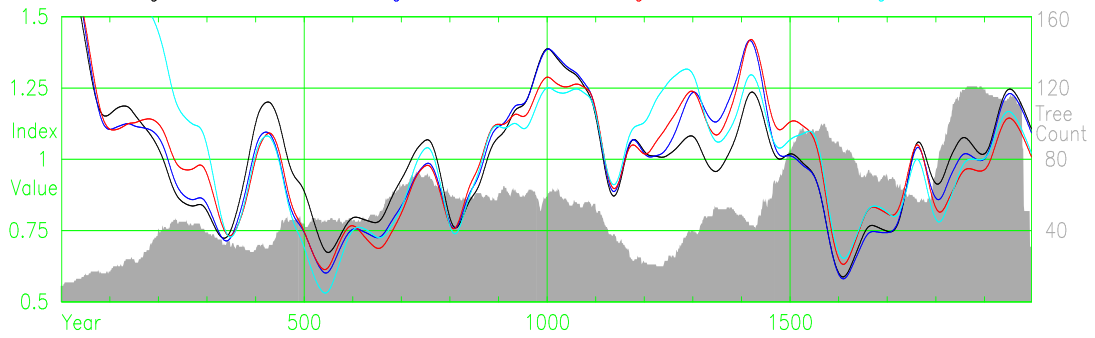


Fig 6.3.8b Counts of overlapping rings – Tornetrask AD Chronology  
 Mean Length 188      Mean Length 108      Mean Length 79      Mean Length 44

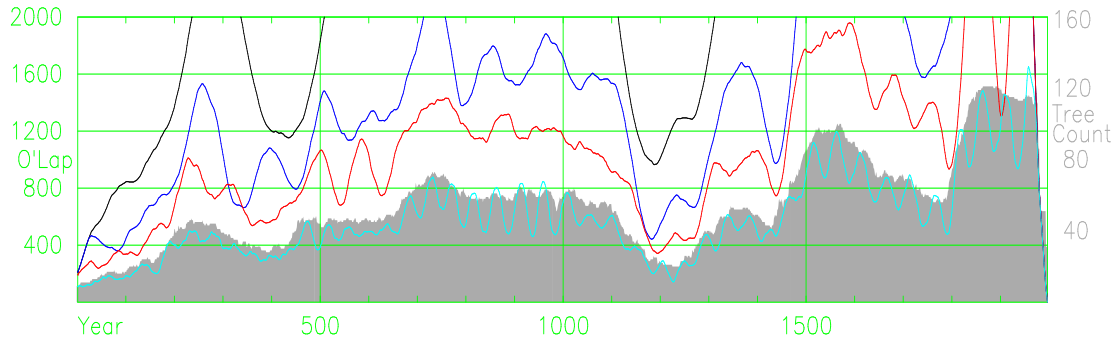


Fig 6.3.8c Chronologies with varying mean tree lengths – Finnish–Lapland AD Chronology  
 Mean Length 178      Mean Length 105      Mean Length 79      Mean Length 44

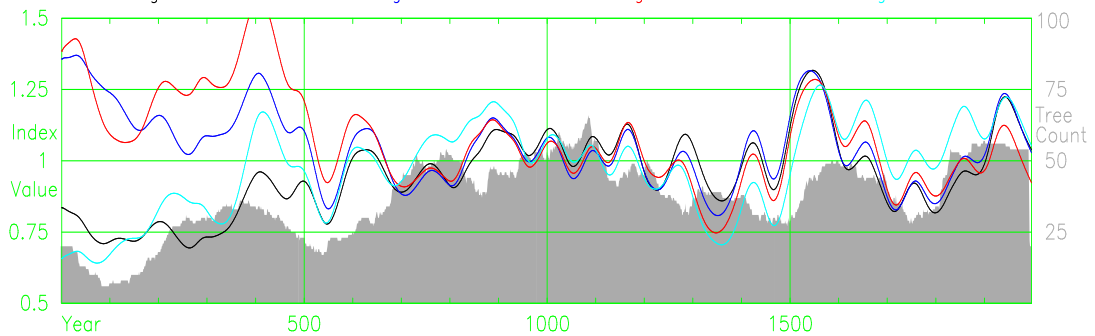


Fig 6.3.8d Counts of overlapping rings – Finnish–Lapland AD Chronology  
 Mean Length 178      Mean Length 105      Mean Length 79      Mean Length 44

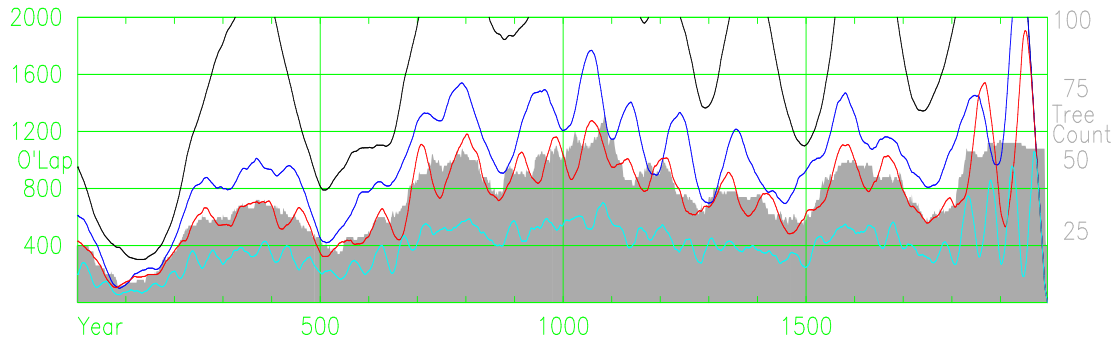


Figure 6.3.8 Chronologies of SARCS derived indices, series sub-divided to reduce mean length and averaged using BFM, with each chronology slope set to zero and mean to 1.0 for period 600 to 1600. Chronologies (a) and (c) and counts of overlapping rings (b) and (d).

### 6.3.5. SARCS Method used on Modern chronologies

The SARCS method derives expected growth curves in a novel manner and a demonstration, that SARCS method retains the low-frequency characteristics of the RCS method and can preserve low-frequency variance to the length of the chronology using modern chronologies, is presented here. For this demonstration the SARCS method is compared to the RCS method using chronologies created from “living” trees. Because the comparison is of variance at half the length of a chronology the overall slope of both RCS

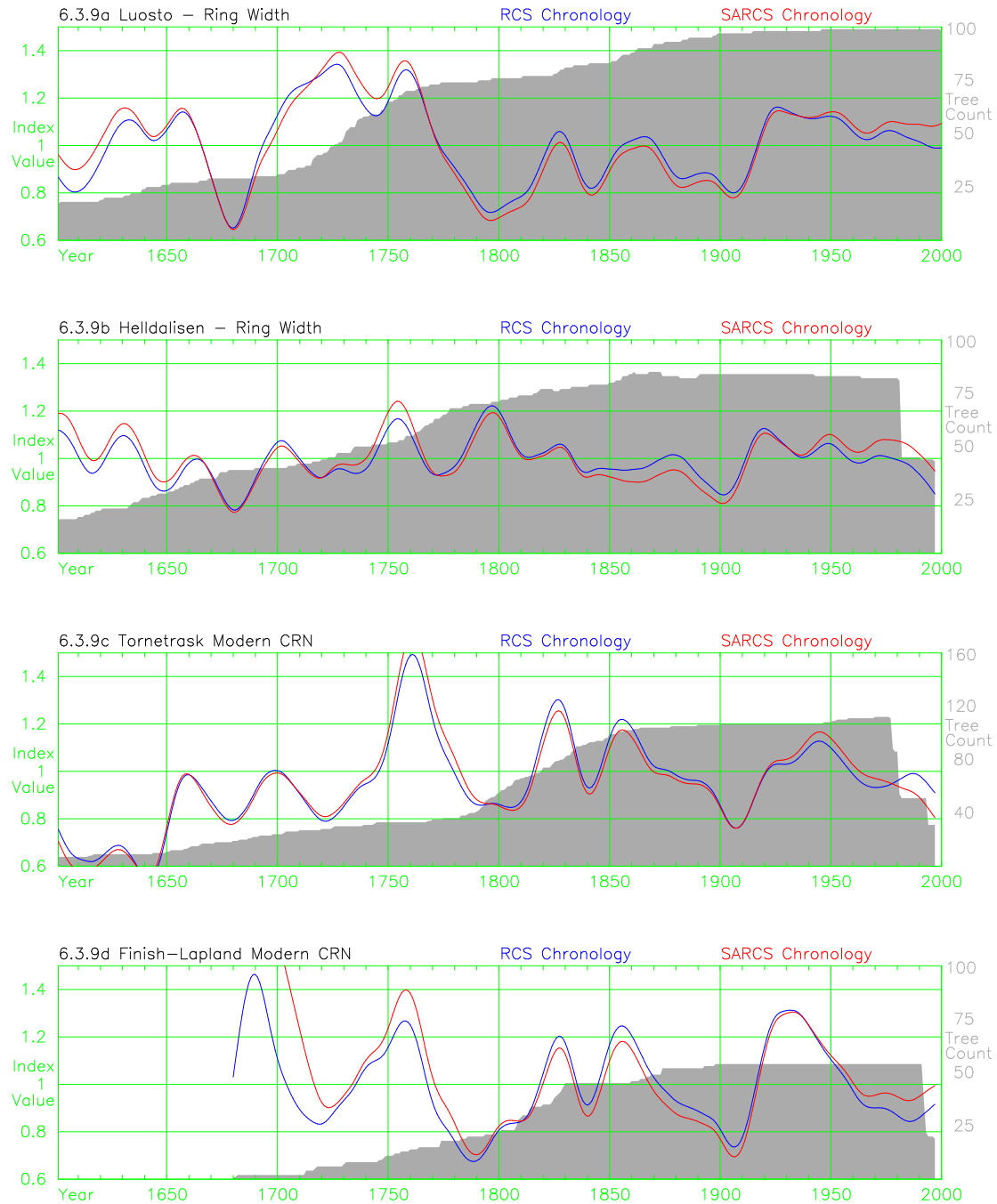


Figure 6.3.9 Comparison of modern chronologies, with adjusted slopes and means, created with the SARCS and RCS methods using trees from (a) Luosto, (b) Helldalisen, (c) Tornetrask, and (d) Finnish–Lapland.

and SARCS chronologies is set to zero and the mean values of both sets of indices are set to 1.0 after chronology creation using the methods described in Section 4.2.5. This rotation of the RCS chronologies removes the main effects of modern sample bias. The resulting chronologies are shown in Figure 6.3.3.

The modern chronologies of Luosto (a) and Helldalisen (b) are used along with “modern” chronologies created from the Tornetrask (c) and Finnish-Lapland (d) sites by only using trees with rings after AD 1980, i.e. trees that were living when sampled. Tree counts are lower in the earliest periods of all chronologies and the results will be less robust. The SARCS method produces chronologies whose medium-frequency variance (one to two centuries) is similar to that produced by the RCS method. The stretching of trees to fit the RCS curves (Section 5.8), the use of the BFM method (Section 4.3), the use of signal-free RCS curves, and signal-free trees (Section 5.5.8) are producing similar results to those of the RCS method with slope adjustment. The main differences between RCS and SARCS chronologies, after adjustment of slopes and means, are in the end effects which are discussed in Section 5.5. The most recent decades, which figure prominently in any temperature reconstructions, are noticeably different.

## **6.4. Tree Growth and Temperature**

### **6.4.1. Correlations**

The main objective of this study is to isolate the common signal found in tree growth measures, but having proposed some new methods, it is necessary to examine the differences these methods might make in climate reconstruction. In previous studies the Tornetrask chronology was used to reconstruct summer temperatures (Grudd et al. 2002), the mean of June, July and August, at the Abisko meteorological station. The Finnish-Lapland chronology was used to reconstruct July temperatures (Helama et al. 2002) for the Karesuando and Karasjok meteorological stations. Simple linear regression was used with the Tornetrask reconstruction based on a single (current year) chronology index as a predictor whereas the Finnish-Lapland reconstruction used both the current and previous year’s chronology indices. The procedures followed here were intended to explore the direct relationships between chronologies and mean monthly temperatures; use the results from this exploration to select a regression model suitable for all chronologies; and then to use this regression model to make comparisons between the different standardisation methods based on the effect on climate reconstructions themselves, as well as on the

variance of the chronologies themselves. The two longest series of mean monthly temperature measures, those from Bödö and Tornedalen, are used to provide predictand data.

Bödö Months	Previous Year								Current Year								
	M	J	J	A	S	O	N	D	J	F	M	A	M	J	J	A	S
Tornetrask AD (1868-1997)																	
Hugershoff	.29	.37				.27	.23							.18	.59	.28	
RCS	.36	.36				.31	.24	.20				.17	.24	.19	.55	.30	.22
MRCS	.32	.38	.18			.29	.24	.20					.21	.20	.59	.30	.19
SARCS	.33	.38	.18			.29	.24	.20					.22	.20	.58	.30	.20
Finnish-Lapland (1868-1997)																	
Hugershoff	.25	.21	.28	.21	.18		.25	.25	.19			.18			.58	.35	
RCS	.25	.20	.28	.22	.19		.25	.25	.19			.18			.58	.35	
MRCS	.27	.21	.29	.23	.20		.26	.28				.18	.19		.57	.36	
SARCS	.29	.21	.28	.23	.20		.26	.28				.19	.21		.57		
Luosto, north Finland (1868-2000)																	
Hugershoff	.35	.23			.18	.19	.20	.21				.17	.20		.39		
SARCS	.36	.23			.20	.20	.21	.22				.17	.22		.39		
Helldalisen, west Norway (1868-1997)																	
Hugershoff	.24	.27										.21	.30	.30	.47	.34	
SARCS	.27	.28									.18	.21	.33	.31	.45	.34	

\* Only values with  $P > 0.05$  shown

Table 6.4.1 Cross-correlation table of Bödö mean monthly temperatures (previous May to current September) against chronologies using various (specified) standardisation methods and sites.

Relationships between temperature measures and chronologies were first explored through cross-correlation. Individual mean monthly climate measures for the months from the previous year's May to the current year's September were separately correlated against the different chronologies and the results of the correlations that are significant at the  $p < 0.05$  level are recorded in Tables 6.4.1 for Bödö and Table 6.4.2 Tornedalen. For the Tornetrask and Finnish-Lapland chronologies the Hugershoff, RCS, MRCS and SARCS methods were used whilst for the modern chronologies from Luosto and Helldalisen only the Hugershoff and SARCS methods were used because the RCS and MRCS methods are not suitable for modern chronologies with limited numbers of trees. The strongest overall relationship, based on all chronologies compared with data for both meteorological stations was that with mean July temperature of the current year, with a consistent (though weaker) secondary relationship with the previous spring, represented by mean May and June temperatures. The southern sites (Luosto and Helldalisen) tend to have a longer and earlier relationship (May to July) in early summer whilst the northernmost sites (Tornetrask and Finnish-Lapland) have a later response into August,

the August relationship is stronger against the northern meteorological site of Bödö. The Hegershoff chronologies tend to have a weaker response to the longer meteorological series of Tornedalen than to the shorter Bödö series.

Tornedalen Months	Previous Year								Current Year								
	M	J	J	A	S	O	N	D	J	F	M	A	M	J	J	A	S
Tornetrask AD (1816-1997)																	
Hegershoff	.23	.36				.16	.17							.31	.47		
RCS	.34	.40	.21			.20	.25	.17			.17	.16	.27	.35	.52		
MRCS	.29	.39	.20			.17	.24	.16					.22	.34	.52		
SARCS	.31	.40	.20			.18	.25	.17					.24	.35	.52		
Finnish-Lapland (1816-1997)																	
Hegershoff	.21	.25	.24	.17			.17	.16						.25	.52		
RCS	.22	.24	.28	.19			.23	.20	.19				.19	.23	.56	.21	
MRCS	.26	.26	.29	.19			.26	.22	.20				.24	.24	.56	.22	
SARCS	.28	.26	.29				.26	.23	.20		.17	.16	.25	.25	.56	.23	
Luosto, north Finland (1816-2000)																	
Hegershoff	.30	.25	.21		.17		.15				.16	.18	.28	.27	.49		
SARCS	.32	.26	.22		.18		.17	.15			.18	.20	.30	.27	.49		
Helldalisen, west Norway (1816-1997)																	
Hegershoff	.27	.29					.21	.23				.18	.29	.32	.37		
SARCS	.32	.30					.25	.25			.18	.23	.33	.34	.39	.18	

\* Only values with P<0.05 shown

Table 6.4.2 Cross-correlation table of Tornedalen mean monthly temperatures (previous May to current September) against chronologies using various (specified) standardisation methods and sites.

### 6.4.2. Regressions

Examination of the Tables 6.4.1 and 6.4.2 led to a decision to focus the regression on summer temperatures and six different mean temperature series were created for each meteorological station; June, July, August, June and July, July and August, and all three months of June, July and August. The existence of a previous year's relationship and the high levels of autocorrelation in the chronologies led to the selection of current year and previous year in the regression model and a constant was also included, which is similar to the Finnish-Lapland reconstruction (Helama et al. 2002). The predicted temperature (T) is derived from the chronology indices (CRN) and three constants (Beta) for year (i) as follows:

$$T(i) = \text{Beta}0 + \text{Beta}1 * \text{CRN}(i) + \text{Beta}2 * \text{CRN}(i-1) \quad (1)$$

The variance explained by this regression model for the full period, first half period, and second half period of overlap between temperature series and chronologies are shown for four of the chronology / temperature series; the Tornetrask chronologies and Bödö temperatures in Table 6.4.3, the Finnish-Lapland and Tornedalen temperatures in Table

Tornetrask	Period	Bödö – Explained variance (R squared %)					
		June	July	August	June to July	July to August	June to August
Hugershoff	1868-1997	4	37	8	26	29	25
	1868-1932	8	39	9	30	32	29
	1933-1997	1	33	8	17	25	17
RCS	1868-1997	4	35	10	25	29	26
	1868-1932	7	42	10	31	35	30
	1933-1997	0	30	8	15	23	15
MRCS	1868-1997	5	37	10	27	31	27
	1868-1932	8	41	10	31	34	31
	1933-1997	1	35	8	18	25	18
SARCS	1868-1997	5	37	10	26	30	27
	1868-1932	7	42	10	31	34	30
	1933-1997	1	34	8	17	25	18

Table 6.4.3 Variance explained by the regression model (1) using the Tornetrask chronologies against the Bödö temperature data for full period, first half of period, and second half of period.

Finnish-Lapland	Period	Tornedalen – Explained variance (R squared %)					
		June	July	August	June to July	July to August	June to August
Hugershoff	1816-1997	7	31	3	25	22	22
	1816-1906	19	29	4	33	18	25
	1907-1997	0	34	12	16	33	21
RCS	1816-1997	6	35	4	26	26	25
	1816-1906	18	30	4	34	19	26
	1907-1997	0	34	12	15	33	20
MRCS	1816-1997	6	35	5	27	27	26
	1816-1906	18	30	4	33	18	25
	1907-1997	1	33	13	16	33	22
SARCS	1816-1997	7	35	5	27	28	26
	1816-1906	18	30	4	33	18	25
	1907-1997	1	33	13	16	33	22

Table 6.4.4 Variance explained by the regression model (1) using Finnish-Lapland chronologies the Bödö temperature data for full, first half, and second half periods.

6.4.4, the Helldalisen and Bödö temperatures in Table 6.4.5, and the Luosto and Tornedalen temperature in Table 6.4.6. The explained variance of the mean July temperatures is larger than that of the other temperature series for the northernmost sites (Tornetrask and Finnish-Lapland) and the explained variance of July temperatures is of similar magnitude to that of the two and three month temperature means for southernmost sites (Helldalisen and Luosto). The explained variances of Tornetrask to Tornedalen and Finnish Lapland to Bödö are of similar magnitudes to those for Tornetrask to Bödö and Finnish Lapland to Tornedalen and these figures are not displayed. The explained variance, by the Helldalisen chronology in the Tornedalen July temperatures and the Luosto chronology in Bödö July temperature, are around 20% and these data are not



presented. Because the explained variance of the mean July temperatures is generally higher than for alternative months, or combinations of months, the mean July temperatures are used here for further work.

Helldalisen	Period	Bödö – Explained variance (R squared %)					
		June	July	August	June to July	July to August	June to August
Hugershoff	1868-1997	10	23	12	24	25	27
	1868-1932	13	34	19	31	37	37
	1933-1997	5	16	8	15	16	16
SARCS	1868-1997	10	23	12	24	24	27
	1868-1932	13	34	19	30	37	36
	1933-1997	6	17	8	15	17	16

Table 6.4.5 Variance explained by the regression model (1) using Helldalisen chronologies against the Bödö temperature data for full period, first half of period, and second half of period.

Luosto	Period	Tornedalen – Explained variance (R squared %)					
		June	July	August	June to July	July to August	June to August
Hugershoff	1816-1997	7	26	1	23	15	17
	1816-1906	15	29	7	30	17	22
	1907-1997	1	16	2	11	10	8
SARCS	1816-1997	8	26	1	23	16	18
	1816-1906	15	29	6	30	17	22
	1907-1997	2	15	3	11	9	9

Table 6.4.6 Variance explained by the regression model (1) using Luosto chronologies against the Tornedalen temperature data for full period, first half of period, and second half of period.

Tree Data Sites	Meteorological Stations	Months	Period	Variance Explained	Source
Tornetrask	Abisko (and neighbours)	June-August	1869-1997	36%	Grudd
	Bodo	July	1868-1997	35%	This study
Finnish-Lapland	Mean of Karasjok and Karesuando	July	1879-1992	37%	Helema
	Tornedalen	July	1816-1997	35%	This study

Table 6.4.7 Variance explained by regression models for the Tornetrask and Finnish-Lapland sites using RCS chronologies.

The amount of variance explained by the different chronologies (standardisation methods) from the same site is similar and the differences are not sufficient to conclude that one method is better than the others on the basis of the climate correlations here.

Table 6.4.7 shows a comparison of the amounts of variance explained in regressions

using the RCS method with the results of previous work. There are differences in the choice of meteorological stations, the season used, and the period covered by the regression but overall the amount of explained variance is similar.

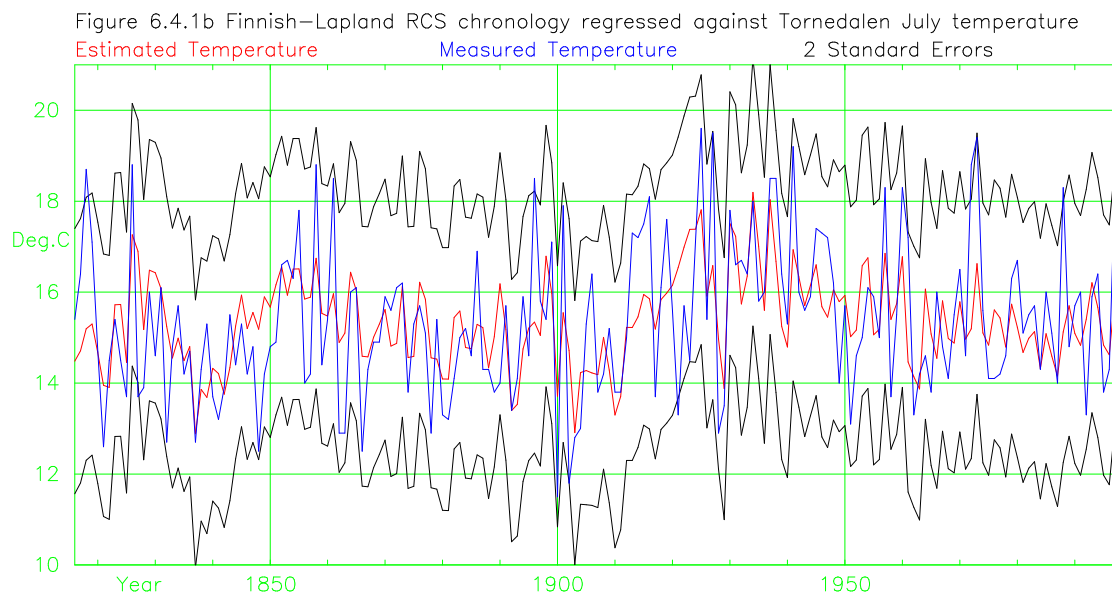
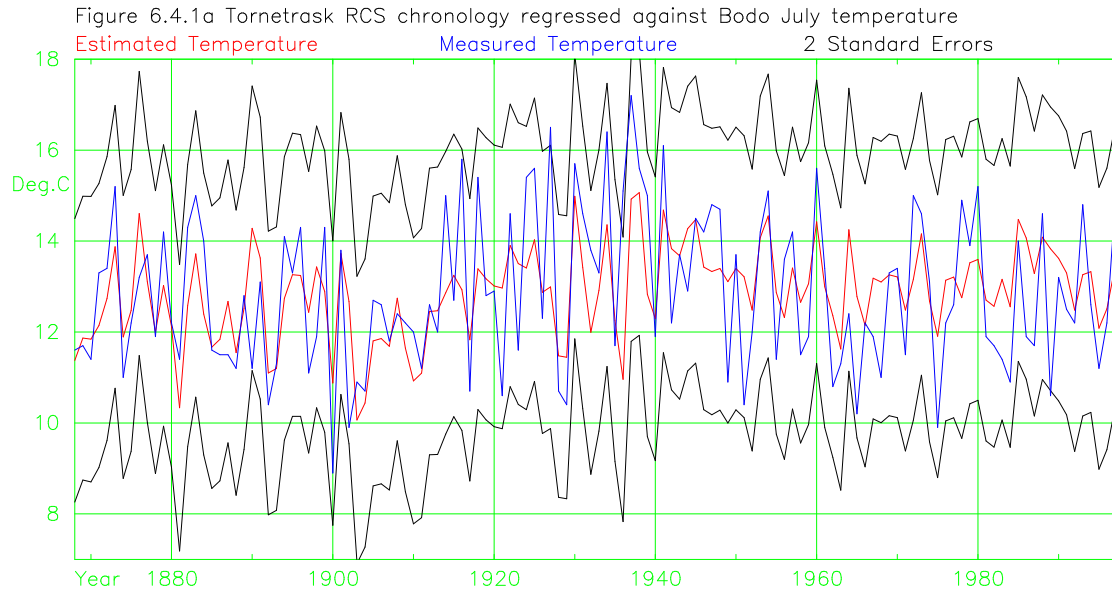


Figure 6.4.1 Measured and estimated mean July temperature showing two standard error limits, from RCS generated chronologies for (a) Tornetrask AD regressed against Bodo and (b) Finnish-Lapland AD regressed against Tornedalén.

The Tornetrask and Finnish-Lapland chronologies explain similar amounts of temperature variance in regressions based on only the first and second half of the data span, whereas the Luosto and Helldalisen chronologies explain twice as much variance in the early period as they do over the later period. It is not wise to over-interpret these differences, given the large error uncertainty associated with these regressions. This is

demonstrated by plotting measured and estimated (by the regression) mean July temperatures along with their two standard errors in Figure 6.4.1 for the Tornetrask RCS chronology and Bödö July temperatures and the Finnish-Lapland chronology and Tornedalen July temperatures. The regression error for year  $i$  (Total Error  $i$ ) was calculated using the standard errors of the three regression coefficients of constant, current year and previous year ( $SE\beta_0$ ,  $SE\beta_1$  and  $SE\beta_2$ ), the standard deviation of the residuals i.e. difference between measured and predicted temperature ( $SET$ ), and the differences between chronology and chronology mean for year  $(x_i)$  and previous year  $(x_{i-1})$  using the following equation (Briffa et al. 2002):

$$(\text{Total Error } i)^2 = (SET)^2 + SE\beta_0^2 + (SE\beta_1 * x_i)^2 + (SE\beta_2 * x_{i-1})^2$$

One observation from Figure 6.4.1 is that the low-frequency variance in predicted temperatures (red) and in measured temperatures (blue) is of similar magnitude whilst the high-frequency variance in predicted temperatures has roughly half the magnitude of the high-frequency variance in the measured temperatures series. The second observation is that the two standard deviation error bars cover a  $4^\circ \text{C}$  temperature range; primarily controlled by the standard deviation of the residuals i.e. the two thirds of variance unexplained by the regression model.

The chronologies created by the various standardisation methods diverge more in the modern period than in their central portions and, because reconstructed temperatures are based on the most recent century or two, there are large variations in the reconstructed temperatures. Figure 6.4.2 shows smoothed series of climate reconstructions representing the mean July temperature of the selected meteorological station for the various regional chronologies. The reconstructions use the methods of Section 6.4.2 and chronologies were created using the Hugershoff, RCS, MRCS (only for sub-fossil chronologies) and SARCS methods are shown. The Tornetrask (Figure 6.4.2a) and the Helldalisen (Figure 6.4.2d) chronologies were used to reconstruct Bödö mean July temperature and the Finnish-Lapland (Figure 6.4.2b) and the Luosto (Figure 6.4.2c) chronologies were used to reconstruct Tornedalen mean July temperature. The Hugershoff method reconstructs temperatures series with variance limited to about a century which matches the other methods in the calibration period as can be seen in Figures 6.4.2 (c) and (d). The MRCS and SARCS methods produce similar results as can be seen in Figures 6.4.2 (a) and (b).

Generally the reconstructed temperatures in the first half of each chronology for Hugerhoff, RCS and MRCS/SARCS differ.

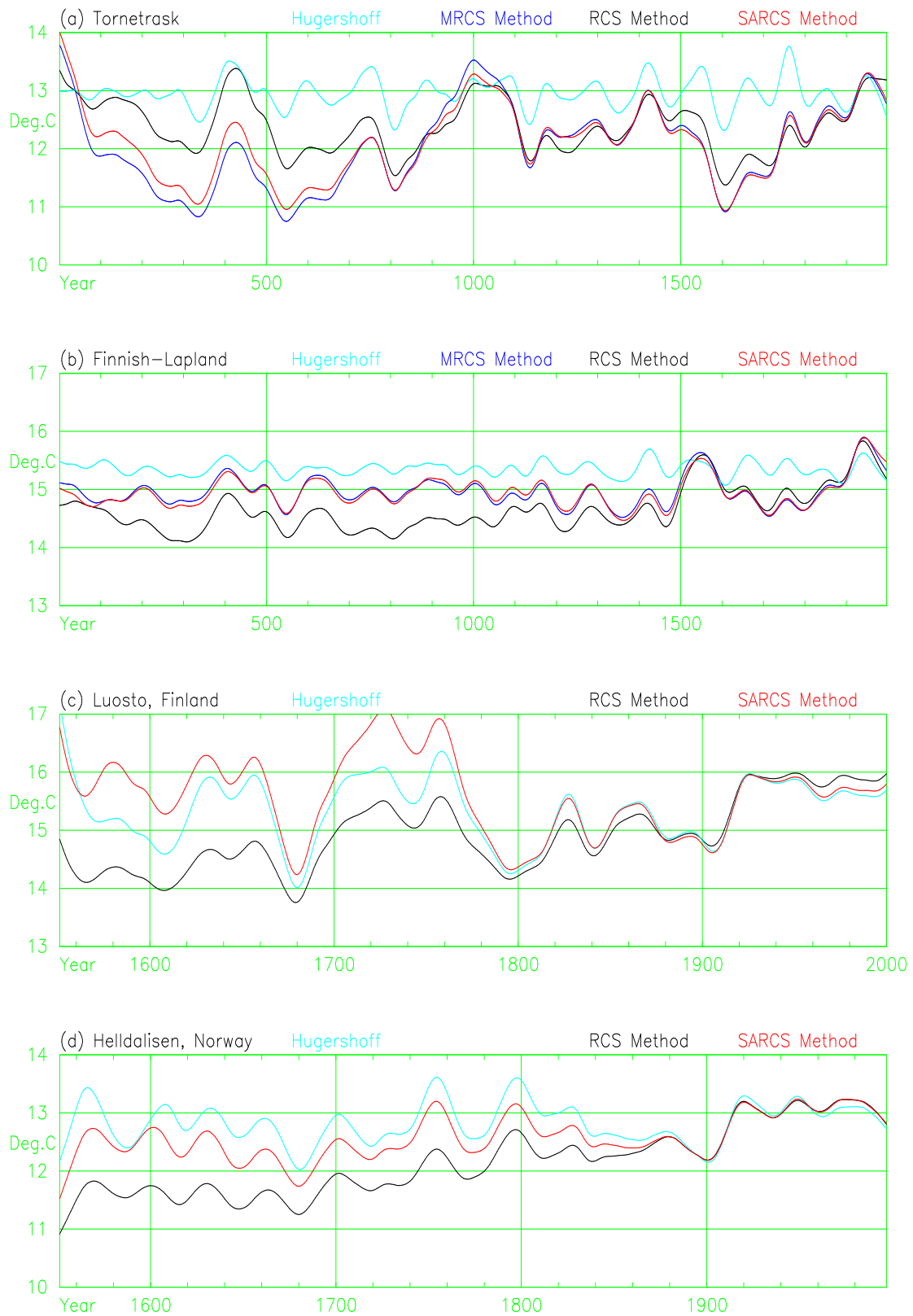


Figure 6.4.2 Various mean July temperature reconstructions based on chronologies created by different standardisation techniques: RCS,Hugerhoff, MRCS and SARCS methods from regression against current and previous years tree growth indices for (a) Tornetrask AD and (d) Helldalisen to Bodo, (b) Finnish-Lapland AD and (c) Luosto to Tornedalen.

### 6.4.3. Low and High pass Filtered Comparisons

The outcomes of different standardisation approaches are likely to manifest differently in long, as opposed to short-timescale variability of the various chronologies. It was considered worthwhile to quantify the association between chronologies and temperature data separately for high and low-frequency variability. Filtering was performed using a Gaussian-weighted filter (Osborn & Briffa 2000). Because measured temperature series have a maximum length of 180-years, all chronologies and temperature series were filtered using a high-pass filter with a 50% magnitude reduction at 180-year frequency. This action created the 180-year high-pass filtered series. The high-pass filtered chronologies and temperature series were filtered again using a low-pass, with 50% magnitude reduce at 10-year frequency filter, to produce band-pass 10-180 year filtered series. The band-pass series were subtracted from the high-pass 180-year series to create high-pass 10-year filtered series. Table 6.4.8 shows correlation values between chronologies, produced by various standardisation methods, and mean July temperatures for the three classes of filtered data. Each filtering method and site combination produces a different level of correlation but the various standardisation methods produce similar

Standardisation Method	High-Pass 180 year	Band-Pass 10-180 year	High-Pass 10 year
Tornetrask AD to Bodo mean July Temperature (1868-1997)			
Hugershoff	0.59	0.53	0.68
RCS	0.60	0.55	0.68
MRCS	0.60	0.57	0.68
SARCS	0.60	0.56	0.68
Finnish-Lapland AD to Tornedalen mean July Temperature (1816-1997)			
Hugershoff	0.50	0.51	0.61
RCS	0.51	0.53	0.62
MRCS	0.51	0.54	0.61
SARCS	0.51	0.54	0.61
Luosto to Tornedalen mean July Temperature (1816-2000)			
Hugershoff	0.43	0.38	0.52
RCS	0.44	0.41	0.52
MRCS	0.44	0.40	0.52
Helldalisen to Bodo July mean Temperature (1868-1997)			
Hugershoff	0.47	0.42	0.55
RCS	0.46	0.36	0.57
MRCS	0.47	0.39	0.56

Table 6.4.8 Correlations of chronologies, created using various (specified) standardisation methods and mean July temperature series which have been filtered using high-pass and band-pass filters.

results i.e. the differences are small. In all cases the high-pass 10-year filtered series produce higher correlation values than the high-pass 180-year, Band-pass 10-180 year, and unfiltered series (Tables 6.4.1 and 6.4.2).

A sample set of filtered series, as used in Table 6.4.8, is plotted in Figure 6.4.3 to show how the filtered chronology and temperatures series correspond. The plots are centred on the mean value with a range of  $\pm 3.0$  standard deviations shown. The Finnish-Lapland chronology generated by the RCS method (blue) and the Tornedalen mean July temperatures (red) are plotted for the high-pass 180-year (a), band-pass 10-180 year (b),



Figure 6.4.3 Tornedalen mean July temperature and Finnish-Lapland RCS chronology filtered as (a) high-pass 180 year, (b) band-pass 10 to 180 year, and (c) low-pass 10-year.

and high-pass 10-year (c) filtered series. One problem highlighted is that the high-frequency magnitude of the temperature series is greater than the high-frequency magnitude of the chronology indices, in Figure 6.4.3a there is at least one temperature value in each decade which is above and one below the mean value of the temperature series whereas the chronology indices are consistently above or below their mean value for more than a decade. (This applies to MRCS and SARCS chronologies as well as the RCS chronology but not to the Hugershoff chronology which has less low-frequency variance.) Temperature reconstructions based on separately identified frequency bands (Guiot 1985; Osborn & Briffa 2000) are likely to explain more variance than the simple regressions used above. A more satisfactory method would be to re-examine the standardisation methods in order to obtain a suitable frequency balance in generated chronologies.

## **6.5. Conclusions**

In this chapter, comparisons of tree and chronology indices have been used to demonstrate that some of the problems of the RCS method are solved and that the MRCS and SARCS methods:

1. Generate *expected growth curves* which are a closer fit to series of measurements.
2. Create series of tree indices with reduced variance relative to the chronology.
3. Create series of tree indices with less age and diameter related bias.
4. Give more equal weight to each tree in the final chronology.
5. Create tree indices which approximate to fractional deviations.
6. Can be used to process “modern” chronologies, provided sufficient trees with a wide age distribution are available.
7. Generate chronologies with an arbitrary slope, but with consistent variance.
8. Extract long-timescale variance from the later years (3<sup>rd</sup> century and beyond) of trees.

Without a priori knowledge of the nature of the low-frequency signal, the magnitude of the common forcing on tree growth over time, there is no way of deciding which method produces the “best” results. The chronologies generated by the MRCS and SARCS methods are similar to each other, but differ from the chronology generated by the RCS method, particularly in the earliest and latest centuries. The MRCS and SARCS methods produce more consistent results, indicative of a significant improvement over the RCS

method. The BFM method is an important element of the processing introduced here to capture long-timescale variance but its detailed characteristics and wider application require further investigation. All methods preserve artificially generated step increases or decreases inserted in the middle or near the end of a chronology. Current methods of standardisation produce chronologies with varying but specified long-timescale characteristics. The MRCS and SARCS methods produce chronologies as having an explicitly defined arbitrary straight line slope which defines the long-timescale variance limitations of these methods. This slope could be calibrated against long series of climate measures.

The BFM method reduces the size of calculated error bars by rescaling each tree and gives the MRCS and SARCS method an advantage over the RCS method in the reduction of tree counts needed for specified confidence limits. Rescaling error bars to remove the effects of varying tree count and varying chronology index values removes most of the time-dependant changes in error bars suggesting that the error bars are not time dependant. The BFM method introduces error in the overlapping of tree indices and methods of assessing the magnitude of this error over time in a chronology are proposed. This overlapping error degrades chaotically and use of the BFM across weak points in a chronology will produce unreliable results for the whole chronology.

The ability of standardisation methods to capture the variance of the common forcing on tree growth should be measured independently of the measured climate signal. The annual variation of the production rate by foliage resulting from climatic variation produces high-frequency variance in ring increments. All standardisation methods appear to be able to capture this high-frequency variance. Medium-frequency variation in the production rate by foliage need not produce similar medium-frequency variation in ring increments because trees are able to adapt to local conditions. Judging the ability of standardisation methods to capture variance at periods of centuries and above by matching chronologies against measured temperature may not be sound because the series of measured temperature are not long enough. Correlation and regression techniques which use least squares methods present another problem in that the extreme values (chronology indices and climate measures) are heavily weighted e.g. a fit in the once a century three standard deviation year carries as much weight as 36 half standard



deviation years in the correlation. If both chronology indices and climate measures have an overall trend then further problems arise.

The Hegershoff, RCS, MRCS and SARCS methods produce chronologies which all appear to perform equally well in the task of estimating mean July temperatures at these north Fennoscandian sites. This appears to be a poor result for the proposed new methods. The problem is that summer temperatures have increased, tree growth rates appear to have increased, and all standardisation methods are able to resolve the high-frequency variability of tree growth. The Hegershoff method, when applied to the Luosto and Helldalisen sites, used a horizontal line to detrend 10% of the trees because series of ring measures from these trees had a positive slope. The Hegershoff chronology is thus forced to have a positive slope and, as temperatures have increased, the consequent medium-frequency fit improves correlations. With only a 20% step increase over 50 years, which is insufficient to trigger the use of a horizontal line detrend, the Hegershoff method performs badly (Figure 4.4.3d) on randomly generated trees. With artificial steps up and down (Figure 4.4.1b) the Hegershoff method produces inconsistent results. Had temperatures dropped, and tree growth rates decreased the Hegershoff method would produce poor results. The RCS method has been shown to have several problems but the most serious, from the point of view of this comparison, is modern sample bias (Section 5.4), which results in an estimated 10% per century positive slope (Figure 5.4.3) in the most recent centuries of all chronologies. Assessing how well the proposed new methods are performing using measured temperature data is problematic, but that they perform as well as commonly used standardisation methods is a positive result.

## Chapter 7. Process Based Standardisation (PBS)

### 7.1. Introduction

In Section 4.1 it was suggested that the rate of production of carbon by foliage would be a more direct measure of the magnitude of the common forcing on tree growth than the variance in series of ring width measures. In this Section an attempt is made to convert series of ring-width measures into estimates of the annual rate of carbon production by foliage in order to assess the magnitude of common forcing on tree growth. The relationship between ring-width and carbon production by foliage is non-linear and a process based standardisation (PBS) model is developed for this purpose. The PBS model is a carbon balance model and uses a “theoretically justified balance between structure and physiological function” (Mäkelä 1997) to develop rates of carbon production by foliage from ring-width measures. A next stage model could be developed, using processes such as photosynthesis, phenology, and soil moisture, to explore the non-linear relationships between various climatic variables such as temperature, precipitation, timing of snow melt and the common forcing signal found in tree growth measures. Such a model is considered beyond the scope of this project and the PBS model developed here is limited to the “standardisation” task of extracting the common forcing signal from series of ring width measures.

From a dendroclimatic point of view the PBS model is an attempt to remove the age-related growth trend from series of ring measures. This is a feasibility study and the question being addressed is “is such a model feasible as a means of standardising tree-growth data”. It is shown that the answer is a qualified “yes”; that the task is feasible in a specific area using limited numbers of tree samples from a single species. Some suggestions, further development and improvements are described.

A model is "*a set of statements embodying our current knowledge or hypotheses about the working of a particular system*" according to Landsberg (1986a, p2). Tree-growth models incorporate knowledge concerning tree growth and some of this knowledge is extracted and used here to create the PBS model. In tree-growth models a “simple” tree is described by the masses of a number of structural compartments. The growth of this tree is considered by the change of the sizes of these compartments over time, and these changes are controlled by a number of processes and empirically derived relationships.

Tree-growth models use time series of measured or simulated climate and environmental data and try to assess how tree growth would proceed over time in these given conditions, leading to a detailed description of model grown trees and forests (Shugart & Smith 1996). Series of ring width measures, as used in dendroclimatology, might be extracted from model-grown trees. Dendroclimatology uses measurements taken from exactly dated tree rings in order to infer the values of various climate variables during the period of interest. The major dendroclimatic input (ring increment) is an output of tree-growth models and the major input of tree-growth models (climate) is a dendroclimatic output. The objective of dendroclimatology (to explore the controls on tree growth) is the reverse of the objective of tree-growth models (use the controls on growth to grow a tree or forest). An attempt to locate commonality between dendroclimatic methods and tree-growth models will find two common areas in ring increments and climate data, but no overlap. In computer programming terms there is a fundamental “structure clash” and such problems can often be solved by reversing one of the processes. The PBS model developed here attempts this; starting with a simple process-based tree-growth model, each process is “inverted” by exchanging inputs and outputs and reversing equations, and then these processes are run in reverse order to “un-grow” a tree. The resulting model follows the sequence of dendroclimatic methods but uses the knowledge and expertise built into tree-growth models.

A sequence of logical stages can be followed to convert ring width measures into foliage production rates and a chronology. Ring width is the radial measurement at breast height of a volume increment (wood) added to the surface of an approximately circular cone (tree stem). If the diameter of this cone is known and there is a suitable rule describing how diameter varies with height, a height growth strategy, then the stem volume increment can be calculated. Mass is the product of volume and density. The mass increment of the stem growth is that portion of the total available mass that the tree has allocated to stem growth in that year. If there is a suitable rule describing the allocation strategy of a tree, then the total mass of carbon consumed by the tree in that year can be calculated. The mass of carbon consumed is presumed to be the carbon generated by photosynthesis in the foliage during the year. If the mass of foliage and the mass of photosynthate are known then photosynthate production by each unit of foliage can be calculated producing a value of “carbon per unit foliage” for each year of each tree (Section 4.1.3). These values are rescaled, by dividing by the mean value for all trees

over all time, to form tree indices, referred to as PBS Indices. The PBS Indices are averaged by calendar year to create a chronology representing the magnitude of tree growth over time.

A schematic diagram, Figure 7.1.1, is presented to illustrate the structure of the PBS model. Efficiency parameters are read at the start. The model then processes each tree reading in the initial diameter and height, calculating the initial size of the tree, and then processing each ring separately. Each ring width is used to calculate height growth, allocate carbon to update the tree sizes, and output a value for growth measured as carbon production by unit of foliage. After all trees have been processed, growth values are divided by their overall mean value to produce PBS tree indices and are averaged by calendar year to produce the PBS chronology. The conversion of each ring to a value for growth has the same effect in the PBS model of removing the age-related growth trend in more traditional standardisation techniques, although the method used is different. The rescaling and chronology production are as used in traditional dendroclimatic procedures.

## **7.2. PBS Model Overview**

Trees are complex living organisms and in order to generate practical models describing the growth of trees many simplifications are made (Cannell & Dewar 1994). Tree-growth models represent trees by a number of state variables which record the size of the basic components of tree structure. Growth processes and empirically-based rules are used to change these state variables to simulate the growth of individual trees on a small plot (or patch) of forest floor (Botkin et al. 1972). The lifecycle of a tree, from sapling to mature tree, is the net result of adding new material to the tree's structure and subtracting dead material. The PBS model, in the application envisaged here, needs to be simple, annual, based on *Pinus sylvestris*, and able to follow the growth of individual trees. There is a wide choice of tree-growth models available and a selection was made based on how well the tree-growth model fits the PBS model requirements. This PBS model is based on a series of carbon balance tree-growth models developed for *Pinus sylvestris* with the investigation of height growth strategies amongst the objectives (Mäkelä & Hari 1986; Mäkelä 1986; Mäkelä & Sievanen 1992; Mäkelä 1997). This tree-growth model is referred to as the “Mäkelä model” in later references. Other models that were examined in detail were HYBRID (Friend et al. 1997), GUESS (Smith et al. 2001), a pipe model

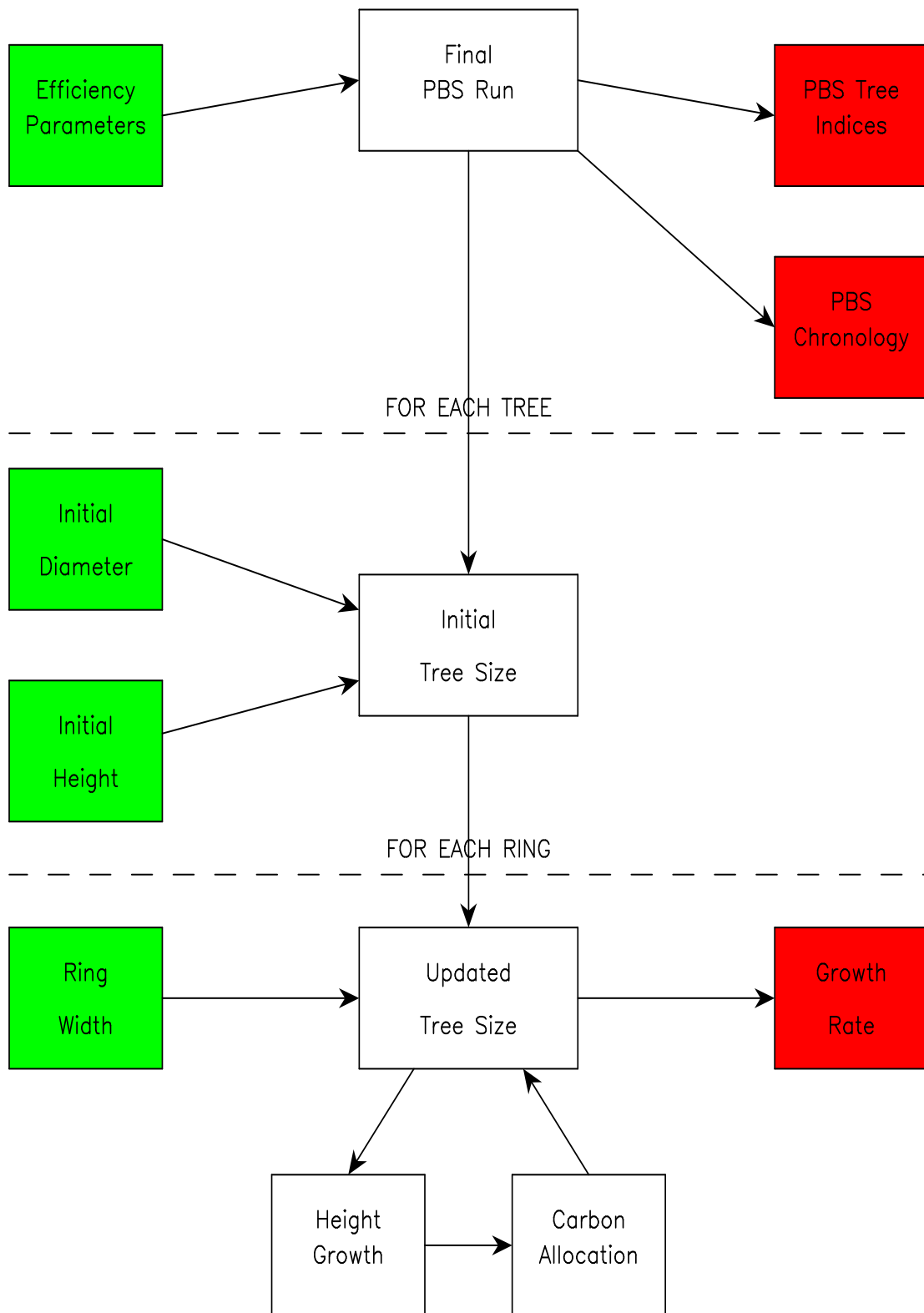


Figure 7.1.1 Schematic diagram of the PBS model chronology processing showing inputs (green), processes (white), and outputs (red).

(Valentine 1988), and the transport-resistance model (Thornley 1991), all of which have provided additional information to the development of the PBS model.

The Mäkelä model represents a tree by the masses of compartments of foliage, fine roots, stem, branches and trunk roots. The Mäkelä model uses a number of structural relationships to conserve a balance between structure and physiological function and is parametrised for *Pinus sylvestris* trees growing in south Finland. The PBS model is similar to the Mäkelä model and many compartments, structural relationships, and empirically estimated parameter values are copied directly from the Mäkelä model. As input, the Mäkelä model has a mass of carbon for each year and the PBS model has a ring increment for each year. The Mäkelä model uses starting foliage mass and stem height to initialise each tree and the PBS model uses initial diameter at breast height for the same purpose. Tree-growth models (Mäkelä 1997; Friend et al. 1997; Smith et al. 2001) use light levels within the canopy to assess the efficiency of foliage at the base of the canopy and to estimate the rate of increase of stem height for each tree. The PBS model is limited to using the efficiency of all foliage of an individual tree to estimate the stem height growth of that tree. Tree-growth models use empirically estimated height – diameter relationships which are selected and tested according to their ability to predict the shape of an “average tree”. The PBS model has the more challenging task (Lindner et al. 1997) of finding a suitable height – diameter relationship which can predict the shape of each individual tree.

The PBS model is developed and tested using the trees from Luosto, Rutajarvi, and Helldalisen developed for this project. The series of ring-width measures originate mainly from living trees and the position of the heartwood – sapwood boundary, relative to the bark, was used to assess the number of rings of sapwood and used with diameter to calculate “measured sapwood area” at breast height for the final year of growth of each tree. The PBS model estimates the sapwood area at crown base throughout the life of each tree and the measured and calculated values of sapwood area for the last year of each tree are compared to assess the ability of the PBS model to predict individual tree growth from series of ring-width measures. A number of diameter - height relationships, different methods of developing stem height growth strategies, and various combinations of parameter values were tried in attempts to obtain a match between measured and calculated sapwood areas. An approximate solution was found using the "mechanical

theory of uniform stress" (Metzger 1893) to relate diameter and height, a method not used by any of the tree-growth models examined in the literature search for this project. This empirical solution, based on mechanical strength and variable rates of sapwood senescence, leads to some novel methods within the PBS model.

The output of the PBS model is a series of values of the carbon production rate per unit foliage for each year of each tree (growth rate measures). Following standard dendroclimatic methods, the mean value of all growth rate values is set to 1.0 to create PBS Indices and these PBS Indices are averaged by calendar year to form a chronology. The series of PBS Indices and the chronologies are compared to their equivalents, produced by other methods of standardisation, and series of temperature measures to assess the potential value of the PBS model approach.

### 7.3. PBS Model - General Properties

#### 7.3.1. State Variables

Name	Description (Units)
Wf	Foliage mass (kg)
Wr	Fine root mass (kg)
Wch	Crown wood mass (kg)
Wc	Crown sapwood mass (kg)
Wsh	Stem wood mass (kg)
Ws	Stem sapwood mass (kg)
Wbh	Branch wood mass (kg)
Wb	Branch sapwood mass (kg)
Wt	Trunk root sapwood mass (kg)
Hc	Crown height (m)
Hs	Stem height (m)
D13	Diameter at breast height (m)
rg	Radial ring increment (m)
Asap	Sapwood area at crown base (m <sup>2</sup> )
Wmech	Mechanical stem wood mass (kg)
Pard	Mechanical diameter-height constant for each year
Resp	Carbon consumed by respiration (kg)
Litter	Carbon deposited as litter (kg)
Frac	Efficiency fraction (dimensionless)
Grow1	Annual carbon mass consumed (kg)
Grow2	Mass of carbon per unit foliage (kg/kg)

Table 7.3.1 State variables used in the PBS model

Figure 7.3.1a is a schematic diagram describing the tree structure as envisaged here. Each tree is considered to consist of compartments of foliage, fine roots, stem, branches, and trunk roots (Mäkelä 1997). The stem is subdivided into crown wood (stem within the crown) and stem wood (stem below the crown base) because these sections of stem have different mechanical shapes and sapwood profiles. The masses of sapwood within crown

Figure 7.3.1a Schematic diagram of a tree

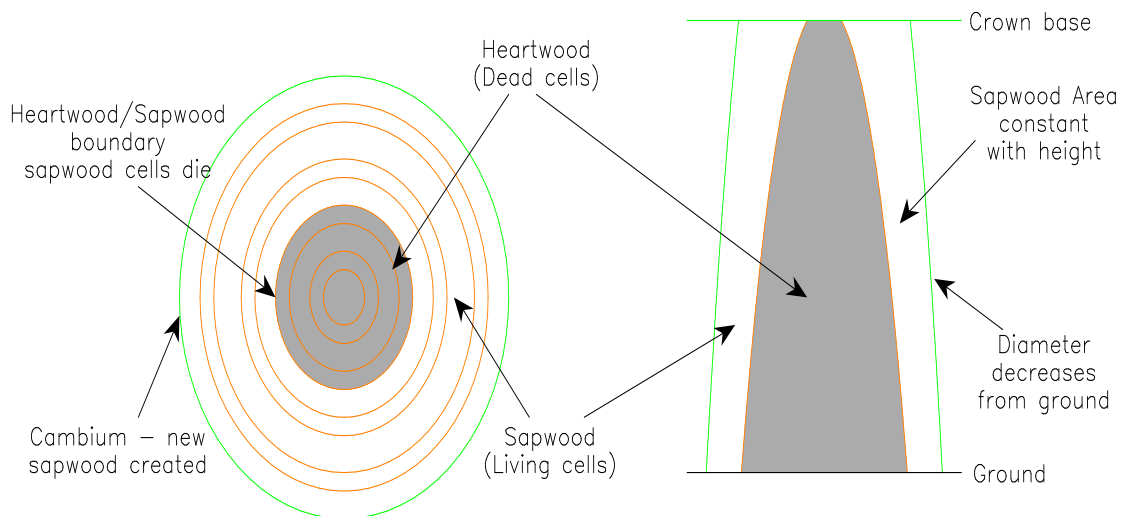
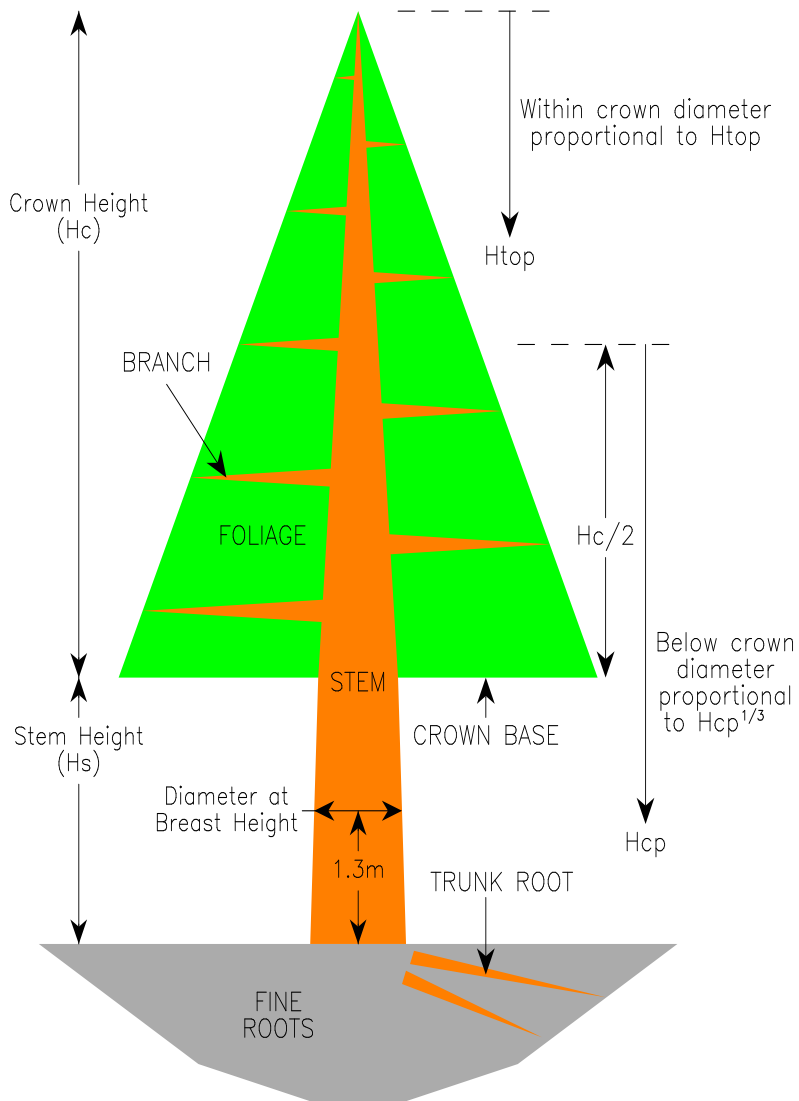


Figure 7.3.1b Stem cross section

Figure 7.3.1c Stem vertical section



wood, stem wood, and branch wood are recorded in addition to wood masses. Trunk root heartwood is not monitored so trunk roots are represented by their sapwood mass and trunk root heartwood becomes soil litter. Wood masses are calculated from density and volume. Volume is obtained using three state variables of length, stem height, crown height and diameter at breast height. Some additional derived variables are used to simplify calculations: these are input ring width measures, sapwood area at crown base, mechanical wood mass, respiration mass, litter mass, total mass consumed by growth, and the output values of carbon generated per unit foliage. Each variable has a value for each growth year of each tree. State variables listed in Table 7.3.1.

### 7.3.2. Parameters

As far as possible, pre-existing parameters are used and their empirically estimated values are taken directly from the Mäkelä model. Values taken from the Mäkelä model represent trees growing in south Finland, but as many will be “species” related they are suitable for the PBS model. Where the need for new parameters was identified, parameters were introduced and “best fit” values were sought in order to achieve a match between calculated and measured sapwood areas and also to produce mean growth by age and mean growth by diameter curves which are horizontal. Some explanation of why these particular parameters were selected and further description of these parameters is provided, along with the specification of the algorithms developed within the PBS model, in the following discussions.

Name	Description	Default value & units	Source
Wden	Wood density	400.0 kg carbon / m <sup>3</sup>	M
Closs	Maximum crown recession rate	0.21 / year	E
Alf0	Sapwood area to foliage mass ratio	2.0 * 10 <sup>-3</sup> m <sup>2</sup> / kg	M
AlfB	Branch/crown sapwood ratio	0.55 kg/kg	M
AlfT	Trunk root / stem sapwood area ratio	0.21 m <sup>2</sup> /m <sup>2</sup>	M
AlfR	Fine root mass to foliage mass ratio	0.2 kg / kg	M
Maxh	Crown height of a large tree	28.0 m	E
Rgrow	New material growth respiration	0.65 kg grown/kg used	M
Rfol	Foliage maintenance respiration.	0.2 kg/kg foliage/year	M
Rroot	Fine root maintenance respiration.	0.2 kg/kg fine root/year	M
Rsap	Sapwood maintenance respiration.	0.02 kg/kg sap/year	M
Sfol	Senescence of foliage	0.25 / Year	M
Sroot	Senescence of fine roots	1.0 / Year	M
ZZ	Foliage to crown height power	2.5 dimensionless	M
Eta	Foliage to crown height ratio	0.05 kg foliage / m <sup>ZZ</sup>	M
Mpwr	Power to raise annual constant Pard	0.5 dimensionless	E
Gfbot	Fraction crown decay	-1.0 Stand. Deviations	E
Gftop	Fraction no stem rise	+1.5 Stand. Deviations	E
Saph	Height at which sapling becomes tree	4.0 m	E

M – from tree growth model, E – Values estimated for PBS model

Table 7.3.2 Parameters used in the PBS model

### 7.3.3. Conservation of Mass

Following the Mäkelä model, the only material that is considered is carbon and the mass of all structure is represented by the carbon content of that structure. Carbon is present in the initial tree or sapling and carbon is stored in both living matter and in enclosed heartwood in stem and branches. Carbon is absorbed from the atmosphere by photosynthesis in the foliage. Carbon is returned to the environment as carbon dioxide by respiration and carbon is deposited as litter by senescence (and eventually by mortality). The law of conservation of mass is applied to the carbon mass at each annual step throughout the lifecycle of each tree.

### 7.3.4. Some Assumptions

A model needs many major components in place before any results are possible. To get this novel PBS model working, some sweeping assumptions and simplifications were made. Assumptions used in tree-growth models and some specific to the PBS model, arrived at after trying numerous alternatives, are listed and details of their source and implications are left to the fine tuning and discussion stages. Photosynthesis is not modelled explicitly. The limitations on growth due to soil and nutrient variation within a site are also not included explicitly. The costs of bark and reproduction are ignored. Wood profiles are presumed to be circular, the tree stem is considered to be vertical, and branches are considered to be horizontal for volume calculations. Wood and sapwood volume are the integrals of wood and sapwood areas over tree height or branch length. All wood has the same constant density. Below the crown base, sapwood area is constant. Conservation of height is assumed in that the height of the crown base can never decrease, overall tree height can never decrease, and crown recession takes place by raising the crown base (Figure 7.3.1). The internal transport requirement of sapwood is ignored as minor (a few kilograms per year) and transport between fine roots and foliage (a few litres per hour) is considered to be the main constraint on sapwood area. The assumption is made that any sapwood in excess of that required to supply transport facilities will be senesced. All generated photosynthate is presumed to be consumed each year, with no year to year storage. A tree can never have more foliage than its mechanical strength can support. A tree can never have more foliage than can be supported by its sapwood transport facilities.

### 7.3.5. Mathematical Procedures

The equations below are generally based on empirical observations and are approximations based on the average behaviour of observed trees. Measurements have been made to accuracies of one part in 1,000 or less and calculations that are approximations are made to accuracies of one part in 1,000,000. The PBS model is based on annual time steps and the annual change of a variable is described using a suffix of lower case "d", e.g. the annual change of crown height ( $H_c$ ) is referred to as ( $dH_c$ ). Where a temporary, mid year, value is needed for a variable the suffix of lower case "z" is used, e.g. if stem height increases, the new crown height created by this increase ( $zH_c$ ) is used until the final new crown height ( $H_c$ ) can be calculated. The term "wood" is used to describe all wood which thus includes both sapwood and heartwood. Mathematical notation from FORTRAN 90 is used in which "\*" is multiplication, "/" is division, "\*\*" is raise to the power, the suffix "(1:n)" is used to represent an array of values, and "SUM(...)" is the arithmetic sum of the enclosed array. Nomenclature was taken from the Mäkelä model where masses are described by (W) with a suffix detailing the tree compartment (c = crown, s = stem, t = trunk roots, b = branches, f = foliage, and r = fine roots). Upper case 'H' is used for heights and an additional lower case 'h' indicate the inclusion of heartwood, e.g. branch sapwood mass is ( $W_b$ ), crown wood mass is ( $W_{ch}$ ), and stem height is ( $H_s$ ).

## 7.4. Growth Processes

### 7.4.1. Photosynthesis

The PBS model ceases before it reaches the photosynthesis stage of tree growth, i.e. the PBS model assesses carbon consumption without needing to know how the carbon was produced, but because photosynthesis controls carbon production and constrains tree structure a brief description is included here. Photosynthesis is a process which uses energy from light, extracts carbon from the atmosphere, and generates the carbon based chemicals (photosynthates) needed to build tree structure and supply energy to the tree (Landsberg 1986c). The light used in photosynthesis is called photosynthetically active radiation (PAR) and is supplied to the earth on a unit surface area basis by the sun. The intensity of PAR reaching the upper atmosphere is modified at several timescales by the Earth's rotation and orbit. The intensity of PAR reaching the top of the canopy is modified by variation in the angle of incidence and cloud cover. The intensity of PAR at a point within the canopy is modified by overlying foliage i.e. it reduces with depth from

the top of the canopy. Photosynthesis takes place in chloroplasts within stomata located in the leaves of the trees. When stomata open, they present a damp surface to the air which absorbs the carbon dioxide needed to manufacture photosynthate and, as a side effect of the practical implementation of photosynthesis, this damp surface loses water to the atmosphere in a process called transpiration. Stomata open and close like switches in sub-second time scales in direct response to the presence or absence in the local environment of the conditions required for photosynthesis. Photosynthesis is a non-linear process, and is dependent on air temperature, air velocity, air humidity, the intensity of PAR, the concentration of carbon dioxide in the air, and the availability in foliage of nutrients and water.

Photosynthesis is usually modelled as a canopy process in which the foliage of many trees is considered as a unit for the calculation of photosynthate production (Landsberg 1986c). A time step is selected, such as month, day, or hour. Values of various climatic variables, such as PAR at the top of the canopy, cloud cover and air temperature, are extracted from measured or simulated data and are averaged over the selected time step. Soil moisture availability is tracked using soil models, daily precipitation, and calculated transpiration rates. Moisture availability in foliage is used by tree-growth models to limit photosynthesis rates. Foliage distribution and mass are calculated for each tree using temperature-dependent phenological models of the start and end of each growing season and foliage is summed to describe the canopy of a patch. The light intensity is calculated at a number of levels in the canopy using models of light extinction and calculated foliage distribution. The masses of photosynthate generated by foliage at each canopy level during the selected time step are calculated. In simple tree-growth models photosynthesis is simulated using sets of procedures whose output is the calculated mass of photosynthate generated by the foliage of each tree in a small patch of forest over a year.

Photosynthesis is not modelled explicitly in the PBS model. Interpretation of the annual production of carbon by foliage, the output of the PBS model, in terms of temperature or precipitation may need to use knowledge of photosynthesis processes. The calculated light intensity level in the canopy is used by tree-growth models to establish the stem height growth rate of trees (Mäkelä 1997) and the PBS model must find an alternative method to establish a height growth strategy for each tree.

#### 7.4.2. Allocation

Having produced photosynthate, the tree must allocate this material to the growth and the maintenance of structural parts in a way that retains a functional balance for the current environment (Cannell & Dewar 1994). In order to photosynthesise, foliage must be supported in a position to intercept PAR leading to a requirement for a mechanical support structure of branches, stem and trunk roots. Photosynthesis must have water and nutrients which leads to a requirement for fine roots to absorb moisture and nutrients. Fine roots need support structure leading to a requirement for trunk roots. The water, nutrients and photosynthate need to be transported around the tree leading to a requirement for sapwood in branches, stem and trunk roots. To survive in harsh conditions and competitive situations a tree needs to be efficient leading to the ability to senesce unwanted structure and to adapt to current local conditions. A successful plant needs descendents leading to the requirement to reproduce. Trees appear to achieve functional balance at a cell level whereas in tree-growth models this functional balance is calculated at a tree level and is usually described in terms of empirical rules and parameters which relate the masses of various tree structures.

Allocation is generally modelled as a complex balancing process. In tree-growth models the starting positions are the sizes of each compartment, the rules to be followed for senescence, the requirement for reproduction, maintenance respiration rates, growth respiration rates, and the mass of photosynthate available. The balancing follows a number of empirical rules that must be satisfied. The main ones are the law of conservation of mass; the relationship between foliage mass and sapwood area; the relationship between fine root mass and foliage area; the relationship between diameter and height; the relationship between crown size and branch mass; the relationship between tree mass and trunk root mass; foliage distribution rules; bark requirement; and reproductive strategy. The output is an allocation of the available photosynthate which generates a new set of compartment masses that describe a “balanced” tree.

#### 7.4.3. Respiration

Respiration returns carbon to the environment. A tree requires energy to synthesise new structure (growth respiration) and energy to maintain the functionality of existing living structure (maintenance respiration) which includes foliage, fine roots and sapwood but excludes the dead heartwood. Except for the direct use of energy in photosynthesis, this

energy is obtained via the process of respiration which uses the chemical energy stored in photosynthates and releases carbon to the external environment. Measurements of the rate of release of carbon dioxide in various structures of trees have led to the establishment of empirical relationships describing respiration in terms of growth respiration and maintenance respiration (McCree 1970). Measured maintenance respiration rates are temperature dependent at sub-day time scales (Dewar et al. 1999) but at annual timescales the empirically-derived values of maintenance respiration depend on functions representing work done such as transporting water and matter, frost hardening of foliage, and damage repair, which are not usually considered to have a direct relationship with annual temperature (Thornley & Cannell 2000). The mass of photosynthate consumed in the manufacture of living structure each year, growth respiration, is treated as proportional to the mass of new structure. In simple tree-growth models, using annual time steps, growth and maintenance respiration are considered as overheads which consume photosynthate each year with growth respiration proportional to the mass of new structure generated in a year and maintenance respiration proportional to the mass of existing living structure in that year (Mäkelä & Hari 1986). The PBS model follows these commonly used method of calculating the consumption of photosynthate by respiration at annual time steps, which ignores the dependency of respiration rate on temperature.

The PBS model calculates maintenance respiration rates annually using the masses of foliage ( $W_f$ ), fine roots ( $W_r$ ), and sapwood ( $W_c + W_s + W_b + W_t$ ) at the start of each year and respiration parameters  $R_{fol}$ ,  $R_{root}$ , and  $R_{sap}$  respectively. Growth respiration is calculated from the mass of new material ( $dW_f + dW_r + dW_c + dW_s + dW_b + dW_t$ ) generated during the year and parameter  $R_{grow}$ . Empirically estimated parameter values for *Pinus sylvestris* were extracted from the Mäkelä model.

$$\text{Resp} = W_f * R_{fol} + W_r * R_{root} + (W_b + W_t + W_c + W_s) * R_{sap} + (dW_f + dW_r + dW_b + dW_t + dW_c + dW_s) * (1.0 - R_{grow}) / R_{grow}$$

#### 7.4.4. Senescence

Senescence returns unwanted parts of the tree structure to the environment as soil litter and “unwanted” is interpreted here as those cells not performing efficiently. Foliage consists of living cells which incur maintenance costs. Leaves which do not intercept sufficient PAR will be senesced (Mäkelä 1997). In boreal conifers the efficiency of

foliage reduces with age (Nikinmaa 1990) and older leaves with low productivity rates are senesced. New leaves are grown in areas of the crown where there is sufficient light leading to continuing regeneration of foliage and the movement of foliage to places in the canopy with sufficient light. Branches which do not have foliage to support will be lost as all cells in those branches die. In a canopy the intensity of light decreases from the top downwards leading to a situation where foliage and branches below some minimum level of PAR (height in the canopy) will be senesced and the base of the crowns of all trees rise. The position of the base of the canopy, i.e. the base of the crowns of all trees of a patch, is set in simple tree-growth models by the empirically-assessed minimum level of light needed for photosynthesis. Light levels are calculated from the canopy top for successive layers of foliage to the canopy base. Senesced foliage and branches fall onto the soil as litter. In *Pinus sylvestris* fine roots have a lifespan of a few weeks to months (Vanninen & Mäkelä 1999) and all are senesced each year leaving litter in the soil. Trunk roots have life spans approaching the age of the tree, but may be senesced when not needed for mechanical strength or transport purposes (Section 7.5.6).

In tree-growth models the senescence of foliage and fine roots is modelled as an annual loss of material, based on empirically estimated life-spans, e.g. in boreal forest *Pinus sylvestris* 25% of foliage and 100% of fine roots are lost each year (Mäkelä & Hari 1986). In many tree-growth models, foliage and branch losses occurring when stem height increases are calculated explicitly from the levels of PAR in the canopy. Calculations of the rise of crown base of trees by the PBS model are described in Section 7.5.9. If the crown base rises ( $dH_s > 0$ ) the PBS model calculates new (temporary) masses of branch wood ( $zW_{bh}$ ) and crown foliage ( $zW_f$ ) and the losses of foliage and branches, now below the crown base, are deposited as litter. The PBS model calculates senescence rates annually for remaining foliage ( $zW_f$ ) and all fine roots using the parameters  $S_{fol}$  and  $S_{root}$  and deposits the senesced mass as litter. Empirically estimated parameter values for *Pinus sylvestris* were extracted from the Mäkelä model.

$$\text{Litter} = \text{Litter} + (W_f - zW_f) + (W_{bh} - zW_{bh}) + zW_f * S_{fol} + W_r * S_{root}$$

The PBS model transfers wood from the crown to the stem when the stem height increases. Temporary values of crown wood ( $zW_{ch}$ ) and crown sapwood ( $zW_c$ ) masses are calculated and the excess wood is transferred from crown ( $W_c$  and  $W_{ch}$ ) to stem ( $W_s$  and  $W_{sh}$ ).

$$W_{sh} = W_{sh} + (W_{ch} - zW_{ch})$$

$$W_s = W_s + (W_c - zW_c)$$

These calculations ignore the slight difference in the profiles of stem in the crown and stem below the crown shown in Figure 7.3.1 and described in Section 7.5.4. Carbon mass balances are used, i.e. a volume of wood from within the crown becomes a volume of wood below the crown and stem shape is assumed to have a profile, after the exchange, calculated using the new position of the crown base.

Sapwood is living and incurs maintenance costs. Sapwood provides a transport mechanism, functions as a temporary storage facility, and provides mechanical support. Heartwood is dead and provides some mechanical support without the consumption of maintenance energy. Heartwood remains as part of the tree stem for the life of a tree and the proportion of heartwood is difficult to predict from stand variables (Bjorklund 1999). Measurements show that storage in sapwood (Magel et al. 1994) and the transport of water in sapwood (Ewers & Oren 2000) preferentially use the sapwood nearest the cambium and, in the presence of excess sapwood, the sapwood cells near the sapwood/heartwood boundary will be doing least work. The sapwood area needed to meet transport requirements at each height creates a profile which differs from the profile of wood area needed to supply mechanical strength at each height (Figure 7.3.1c). It was found in the PBS model that an increase in stem area (a new ring) is able to supply transport services to more foliage than the increase in mechanical strength is able to support. The maintenance cost of supporting living sapwood is an overhead cost and the assumption is made here that sapwood cells that do not transport or store material will die and become heartwood cells. The sapwood area below the crown base will be constant as there is no foliage between crown base and ground level and the transport requirement does not change in this section of the stem. The wood area needed for mechanical support will increase from crown base towards ground level (Figure 7.3.1c) because the distance from the centre of pressure of wind forces on the crown increases with distance from the crown. Detailed equations and further explanation are provided in Section 7.5.3 (sapwood volume and mass) and Section 7.5.4 (wood volume and mechanical strength).

Many tree-growth models calculate heartwood shape and mass by accumulating senesced sapwood over the life of a tree; a fixed proportion of sapwood is lost each year and is added to a growing cone of heartwood (Friend et al. 1997; Smith et al. 2001). This method was tried but failed to predict the final proportions of sapwood and heartwood of



the individual trees from Luosto and Helldalisen. In the PBS model sapwood senescence is considered as variable and annual values are calculated using the mechanical ability of the tree stem to support foliage. The presumption is made in the PBS model that a tree will grow sufficient wood to maintain mechanical strength but will only retain enough sapwood to meet the transport requirements of the foliage. The balance is produced by the senescence (cells die) of excess sapwood. The PBS model assumes that variation with height of the profile of tree ring increments will match the taper of the mechanical stem profile (Section 7.4.7) unless the tree has excess mechanical strength, in which case the profile of tree ring increments will follow the required sapwood profile, i.e. will be a cylinder below the crown. The PBS model constrains diameter to fit the mechanical strength profile when the tree has “minimum” strength. If the tree has more wood than is required by the mechanical strength then diameter at breast height will be correct (measured values) and the sapwood profile will be correct, but diameters at other heights within the stem are greater than the minimum requirement but are not explicitly calculated. (An early version of the PBS model used 10cm steps through stem height to track diameter but these calculations were removed because the extra processing involved did not produce any benefits.)

The PBS model does not use specific senescence rates for sapwood to heartwood conversion. Each year the newly grown wood in each compartment (crown, stem, branches and trunk roots) is added to the existing sapwood (Section 7.5.3) and if there is an excess, i.e. that sapwood not needed to supply transport facilities for foliage, this excess becomes heartwood. The mass of foliage is calculated to fit the limit set by the minimum of the mass of foliage that can be mechanically supported or the mass of foliage for which transport facilities exist. The heartwood masses in each compartment do not decrease with the exceptions that trunk root heartwood goes straight to litter, branch heartwood may drop off to become litter as a consequence of stem rise, and crown heartwood may become stem heartwood as stem height increases. The increase in heartwood (death of sapwood cells) in any year depends on changes in foliage mass which will depend on ring-width, and also will vary with crown height and stem height which are products of the tree's growth history. In the event of the crown becoming smaller (base of crown rises faster than tip of crown grows) a tree may have excess mechanical strength (a smaller crown generates less wind force) and for a limited period will be able to grow new wood purely as sapwood with zero senescence of sapwood,

allowing a more rapid recovery from extreme events. Several of the oldest trees sampled for this project were beyond the stage of exponentially increasing growth (Section 4.1.4), had excess mechanical strength, and had more than 100 sapwood rings. Crown recession leads to excess mechanical strength and immediate sapwood loss which can remove the need for sapwood senescence in subsequent years. Where tree stems are supported then stem growth above the support is observed to be greater than stem growth below the support (Matthegek 1991a, Fig. 37) lending credence to this mechanical model of sapwood senescence introduced here.

#### 7.4.5. Reproduction

In pine trees the growth and loss of reproductive organs is annual. The buds and shoots required to form reproductive organs are seen to develop in the year prior to seeding and once started the growth of reproductive organs appears to take on a high priority for resources (Cannell & Dewar 1994). In the boreal forest, pine trees generally do not produce seeds in the first few decades of life and may cease seed production in old age. Seed production in pine trees is irregular with high seed mass every few years and in harsh climates high seed mass years are less frequent (Tappeiner 1969). Seed production rates in trees at the same site are only partially synchronised. Climatic variables may control the annual variation of seed production and thus indirectly influence the resources available for structural growth in the following year. Reproduction can create large year to year variations in tree growth measures which may be unrelated to the values of climatic variables in that growth year (Cannell 1985). Reproductive organs become soil litter after use and in tree-growth models reproduction is an overhead which consumes photosynthate. Seed generation in boreal forest conifers has been estimated in model LPJ (Sitch et al. 2003) to consume 10% of annual production each year. If methods were available to estimate the irregular consumption of resources by reproduction then these could be incorporated into the PBS model with consequent improvements in the retrodiction of the values of climatic variables. The simplest alternative, of the addition of 10% to all growth values, is of no benefit to the PBS model as all growth values are rescaled. As a result, this first stage development of the PBS model ignores reproduction costs entirely.

#### 7.4.6. Mortality

Trees do not appear to die of old age (Franklin et al. 1987) and mortality is generally the result of various other factors. Mortality from self-thinning is dependent on stand density

and canopy thickness (Peet & Christensen 1987). In some tree-growth models unhealthy trees with low productivity (photosynthate per unit leaf) are given an increased risk of mortality or killed (Friend et al. 1997; Smith et al. 2001). Abiotic effects such as forest fires, storms and insect attacks can be modelled explicitly or as random events and mortality, based on maximum age or maximum size, is often included in tree-growth models (Hawkes 2000). The PBS model should be able to “predict” that trees which died because of low productivity had little or no remaining foliage or sapwood at the time of death (discussed in Section 7.7). Foliage that is not productive is lost and the associated sapwood, no longer required, is converted to heartwood. Trees with low-productivity will have little sapwood and on death no sapwood. In Figure 7.7.1b the 23<sup>rd</sup> and 43<sup>rd</sup> trees from Helldalisen had no apparent sapwood which suggests death by steadily reducing productivity. Trees that die whilst having sapwood e.g. trees that were harvested retain their sapwood / heartwood boundary at the time of death.

#### 7.4.7. Mechanical Strength

The mechanical strength of wood can be measured as the ability of a cube of wood to withstand a force (compression or tension) applied across opposite faces. The total forces on the stem of a tree increase from the top down to the ground and then decrease to the tips of the roots. By increasing diameter from the top of the stem down to ground level the maximum force per unit area at all heights within the stem can be maintained roughly constant, wider radius (lever arm) and longer circumference over which to spread the load both contributing. A tree requires sufficient mechanical strength in branches, stem and trunk roots to support itself. When trees bend in the wind, they receive maximum bending stress at the outer surface of their stems. "*One of the most enduring theories in tree biology is that the cambium produces new wood in such a way as to equalise the distribution of stress along the outer surface of the stem*" (Morgan & Cannell 1994a), referred to as the "mechanical theory of uniform stress" (Metzger 1893). The bending stress will increase with distance (lever arm length) from the centre of pressure of the wind forces on the crown (force) and to avoid points of weakness the stem needs to taper, being wider near the base (Spatz & Bruechert 2000). Measurements of the stem taper of saplings and mature *Pinus contorta* suggest that the uniform stress model functions similarly in both classes (Dean & Long 1986). Detailed measurements and calculations using wind velocity profiles, foliage distribution within the crown, and stem diameter measurements (Morgan & Cannell 1994a) support the uniform stress theory, with the

additional observations that normal average wind speeds (2.5 m/s to 10.0 m/s at the top of the canopy) give similar calculated stress profiles and that trees tend to develop shapes in response to average conditions. Stem loading experiments in both summer and winter showed that *Pinus sylvestris* retain information about mechanical forces over winter and respond in the following growth season (Lundqvist & Valinger 1996). Wind speeds vary over time and in extreme conditions the distribution of stress is not uniform, above average wind speeds lead to higher stresses near the base of the stem (Morgan & Cannell 1994a). Where the strongest winds are consistently from one direction, such as at a coastline, then trees develop elliptical cross sections in order to maintain uniform stress in average conditions (Mattheck 1991a, Fig. 36).

Crown size and height above the ground will change over the life of a tree. The average wind speed will change due to the changes in neighbouring trees and possible climatic variation. Stem mass increases over time. Trees will adjust their stem profiles to track the changing mechanical strength requirements, although there may be a lag of years to decades and diameter can only increase. The results of measurements lead to the empirical conclusion that trees limit their mechanical strength (carbon cost) to a minimum safety level (benefit) related to absolute stress levels (Cannell & Dewar 1994). Mechanical strength depends on elasticity and wood density which vary considerably from species to species and from tree to tree. Saplings are more elastic and their wood is less dense than for mature trees, and density varies both with climatic factors and in the varying proportion of intra annual ring latewood to earlywood. The absolute stress on open grown trees is large, leading to short fat stems. In tightly packed canopies wind forces on individual trees are low and tree crowns are less densely packed with foliage leading to tall thin stems. One could speculate that in highly competitive situations the mechanical safety levels might be temporarily relaxed leading to the observation that excessive thinning can lead to increased stem breakage (Valinger & Pettersson 1996). Trees that survive the self thinning process to become widely spaced dominant trees need to develop sufficient mechanical strength to withstand wind forces.

The "elastic instability model" considers the stem of a tree to be a uniform pole that resists buckling due to its own weight and arises from the observation that the height of very large trees tends to be limited to one quarter of the height that would cause a solid cylinder of the same diameter to buckle (McMahon 1973). This conclusion is based on

observations from 576 trees of various species found in the register of large trees in the United States is the basis for the equation:

$$\text{Diameter} \propto \text{Height}^{3/2}$$

Measurements of *P. contorta* showed that mature trees conform to the "elastic instability model" and that saplings do not fit this model (Dean & Long 1986). In order to be self supporting with a minimum amount of wood a tree stem must increase in diameter towards the base. If a tree requires the addition of a vertical cylinder of sapwood (tree ring) to the stem to increase water transport capacity in support of increased foliage mass then, in order to maintain the presumed "minimum" safety level of mechanical strength, the tree must add a tapering cylinder of wood to the stem. The new wood added to the outside of the stem will be sapwood and the excess sapwood at each height will be converted to heartwood at the sapwood/heartwood boundary (Figures 7.3.1 b and c) to produce the net gain of the required cylinder of sapwood. Generally tree-growth models do not use mechanical constraints, to relate diameter and height. The PBS model uses these mechanical rules in the absence of other methods of calculating stem profiles for individual trees.

#### 7.4.8. Stem Diameter and Compartment Lengths

All ring measures are presumed to have been made at breast height (traditionally considered in dendroclimatic studies to be 1.3 m above the ground). In order to establish tree diameter an estimate is needed of the missing diameter from the first measured ring-width to the pith at the centre of the tree, called the initial diameter (iD13) for each tree. These estimates were made by examination of the tree cores and comparison of the early rings with a series of concentric circles. The diameter at the start of each year (D13) is the initial diameter plus twice the sum of all previous rings measures. A tree is considered to be made of a crown containing foliage, supported by a bare stem and a below ground root system (Figure 7.3.1). In the PBS model, the crown height (Hc) and stem height to the crown base (Hs) make up the above ground tree height (Hs + Hc). Because ring width measurements are presumed to be taken at breast height, when stem height is less than 1.3m ring-width measurements were made within the crown and when stem height is greater than 1.3m ring-width measurements were made in the stem and, because the stem profile changes at crown base (Section 7.5.4), two sets of calculations are needed. Over the life of a tree it is assumed that both above ground tree height and stem height can never decrease (Mäkelä & Sievanen 1992). Crown height can only decrease by raising

the crown base and thus increasing stem height. Both stem height and crown height can change in a given year and these are treated as smoothly varying events for arithmetic calculations. Calculations assume that the growth represented by an annual change in stem height (dHs) and an annual change in crown height (dHc) took place by adding equal proportions of both dHs and dHc to the existing structure throughout the year, thus simulating a smooth progression from one year to the next.

Height growth is problematical because "*The ratio of height to almost any other quantity describing the state of the tree is highly variable*" (Mäkelä 1997). Open grown trees tend to produce short but fat stems, a result of the requirement to withstand wind forces and the availability of light near the ground. In dense stands tree stems are tall and thin in response to the need to compete for light, reduced light levels near the ground, and the reduced requirement for mechanical strength created by mutual shelter from wind forces (Bruchert et al. 2000). The rise of crown base is related to minimum light levels in the canopy (Mäkelä 1997). Maximum height at a site is generally dependent on soil quality at that site and the rate at which trees approach the maximum height found at a site is dependent on stand density for a given climate and soil fertility (Mäkelä & Sievanen 1992). The process of self-thinning in stands leads to increasing wind forces on individual trees which must increase diameter growth, relative to height growth, in order to remain mechanically sound. In tree-growth models, light levels are explicitly modelled and the rise of crown base can be estimated from empirically derived parameters. In tree-growth models self-thinning is modelled explicitly and the mortality of the losers leads to changing canopy conditions for the survivors.

## **7.5. PBS Model Calculations**

### **7.5.1. Overview**

Ideally the PBS model should consider each tree in isolation and for each tree use each ring to calculate the rate of production of carbon in that year (Grow2) in sequence without "looking" ahead in this tree or "across" at other trees. Exceptions are made to these rules in that iterative methods are used to estimate site-level efficiency limits to implement a height growth strategy (Section 7.5.9) and the first 12 rings of each tree are used in the estimation of initial stem height (Section 7.5.10). Having assessed efficiency limits and initial stem heights, each tree and each ring within a tree are processed independently. The carbon mass of each compartment of a tree is estimated from the

initial diameter (iD13) and initial tree height (iHs). Each year is then processed in sequence. The compartment masses of the current year, the current diameter at breast height (D13), and the current ring-width are all used in the current year's calculations to estimate Grow2 and to update compartment masses ready for the following year. The values of Grow2 are estimates of carbon production per unit foliage for each year of growth of each tree and the Grow2 values for each ring are converted to PBS Indices by being divided by the mean value of Grow2 for the site (Section 4.1). Series of PBS Indices are developed without reference to calendar year, i.e. the trees do not need be crossdated in order to generate series of PBS Indices. If sufficient trees are available to estimate efficiency parameters for a site, then a single series of PBS Indices can be produced. The final task of averaging PBS Indices to create a chronology requires some form of dating, calendar or relative.

The assumptions and rules of the PBS model enable the sizes of all state variables to be derived from diameter (which is known) and a length variable (or direct derivative of a length variable). Stem height (Hs) is used with diameter to derive crown height (Hc) using mechanical and/or sapwood area constraints. The masses of foliage, fine roots, crown sapwood, crown heartwood, branch sapwood and branch heartwood are all derived from crown height and a series of constants. The masses of stem sapwood, stem heartwood and trunk root sapwood are all derived from crown height, stem height and a series of defined constants. Growth respiration, maintenance respiration, and senescence rates are derived from compartment sizes and a series of constants. Stem height is obtained from efficiency measures and efficiency measures are generated using stem height estimates a situation resolved using iterative procedures. The state of the tree through time is derived from tree-rings and detailed descriptions of how and, in some cases why, follow.

#### 7.5.2. Foliage and Fine Root Mass

The PBS model needs to relate total foliage mass ( $W_f$ ) and crown height ( $H_c$ ). For a conical crown, if foliage is distributed evenly through the crown volume then foliage mass will be proportional to crown height cubed and if foliage is distributed over the crown surface area then foliage mass will be proportional to crown height squared. The distribution of foliage is constrained by light levels. The crowns of large pine trees are generally hollow, due to self shading, with foliage concentrated on the outer surface of

the crown. Vigorously growing trees have more densely packed foliage. In dense stands where competition is high, or on poor soils, or in drought situations, or in very old trees foliage distribution may be less dense (Mäkelä & Albrekson 1992). The PBS model assumes that the foliage distribution of all trees of the same species from the same site can be described by the site level constants for foliage density (Eta) and the allometric ratio to crown height (ZZ) (Mäkelä 1997).

$$W_f = \text{Eta} * H_c^{ZZ} \quad (1)$$

Fine root mass (Wr) is related to foliage mass by the functional requirements to supply water and nutrients to support photosynthesis and growth. The ratio of fine root mass to foliage mass varies considerably depending on availability of nutrients (soil fertility) and availability of water (drought) (Vanninen & Mäkelä 1999). Simple tree-growth models use a linear relationship between foliage and fine root masses, whereas more complex tree-growth models use non-linear relationships derived from explicit soil moisture and nutrient modelling. The transport-resistance model (Thornley 1991) uses concentrations of photosynthate in foliage, water pressure gradients, and nutrient concentrations in roots to calculate the proportions of growth material allocated to foliage, roots and sapwood in order to achieve a functional balance. In *Pinus sylvestris* fine roots are grown and senesced in sub-annual timescales and the total mass of fine roots grown in a year (Wr) is used in this model. The PBS model assumes that the ratio of the mass of fine roots to the mass of foliage in each tree is a site constant (AlfR) (Mäkelä 1997).

$$W_r = \text{AlfR} * W_f \quad (2)$$

### 7.5.3. Sapwood Volume and Mass

In order to estimate the amount of sapwood there is a need to relate sapwood area (Asap) to foliage mass (Wf) and the constant ratio implied by the pipe-model theory (Shinozaki et al. 1964) is used. The requirement for sapwood to transport water to support photosynthesis has led to the approximation that sapwood area at any height (h) is proportional to the mass of foliage (Wf (h)) above that height. There is empirical evidence to support this although the measured relationship is only approximate. Variation is found from tree to tree. The relationship is better at crown base than at the base of the stem, the relationship may be to leaf area rather than leaf mass (Mäkelä & Albrekson 1992), and there may be variation with tree height due to hydraulic considerations (Magnani et al. 2000). The requirement (for mechanical purposes) for more wood at the base of the stem than at the base of the crown would allow trees to



adjust the distribution of sapwood within the stem in order to optimise the structural costs. The area of the hollow, tapering cylinder of sapwood in the stem below crown base might be made smaller at crown base and larger near the ground in order to retain the transport capacity of a parallel cylinder but with reduced mechanical overhead costs. Modelling this is not practical without detailed measurements with which to calibrate the relationship, so the assumption is made in the PBS model that sapwood area is constant between crown base and the ground.

The PBS model assumes that at site level the ratio of sapwood area to foliage mass above measurement height ( $h$ ) is constant ( $Alf_0$ ) (Mäkelä 1997).

$$Asap(h) = Alf_0 * Wf(h) \quad (3)$$

Combining (1) and (3) gives sapwood area within the crown at height ( $h$ ) from the top of the crown as:

$$Asap(h) = Alf_0 * \eta * h^{ZZ} \quad (4)$$

Sapwood area at crown base ( $Asap(cb)$ ) and below will be constant because all foliage is above the crown base, so:

$$Asap(cb) = Alf_0 * \eta * Hc^{ZZ} \quad (5)$$

Within the crown, sapwood area increases from the top ( $h = \text{zero}$ ) to a maximum at the crown base ( $h = Hc$ ). Sapwood volume in the crown ( $Vcsap$ ) is the integral over crown height of sapwood area:

$$Vcsap = Alf_0 * \eta * \left( \int_0^{Hc} [ h^{ZZ} ] dh \right)$$

$$Vcsap = Alf_0 * \eta * Hc^{(ZZ+1.0)} / (ZZ+1.0)$$

Sapwood volume below the crown ( $Vssap$ ) is the product of area and length:

$$Vssap = Alf_0 * \eta * Hc^{ZZ} * Hs$$

The densities of earlywood and latewood vary within tree rings. Mean wood density varies between species. Mean wood density increases with wind exposure (Dean & Long 1986). Wood density increases through juvenile, adolescent and adult tree growth stages (Bruchert et al. 2000), and RCS curves of maximum late wood density (Briffa et al. 1992b) show steadily decreasing values of density over centuries. The PBS model, which uses annual time steps, ignores these complexities and, following simple tree-growth models, assumes that wood density ( $Wden$ ) is a site-level constant which can be used to derive the mass of wood from volume (Mäkelä 1997). Heartwood and sapwood are assumed to have the same density.

$$Wc = Wden * Alf_0 * \eta * Hc^{(ZZ+1.0)} / (ZZ+1.0) \quad (6)$$

$$W_s = W_{den} * A_{lf0} * \eta * H_c^{ZZ} * H_s \quad (7)$$

#### 7.5.4. Wood Profile from Mechanical Strength

A good approximation of the diameter-height relationship based on the mechanical theory of uniform stress can be obtained from Matthegek (1991c, Fig. 18), within a roughly conical shaped crown where height is measured from the top (Htop)

$$\text{Diameter} \propto H_{top} \quad (8)$$

Below crown base (in the stem) where height is measured from the centre of pressure of the wind force on the crown (Hcp)

$$\text{Diameter} \propto H_{cp}^{1/3} \quad (9)$$

(Htop and Hcp are shown in Figure 7.3.1a.) Equations (8) and (9) apply to the profile of a tree stem at a specific time. These equations result from the empirical observation that tree stems adopt a profile which equalises the time-averaged stress throughout the outer surface of the stem. The constant of proportionality will vary from year to year because it depends on complex mechanical factors such as tree height, tree mass distribution, crown profile, variation of wind velocity within the crown, time averaged maximum wind velocities, wood density, and wood elasticity. Wind forces on the stem are ignored by the PBS model. The difficulty was in finding a consistent method of assessing the value of the constant of proportionality for each year over the life of a tree which could be applied equally to all trees. For a conical crown in uniform wind, then the position from which Hcp is measured will be one third of crown height above crown base, the integral of force per unit area over the crown height. Uniform wind conditions may be approached by the crowns of open grown trees but wind velocity generally increases with distance from the ground. Empirical measurements of wind velocity and detailed calculations of stress indicate that in a canopy, where wind speeds reduce with depth from the top of the canopy, then Hcp will be roughly half way up the crown (Morgan & Cannell 1994b). In the PBS model Hcp is assumed to be half way up the crown. A single constant of proportionality for a specific year (Pard) results after elimination because diameter at the base of the crown (Dcb) is the same in equations (8) and (9) and eliminating Dcb gives (12).

$$D_{cb} = P_{ard} * H_c \quad (10)$$

$$D_{cb} = P_{ar2} * (H_c / 2.0)^{1/3} \quad (11)$$

$$P_{ar2} = P_{ard} * (H_c^{2/3}) * (2.0^{1/3}) \quad (12)$$

For a tree where diameter at breast height (Dbh) is within the crown then:

$$Dbh = Pard * (Hc + Hs - 1.3) \quad (13)$$

For a tree where Dbh is below the crown base then:

$$Dbh = Pard * (Hc^{2/3}) * (2.0^{1/3}) * (Hc/2.0 + Hs - 1.3)^{1/3}$$

$$Dbh = Pard * (Hc^{2/3}) * (Hc + 2*Hs - 2.6)^{1/3} \quad (14)$$

The area of wood (Area) at any height (h) is calculated from the diameter (Diam) in a circular stem:

$$Area = \pi * Diam^2 / 4.0 \quad (15)$$

Area of wood at crown base (Acb) is

$$Acb = (Pard^2) * (\pi / 4.0) * Hc^2 \quad (16)$$

The volume of stem wood contained within the crown (Vwc) is the integral from zero to Hc of the area.

$$Vwc = (Pard^2) * (\pi / 4.0) * \int_0^{Hc} [ h^2 ] dh$$

$$Vwc = (Pard^2) * (\pi / 4.0) * Hc^3 / 3$$

The volume of wood in the stem below the crown (Vws) is the integral from zero to Hs of the area.

$$Vws = (Pard^2) * (Hc^3) * (\pi / 4.0) * \int_0^{Hs} [ (1 + 2*h/Hc)^{2/3} ] dh$$

$$Vws = (Pard^2) * (Hc^3) * (\pi / 4.0) * [(1.0 + 2*Hs/Hc)^{5/3} - 1.0] * 3/10$$

The masses of wood are derived from volumes using wood density (Wden) and using Par3 to simplify the equations then:

$$Par3 = Wden * (Pard^2) * (\pi / 4.0)$$

$$Wch = Par3 * Hc^3 / 3 \quad (17)$$

$$Wsh = Par3 * Hc^3 * [(1.0 + 2*Hs/Hc)^{5/3} - 1.0] * 3/10 \quad (18)$$

#### 7.5.5. Branch Wood

In the PBS model the crown is considered as conical and branches are considered as horizontal (Figure 7.3.1) so that branch length is proportional to crown height above that branch (Mäkelä 1997). An empirically estimated value for *Pinus sylvestris* has branch length as one quarter of crown height (Mäkelä 1997). The sum for all branches of branch sapwood area has been found to be approximately proportional to stem sapwood area at crown base (Mäkelä 1997). In the PBS model all branches are lumped together and considered as one branch of length equal to one quarter of crown height. Symmetry results in the foliage distribution over the length of this branch being the same as the foliage distribution over the height of the crown. Using the constant of proportionality

(AlfB), and presuming a constant ratio of branch length to crown height, and integrating finds branch sapwood (Wb) proportional to crown sapwood (Wc).

$$Wb = AlfB * Wc \quad (19)$$

Mechanical strength calculations for a horizontal branch should be different from those for a vertical stem, but because branches also point upwards (in conifers) the assumption is made in this model that the same mechanical constraints apply to stem and branches within the crown and the constant of proportionality AlfB can be used to relate branch wood mass (Wbh) to the mass of stem wood within the crown (Wch).

$$Wbh = AlfB * Wch \quad (20)$$

#### 7.5.6. Trunk Root Wood

Trunk root heartwood is not tracked in the PBS model because it requires no maintenance respiration, is not used in mechanical strength calculations, and soil litter is not tracked. Trunk root sapwood (Wt) is needed for growth and respiration calculations and is assumed to be proportional to both sapwood area at crown base and to tree height (Mäkelä 1997). AlfT is the constant of proportionality. Senesced trunk root sapwood is added directly to soil litter for carbon balance purposes. Trunk root sapwood is thought of as “connected” to stem sapwood. The senescence of trunk root sapwood area is calculated as proportional to the senescence of stem sapwood area (and existing tree height) and the growth of new trunk root sapwood area is calculated as proportional to the growth of new sapwood area (and the new tree height).

$$Wt = Wden * AlfT * Asap * (Hs + Hc) \quad (21)$$

$$dWt = Wden * AlfT * dAsap * (Hs + Hc) \quad (22)$$

#### 7.5.7. Pard - Increases as Trees Grow

The mechanical strength equations (8 and 9) predict the profile of the stem of a tree with known stem height (Hs) and known crown height (Hc) at one point in time such that the tree conforms to the mechanical theory of uniform stress. For a specific tree in a specific year then Pard, in equations 13 and 14, is a constant that can be used to calculate diameter at any height both within and below the crown. A method of estimating suitable values of Pard for all years of all trees was sought based on the following logic. The parameter values which produce “acceptable” empirical results do not match the theory presented which suggests there may be a “better” solution. Suitable values of Pard can be selected to describe both short fat stems and tall thin stems. Observed limits on the sizes of very

large trees and on the structure of saplings are used to develop a method to estimate values of  $Pard$ .

For very large trees with tall and very fat stems the value of diameter at breast height is approximately related to tree height by the mechanical rules applying to self supporting cylinders (McMon 1976) giving equation (23) which can be equated with equation (14).

$$Dbh \propto (Hc + Hs - 1.3)^{3/2} \quad (23)$$

$$Dbh = Pard * Hc^{2/3} * (Hc + 2*Hs-2.6)^{1/3} \quad (14)$$

For these large trees, if diameter at the base of the stem is used (ignoring any butt swell) then the 1.3 and 2.6 terms disappear and eliminating diameter gives:

$$Pard \propto (Hc+Hs)^{3/2} / [Hc^{2/3} * (Hc+2*Hs)^{1/3}] \quad (24)$$

The sapwood of young trees (juvenile sapwood) is mechanically different from the sapwood of mature trees in terms of density and elasticity (Bruchert et al. 2000). Saplings are able to reduce the surface area they present to the wind and thus reduce maximum wind forces by bending, whereas mature trees are far less flexible and need greater mechanical strength. The differences between juvenile and adult wood led to the need to use different methods of incorporating mechanical constraints into the PBS model and a definition of “Sapling” as “a tree below a specific height (Saph)” was adopted and is described further in Section 7.5.8. Saplings generally contain very little heartwood and the presumption that stem area and sapwood area are equal at crown base is used. From equations (5) and (15) diameter at crown base ( $Dcb$ ) is proportional to crown height to the power of  $ZZ/2$  and this with equation (10), after eliminating  $Dcb$ , gives equation (25) as an approximation of the relationship between  $Pard$  and crown height ( $Hc$ ) in saplings.

$$Dcb \propto Hc^{(ZZ/2)}$$

$$Dcb = Pard * Hc \quad (10)$$

$$Pard \propto Hc^{(ZZ/2-1.0)} \quad (25)$$

For saplings, using the empirically derived value of 2.5 (Mäkelä 1997) for the constant  $ZZ$ , then a rough approximation is that  $Pard$  is proportional to the fourth root of crown height. As a tree gets larger the rate of change of  $Pard$  must increase to a value in equation (24) which approximates to  $Pard$  being proportional to the square root of crown height (plus a bit extra for stem height). The value of  $Pard$  changes from its value in (25) to the value in (24) because the tree grows and  $XX$  is introduced as the power needed to describe such a change in  $Pard$ .

$$Pard \propto [ (Hc+Hs)^{3/2} / (Hc^{2/3} * (Hc+2*Hs)^{1/3} ) ]^{XX} \quad (26)$$

Theoretically, XX needs to vary from 0.5 for a small tree to 1.0 for a large tree as the tree grows. The size of tree could be defined by tree height or by tree mass, but because in competition tall thin trees need to have smaller values of Par1 than those needed for short fat trees, it seems more reasonable to define a large tree as one that approaches a defined maximum crown height (Maxh). The value of 0.5 is replaced by a parameter (Mpwr) to enable the sensitivity of the PCB model to the value 0.5 to be assessed. With no reason to do otherwise, XX is set to vary linearly (though it could vary with mass to fit self supporting cylinder equations) with crown height as follows:

$$XX = Mpwr * (Maxh + Hc) / Maxh \quad (27)$$

For a small tree at crown base then

$$Asap = Alf0 * eta * Hc^{ZZ} \quad (5)$$

$$Dcb = [ (Alf0 * eta * 4.0 / \pi)^{1/2} ] * Hc^{(ZZ/2)} \quad (28)$$

$$Dcb = Pard * Hc \quad (12)$$

From (28) and (12), for a small tree

$$Pard = (Alf0 * eta * 4.0 / \pi)^{1/2} * Hc^{(ZZ/2-1.0)} \quad (29)$$

When ZZ = 2.5 then ZZ/2 - 1.0 = 1/4.

When Hc is small compared to Maxh, then XX = 1/2.

When Hs is small compared to Hc, then

$$[ (Hc+Hs)^{3/2} / (Hc^{2/3} * (Hc+2*Hs)^{1/3} ) ] **XX \quad \rightarrow \quad Hc^{1/4}$$

Pard thus increases from being proportional to the fourth root of crown height for a sapling to being proportional to the square root of crown height for a large tree. In order to have exact values of Pard for all years then a value for the constant of proportionality (equation 26) must be found. While the tree is a sapling the mechanical constant for all saplings (Smech) is used and sapwood area at crown base is equated to wood area at crown base giving:

$$Smech = (Alf0 * eta * 4 / \pi)^{1/2}$$

$$Pard = Smech * Hc^{(ZZ/2-1.0)}$$

Within the crown of a sapling the mechanical equation (8) operates:

$$\text{Diameter} = Pard * Htop$$

In a sapling below the crown base, with Hc constant, the mechanical equation (9) operates:

$$\text{Diameter} = Pard * Hc^{2/3} * Hcp^{1/3}$$

The change from a sapling at height Saph to a tree at height Saph needs to be smooth and the constant for a tree, Tmech, is set to equate Pard for sapling and tree at height Saph.

$$XX = Mpwr * (Maxh + Hc) / Maxh \quad (27)$$

$$Tmech = Smech * Hc^{(ZZ/2-1.0)} * (Hc^{2/3} * (Saph+Hs)^{1/3} / Saph^{3/2})^{XX}$$

Tmech remains constant for the rest of the tree's life while XX varies as the tree becomes larger and both are used to derive Pard for a tree in a specific year:

$$Pard = Tmech * [ (Hc+Hs)^{3/2} / (Hc^{2/3} * (Hc+2*Hs)^{1/3} ) ]^{XX} \quad (30)$$

Within the crown of a tree the mechanical equation (8) operates:

$$\text{Diameter} = Pard * Htop$$

In a tree below the crown base, with Hc constant, the mechanical equation (9) operates:

$$\text{Diameter} = Pard * Hc^{2/3} * Hcp^{1/3}$$

Summarising the above then the stem profile of every tree at a specific time follows the observed mechanical constraints (Equations 8 & 9). The rate of change of diameter with respect to height of small trees matches the rate of change produced by sapwood requirements (25). The rate of change of diameter with respect to height of large trees matches the rate of change produced by mechanical constraints (24). The rate of change of diameter with respect to height for in-between sized trees is set by smoothly changing values of Pard, from the sapling rate to the large tree rate, obtained from equation (30) using a smoothly varying exponent (XX) which is dependent on crown height.

#### 7.5.8. Par1 - Open Grown > Closed Canopy

As a tree progresses from the juvenile stage to the mature stage the density and elasticity of the wood changes and, although the stem profile still follows the mechanical constraints (8 & 9), the mechanical constant "Pard" needs to change considerably. The wood in the crown of small trees is almost entirely sapwood and the term sapling is used here to describe small trees. The PBS model assumes that for a sapling all wood above the crown base is sapwood and for calculations involving saplings "Pard" is set to the value that calculates wood area at crown base as the same as sapwood area at crown base. The wood in the stem of saplings below the crown is set to taper as in equation (9). There is a small difference in the volume of wood and the volume of sapwood in the crown (Equations 6 and 17) and in order to produce a smooth change from sapling to tree the volume of sapwood in the crown is assumed to be the maximum of the volume calculated using mechanical wood constraints (17) and the volume of sapwood due to foliage distribution (6).

The PBS model needs to be able to follow the progress of open grown trees (short and fat) and closed canopy trees (tall and thin) and the differences are described by setting appropriate values of “Pard”. If Saph is set at 4.0m then the diameter of an open grown tree with a small stem height ( $H_c = 3.5\text{m}$  and  $H_s = 0.5\text{m}$ ) will be larger than the diameter of a closed canopy tree with a longer stem ( $H_c=2.0\text{m}$  and  $H_s=2.0\text{m}$ ) and at the changeover point from sapling to tree these two trees will be allocated differing values of Pard based on sapwood area at crown base. The value of Pard is set when tree height ( $H_s + H_c$ ) reaches the specific value of Saph, interpolated where necessary, and this value is the starting value which changes over the rest of the tree’s life (equation 30). Because the tree gets bigger, Pard increases with changes in stem and crown height and also changes as exponent XX increases. The ratio of crown height to stem height at the time the sapling becomes a tree is used to distinguish between open grown and closed grown trees and success has not been tested directly. The PBS model has the nature of growth of the open grown and closed canopy trees different for the rest of their lives and because trees that increase their height at a slower rate, relative to diameter increase, tend to achieve a larger overall size (Mäkelä & Hari 1986) this may be a reasonable approximation. However “speculative” this explanation is, this somewhat contrived approximation appears to produce acceptable results. These are only useful if a sensible height growth strategy can be developed.

#### 7.5.9. Height Growth Strategy

In tree growth models, stem height increases because of the senescence of foliage and branches which are below some empirically measured minimum light level (Mäkelä 1997). In HYBRID “*the carbon balance of the lowest foliage layer is a linear function of the whole crown rates of daytime photosynthesis and night-time respiration*” (Friend et al. 1997) which allows the use of the crown production rate to estimate stem height increase. The PBS model cannot use light levels so needs to use crown production rates to estimate height growth. Because crown production rates vary with latitude and altitude, the use of crown production rates has the disadvantage that it introduces a dependency at site level. In the PBS model, ring width measures are used to estimate the foliage mass and the mass of photosynthate generated by that foliage in a year. These values give an indication of how efficient the foliage was during the year. If foliage performs poorly, stem height increases and if foliage performs well then only crown height increases. An estimate of foliage efficiency is used to decide the height growth strategy in terms of the



relative sizes of crown height (dHc) and stem height (dHs) increments. From the relative sizes of dHs and dHc, absolute values can be calculated that are consistent with the measured diameter increment. The cause of poor performance by foliage need not be low light levels, as trees will senesce foliage that is inefficient. Foliage that is considered inefficient (by a tree) in south Finland may be considered as highly productive in north Finland. The reduction of light levels within the canopy leads to foliage at the base of the crown being “least efficient” and foliage at the crown base is generally the first to be lost.

To survive, a tree must generate sufficient carbon for maintenance respiration and the replacement of senesced foliage and fine roots, otherwise the tree will die within a few years. The PBS model calculates the “minimum mass of material needed to survive” from compartment masses at the start of the year and this mass is used as a base value for assessing the efficiency of foliage. The mass of material needed to generate the measured ring increment of the current year with no stem rise (dHs = 0) is calculated and divided by the minimum mass needed to survive to give an estimate of foliage efficiency as a “Fraction”. If the ring increment is zero then Fraction = 1.0 and larger ring increments produce values of Fraction greater than 1.0. The relative sizes of dHs and dHc must be able to vary smoothly over the range of possible ring increments.

Three stages in height increase are identified. Firstly, when dHs is zero and all height increase is allocated to crown increase. Secondly, when dHc is zero and all height increase is allocated to stem rise. Thirdly, when dHc is negative and the crown recedes. The first limit was called Gftop (growth fraction top) and if Fraction is greater than this value, dHs is set to zero and all height increase is in the crown. The second limit was called Gfbot (growth fraction bottom) and if Fraction equals this value, dHc is set to zero and all height increase is in the stem. If Fraction is between Gftop and Gfbot then height increase is divided between stem and crown. The lowest possible value of Fraction is 1.0 and when Fraction is 1.0 the crown recesses by an amount specified by a parameter which sets the maximum amount of crown loss in any year “Closs” and the stem height increases. Closs was initially set to 0.3 which means that when the ring increment is zero then 30% of the crown height (and more than 50% of foliage mass as  $W_f \propto H_c^{2.5}$ ) are lost. To calculate the new heights (Hs and Hc) from the existing heights and the new diameter, one of dHc, dHs, or the ratio of dHs to dHc must be known. To produce a smoothly

changing range then the relative proportions of height increase allocated to stem and crown are derived linearly as follows:

If Fraction  $\geq$  Gftop then

$$dH_s = 0, dH_c = \text{calculated crown rise}$$

If Fraction  $<$  Gftop and Fraction  $\geq$  Gfbot then

$$dH_s / dH_c = (Gftop - \text{Fraction}) / (\text{Fraction} - Gfbot)$$

dH<sub>s</sub> and dH<sub>c</sub> values are calculated from the dH<sub>s</sub> to dH<sub>c</sub> ratio

If Fraction  $<$  Gfbot

$$dH_c = -H_c * Closs * (Gfbot - \text{Fraction}) / (Gfbot - 1.0)$$

dH<sub>s</sub> = Calculated stem rise for this negative value of dH<sub>c</sub>

Initial values of 1.2 for Gfbot, 1.8 for Gftop, and 0.3 for Closs, using the North Finnish trees, produced “reasonable” results. A problem arises in that as a tree gets larger and older, both the local mean value and the variance of Fraction reduce as the proportion of carbon consumed by maintenance respiration in the sapwood increases steadily. (This problem is exaggerated in the current formulation of this PBS model because the effects of bark and reproduction are included in the respiration parameter, as discussed in Section 7.6.5.). Gfbot and Gftop need to vary with age or size. The foliage of trees from Rutajarvi generates more photosynthate than does the foliage of trees from Luosto in the PBS model, expected because of higher summer temperatures. The production rate of foliage at the top of the canopy depends on temperature and sunlight and overall production rate varies by site. Gfbot and Gftop thus need values which are also site dependent. To avoid these problems, ring age and diameter based RCS curves of Fraction are created. The upper limit (Gftop) was set at +1.5 standard deviations, above the age or diameter based curve, and the lower limit (Gfbot) was set to -1.0 standard deviations, below the age or diameter based curve. The four curves created from Fraction by age or diameter + 1.5 and -1.0 standard deviations all decay in the manner of negative exponential curves (Figure 7.7.6a). Modified (by the addition of a constant) negative exponential curves (Fritts et al. 1969) were fitted to these curves producing a series of 12 parameters (Gfpar), 3 for each exponential curve, which can be used to calculate the upper and lower efficiency limits for all ring ages and tree diameters.

The decision was made to use the average value of the ring age and diameter values for both upper and lower curves to calculate stem height increments. Thus age and diameter are both used as predictors. The parameters Gftop and Gfbot are the number of standard deviations to add-to or subtract-from the mean Fraction curves to generate values of Gfpar. This does entail iterative methods. The first run uses default values of Gfpar from which site dependent values of Fraction and Gfpar are created. Subsequent runs use previously calculated Gfpar values to create “better” fitting values of Gfpar. Gfpar values change by less than one part in 1000 between the 5th and 6th iterations so 6 iterations are used in the PBS model. This height growth strategy allows for the extremes of stem and crown height growth rates; is dependent on the overall distribution of foliage growth rates at a site; and allows each individual tree to develop independently.

#### 7.5.10. Estimating Initial Height

In HYBRID “*The initial tree seedling diameter is set as a uniform random number between 0.001 and 0.002 m, with the height set to 1m.*” (Friend et al. 1997) and this randomness in diameter at 1m height produces adequate variation of sapling size, tree growth rates, and subsequently tree sizes on each plot. The PBS model has estimates of the initial diameter (iD13) for each tree and must develop estimates of initial stem height (iHs) for each tree consistent with the initial diameter and subsequent growth. The first ring alone is not suitable as an estimator because ring-width measures are noisy so sufficient rings are needed to overcome the effects of this noise. Because trees (grown by the PBS model) adapt over decades to local growing conditions the number of rings that could be used as estimators for initial stem height is limited. By trial and error with different numbers, the first 12 rings were selected in the PBS model as the basis for estimating iHs. The values of the diameter based “Fraction” curve give an estimate of the values of Fraction expected at each diameter. Diameters are known and a procedure was written to select a value of iHs which produces values of Fraction for the first 12 rings of each tree with a sum equalling the sum of the 12 values of the diameter-based “Fraction” curve for that tree’s known diameters for each of the 12 rings. Testing showed that in the PBS model only the first 20 years of each tree are sensitive to the choice of initial height. Variation of iHs by  $\pm 50\%$  has negligible effect after the 20th year. If stem height is too large, crown height is too small, foliage is very efficient and height growth is allocated to the crown. If stem height is too small, crown height is too large and foliage is inefficient

resulting in increased stem height growth. PBS model grown trees adapt to achieve a “balanced” state.

## **7.6. Evaluating the PBS Model**

### **7.6.1. Testing Methods**

A problem with testing tree-growth models is that, with large numbers of parameters and results which are compared to average measured values, it is difficult to test the interrelationships between parameters because of the number of separate program runs needed. The PBS model has an advantage in that it must satisfy an equation for each measured ring-width. For the regions used here, with 20 parameters, 100 trees, 500 years, and high-frequency noise to remove, there is scope for best fit values to be assessed from the 20,000 equations formed by each ring measure and it is possible to tune parameters and examine options within algorithms. The principle of treating each tree ring separately guided program development. Compartment sizes at the start of each year and measured ring increment provide almost all the data needed for each annual calculation. One exception was the need to estimate initial stem height but this is not critical to the overall results (Section 7.5.10). Another exception was the need to develop site specific efficiency measures and this requires the use of all trees in an iterative manner (Section 7.5.9). The initial iterative procedures estimate the 12 values of  $G_{fpar}$  and an initial height ( $iHs$ ) for each tree. These values, the other parameters, and state variables are used to process each ring width measure independently, although in sequence, to produce a tree index value for that ring. Compartment sizes are changed by each ring width simulating the growth of each tree. The Luosto trees were used for most of the development and testing. The Helldalisen trees were used as an independent data set to evaluate progress. Problems with the PBS model using the Rutajarvi trees rendered these of limited value at this stage of development of the PBS model (Section 7.6.4).

Initial diameter (from pith to first ring) is a variable for each tree which could be used to set the mean value of series of PBS Indices and is not available for some existing dendroclimatic chronologies. In order to widen the applicability of the PBS model, attempts were made to estimate the initial diameter of each tree from the series of ring measures. A number of equations can be developed (two unknowns  $iD13$  and  $iHs$  require two or more equations for each tree) by reducing the length of series of indices, i.e. by comparing the results of growing a tree from the start and growing a tree from the middle.

Results were inconsistent, in that a tree's growth adjusts over decades in an unpredictable manner which is dependent on the ratio of stem height and crown height when the sapling becomes a tree i.e. the Parm parameter. It would be possible to use initial tree diameters and heights to achieve specific goals such as to reduce the standard deviation of PBS Indices, increase correlation with climate variables, or obtain "best fit means" of PBS Indices (Section 7.7). In the PBS model, the default option of presuming that the diameter of the first ring is zero will fail so the decision was made to use visually estimated values for the initial diameter of each tree, at least until a method can be found to estimate initial diameter.

### 7.6.2. The PBS Program

The computer program is written in FORTRAN 90 and consists of a series of procedures which run within a menu system. The main calculations are performed by a procedure called "Tree\_grow" which, given diameter measures, the initial stem height, and parameter values, processes each year sequentially to "grow a tree" producing a series of Grow2 values as output. There is a procedure called "Tree\_height" which uses the first 12 rings of a tree to estimate an initial height for that tree which is consistent with the default parameters (1<sup>st</sup> run of program) or the site specific efficiency parameters Gfpar (subsequent runs). There is a procedure called "Tree\_frac" which calculates the parameter values (gfpar) of the exponential curves used to assess the efficiency of foliage. Tree\_frac runs iteratively six times to produce stable values and outputs the 12 numbers (gfpar) needed to specify the upper and lower limits of efficiency. There is a procedure called "Tree\_stats" which creates calendar, ring-age, and diameter-based chronologies for analysis purposes. There are various procedures, controlled by the menu system, which read data, save data, and display data. The menu system allows a hierarchical selection of a site, and a tree. The values of state variables for each tree can be plotted. The values of various chronologies can be plotted by calendar year, ring age, or diameter. Values for each tree can be sorted and compared, such as final height and sapwood area. Parameters can be selected and their values changed online to examine the sensitivity of the outputs to individual parameter values. The sensitivity to parameter values can also be tested by a menu option which runs the programs with parameter values systematically varied by specified increments over a specified range and displays the values of some key chronology statistics, thus allowing the selection of "better fitting" parameter values. The development of this flexible, menu driven interface in

which to test and evaluate the PBS model has enabled all subsequent work. The development of this novel and complex model would not have been feasible without such an environment.

### 7.6.3. Parameter Values

Where possible, empirically estimated parameter values were taken from the Mäkelä model and estimated values are used for the “newly introduced” parameters. The default parameter values were varied in order to find a suitable set of parameter values which produced a good match between measured and calculated sapwood areas for the last ring in each tree and also produced mean signal-free PBS Indices which, when plotted by ring age or tree diameter, were approximately horizontal (Signal-free PBS Indices are PBS Indices which have been divided by chronology indices as described in Section 5.5.8 and are necessitated by the use of modern chronologies with an estimated 40% growth rate increase since 1920). Because the trees used here were living and at different stages in their lifecycles at the time of sampling then matching sapwood area for the last ring of each tree tests the ability of the PBS model to predict sapwood area at differing (although generally later) stages during the lifecycle of trees. It was possible to use the same set of parameter values for the Luosto and Helldalisen sites while the faster growing trees of the Rutajarvi site required different parameter values for Eta, Mpwr and Gftop (Table 7.3.1). Luosto, Helldalisen and Rutajarvi were allowed to generate their own site specific efficiency parameters (Gfpar).

Name	Luosto	Helldalisen	Rutajarvi
Wden	400 (M)	400 (M)	400 (M)
Closs	0.21 (E)	0.21 (E)	0.21 (E)
Alf0	0.0022 (M)	0.0022 (M)	0.0022 (M)
AlfB	0.8 (E)	0.8 (E)	0.8 (E)
AlfT	0.20 (E)	0.20 (E)	0.20 (E)
AlfR	0.23 (E)	0.23 (E)	0.23 (E)
Maxh	28 (E)	28 (E)	28 (E)
Rgrow	0.65 (M)	0.65 (M)	0.65 (M)
Rfol	0.16 (E)	0.16 (E)	0.16 (E)
Rroot	0.25 (E)	0.25 (E)	0.25 (E)
Rsap	0.03 (E)	0.03 (E)	0.03 (E)
Sfol	0.25 (M)	0.25 (M)	0.25 (M)
ZZ	2.5 (M)	2.5 (M)	2.5 (M)
Eta	0.05 (M)	0.05 (M)	0.065 (E)
Mpwr	0.4 (E)	0.4 (E)	0.22 (E)
Gfbot	1.0 (E)	1.0 (E)	1.0 (E)
Gftop	1.6 (E)	1.6 (E)	1.2 (E)
Saph	5.6 (E)	5.6 (E)	5.6 (E)

Note: M = values from Mäkelä, E = Estimated or tuned values

Table 7.6.1 Parameter values selected for the Luosto, Helldalisen, and Rutajarvi sites.

A set of parameter values was established which achieve the above objectives and these values, used in all subsequent testing, are shown in Table 7.6.1. Parameter values could be adjusted for specific purposes e.g. to improve correlations with temperature, to produce better height growth characteristics, to reduce the mean autocorrelation in series of PBS Indices, but such tuning has not been attempted at this stage of model development. There are 20 parameters which are allowed to vary within the PBS model and there are a few fixed values, which might be considered as adjustable parameters, in future PBS model development. Some of the parameters are closely linked in that direct relationships might be found between parameter values. Detailed testing of the effects and sensitivity of each parameter and of some of the assumed relationships and algorithms has not been attempted. This detailed testing will require more trees and a number of other measures taken in conjunction with series of ring measures against which to validate the PBS model.

#### 7.6.4. Trees and the PBS Model

In section 7.5.7 the problems of dealing with the mechanical properties of saplings were discussed and here the problem that the PBS model produces larger values for the rate of production of carbon by foliage in the earliest decades of trees is discussed. Mean values of growth (carbon per unit foliage) are shown in Figure 7.6.1 for the Luosto (a) and Rutajarvi (b) sites. The RCS curve of mean growth by ring age (Figure 7.6.1a blue) for Luosto shows that mean growth rate by ring age decays in the earliest decades, is roughly horizontal for two centuries and then rises after the third century. The rise after the third century is the result of the 40% step increase in growth rates from 1920 onwards found in these trees and is distortion created in the RCS curve by the presence of a common forcing signal (Section 5.5.8). The solution to this problem is to use signal-free growth measures i.e divide the growth measures by the chronology signal before averaging growth to produce age or diameter related growth curves. The RCS curve of mean growth by ring age (Figure 7.6.1b blue) for Rutajarvi shows larger growth rate decay in the earliest decades than at Luosto. The RCS curves of mean growth plotted by diameter (black) show similar trends to those of the RCS curves plotted by ring age (blue).

There is a steady increase in tree count (grey shaded area) over time at Luosto whereas at Rutajarvi 70% of trees were between 80 and 120 years old at the time of sampling. The mean growth by calendar year (red) when scaled by its overall mean becomes the

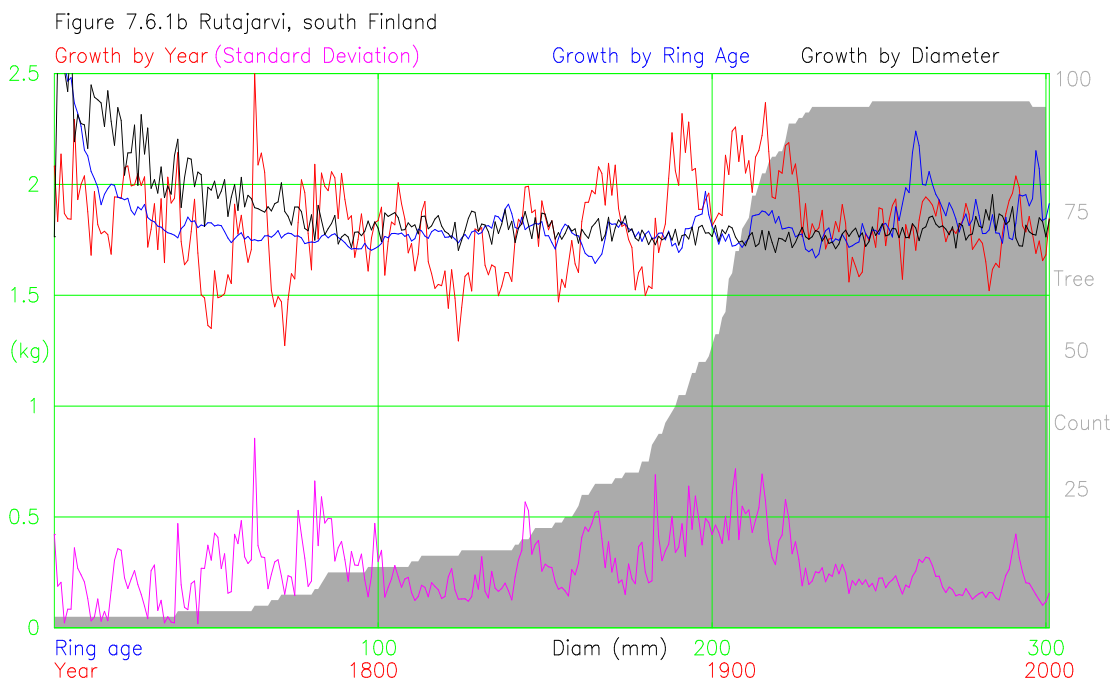
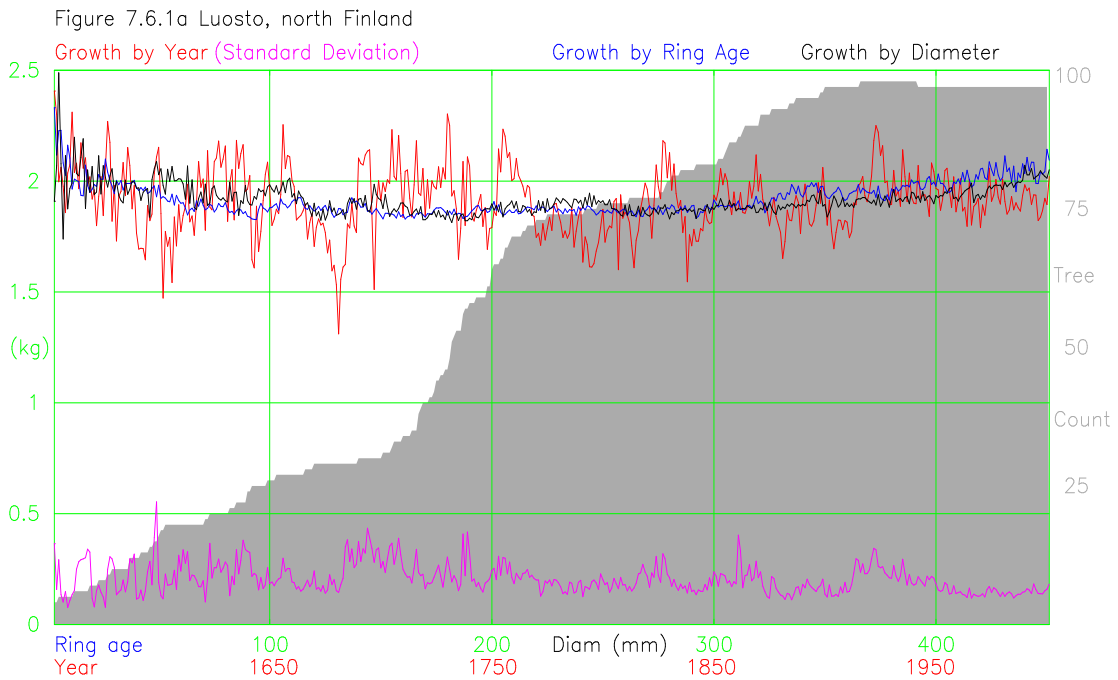


Figure 7.6.1 Growth, carbon per unit foliage, by calendar year (with standard deviation), ring age, and diameter for (a) Luosto and (b) Rutajarvi. Scales for calendar year add 1550 (a) and 1700 (b), ring age units of years, and diameter units of mm.

chronology for each site. The growth rates (carbon per unit foliage) by calendar year and the standard deviation of this curve (magenta) show increases during periods when there are several young trees i.e. when tree counts are rising. This signal, as ring-age based distortion, is not part of the wanted signal. At the Luosto site the steady change in tree counts renders this problem acceptable, at least in this stage of development of the PBS model. The magnitude of distortion at Rutajarvi is larger than the common signal, for ring



ages 190 to 220 and as a consequence the PBS generated chronology at Rutajarvi is not used in subsequent testing. The faster growing trees of Rutajarvi have proved valuable in demonstrating this problem and have suggested some PBS modifications in order to avoid the problem.

The PBS model “grows” trees, by expanding series of ring width measures into a description of trees over time, and some characteristics of these trees are discussed using examples. Two sample trees were selected from Luosto which had reached the stage of growth where sapwood area ceases to expand i.e. trees beyond the stage of exponential growth. Modelled ring-width, stem area, sapwood area, and tree heights are plotted over time for both trees (Figure 7.6.2) to show how the PBS model values evolved over the life of these trees. The vertical scale, labelled from 0 to 1.0 (Figures 7.6.2a and b), represents the magnitude and units which are shown separately for each variable. Stem area (at breast height) is derived directly from visually made estimates of initial diameter and ring measurements. Stem area (blue) increases steadily over the life of each tree. Ring-width measures (red) are highly variable but both trees start with larger values of ring width and finish with smaller values. Sapwood area (black) starts off with small values (first century), which then increase rapidly, and in the final century decay slightly. Despite ring widths being twice as large in the first century of growth as in the last century, the growth rates (gain in wood volume per year) of both trees are roughly eight times greater in the last century than in the first century; sapwood area is proportional to foliage mass and foliage mass (modified by climate) sets the rate of carbon sequestration. Small ring widths measures, relative to the local mean, produce a reduction in sapwood area (and foliage mass) e.g. 1795 and 1837 for tree “tu152” (Figure 7.6.2a) and 1680 and 1780 to 1800 for tree “vy131” (Figure 7.6.2b). Tree heights are a problem because these trees, using a rough approximation, should reach roughly three-quarters maximum height in half their maximum age (Botkin et al. 1972). In the second century, both trees are 25% shorter than they ought to be. This is a PBS model problem that needs to be sorted out.

The PBS model creates series of PBS Indices from series of ring-width measures using non-linear methods. Some sample trees from Luosto are used to show the relationship between ring-width measures (blue) and PBS Indices (red) in Figure 7.6.3. The general decline in radial ring width with age is removed creating series of roughly horizontal indices. The indices of the slowest growing tree (c) have less variance than the indices of

Figure 7.6.2a Tree = tu152

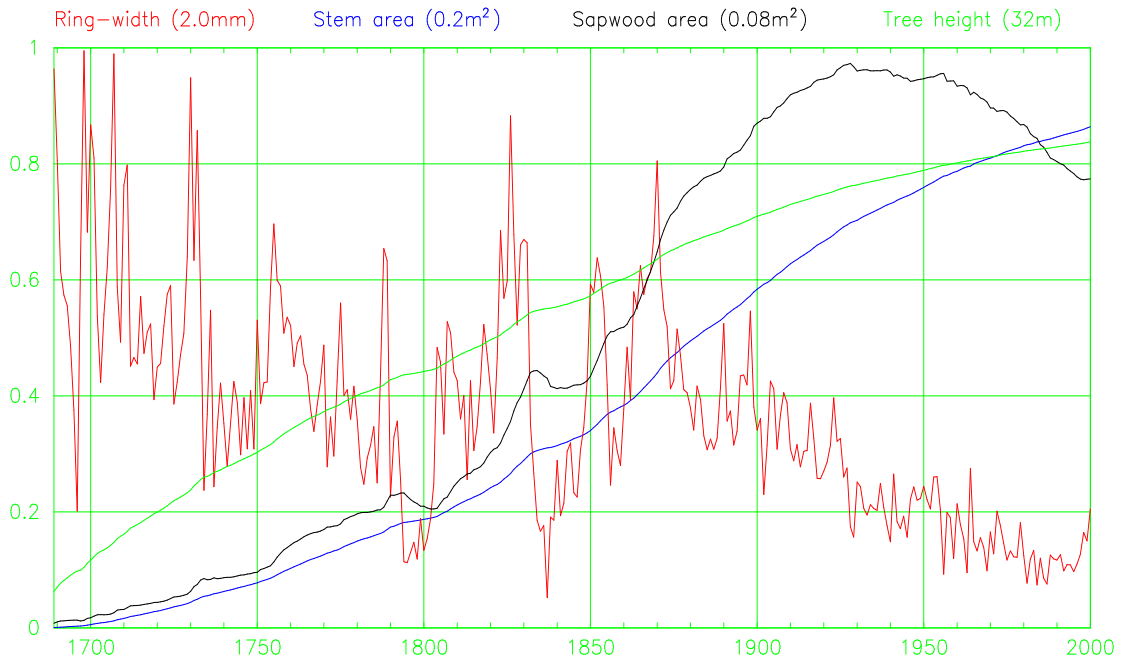


Figure 7.6.2b Tree = vy131

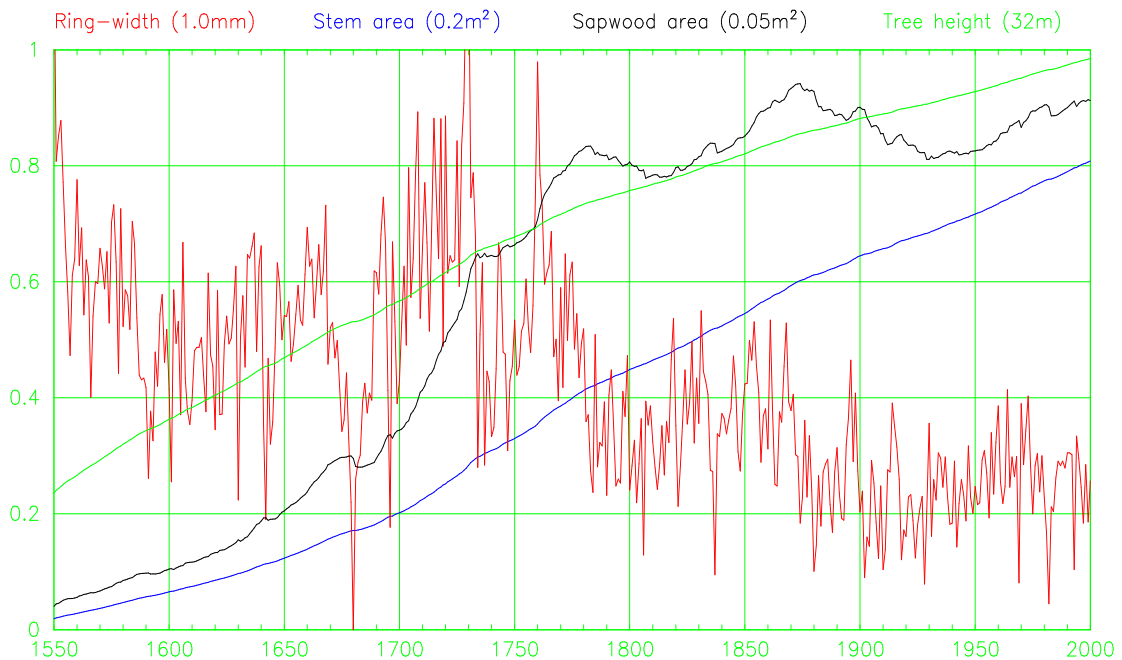


Figure 7.6.2 Ring width, stem area, sapwood area and tree height over the life of each tree for sample trees from Luosto. (1.0 on the vertical scale represents the magnitude and units shown separately for each variable).

the other trees which may indicate a problem in the PBS model. The magnitude of the inter-annual variance is lower in the PBS Indices than in the measured ring widths. Some changes, such as the magnitude of the spikes at 1793 and 1935 (Figure 7.6.3a) are retained, whilst others, such as the spikes at 1948 and 1953 (Figure 7.6.3b) have been considerably reduced in magnitude. The PBS model generates series of PBS Indices

whose medium-frequency variance is substantially different from that of series of tree indices generated by other standardisation methods as can be seen in Figure 7.6.4, in which indices, for the sample trees of Figure 7.6.3, created by the SARCS (blue), PBS (red) and Hugershoff (Black) methods are compared.

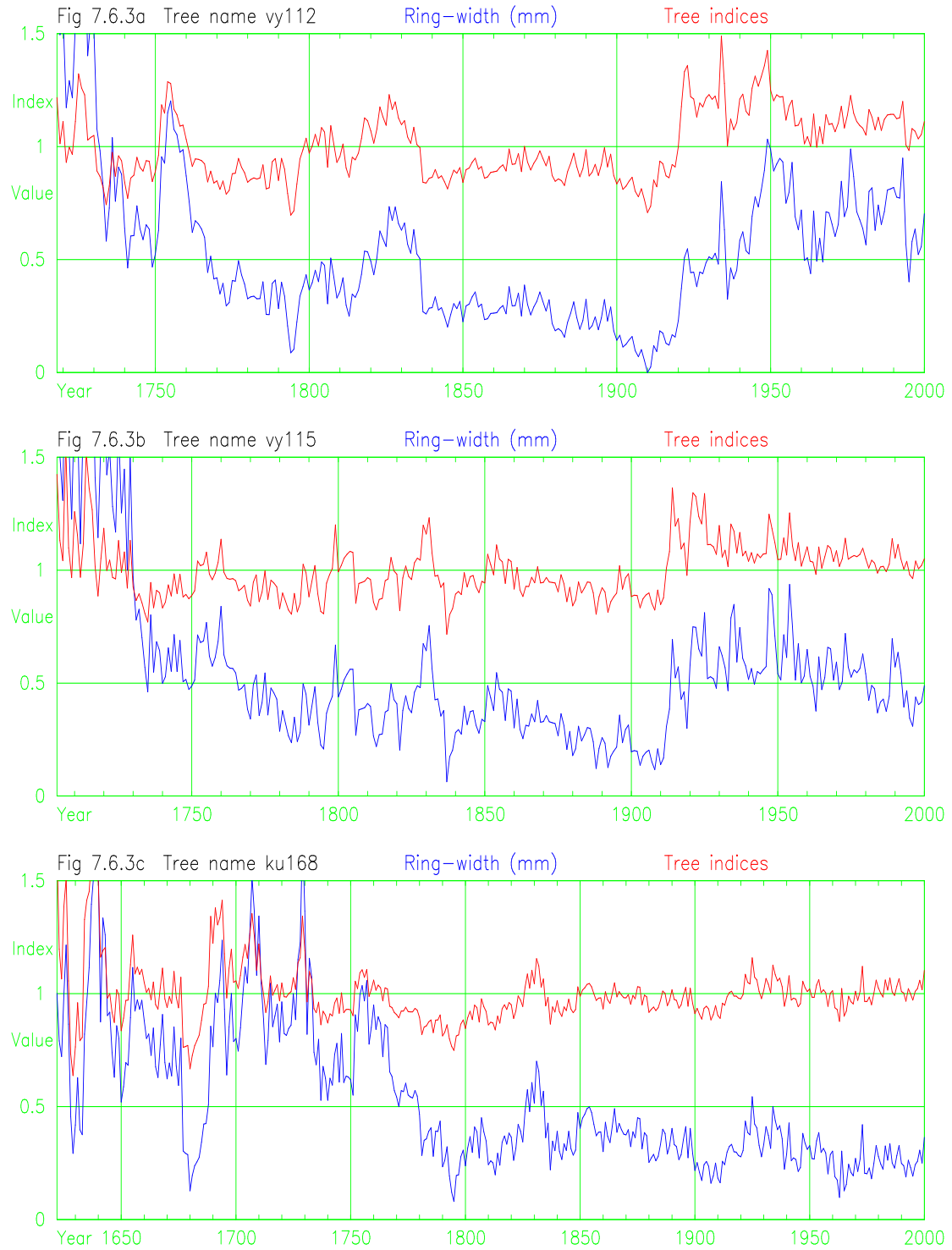


Figure 7.6.3 Sample trees showing ring width and PBS indices over the life of the trees.



Figure 7.6.4 Comparison of tree indices for sample trees from Luosto created using the SARCS, PBS and Hegershoff methods of standardisation.

### 7.6.5. Measured v Calculated Sapwood Areas

The PBS model calculates the sapwood area ( $A_{sap}$ ) at crown base for each year of each tree's growth. The sapwood-heartwood boundaries in each tree core were used to assess the sapwood area of each tree in the year the tree cores were sampled. Trees whose last measured ring is not the year beneath the bark (Luosto 1 tree, Rutajarvi 1 tree, and

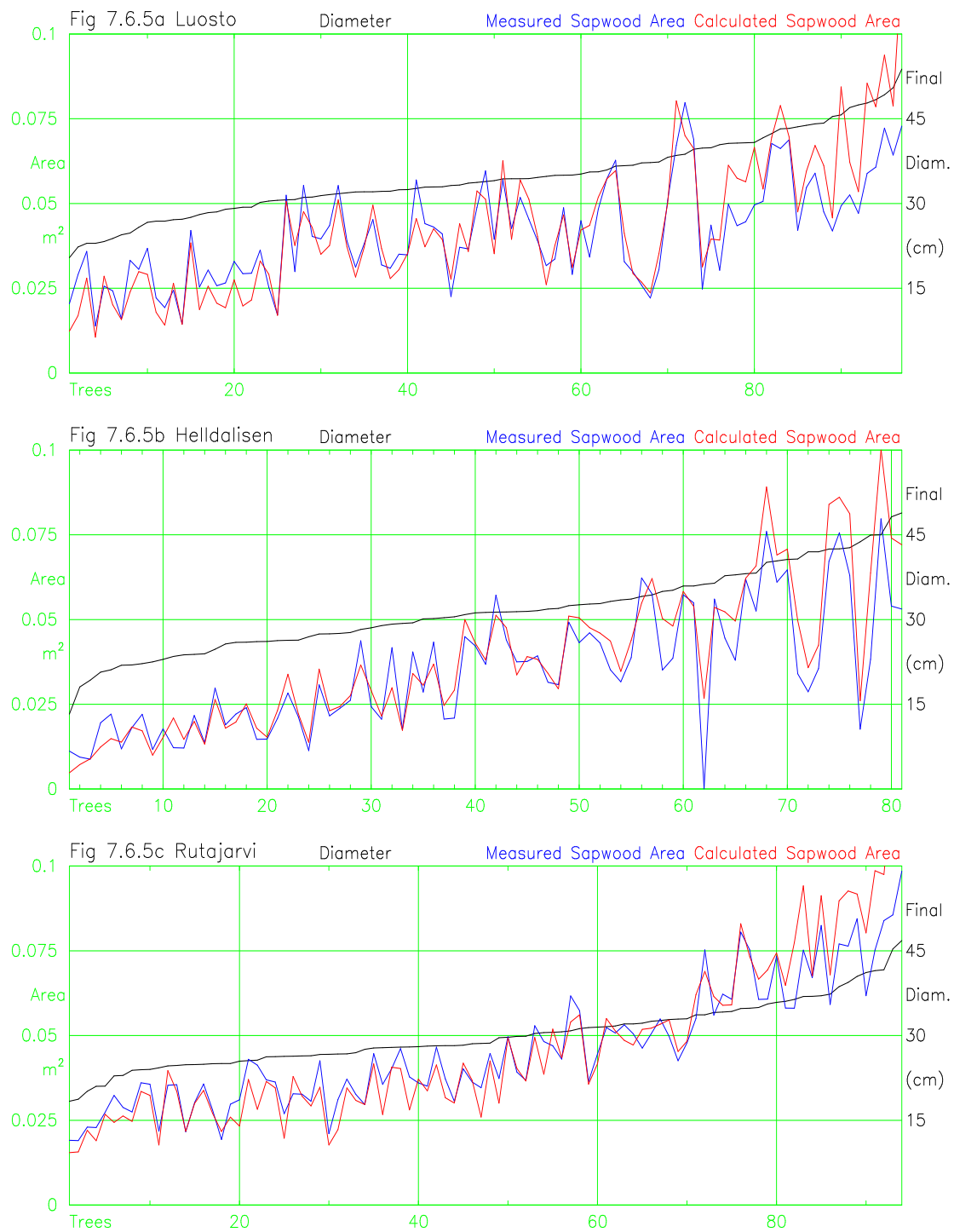


Figure 7.6.5 Comparison of measured sapwood area and calculated sapwood area sorted on ascending final tree diameter for (a) Luosto, (b) Helldalisen, and (c) Rutajarvi.

Helldalisen 7 trees) are excluded from this comparison because final sapwood areas are not known. The sampling date of the living trees at the sites used here represent a range of life cycle stages in different trees and, because trees generally become larger, increase foliage mass, and increase sapwood area with age, final tree diameter will be a predictor of final sapwood area. Figure 7.6.5 demonstrates the ability of the PBS model to predict final sapwood area, beyond the effects of changing diameter. Measured and predicted

sapwood areas for each tree are shown sorted by ascending order of final diameter (black). Data are shown for each of three sites. The selected parameter values produce “model grown” trees whose final sapwood area (red) closely matches the measured sapwood area (blue). There is a small diameter related bias in that sapwood areas are somewhat underestimated for smaller diameter trees and overestimated for larger diameter trees, a problem that will need to be addressed at a later stage of PBS model development.

In contrast to the good prediction of sapwood areas, the calculated stem and crown heights (not shown) do not match the measured values in the final year of the trees from Luosto and Rutajarvi (Tree height measurements were not available for Helldalisen). The problem with heights is that the foliage density within the crown of trees can vary considerably and trees distribute their foliage within the canopy making the modelled and measured heights differ. The PBS model presumes a constant distribution of foliage within the crown of trees (Section 7.5.2). A conversion algorithm could be used within the PBS model to generate estimates of crown height from stem strength (a proxy for canopy openness), estimated from diameter, and tree age. Ring measures in conjunction with stem and crown height measures are needed to test the PBS model and these could be used to develop a more “realistic” description of foliage distribution and consequently crown height for closed and open canopy situations.

#### 7.6.6. PBS Indices by Year, Ring Age and Diameter

The PBS model generates series of values representing the rate of production of carbon by unit foliage for each year, these are divided by their mean value (over all trees and years) to produce series of PBS Indices. The chronology is created as the simple arithmetic mean of PBS Indices for each year. The chronologies produced by the PBS model for the Luosto and Helldalisen sites are plotted in Figure 7.6.6a. There are periods when these chronologies correspond and periods when they are markedly different. The magnitude of the variance is similar for the two sites and a slight reduction in variance over time is apparent, above that expected from changing tree counts. There are a number of potential causes for this effect which need to be investigated, one of which is the higher production rate values (Grow2) of the first few decades of each tree. Aligning series of tree indices by ring age or tree diameter is expected to remove the common signal and produce mean indices that are horizontal, but the low-frequency common

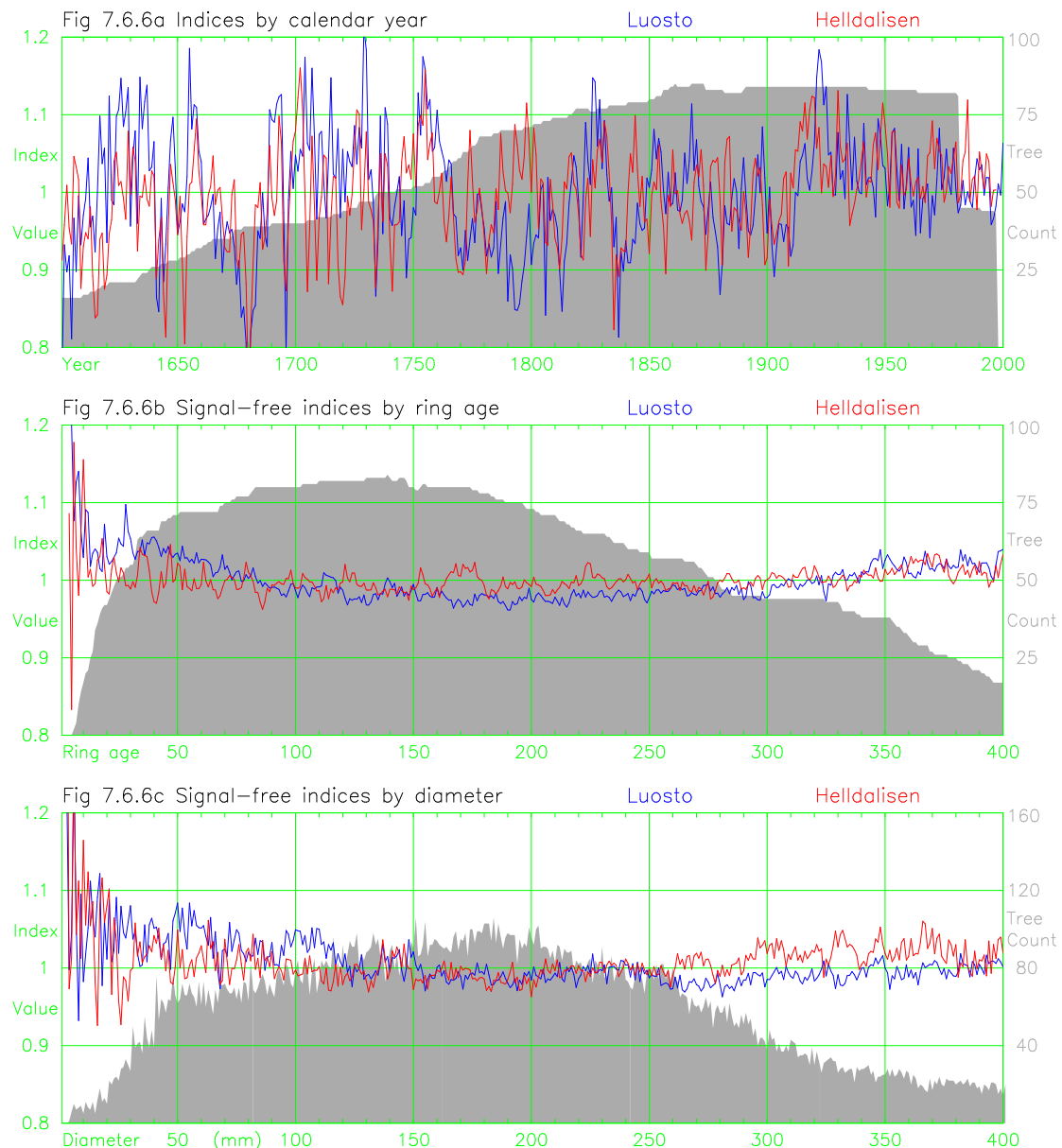


Figure 7.6.6 Mean PBS indices (carbon per unit foliage) for Luosto and Helldalisen (a) by calendar year, (b) signal-free by ring age, and (c) signal-free by diameter.

signal in “modern” chronologies can distort these curves in a similar way to its distortion of RCS curves (Section 5.5.8). Therefore, signal-free series of PBS Indices were created here by dividing each series of PBS Indices by the values of the chronology over their common period and aligning these by age and diameter. (There is no expectation that this division is “valid” because series of PBS Indices are not necessarily “fractional deviations” as are tree indices created by traditional standardisation methods and no attempt is made to rescale PBS Indices prior to averaging. If variance is proportional to the local mean then division may be suitable but tests of this are left until some of the larger magnitude problems are corrected.) The means of signal-free PBS Indices plotted by ring age are shown in Figure 7.6.6b and plotted by diameter in Figure 7.6.6c.

As trees become taller and older the ratio of sapwood mass to foliage mass increases and the overhead of sapwood maintenance per unit foliage become larger. If the value of sapwood maintenance respiration ( $R_{sap}$ ), is too large all series of PBS Indices slope up and if the value is too small all series slope down.  $R_{sap}$  controls the slope of the resulting series of indices more than any of the other parameters (other parameters can vary the slope of series of indices but  $R_{sap}$  produces by far the largest magnitude change). A value of sapwood maintenance respiration was selected to produce mean signal-free PBS Indices by ring age which, excluding the first 40 years, are nearly horizontal for both sites. The first 20 years of the ring-age aligned curves have a greater variance than the later years indicating that the PBS model is poor at tracking growth rate changes in the early decades of saplings. The probable cause is that the early rings of *Pinus sylvestris* often contain reaction wood which is grown for mechanical purposes but is presumed by the PBS model to be sapwood. Removing the first two decades of each series of PBS Indices, prior to averaging to create a chronology, produced a small improvement in correlations with temperature at both sites. In initial versions of the PBS model, mean PBX indices by age (and diameter) sloped downwards in the first century (10 cm of diameter) and created a need to treat saplings separately (Section 7.5.7). The introduction of “saplings” with differing mechanical shape to that of mature trees reduced this slope to the levels seen in Figures 7.6.6 (b) and (c). This residual slope in the first century shows that the PBS model has not completely solved the problem. A more realistic solution would be to have wood density steadily increasing from the density of juvenile sapwood (maybe 20% below current density) to the density of mature sapwood because wood density increases in this way. With 20% less material needed for wood growth and fixed diameter at breast height, saplings would use less carbon per unit foliage (lower growth indices) and their initial height growth would be larger (better match to measured values). This is not practical without forestry data against which to calibrate the assumptions.

The means of signal-free PBS Indices plotted by stem diameter (units of mm) are shown in Figure 7.6.6c. These curves are similar to the ring age based curves with the exception that the curvature at both ends is slightly larger. The sapwood maintenance respiration (parameter  $R_{sap}$ ) is set to higher levels than the empirically estimated values (Mäkelä 1997). The PBS model did not explicitly account for the cost of bark production which increases as trees become larger, but this is implicitly included by using a higher cost of



maintaining sapwood. The PBS model also ignored the cost of reproduction, which starts after trees become mature and continues until trees become old, and again this is implicitly included by using a higher cost of maintaining sapwood. A steadily increasing efficiency of carbon production by foliage due to increasing partial pressure of carbon dioxide, if it occurred in these modern chronologies, will also be explained (and removed) within the increased value of the sapwood maintenance parameter. The effect of finding a “best fit” value for sapwood maintenance on the preservation of low-frequency variance in the final chronology will be similar to that of using an RCS curve to remove the age-related growth trend of trees. The preservation of low-frequency variance in the slope of each series of indices will be limited to the length of the chronology and to investigate multi-century variance, sub-fossil chronologies will be needed. The PBS model has the alternative of using an empirically-measured value for sapwood maintenance which would then require an explicit description of the carbon consumption by bark and reproductive organs.

The random variations in tree growth rates (Section 5.4.2) which lead to modern sample bias are preserved in the mean value of series of indices. Mean PBS indices are examined by tree growth rate, tree age, and tree size to look for potential problems. Figure 7.6.7 shows sub-chronologies created from indices of the slowest and fastest growing trees (a), the youngest and oldest trees (b), and the biggest and smallest trees (c) from the Luosto site. Slowest and fastest were defined by the time taken (or projected to have taken) to reach 10cm radius and smallest and largest were defined by final tree diameter. The chronologies are very similar except that the smallest (slower growing) trees tend to have lower index values than the largest (fastest growing) trees. Figure 7.6.8 shows plots of mean PBS Indices by ring age (RCS curves) for all trees and the sub-chronologies for growth rate, tree age and tree diameter. Sub-chronologies are smoothed for display purposes. Similar patterns were found for the Helldalisen site (not shown). The consistent differences, between the sub-classes of trees, produced by the PBS model is constant over the life of trees whereas the differences between the sub-classes created by the RCS, MRCS and SARCS methods (Figure 5.9.2) are larger and vary with tree age. The difference in magnitudes between classes, with RCS 100%, SARCS and MRCS 20% and PBS model (5%), are not directly comparable due to overall differences in variance. The PBS model generates PBS Indices with little bias due to age, diameter or rate of growth.

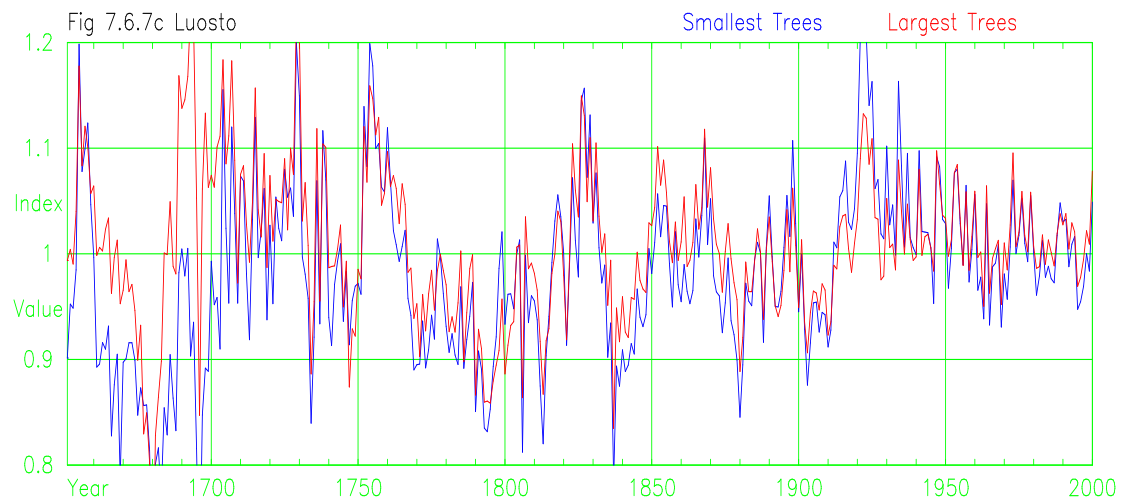
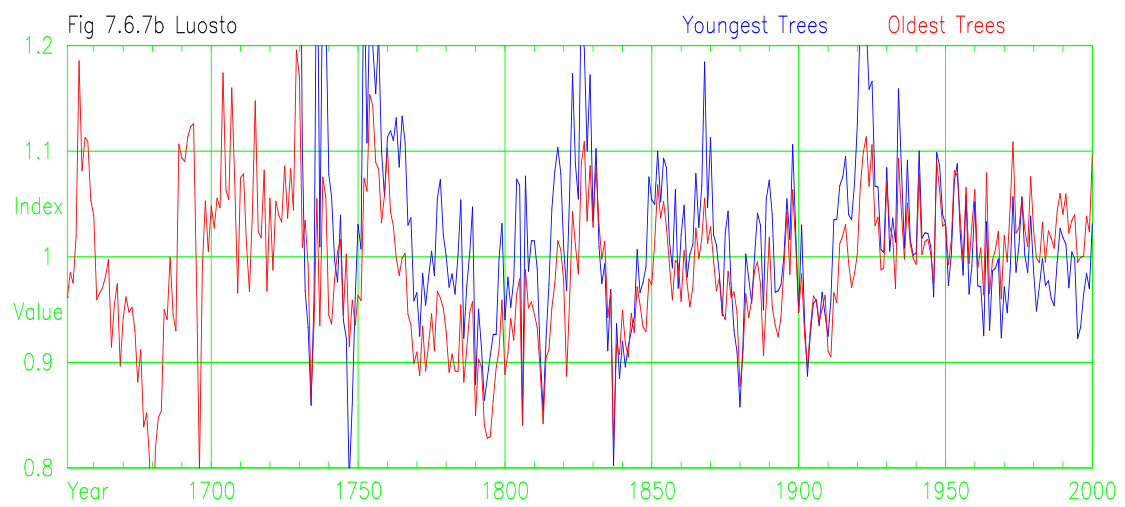
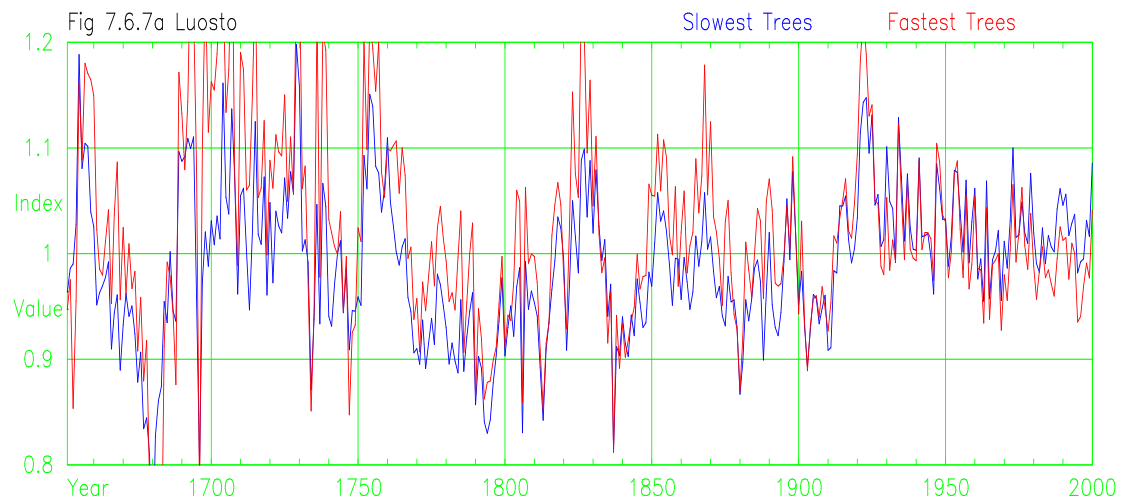


Figure 7.6.7 Mean PBS indices for the Luosto site by calendar year showing (a) slowest and fastest growing trees, (b) youngest and oldest trees, (c) smallest and largest trees.

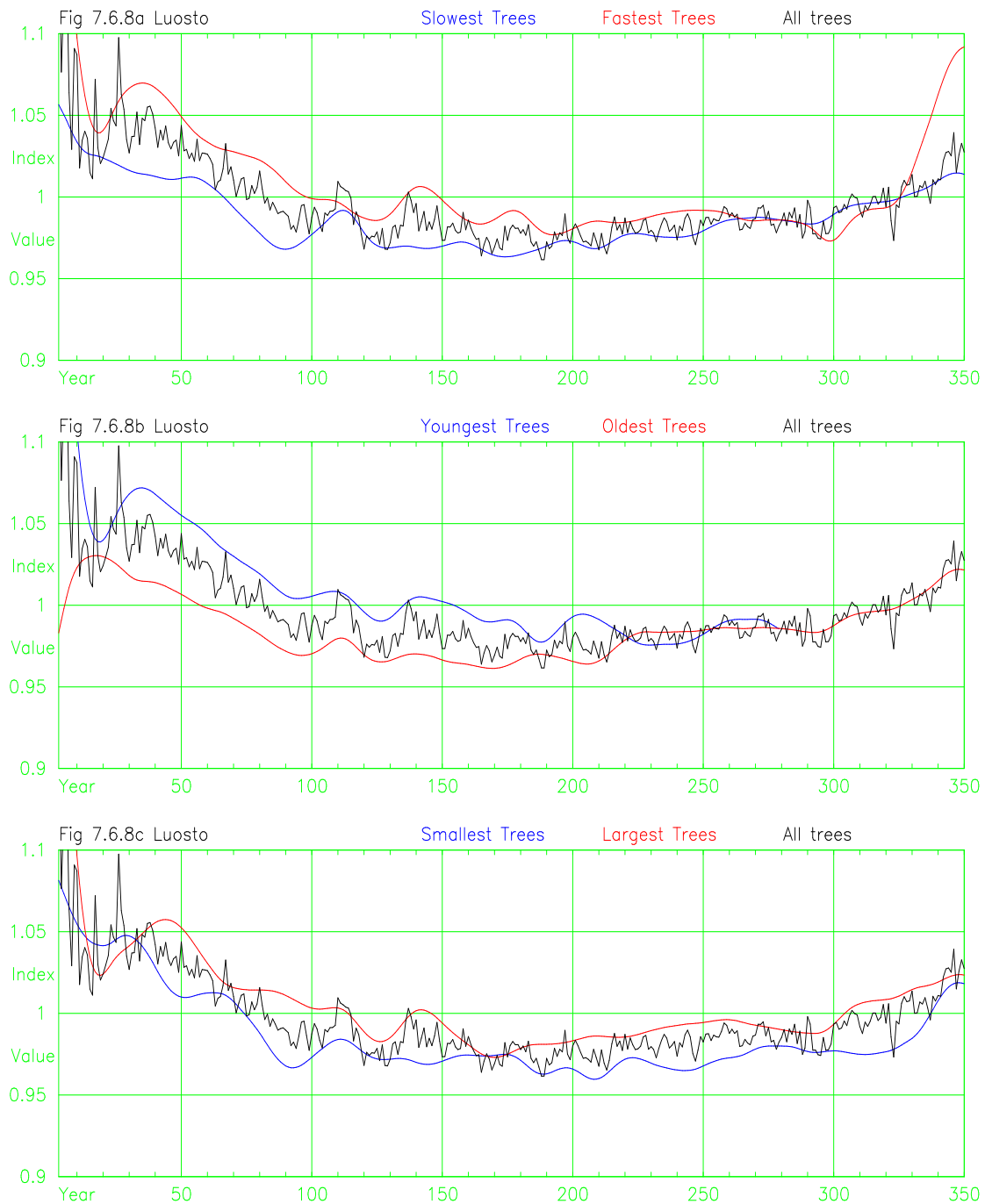


Figure 7.6.8 Mean PBS indices for the Luosto site by ring age showing (a) slowest and fastest growing trees,(b) youngest and oldest trees, (c) smallest and largest trees.

### 7.6.7. Growth Efficiency of the PBS Model

Growth efficiency (Fraction) in the PBS model is estimated for each year of growth of each tree and is used to set site level upper and lower efficiency limits (Section 7.5.9).

“Fraction” is defined as the ratio of the carbon mass needed to grow the current ring and the carbon mass needed survive which is the cost of maintenance and replacement of senesced foliage and fine roots. Stages in the development of growth efficiency limits are shown in Figure 7.6.9 for the Luosto site. The age (a) and diameter (b) based RCS curves

for Fraction (red) are derived by averaging values of Fraction for each ring age and for each diameter. The mean value (red) and standard deviation (magenta) of Fraction by ring age (a) and diameter (b) are relatively smooth curves which have a roughly exponential decay. The upper “efficiency” limits for a site are created by multiplying the standard deviation by Bftop, adding this value to the mean, and fitting a modified negative exponential curve to the resulting values. The lower “efficiency” limits are created by multiplying the standard deviation by Bfbot, subtracting this value from the mean, and fitting a modified negative exponential curve to the resulting values. The upper (lower) efficiency limit used on each year of growth of each tree to implement the height growth strategy is the average of the upper (lower) limits for that ring age and that tree diameter. The values obtained from the diameter based and ring-age based Fraction curves by a tree will differ because diameter increase and age increase progress at differing rates.

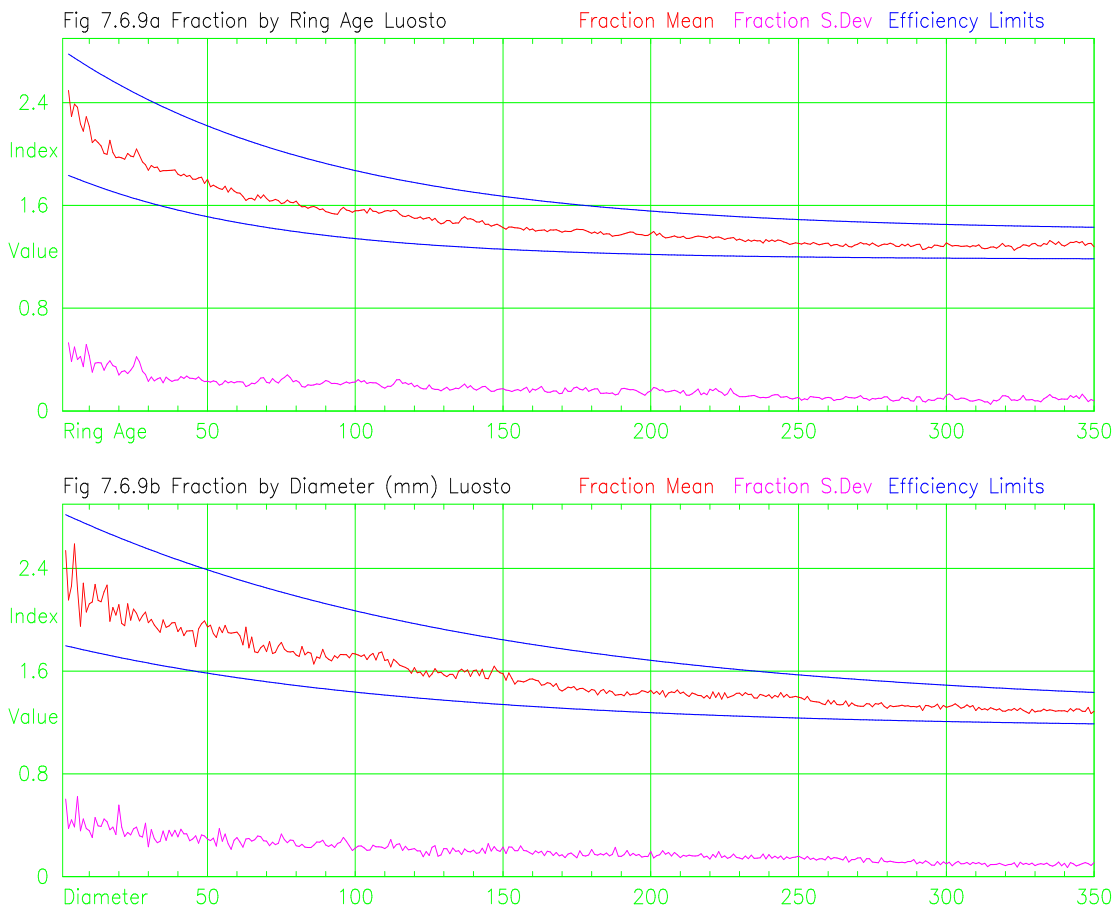


Figure 7.6.9 Fraction values and standard deviations plotted by (a) ring age and (b) calendar year with calculated upper and lower efficiency limits.

There is a requirement in the PBS model to have upper and lower “efficiency” limits and this method was chosen, by trial and error, from a number of possible alternatives because it appears to succeed. Once installed, this “efficiency based height growth strategy” is mainly controlled by three parameters (Gftop, Gfbot and Closs) with secondary control by three additional parameters (Saph, Maxh and Mpwr). Finding best fit values of these parameters for height growth would be possible as they are currently “best fitted” to sapwood area prediction. The main problem being the lack of tree measures from the sapling stages of tree growth, such as stem height, crown height and foliage mass, against which to evaluate best fit.

#### 7.6.8. Comparisons of the PBS model and other methods

The original RCS method is not suitable for use on “modern” chronologies in northern Fennoscandia because of the effects of modern sample bias (Section 5.4) and the distortion that is created in the RCS curve (Section 5.5.8) by the estimated 40% step increase in growth after 1920. There are insufficient trees in these chronologies to use the MRCS method (Section 5.7), so the SARCS method (Section 5.8) is used in these comparisons. Some comparison is also made against chronologies created using the Hugerhoff method as a representative of curve-fitting methods (Section 2.5.4). The preservation of long-timescale variance by the SARCS and Hugerhoff methods is limited to approximately half the length of the chronology. The preservation of long-timescale variance by the PBS model is limited to half the length of the chronology, at this stage of development, by the use of the Rsap parameter but there may be other, as yet undiscovered, restrictions. For these comparisons all three methods are considered here to have similar low-frequency variance restrictions.

The difference in the variance of chronologies (Table 7.6.2) has been reduced for presentation purposes, by setting the scales in Figures 7.6.10 and 7.6.11 to display from -3 to +3 standard deviations about the mean value, calculated over the period displayed. Chronologies created using the SARCS method (blue) and the PBS method (red) are plotted in Figure 7.6.10 for Luosto (a) and Helldalisen (b). These chronologies look remarkable similar, considering the completely different methods used to create the chronologies, and this gives hope that some degree of “common signal” is being found. Because the Helldalisen and Luosto chronologies both correlate well with July temperature, mean monthly July temperatures are used for comparison of the

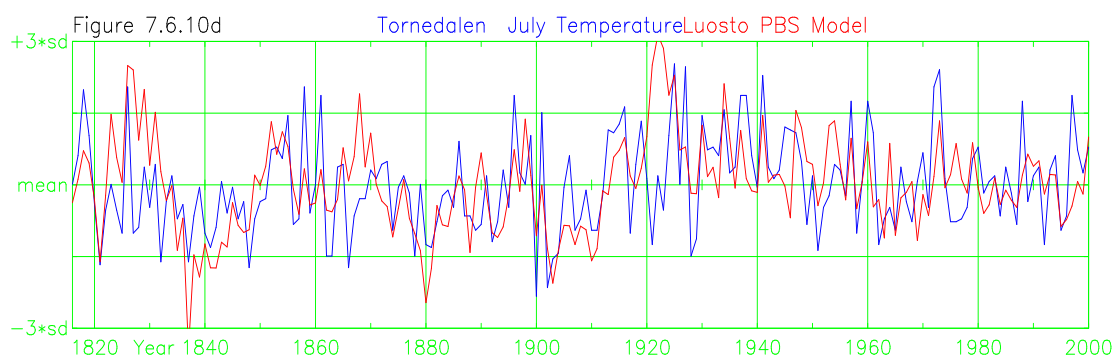
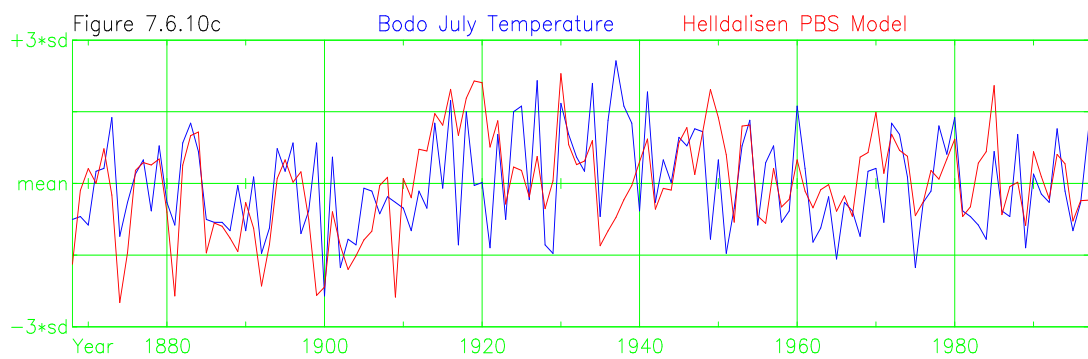
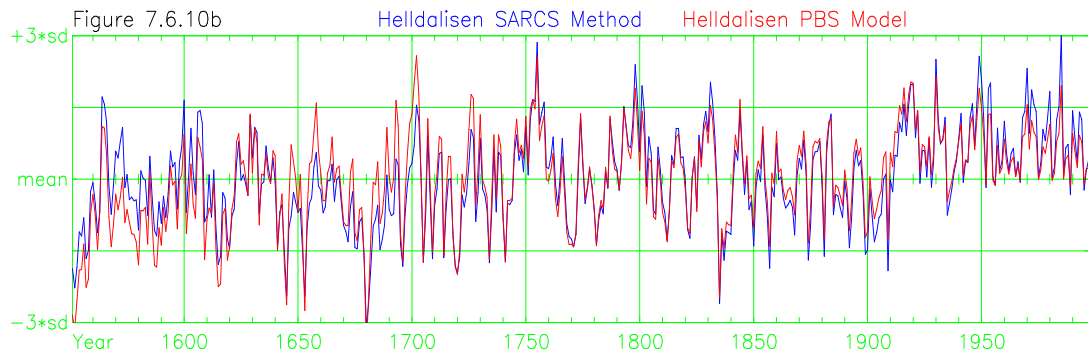
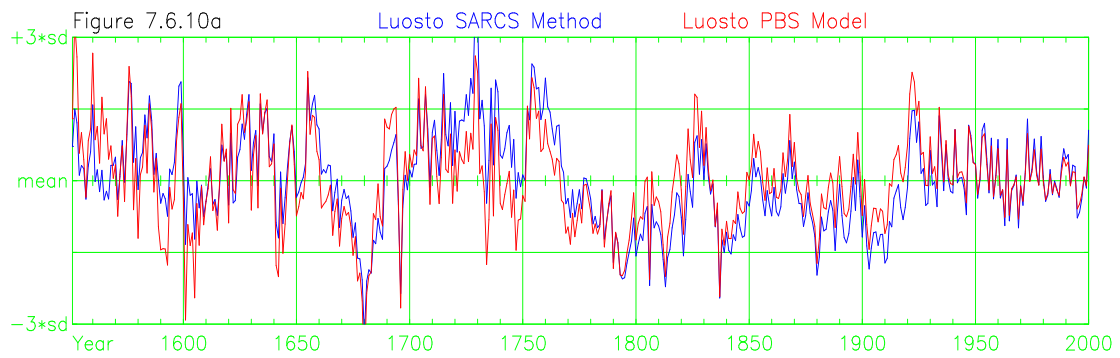


Figure 7.6.10 PBS model and SARCS method chronologies from (a) Luosto and (b) Helldalisen and PBS model chronologies and July temperatures (c) Helldalisen and Bodo and (d) Luosto and Tornedalen.

chronologies with measured climate data. In Figure 7.6.10c the PBS model generated chronology for Helldalisen (red) is plotted against the local July temperature record from Bödö (1867 to 1997) and the correspondence between the two is clear. There are periods, such as 1936-1940, when chronology indices and July temperature do not match but overall there is a reasonable match at decadal and longer timescales. In Figure 7.6.10d the

PBS model generated chronology for North Finland (red) is plotted against the, more distant (but longer) July temperature record from Tornedalen (1816 to 2000) and again the correspondence between the two is clear but in this case chronology indices and July temperatures do not match for the period 1921-1924.

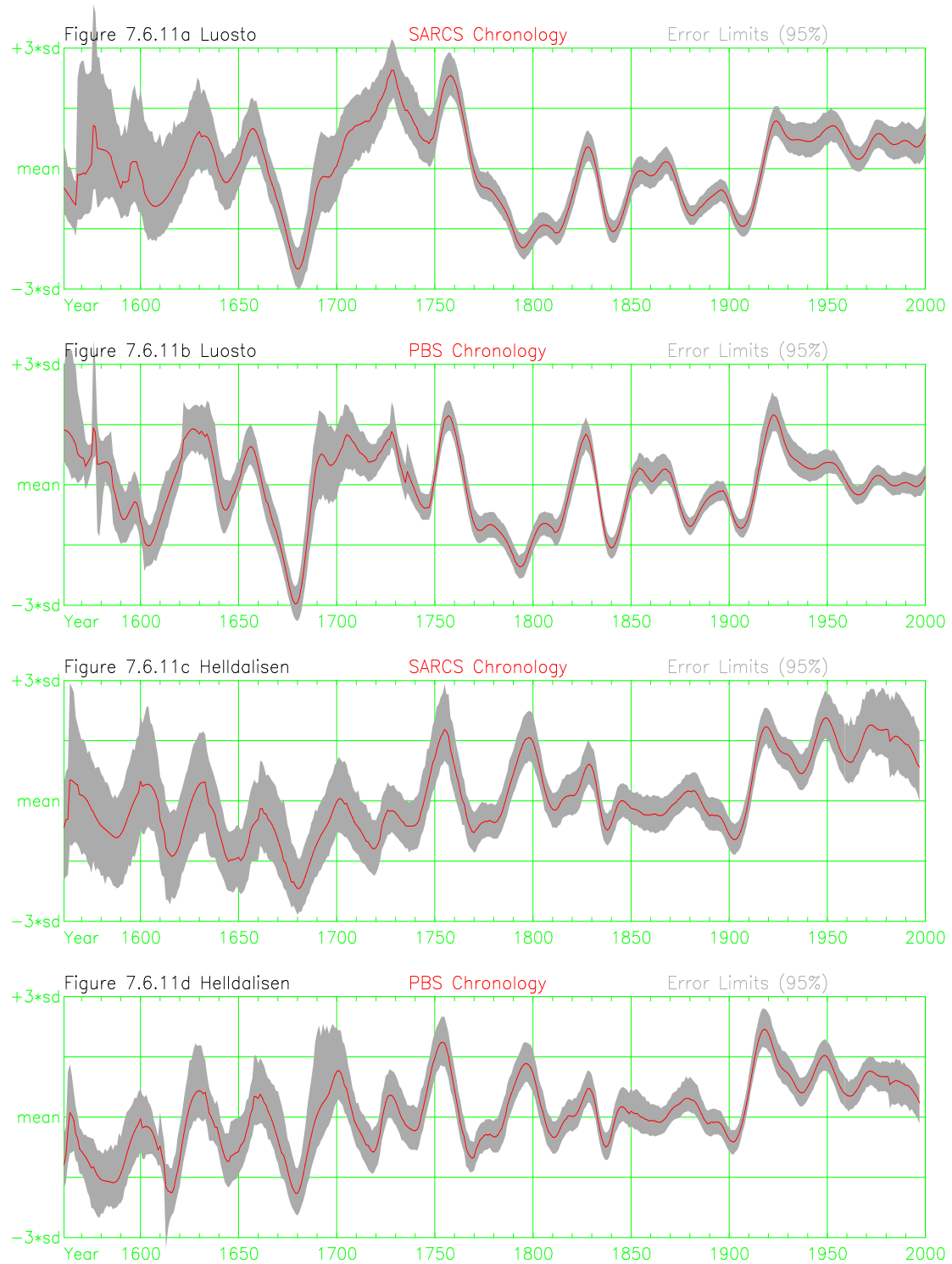


Figure 7.6.11 Chronology indices and their 95% confidence error limits, after smoothing tree indices with a 20-year spline, for (a) Luosto using SARCS method, (b) Luosto using PBS model, (c) Helldalisen using SARCS method, and (d) Helldalisen using PBS model.

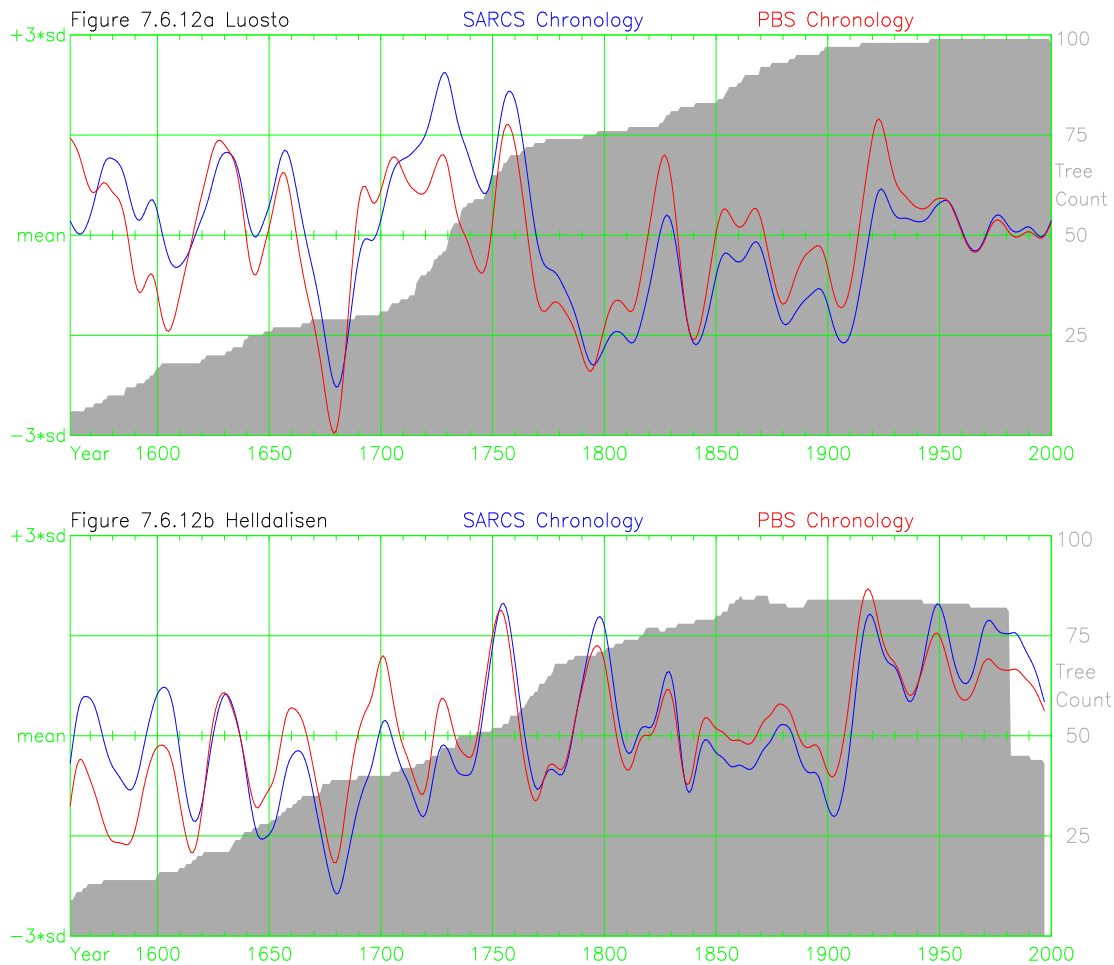


Figure 7.6.12 Comparison of SARCS and PBS chronologies after smoothing with a 20-year spline, for (a) Luusto, Finland and (b) Helldalisen, Norway.

Chronology indices and their 95% confidence limits, calculated using a bootstrap procedure (Cook 1990), are shown in Figure 7.6.11. The tree indices were smoothed with a 20-year smoothing spline (Cook & Peters 1981) prior to chronology creations and the error limits are for smoothed trees. The 95% confidence error limits for the PBS method are smaller than those for the SARCS method (albeit scaled in standard deviations). The first centuries of both chronologies have wider error limits reflecting lower tree counts and, in the case of the PBS model, problems in dealing with saplings. In the final 50 year period the PBS model has narrower error limits although this may be due to the reduced overall variance (approaches closer to the mean) rather than a genuine advantage in extracting the common signal and needs further investigation. Interestingly both chronologies have wider error limits during the period 1690 to 1720 and 1850 to 1870 despite the large distance between these sites. One important difference is that the step increase from 1920 onwards is maintained by the SARCS method whilst the PBS model chronologies become progressively closer to the mean after 1920. To highlight the differences between the SARCS and PBS the 20-year smoothed chronologies are plotted



in Figure 7.6.12. There are distinct differences in some periods which depend in part on the selection of slope for the SARCS method and, at this stage of development, the choice of parameter values for the PBS model.

Statistic (Standard Deviation)	Method	Luosto	Helldalisen
Mean Tree Indices	SARCS	1.0 (0.44)	1.0 (0.48)
	PBS	1.0 (0.13)	1.0 (0.13)
Mean Chronology Index	SARCS	1.0 (0.23)	1.0 (0.21)
	PBS	1.0 (0.08)	1.0 (0.07)
Mean correlation (tree to chronology)	SARCS	0.51 (0.21)	0.41 (0.20)
	PBS	0.53 (0.12)	0.47 (0.14)
R.Bar (mean tree to tree correlation)	SARCS	0.28 (0.29)	0.20 (0.23)
	PBS	0.31 (0.19)	0.24 (0.16)
Tree Indices - Mean Autocorrelation	SARCS	0.80 (0.09)	0.76 (0.09)
	PBS	0.68 (0.09)	0.67 (0.09)
Chronology Indices Autocorrelation	SARCS	0.72	0.67
	PBS	0.62	0.64
Correlation with Bødö July temperatures (1869 – 1997).	SARCS	0.38	0.45
	PBS	0.38	0.47
Correlation with Tornedalen July temperatures (1816 – 1997).	SARCS	0.49	0.39
	PBS	0.49	0.39

Table 7.6.2 Statistics comparing tree and chronology indices created using the SARCS and PBS methods and the Luosto and Helldalisen trees.

	PBS Luosto	SARCS Helldalisen	PBS Helldalisen
Full period (1550-1997)			
SARCS – Luosto	0.84	0.31	0.30
PBS – Luosto	-	0.25	0.25
SARCS – Helldalisen	-	-	0.91
Ignoring first 50 years (1600-1997)			
SARCS – Luosto	0.88	0.34	0.37
PBS – Luosto	-	0.35	0.43
SARCS – Helldalisen	-	-	0.92
High-Pass Filtered (1600-1997)			
SARCS – Luosto	0.96	0.40	0.40
PBS – Luosto	-	0.41	0.42
SARCS – Helldalisen	-	-	0.98
Low-pass filtered (1600-1997)			
SARCS – Luosto	0.85	0.33	0.37
PBS – Luosto	-	0.32	0.44
SARCS – Helldalisen	-	-	0.90

Table 7.6.3 Correlations between SARCS and PBS chronologies from Luosto and Helldalisen (Filters using spline with 50% cut-off at 10-years).

Table 7.6.2 lists some statistics of tree indices and chronologies created using the PBS model and SARCS method using the Luosto and Helldalisen trees. The overall mean values of tree indices are set to 1.0 by convention but the standard deviation of tree and

chronology indices created by the SARCS method is roughly three times that of those created by the PBS model. Between-tree and tree to chronology correlations at both sites are slightly higher using the PBS model than using the SARCS method. The standard deviations of between-tree and tree to chronology correlations are much lower using the PBS method than using the SARCS method, suggesting that fewer trees are needed to establish critical chronology confidence levels. The mean of autocorrelation within tree indices and the autocorrelation in the chronology are lower when using the PBS model than when using the SARCS method. Correlations between mean July temperatures, from Bödö and Tornedalen, and chronology indices over their common periods are similar for PBS and SARCS chronologies. Table 7.6.3 presents between method and site chronology cross correlations and the results are similar for both methods.

Making detailed interpretations from these results and statistics at this stage of development of the PBS model would be premature. The first 50 years of the Luosto chronology created using the PBS model slopes downwards (Figure 7.6.11b) in comparison to the other chronologies (Figures 7.6.11 a, c, and d). The first 50 years of the Luosto chronology has tree counts less than 10, the SARCS method may well have some residual “end effects”, and the PBS model has problems with saplings leaving a situation difficult to resolve without the use of more sites and trees. The high-pass filtered correlations (Table 7.6.3) are consistent across both methods (SARCS and PBS) suggesting that both methods preserve high-frequency variance. The low-pass filtered correlations are similar to the unfiltered correlations (1600-1997) with the PBS Luosto to PBS Helldalisen correlation between sites being significantly larger than the SARCS correlation between sites. From a dendroclimatic viewpoint the PBS model is producing tree and chronology indices with characteristics similar to those produced by other methods of standardisation and as such this feasibility study can claim to have a positive result, a process-based standardisation model is feasible. The testing of the preservation of multi-century variance by the PBS model must wait until the PBS model is applied to long sub-fossil chronologies.

### **7.7. Conclusions and Further Development**

The need for a “process” model in dendroclimatology arises from the known limitations of existing techniques. The observation, that climate controls the production rate of foliage, suggests the need to convert ring width measures into measures of foliage

production rate. The development of expected growth curves in the RCS method, with its previous focus on the use of ring age, has been improved by the additional consideration of diameter (Chapter 5) and the use of other variables, such as tree heights, are likely to produce further benefits. This logic suggests the value of a process based standardisation model, designed to incorporate the multiple non-linear relationships involved in tree growth. A number of existing tree-growth models were examined, relevant processes and parameters were identified and extracted, and these were developed into the PBS model. To meet the dendroclimatic requirements, some processes not normally found in tree-growth models have had to be developed. The fundamental concept underlying this model is that the main constraint on tree growth is mechanical. This is unique, at least in the context of the tree-growth models examined for this study. The modelling of the senescence of sapwood as a variable to achieve a balance (between sapwood area, foliage mass, and mechanical strength) has apparently not been used in other tree-growth models. That these mechanical and senescence assumptions were needed to make the PBS model work does not guarantee they are correct, but simply that they have value in this application. The mechanical rules used in the PBS model limit its application to trees with circumferential growth, because of the presumed relationship between height and diameter.

The development of a fully operational and rigorously tested PBS model will require considerably more research than has been possible in the limited time available for this study and as such this description should be considered only as a report of progress to date. A large number of assumptions were made in order to produce a model that could grow trees from series of ring measurements and meet the test of estimating the final sapwood area of each tree. Currently, the PBS model grows trees and meets this sapwood area test but suffers from a number of problems arising from some of the processes which have not yet been implemented. Examination of the problems identified so far, suggest that they can be solved with the application of further work. After further modifications that will hopefully resolve these problems, a wider-ranging testing of the capabilities and characteristics of the PBS model is envisaged. The tuning of parameters, as used within this study to investigate the feasibility of a PBS model, will limit the ability to establish the common signal found in tree growth. Standardising dendroclimatic chronologies which have small numbers of trees, typically 15 to 25, will require the use of fixed parameter values in order to maintain levels of “freedom of choice”. The use of the PBS

model as a general tool by people, whose expertise is in other fields, will require the careful development and testing of specific parameters, instructions and descriptions of the general applicability of the PBS model.

An explicit description of bark is needed in the PBS model. Given that for stem, branches and trunk roots the areas and diameters are known this should be relatively straightforward. Parameter values for bark thickness, senescence rate, and respiration costs can be established from forestry data and appropriate algorithms added to the PBS model. An explicit description of the cost of reproduction is needed in the PBS model. The first stage would be to establish the “average” annual cost of reproduction over the life of a tree (from forestry data), which may vary with age, size or productivity rate and then incorporate these costs into the PBS model. (The second stage of attempting to model the year to year variability of reproduction costs is likely to be too difficult for the current PBS model because this annual variability is likely to depend on climatic influences and as yet tree-growth models, using known climate, have limited abilities in the prediction of the annual variability of reproduction costs.) An explicit description of the change in wood density as a tree changes from small sapling to mature tree is needed in the PBS model. Empirical descriptions of wood density over the life cycle of trees are available and can be used to adjust the volume, mass and mechanical strength calculations within the PBS model. An explicit description of the year to year storage of carbohydrate in sapwood is needed in the PBS model and again empirical values can be extracted from tree-growth models and forestry data.

These four additional processes should resolve some of the problems of the PBS model with respect to the first decades of tree growth, restriction in the resolution of long-timescale variance, and the excessive autocorrelation of series of growth indices.

Testing of the PBS model has been limited to date to the use of the mean ring width measures for each tree. Future testing must be undertaken, specifically of the abilities of the height growth strategy and mechanical strength algorithms used to grow trees, using the individual cores for each tree which will enable within-tree comparisons to be made. Testing of the PBS model has been limited to the use of tree measures obtained within this study and there is a need to obtain data from external sources. An important test needed is a comparison of modelled carbon production by foliage in northern

Fennoscandia with available measurements of photosynthesis rates. The PBS model also needs to be applied to long chronologies of sub-fossil trees. The long-timescale characteristics of chronologies created using the PBS model will need detailed investigation. The PBS model needs to be run using trees of other species which are commonly used in dendroclimatology. This will require developing suitable parameter values for other species and will allow the differentiation of parameters; e.g. all species parameters, species specific parameters, site specific parameters and possibly latitude or altitude parameters. Testing PBS models against measured climate variables is problematic because correlations and regressions are unsuited to low-frequency comparisons over the relatively short period of climate measurements.

The assessment of the ability of the PBS model to preserve long-timescale variance is incomplete at this stage. Variation of the carbon production rate by foliage allows different periods of growth to produce series of PBS Indices with differing mean values, thus giving the PBS model (theoretical) unlimited capability to preserve long-timescale variance. The use of a “fitted” value for sapwood maintenance (Section 7.6.6), in the current implementation of the PBS model, limits the preservation of low-frequency variance in the slope of series of tree indices to that of the length of the chronology, i.e. if sapwood maintenance values are tuned to fit, then the average slope of all series of indices is set to zero. The current PBS model thus has the same theoretical low-frequency limits as the RCS method. It can preserve variance in the mean values of series of tree indices but is unable to preserve variance in the slope of series of tree indices beyond the length of the chronology. These limits can only be tested fully using long chronologies of sub-fossil trees and this task has not been performed. The comparisons of Figure 7.6.10 (a) and (b) suggest that the PBS chronologies generated at this stage of model development have similar variance to those of the SARCS chronologies, when used on modern chronologies.

Models can be used to improve understanding of the systems being examined and, in the PBS model case, forcing the “rules” of tree growth to conform to series of annual measures is an exacting test of these rules. The PBS model appears to “predict” mortality based on a combination of tree size and the random probability of extreme (negative) climatic forcing. Trees approaching the maximum size lose so much sapwood in poor growth years that they need a number of average or above average years following a bad

year in order to recover. The PBS model would thus predict that the largest trees will occur in areas with the least climatic (common forcing) variation in the growing season. Average growth rates need not be high but the sort of climate that produces series of tree rings that are so uniform that crossdating is difficult will produce very large trees. (This prediction was not tested here.) The observations from the Fennoscandian trees used in this project, that to become one of the largest trees, a tree must grow quickly, and that to become one of the oldest trees, a tree must remain below maximum size, is consistent with this PBS model prediction in a widely varying climate.

This project started out considering that trees obey macro rules. The learning process of developing the PBS model led a realisation that “decision taking” by trees is best modelled as the result of trees obeying micro rules i.e. each cell responds to its internal state and (maybe) a comparison with neighbouring cells. The difficult calculations required to conform to the macro level "mechanical theory of uniform stress" (Metzger 1893) can be achieved at individual cell level. A modelled cambium cell is only allowed to take growth material to increase the strength of the cell it is growing if that cell is weaker than the strength of all its neighbouring cells. Repeatedly asking this question of all cambium cells in order to control cell growth in a modelled tree will ensure that stress is equalised throughout the outer surface of all wood. If variable fine root to foliage ratios are introduced to the PBS model then methods used by the “transport-resistance” model (Thornley 1991) become attractive because they fit this ideal of cell level decisions. One conclusion is that improvements to the PBS model by the addition of new processes are likelier to be easier to implement and more successful if trees are considered to respond at a cell level (a bottom up approach) as opposed to the presumption that trees follow macro rules (a top down approach).

The value of “growth” produced by the PBS model has units of kilograms per unit foliage and is not relative in any way. Comparison of the series of “growth” values from one tree against those from another tree (or the mean values of a group of trees) is possible (not by correlation but as absolute values) leading to a potential use of the PBS model in the crossdating of trees. The reduced standard deviation of tree-to-chronology and between-tree correlations along with the small increase in the values of these correlations leads to the potential to apply the PBS model to the crossdating of trees. Current crossdating methods only use high-frequency variance and correlation techniques which give

considerable weight to a few extreme values. Foliage production rates are possibly a more consistent measure of common forcing than ring width and the medium-frequency variance is likely less dependent on the characteristics of an individual tree. The use of foliage production rates has the potential to match the common signal of trees with fewer trees or with shorter samples. The extreme reaction by the PBS model, of discarding 50% of sapwood, to zero growth rings (or inserted zero rings) facilitates the correct positioning of missing rings. The potential ability of the PBS model to follow the protracted deviations from normal growth that are sometimes found in ring measures, such as when water logging of roots produces ring widths only 10% of average for a period of decades before the ground dries and the tree recovers, will improve the ability to crossdate trees. Further work is needed to explore this potential application of the PBS model.

The PBS model converts ring measures to estimates of carbon generated by unit foliage and could be run (with adjustment) in the reverse direction. Trees could be used to produce a chronology representing carbon production rates and these annual values could be used to predict the growth rate of individual trees whose final ring is earlier than the end of the chronology (prediction beyond the range of recorded values is not possible using the PBS model). The ability to assess the position of the sapwood-heartwood boundary will enable the prediction of mortality dates for trees with some missing sapwood rings. Trees can be grown from their current end point to a stage where the known sapwood-heartwood boundary is in the correct position and the year of the final ring becomes a prediction of the year mortality occurred.

The PBS model assesses the mass of carbon produced by unit foliage for each year. The photosynthesis modules of tree-growth models, such as GUESS (Smith et al. 2001), also assess the annual mass of carbon produced by foliage. The PBS model generates an important link between dendroclimatic tree growth measures and a key variable used by most tree growth and ecosystem models, and this link has the potential to enable new areas in climatic research. The tree-growth model GUESS could be run using measured climate data and the resulting production rate of carbon by foliage could be compared with the PBS model output. Selected series of climate years (a full set of annual temperature measures, precipitation, cloud cover etc) could be calibrated by their resulting carbon production rates using both GUESS and the PBS model. The difference in tree growth rates, resulting from a specific climate variable, such as mean July

temperature could be investigated. A large number of climate years could be collected for Fennoscandia and tree-ring chronologies such as Tornetrask and Finnish-Lapland could be used to select a several millennia long sequence of climate years that would “grow” the tree samples from these sites. A poor growth year may have many causes e.g. drought, cool summer, or volcanic eruption, so care would be needed. Comparing the output of climate models with a tree-ring derived climate for the Holocene would be an interesting exercise.

Tree-ring chronologies do not give estimates of the rate of carbon sequestration by ecosystems because they lack information concerning stem diameter, tree height, stocking density, species distributions and soil conditions. If the PBS model derived carbon production rates were used to drive a tree-growth model such as GUESS then carbon sequestration rates could be assessed over all periods covered by dendroclimatic samples. Using the output from dendroclimatic chronologies to control tree-growth models has the potential to produce a general improvement to our knowledge of carbon sequestration during the Holocene. The main conclusion is that the PBS model approach is a potential alternative to the traditional standardisation methods used in dendroclimatology.



## **Chapter 8. Conclusions**

### **8.1. Project description and methods**

This thesis makes a major contribution towards methods of isolating the long-timescale variance of climatically controlled tree growth. Knowledge gained from tree-growth models was applied to a detailed analysis of those standardisation methods designed to retain long-timescale variance, in particular the assumptions underlying the Regional Curve Standardisation approach (RCS). This study has highlighted a number of systematic errors and led to the development of alternative methods which avoid or reduce the major biases that can arise in chronologies because of these errors. A fundamental assumption was made, at the outset of this work, that the common forcing on tree growth operates through climatic control of the rate of photosynthesis and that the “climatically” controlled rate of carbon production by foliage in a year is expected to be common to all trees of a specific species at a site. A tree’s foliage mass sets the “expected growth rate” of that tree for a specific year independently of the amount of “climatic forcing” in that year and this definition of tree-growth was used in both the examination of existing standardisation methods and to inform choices made in the development of new techniques. New methods of standardisation - Multiple Regional Curve Standardisation (MRCS) and Size Adjusted Regional Curve Standardisation (SARCS) - were developed in order to overcome some of the problems of the existing RCS method. Comparisons of chronologies generated using the new and old methods were made, assessment of error levels was made, and chronologies were compared with measured climate data. The observation that climate controls the production rate of foliage implies a need to convert ring width measures into measures of foliage production rate and to this end a Process Based Standardisation model (PBS) was developed to incorporate some of the non-linear relationships involved in tree growth. This is an entirely original approach to standardisation in dendroclimatic studies and opens up a new development route for dendroclimatic studies.

### **8.2. Summary of major findings**

A summary of the major findings relating to potential limitations or weaknesses in important implementations of existing approaches (especially RCS) follows, together with the new concepts developed to overcome these problems:

- Bias was found to be caused by estimating the age-related growth trend from series of ring measures which contain the effects of common forcing. This bias has been termed *trend distortion*. A new method of generating expected growth curves from *signal-free* measures which mitigates the problem of *trend-distortion* is presented. For RCS based methods the bias is removed from the RCS curves.
- Tree indices developed using the RCS method were found to have systematically biased age and diameter related slopes for size, age and growth rate classes of tree. New methods of generating expected growth curves from RCS curves that take account of both age and diameter were developed which largely overcome this problem.
- The tree measures used in this study show that fast growing trees generally do not become the oldest trees and that slow growing trees do not become the largest trees. Convincing evidence is presented to demonstrate that this leads to a systematic bias in chronologies generated by the RCS method using tree samples taken from one point in time. This bias has been termed *modern sample bias*. A new method of averaging tree indices, the Best Fit Means method (BFM), was developed which overcomes the problem of *modern sample bias* by rescaling each series of tree indices.
- Examination of tree growth rates and chronology error bars showed that natural, non-climate related, variability of tree growth rates increases the number of trees needed for the existing RCS method to generate chronologies, a problem which is known and accepted. The newly developed BFM method of averaging tree indices also mitigates this problem.
- The reasons why the existing RCS method is unsuitable for the standardisation of *modern chronologies* were investigated and confirmed. A new method of standardisation, SARCS, is presented which is suitable for the standardisation of *modern chronologies* and can preserve long-timescale variance in chronologies without the need for sub-fossil trees which grew in earlier periods.
- Examination of tree-growth models showed that the empirical relationship between tree growth rates and climatic forcing is the result of a number of factors, some of which are known and quantified. The PBS model was designed as a standardisation method which can account for many of the known factors relating

tree growth to climatic forcing and is presented as a potential tool for future investigation.

### **8.3. Project's strengths and weaknesses**

A number of new concepts and methods are introduced in this project and these lead to benefits although there is a cost or limitations attached to some of these benefits. Below, some conclusions and limitations are discussed:

#### **Best Fit Means method (BFM)**

The examination of various published tree-growth models suggested that the size of ring width is not a direct measure of the common forcing on tree growth but that year to year changes in the size of ring width will reflect annual changes in the magnitude of the common forcing on tree growth. The contemporaneous existence of fast and slow growing trees in all years of the Tornetrask AD and Finnish-Lapland AD chronologies is evidence that common forcing does not fully control tree growth rates and the demonstration in this project that fast and slow growing trees independently preserve the same low-frequency "common signal" enable the important conclusion that tree growth rates are not necessary to the preservation of long-timescale variance. The BFM method was introduced to establish long-timescale variance from tree growth indices by *overlapping* the variance of individual trees without the need to use mean tree growth rates. The BFM method requires series of indices which can have an overall slope and is thus limited to indices generated by RCS based standardisation methods and the BFM method requires sufficient *overlapping trees* to accurately generate the long-timescale variance. The main advantages of the BFM method over the traditional arithmetic means method used in the RCS method are that the BFM method reduces some sampling constraints, reduces the magnitude of error bars, overcomes some major bias problems, and allows the use of both age and diameter in the generation of expected growth values from RCS curves.

#### **Growth rate**

The RCS method uses the mean growth rate of trees through time, assessed from ring-width at a given cambial age, and assumes that this mean growth rate is a product of climate forcing. Using the RCS method, it is possible to compare the growth rates of trees between sites or along latitudinal or altitudinal gradients. The ability to compare tree

growth rates is lost by the BFM method because each tree is rescaled. Chronologies built by the BFM method use the change in growth rate over the life of a tree to assess the mean change in growth rates over time which forms the chronology. The RCS method is the only tool for some applications requiring growth rate comparisons.

### **Fractional deviations**

The observation that climate controls the carbon production by foliage leads to the need to remove the effects of foliage mass from series of measures by division. Indices created by dividing ring widths by expected growth values will be fractional deviations which represent the magnitude of common forcing on tree growth. In this work, chronology indices have been assumed to be fractional deviations and this leads to the use of multiplication to manipulate the values of measurements and indices. Multiplication is a commonly used method in standardisation, but for some of the new methods developed here it becomes a necessity. Multiplication is intrinsic to the BFM method, enables the generation of *signal-free* measures, and enables the reversible procedure to *rotate* chronologies with arbitrary slopes.

### **Testing for age/diameter related bias**

Expected growth curves are used to remove the age-related growth trend from series of measures. Testing that the age-related growth trend has been removed from series of tree indices is often performed by examining mean indices aligned by calendar year for different classes of tree. In this thesis testing the presence of age and diameter related bias in tree indices is examined by aligning tree indices by age or diameter for different classes of tree. These methods were used to show that the standard RCS method produces series of tree indices with systematic age and diameter related biases which can seriously distort the modern end of resultant chronologies.

### **History in expected growth**

The conclusion is reached here that in order to remove the age related bias, arising in ring measures from increasing stem diameter and changing foliage mass over the life of a tree, from series of tree indices the history of growth of a tree must be used in the creation of expected growth curves. The foliage mass and hence expected growth rates of a tree are dependent on the history of growth of a tree and both age and diameter will be needed to estimate expected growth values capable of reducing/removing the age related bias..

### **Signal-free measures**

Expected growth and RCS curves are often generated using series of measurements which contain the effects of common forcing and in this thesis it is shown that expected growth and RCS curves can be distorted by the presence of the common forcing signal. The concept of signal-free measures, created using iterative procedures, was developed into a practical method to reduce the magnitude of this distortion.

### **Rotation of chronologies**

Standardisation methods may produce series of tree indices or chronologies whose slopes are not known and these slopes are usually retained. It is recognised that the new methods of standardisation proposed here produce chronologies with an arbitrary slope. It follows that the overall slope of chronologies is not defined and must be fixed by reference to a default value of slope (e.g. zero), instrumental data, or other external data. The pragmatic decision was made here to generate chronologies whose properties allow slope adjustment i.e. chronologies can be rotated. In setting the slope of the chronology there is potential for error and this will depend on (among other things) the time period over which the slope is set, using longer time periods will reduce error. The conclusion here is that the existence of arbitrary slopes requires careful interpretation and, because arbitrary slopes need to be set to some value, the effect that setting the slope has on the retention of long-timescale variance needs to be stated.

### **Error assessment**

The examination of chronology uncertainty (or error) in this thesis confirmed the known problem that to assess low-frequency variance with similar confidence levels to those of high-frequency variance, several times more tree samples are needed for each year of the low-frequency chronologies than are needed for the high-frequency chronology. A method of assessing the stability of chronologies built using the BFM method is proposed in this thesis to allow confidence levels to be assessed over the span of a chronology. Chronologies created using the BFM method become unstable at points in time where there are insufficient trees or *overlapping rings* and this leads to the conclusion that all chronologies created using the BFM method **must** be checked for stability.

## **MRCS and SARCS**

Two new methods of standardisation were developed in this thesis and are proposed to overcome some of the problems inherent in the traditional RCS method. MRCS and SARCS are based on the concepts of the RCS method. Both methods use diameter and ring age to produce expected growth values, use signal-free measures to produce RCS curves, use the BFM method to average tree indices, generate chronologies with an arbitrary slope which can be reset by rotation, and retain long-timescale variance to the length of the chronology. The MRCS method uses multiple RCS curves and requires several hundred trees whilst the SARCS method stretches RCS curves to fit and can be used on modern chronologies with fewer trees. Comparisons of the RCS, MRCS and SARCS methods showed that they produce similar low-frequency signals in the central portions of chronologies. There are notable differences between old (RCS) and new methods (MRCS and SARCS) in the most recent centuries and the conclusion here is that this is the result of a reduction of systematic bias by the MRCS and SARCS methods. Comparison of chronologies with measured temperature series showed that variance of the common signal derived from trees matches variance in the temperature records but the methods used to compare chronologies and temperature series (correlation and regression techniques) failed to distinguish between the standardisation methods analysed in this thesis. The observation that chronologies contain high-frequency variance in common with temperature measurements does not confirm the assumption that there will be low-frequency variance in common.

The BFM method, the use of climate-free measures, the allowance for diameter in developing expected growth curves, and the rotation of chronologies are all techniques which might be singly applied to improve existing standardisation methods. The MRCS and SARCS methods are presented as internally consistent methods of standardisation which can be used, within specified constraints, by dendroclimatologists.

## **PBS Model**

The benefits obtained in this study from the identification and removal of major sources of age and diameter related bias from tree growth indices by generating “better fitting” expected growth curves is only a partial solution to this problem. The PBS model was designed to incorporate the multiple non-linear relationships involved in tree growth. A large number of assumptions were made in order to produce a model that could grow

individual trees from series of ring measurements and meet the test of estimating the final sapwood area of each tree. Two concepts not normally found in tree-growth models, that a major constraint on tree growth is mechanical and that the senescence of sapwood is variable, were needed in order to develop this working model. The PBS model directly estimates the mass of carbon generated by unit foliage and forms an important link between dendroclimatic tree growth measures and tree-growth models. An important conclusion of this project is that the PBS model approach is a potential alternative to the traditional standardisation methods used in dendroclimatology.

### **PBS Future**

In order to improve the PBS model explicit descriptions of bark, the cost of reproduction, and the storage of carbohydrate in sapwood are needed. The PBS model needs to be run using long chronologies of sub-fossil trees in order to fully test the long-timescale characteristics of generated chronologies. The PBS model needs parameter sets and relevant testing with other tree species. The outputs from the PBS model need to be compared with the outputs of photosynthesis and tree-growth models driven by measured climate data. Future development of the PBS model is justified by the results generated in this thesis, but development will require a project of one or more years.

Process based modelling has the potential to supplant existing dendroclimatic standardisation methods in the coming decade but much work is needed to develop the methods and skill of modelling to the levels required for the application of the PBS model to dendroclimatic data sets representing tree growth on a worldwide basis.

## Reference List

- Badeau, V., Becker, M., Bert, D., Dupouey, J., Lebourgeois, F. & Picard, J. F. 1996. Long-term growth trends of trees: Ten years of dendrochronological studies in France. In Spiecker, H., Mielikainen, K., Kohl, M. & Skovsgaard, J. P. (Eds) *Growth Trends in European Forests* (pp. 167-181). Berlin: Springer.
- Baillie, M. G. L. 1994. Dendrochronology raises questions about the nature of the A.D. 536 dust-veil event. *Holocene* 4: 212-217.
- Becker, M. 1989. The role of climate on present and past vitality of silver fir forests in the Vosges mountains of northeastern France. *Canadian Journal of Forest Research-Revue Canadienne de Recherche Forestiere* 19: 1110-1117.
- Beerling, D. J. & Woodward, F. I. 1996. In situ gas exchange responses of boreal vegetation to elevated CO<sub>2</sub> and temperature: First season results. *Global Ecology and Biogeography Letters* 5: 117-127.
- Biondi, F., Myers, D. E. & Avery, C. C. 1994. Geostatistically modeling stem size and increment in an old-growth forest. *Canadian Journal of Forest Research-Revue Canadienne de Recherche Forestiere* 24: 1354-1368.
- Bjorklund, L. 1999. Identifying heartwood-rich stands or stems of *Pinus sylvestris* by using inventory data. *Silva Fennica* 33: 119-129.
- Bonan, G. B., Pollard, D. & Thompson, S. L. 1992. Effects of Boreal forest vegetation on global climate. *Nature* 359: 716-718.
- Botkin, D. B., Janak, J. F. & Wallis, J. R. 1972. Some ecological consequences of a computer model of forest growth. *Journal of Ecology* 849-873.
- Bradley, R. S., Briffa, K. R., Cole, J. & Osborn, T. J. 2003. The climate of the last millennium. In Alverson, K. D., Bradley, R. S. & Pedersen, T. F. (Eds) *Paleoclimate, Global Change and the Future* (pp. 105-141). Berlin: Springer.
- Bradley, R. S. & Jones, P. D. 1992. Climate Since A.D. 1500: Introduction. In Bradley, R. S. & Jones, P. D. (Eds) *Climate Since A.D. 1500* (pp. 1-16). London: Routledge.
- Braker, O. U. 1981. Der Alterstrend bei Jahrringdichten und Jahrringbreiten von Nadelholzern und sein Ausgleich. *Mitteilungen der Forstlichen Bundesversuchsanstalt Wien* 142: 75-102.
- Briffa, K. R. Tree climate relationships and dendroclimatological reconstructions in the British Isles. 1984 Thesis. University of East Anglia, Norwich, UK.
- Briffa, K. R. 1995. Interpreting high-resolution proxy climate data - the example of dendroclimatology. In von Storch, H. & Navarra, A. (Eds) *Analysis of climate variability: applications of statistical techniques* (pp. 77-94). Berlin: Springer.
- Briffa, K. R., Bartholin, T. S., Eckstein, D., Jones, P. D., Karlen, W., Schweingruber, F. H. & Zetterberg, P. 1990. A 1,400-year tree-ring record of summer temperatures in Fennoscandia. *Nature* 346: 434-439.
- Briffa, K. R. & Jones, P. D. 1990. Basic Chronology Statistics and Assessment. In Cook, E. R. & Kairiukstis, L. A. (Eds) *Methods of Dendrochronology* (pp. 137-152). Kluwer Academic Publishers.
- Briffa, K. R., Jones, P. D., Bartholin, T. S., Eckstein, D., Schweingruber, F. H., Karlen, W., Zetterberg, P. & Eronen, M. 1992a. Fennoscandian summers from AD-500 - Temperature-changes on short and long timescales. *Climate Dynamics* 7: 111-119.



- Briffa, K. R., Jones, P. D. & Schweingruber, F. H. 1992b. Tree-ring density reconstructions of summer temperature patterns across western North-America since 1600. *Journal of Climate* 5: 735-754.
- Briffa, K. R., Jones, P. D., Schweingruber, F. H., Karlen, W. & Shiyatov, S. G. 1996. Tree-ring variables as proxy-climate indicators: Problems with low frequency signals. In Jones, P. D., Bradley, R. S. & Jouzel, J. (Eds) *Climatic Variations and Forcing Mechanisms of the Last 2000 Years* (pp. 9-41). Berlin: Springer-Verlag.
- Briffa, K. R., Jones, P. D., Schweingruber, F. H., Shiyatov, S. G. & Cook, E. R. 1995. Unusual 20th-century summer warmth in a 1,000-year temperature record from Siberia. *Nature* 376: 156-159.
- Briffa, K. R. & Matthews, J. A. 2002. ADVANCE-10K: a European contribution towards a hemispheric dendroclimatology for the Holocene. *Holocene* 12: 639-642.
- Briffa, K. R. & Osborn, T. J. 1999. Perspectives: Climate warming - Seeing the wood from the trees. *Science* 284: 926-927.
- Briffa, K. R., Osborn, T. J., Schweingruber, F. H., Harris, I. C., Jones, P. D., Shiyatov, S. G. & Vaganov, E. A. 2001. Low-frequency temperature variations from a northern tree ring density network. *Journal of Geophysical Research-Atmospheres* 106: 2929-2941.
- Briffa, K. R., Osborn, T. J., Schweingruber, F. H., Jones, P. D., Shiyatov, S. G. & Vaganov, E. A. 2002. Tree-ring width and density data around the Northern Hemisphere: Part 1, local and regional climate signals. *Holocene* 12: 737-757.
- Briffa, K. R., Schweingruber, F. H., Jones, P. D., Osborn, T. J., Harris, I. C., Shiyatov, S. G., Vaganov, E. A. & Grudd, H. 1998a. Trees tell of past climates: but are they speaking less clearly today? *Philosophical Transactions of the Royal Society of London Series B-Biological Sciences* 353: 65-73.
- Briffa, K. R., Schweingruber, F. H., Jones, P. D., Osborn, T. J., Shiyatov, S. G. & Vaganov, E. A. 1998b. Reduced sensitivity of recent tree-growth to temperature at high northern latitudes. *Nature* 391: 678-682.
- Bruchert, F., Becker, G. & Speck, T. 2000. The mechanics of Norway spruce [*Picea abies* (L.) Karst]: mechanical properties of standing trees from different thinning regimes. *Forest Ecology and Management* 135: 45-62.
- Cannell, M. G. R. 1985. Dry matter partitioning in tree crops. In Cannell, M. G. R. & Morgan, J. (Eds) *Attributes of Trees as Crop Plants* (pp. 160-193). UK: Institute of Terrestrial Ecology.
- Cannell, M. G. R. & Dewar, R. C. 1994. Carbon allocation in trees - a review of concepts for modeling. *Advances in Ecological Research, Vol 25* 25: 59-104.
- Cook, E. R. A time-series analysis approach to tree-ring standardisation. 1985, Thesis. University of Arizona, Tucson.
- Cook, E. R. 1990. Bootstrap confidence-intervals for red spruce ring-width chronologies and an assessment of age-related bias in recent growth trends. *Canadian Journal of Forest Research-Revue Canadienne de Recherche Forestiere* 20: 1326-1331.
- Cook, E. R., Briffa, K. R., Meko, D. M., Graybill, D. A. & Funkhouser, G. 1995. The Segment Length Curse in long Tree-ring Chronology Development for Paleoclimatic Studies. *Holocene* 5: 229-237.
- Cook, E. R., Briffa, K. R., Shiyatov, S. & Mazepa, V. 1990. Tree-Ring Standardisation and Growth Trend Estimation. In Cook, E. R. & Kairiukstis, L. A. (Eds) *Methods of Dendrochronology* (pp. 104-123). Kluwer Academic Publishers.
- Cook, E. R. & Kairiukstis, L. A. 1990. *Methods of Dendrochronology*. Kluwer Academic Publishers, Dordrecht: International Institute for Applied Systems Analysis.

- Cook, E. R., Palmer, J. G. & D'Arrigo, R. D. 2002. Evidence for a 'Medieval Warm Period' in a 1,100 year tree-ring reconstruction of past austral summer temperatures in New Zealand. *Geophysical Research Letters* 29: art-1667.
- Cook, E. R. & Peters, K. 1981. The Smoothing Spline: A new approach to standardizing forest interior tree-ring width series for dendroclimatic studies. *Tree-Ring Bulletin* 41: 45-53.
- Cook, E. R. & Peters, K. 1997. Calculating unbiased tree-ring indices for the study of climatic and environmental change. *Holocene* 7: 361-370.
- Dale, V. H. & Rauscher, H. M. 1994. Assessing impacts of climate-change on forests - The state of biological modeling. *Climatic Change* 28: 65-90.
- Dean, T. J. & Long, J. N. 1986. Validity of constant-stress and elastic-instability principles of stem formation in *Pinus contorta* and *Trifolium-pratense*. *Annals of Botany* 58: 833-840.
- Dewar, R. C. 1993. A mechanistic analysis of self-thinning in terms of the carbon balance of trees. *Annals of Botany* 71: 147-159.
- Dewar, R. C., Medlyn, B. E. & McMurtrie, R. E. 1999. Acclimation of the respiration photosynthesis ratio to temperature: insights from a model. *Global Change Biology* 5: 615-622.
- Dickinson, R. E., Meleshko, V., Randall, D., Sarachik, E. & Silvva-Dias, P. 1996. Climate Processes. In Houghton, J. T., Meira Filho, L. G., Callander, B. A., Harris, N., Kattenberg, A. & Maskell, K. (Eds) Climate change 1995. Contribution of WG I to the second Assessment report of the IPCC Cambridge, UK: Cambridge University Press.
- Douglass, A. E. 1914. A method of Estimating Rainfall by the Growth of Trees. In Huntington, E. (Ed) The Climate Factor Washington, DC, USA: Carnegie Institution of Washington Publication 192.
- Elfving, B. & Nystrom, K. 1996. Stability of site index in scots pine (*Pinus sylvestris*, L.) plantations over year of planting in the period 1900-1977 in Sweden. In Spiecker, H., Mielikainen, K., Kohl, M. & Skovsgaard, J. P. (Eds) Growth Trends in European Forests (pp. 71-77). Berlin: Springer.
- Enquist, B. J., West, G. B., Charnov, E. L. & Brown, J. H. 2000. Allometric scaling of production and life-history variation in vascular plants (vol 401, pg 907, 1999). *Nature* 408: 750.
- Eronen, M., Zetterberg, P., Briffa, K. R., Lindholm, M., Merilainen, J. & Timonen, M. 2002. The supra-long Scots pine tree-ring record for Finnish Lapland: Part 1, chronology construction and initial inferences. *Holocene* 12: 673-680.
- Esper, J., Cook, E. R., Krusic, P. J. & Schweingruber, F. H. 2003. Tests of the RCS method for preserving low-frequency variability in long tree-ring chronologies. *Tree-Ring Research* 59: 81-98.
- Esper, J., Cook, E. R. & Schweingruber, F. H. 2002. Low-frequency signals in long tree-ring chronologies for reconstructing past temperature variability. *Science* 295: 2250-2253.
- Ewers, B. E. & Oren, R. 2000. Analyses of assumptions and errors in the calculation of stomatal conductance from sap flux measurements. *Tree Physiology* 20: 579-589.
- Foley, J. A., Levis, S., Prentice, I. C., Pollard, D. & Thompson, S. L. 1998. Coupling dynamic models of climate and vegetation. *Global Change Biology* 4: 561-579.
- Franklin, J. F., Shugart, H. H. & Harmon, M. E. 1987. Tree death as an ecological process. *Bioscience* 37: 550-556.
- Friend, A. D., Stevens, A. K., Knox, R. G. & Cannell, M. G. R. 1997. A process-based, terrestrial biosphere model of ecosystem dynamics (Hybrid v3.0). *Ecological Modelling* 95: 249-287.

- Fritts, H. C. 1976a. *Tree Rings and Climate*. London: Academic Press.
- Fritts, H. C. 1976b. Growth and Structure. *Tree Rings and Climate* (pp. 55-117). London: Academic Press.
- Fritts, H. C. 1976c. Dendrochronology and Dendroclimatology. *Tree Rings and Climate* (pp. 1-54). London: Academic Press.
- Fritts, H. C. 1976d. The statistics of ring-width and climatic data. *Tree Rings and Climate* (pp. 246-311). London: Academic Press.
- Fritts, H. C., Mosimann, J. E. & Bottorff, C. P. 1969. A revised computer program for standardising tree-ring series. *Tree-Ring Bulletin* 29: 15-20.
- Grissinomayer, H. D. & Fritts, H. C. 1997. The International Tree-Ring Data Bank: An enhanced global database serving the global scientific community. *Holocene* 7: 235-238.
- Grudd, H., Briffa, K. R., Gunnarson, B. E. & Linderholm, H. W. 2000. Swedish tree rings provide new evidence in support of a major, widespread environmental disruption in 1628 BC. *Geophysical Research Letters* 27: 2957-2960.
- Grudd, H., Briffa, K. R., Karlen, W., Bartholin, T. S., Jones, P. D. & Kromer, B. 2002. A 7400-year tree-ring chronology in northern Swedish Lapland: natural climatic variability expressed on annual to millennial timescales. *Holocene* 12: 657-665.
- Guiot, J. 1985. The extrapolation of recent climatological series with spectral canonical regression. *Journal of Climatology* 5: 325-335.
- Gunderson, C. A. & Wullschleger, S. D. 1994. Photosynthetic acclimation in trees to rising atmospheric CO<sub>2</sub> - A broader perspective. *Photosynthesis Research* 39: 369-388.
- Hamilton, G. J. & Christie, J. M. 1971. *Forest Management Tables (Metric)*. London: HMSO.
- Hawkes, C. 2000. Woody plant mortality algorithms: description, problems and progress. *Ecological Modelling* 126: 225-248.
- Helama, S., Lindholm, M., Timonen, M., Merilainen, J. & Eronen, M. 2002. The supra-long Scots pine tree-ring record for Finnish Lapland: Part 2, interannual to centennial variability in summer temperatures for 7500 years. *Holocene* 12: 681-687.
- Holmes, R. L. 1986. COFECHA. University of Arizona, Tuscon: Laboratory of Tree Ring Research.
- Houghton, J. T., Jenkins, G. J. & Ephraums, J. J. (Eds) 1990. *Climate Change. The IPCC Scientific Assessment*. Cambridge, UK: Cambridge University Press.
- Houghton, J. T. 2001. (Ed) *Climate Change. The scientific basis: to the assessment report of the Intergovernmental Panel on Climate Change*. Cambridge: Cambridge University Press.
- Kalela-Brundin, M. 1999. Climatic information from tree-rings of *Pinus sylvestris* L. and a reconstruction of summer temperatures back to AD 1500 in Femundsmarka, eastern Norway, using partial least squares regression (PLS) analysis. *Holocene* 9: 59-77.
- Kaufmann, M. R. 1996. To live fast or not: Growth, vigor and longevity of old-growth ponderosa pine and lodgepole pine trees. *Tree Physiology* 16: 139-144.
- Klingbjer, P. & Moberg, A. 2003. A composite monthly temperature record from Tornedalen in northern Sweden, 1802-2002. *International Journal of Climatology* 23: 1465-1494.

- LaMarche, V. C. 1974a. Frequency-Dependent Relationships between Tree-Ring Series along an Ecological Gradient and some Dendroclimatic Implications. *Tree-Ring Bulletin* 34: 1-20.
- LaMarche, V. C. 1974b. Paleoclimatic inferences from long tree-ring records. *Science* 183: 1043-1048.
- Landsberg, J. J. 1986a. Introduction. *Physiological Ecology of Forest Production* (pp. 1-5). London, UK: Academic Press.
- Landsberg, J. J. 1986b. Process Rates and Weather. *Physiological Ecology of Forest Production* (pp. 7-29). London, UK: Academic Press.
- Landsberg, J. J. 1986c. The carbon balance of leaves. *Physiological Ecology of Forest Production* (pp. 69-86). London, UK: Academic Press.
- Lindholm, M. & Eronen, M. 2000. A reconstruction of mid-summer temperatures from ring-widths of Scots pine since AD 50 in northern Fennoscandia. *Geografiska Annaler Series A-Physical Geography* 82A: 527-535.
- Lindner, M., Sievanen, R. & Pretzsch, H. 1997. Improving the simulation of stand structure in a forest gap model. *Forest Ecology and Management* 95: 183-195.
- Lundqvist, L. & Valinger, E. 1996. Stem diameter growth of Scots pine trees after increased mechanical load in the crown during dormancy and (or) growth. *Annals of Botany* 77: 59-62.
- Magel, E., Jayallemand, C. & Ziegler, H. 1994. Formation of heartwood substances in the stemwood of robinia-pseudoacacia L.2. distribution of nonstructural carbohydrates and wood extractives across the trunk. *Trees-Structure and Function* 8: 165-171.
- Magnani, F., Mencuccini, M. & Grace, J. 2000. Age-related decline in stand productivity: the role of structural acclimation under hydraulic constraints. *Plant Cell and Environment* 23: 251-263.
- Makela, A. A. 1986. Implications of the pipe model-theory on dry-matter partitioning and height growth in trees. *Journal of Theoretical Biology* 123: 103-120.
- Makela, A. A. 1997. A carbon balance model of growth and self-pruning in trees based on structural relationships. *Forest Science* 43: 7-24.
- Makela, A. A. & Albreksson, A. 1992. An analysis of the relationship between foliage biomass and crown surface area in *Pinus sylvestris* in Sweden. *Scandinavian Journal of Forest Research* 7: 297-307.
- Makela, A. A. & Hari, P. 1986. Stand growth-model based on carbon uptake and allocation in individual trees. *Ecological Modelling* 33: 205-229.
- Makela, A. A. & Sievanen, R. 1992. Height Growth Strategies in Open-Grown Trees. *Journal of Theoretical Biology* 159: 443-467.
- Makela, A. A. & Vanninen, P. 1998. Impacts of size and competition on tree form and distribution of aboveground biomass in Scots pine. *Canadian Journal of Forest Research-Revue Canadienne de Recherche Forestiere* 28: 216-227.
- Makela, A. A. & Vanninen, P. 2000. Estimation of fine root mortality and growth from simple measurements: a method based on system dynamics. *Trees-Structure and Function* 14: 316-323.
- Mateu, J., Uso, J. L. & Montes, F. 1998. The spatial pattern of a forest ecosystem. *Ecological Modelling* 108: 163-174.

- Matthégk, G. C. 1991a. The height-diameter ratio of the trunk, *Trees, the mechanical design* (pp. 53-57). Berlin: Springer-Verlag.
- Matthégk, G. C. 1991b. What is good mechanical design, *Trees, the mechanical design* (pp. 25-27). Berlin: Springer-Verlag.
- Matthégk, G. C. 1991c. The mechanics of trees and the self-optimisation of tree shape. *Trees, the mechanical design* (pp. 42-51). Berlin: Springer-Verlag.
- McCree, K. J. 1970. An equation for the rate of respiration of white clover plants grown under controlled conditions. In Setlik, I. (Ed) *Prediction of Measurement of Photosynthetic Productivity* (pp. 332-339). Wageningen: PUDOC.
- McMahon, T. A. 1973. Size and shape in Biology. *Science* 179: 1201-1204.
- Mendenhall, W., Wackerly, D. D. & Scheaffer, R. L. 1990. *Mathematical Statistics with Applications*. Belmont, California: Duxbury Press.
- Metzger, K. 1893. Der Win als massgebender Faktor für das Wachstum der Baume. *Mundener Forstl* 3: 35-62.
- Mielikainen, K. & Timonen, M. 1996. Growth trends of Scots Pine (*Pinus sylvestris*, L.) in unmanaged and regularly managed stands in southern and central Finland. In Spiecker, H., Mielikainen, K., Kohl, M. & Skovsgaard, J. P. (Eds) *Growth Trends in European Forests* (pp. 41-59). Berlin: Springer.
- Mitchell, V. L. An investigation of certain aspects of tree growth rates in relation to climate in the central Canadian boreal forest. Technical Report 33. 1967. University of Wisconsin, Dept. Meteorology.
- Morgan, J. & Cannell, M. G. R. 1994a. Shape of tree stems - A reexamination of the uniform stress hypothesis. *Tree Physiology* 14: 49-62.
- Morgan, J. & Cannell, M. G. R. 1994b. Shape of tree stems - A reexamination of the uniform stress hypothesis, Fig 4. *Tree Physiology* 14: 49-62.
- Nicoll, B. C. & Ray, D. 1996. Adaptive growth of tree root systems in response to wind action and site conditions. *Tree Physiology* 16: 891-898.
- Nikinmaa, E. 1990. A simplified carbon partitioning model for scots pine to address the effects of altered needle longevity and nutrient uptake on stand development. In Dixon, R. K. (Ed) *Process modeling of forest growth responses to environmental stress* (pp. 263-270). Oregon: Timber Press.
- Norby, R. J., Wullschlegel, S. D., Gunderson, C. A., Johnson, D. W. & Ceulemans, R. 1999. Tree responses to rising CO<sub>2</sub> in field experiments: implications for the future forest. *Plant Cell and Environment* 22: 683-714.
- Osborn, T. J. & Briffa, K. R. 2000. Revisiting timescale-dependent reconstruction of climate from tree-ring chronologies. *Dendrochronologia* 18: 9-25.
- Osborn, T. J., Briffa, K. R., Tett, S. F. B., Jones, P. D. & Trigo, R. M. 1999. Evaluation of the North Atlantic Oscillation as simulated by a coupled climate model. *Climate Dynamics* 15: 685-702.
- Peet, R. K. & Christensen, N. L. 1987. Competition and tree death. *Bioscience* 37: 586-595.
- Pilcher, J. R. 1990. Primary Data. In Cook, E. R. & Kairiukstis, L. A. (Eds) *Methods of Dendrochronology* (pp. 23-96). Kluwer Academic Publishers.
- Prentice, I. C. & Webb, T. 1998. BIOME 6000: Reconstructing global mid-Holocene vegetation patterns from palaeoecological records. *Journal of Biogeography* 25: 997-1005.

Schimel, D., Alves, D., Enting, I., Heimann, M., Joos, F., Raynaud, D. & Wigley, T. 1995. CO<sub>2</sub> and the carbon cycle. In Houghton, J. T., Meira Filho, L. G., Callander, B. A., Harris, N., Kattenberg, A. & Maskell, K. (Eds) *Climate change 1995. Contribution of WG I to the second Assessment report of the IPCC* Cambridge, UK: Cambridge University Press.

Schweingruber, F. H. 1988. *Tree Rings: Basics and Applications in Dendrochronology*. Dordrecht, Netherlands: Kluwer Academic Publishers.

Schweingruber, F. H. 1996a. *Tree-Ring Morphology*. *Tree Rings and Environment Dendroecology* (pp. 71-93). Berne: Paul Haupt Publishers.

Schweingruber, F. H. 1996b. *Tree Rings and Environment Dendroecology*. Berne: Paul Haupt Publishers.

Schweingruber, F. H., Kairiukstis, L. A. & Shiyatov, S. 1990. Sample Selection. In Cook, E. R. & Kairiukstis, L. A. (Eds) *Methods of Dendrochronology* (pp. 24-35). Kluwer Academic Publishers.

Shinozaki, K., Yoda, K., Hozumi, K. & Kira, T. 1964. A quantitative analysis of plant form - the pipe model theory I Basic analyses. *Japenese Journal of Ecology* 14: 97.

Shugart, H. H. & Smith, T. M. 1996. A review of forest patch models and their application to global change research. *Climatic Change* 34: 131-153.

Sitch, S., Smith, B., Prentice, I. C., Arneth, A., Bondeau, A., Cramer, W., Kaplan, J. O., Levis, S., Lucht, W., Sykes, M. T., Thonicke, K. & Venevsky, S. 2003. Evaluation of ecosystem dynamics, plant geography and terrestrial carbon cycling in the LPJ dynamic global vegetation model. *Global Change Biology* 9: 161-185.

Skovsgaard, J. P. & Henriksen, H. A. 1996. Increasing site productivity during consecutive generations of naturally regenerated and planted Beech (*Fagus sylvatica* L.) in Denmark. In Spiecker, H., Mielikainen, K., Kohl, M. & Skovsgaard, J. P. (Eds) *Growth Trends in European Forests* (pp. 89-97). Berlin: Springer.

Smith, B., Prentice, I. C. & Sykes, M. T. 2001. Representation of vegetation dynamics in the modelling of terrestrial ecosystems: comparing two contrasting approaches within European climate space. *Global Ecology and Biogeography* 10: 621-637.

Spatz, H. C. & Bruechert, F. 2000. Basic biomechanics of self-supporting plants: wind loads and gravitational loads on a Norway spruce tree. *Forest Ecology and Management* 135: 33-44.

Spiecker, H. 1996. *Growth Trends in European Forests*. Berlin: Springer.

Stahle, D. W., Cleaveland, M. K. & Heyr, J. G. 1988. North Carolina climate changes reconstructed from tree-rings: A.D. 372 to 1985. *Science* 240: 1517-1519.

Stokes, M. A. & Smiley, T. L. 1968. *An introduction to Tree-Ring Dating*. IL, USA: University of Chicago Press.

Stoll, P., Weiner, J. & Schmid, B. 1994. Growth variation in a naturally established population of *Pinus sylvestris*. *Ecology* 75: 660-670.

Swetnam, T. W., Allen, C. D. & Betancourt, J. L. 1999. Applied historical ecology: Using the past to manage for the future. *Ecological Applications* 9: 1189-1206.

Tappeiner, J. C. I. 1969. Effect of cone production on branch, needle, and xylem ring growth of Sierra Nevada Douglas-fir. *Forest Science* 15: 171-174.

Thornley, J. H. M. 1991. A transport-resistance model of forest growth and partitioning. *Annals of Botany* 68: 211-226.

- Thornley, J. H. M. & Cannell, M. G. R. 2000. Modelling the components of plant respiration: Representation and realism. *Annals of Botany* 85: 55-67.
- Tuomenvirta, H. 2001. Homogeneity adjustments of temperature and precipitation series - Finnish and Nordic data. *International Journal of Climatology* 21: 495-506.
- Valentine, H. T. 1988. A carbon-balance model of stand growth - A derivation employing pipe-model theory and self-thinning rule. *Annals of Botany* 62: 389-396.
- Valinger, E. & Pettersson, N. 1996. Wind and snow damage in a thinning and fertilization experiment in *Picea abies* in southern Sweden. *Forestry* 69: 25-33.
- Vanninen, P. & Makela, A. A. 1999. Fine root biomass of Scots pine stands differing in age and soil fertility in southern Finland. *Tree Physiology* 19: 823-830.
- Vanninen, P. & Makela, A. A. 2000. Needle and stem wood production in Scots pine (*Pinus sylvestris*) trees of different age, size and competitive status. *Tree Physiology* 20: 527-533.
- Vanninen, P., Ylitalo, H., Sievanen, R. & Makela, A. A. 1996. Effects of age and site quality on the distribution of biomass in Scots pine (*Pinus sylvestris* L.). *Trees-Structure and Function* 10: 231-238.
- Warren, W. G. 1980. On Removing the Growth Trend from Dendrochronological Data. *Tree-Ring Bulletin* 40: 35-44.
- Wenk, G. & Vogel, M. 1996. Height growth investigations of Norway spruce (*Picea abies*, L.) in the eastern part of Germany during the last century. In Spiecker, H., Mielikainen, K., Kohl, M. & Skovsgaard, J. P. (Eds) *Growth Trends in European Forests* (pp. 99-106). Berlin: Springer.
- Wigley, T. M. L., Jones, P. D. & Briffa, K. R. 1987. Detecting the effects of acid deposition and CO<sub>2</sub>-fertilisation on tree growth. In Kairiukstis, L. A., Bednarz, Z. & Feliksik, E. (Eds) *Methods of Dendrochronology* (pp 239-254) International Institute for Applied Systems Analysis, Laxenburg, Austria and Polish Academy of Sciences-Systems Research Institute, Warsaw, Poland.
- Woodward, F. I. 1987. *World Climate. Climate and Plant Distribution* (pp. 39-58). Cambridge, UK: Cambridge University Press.